MICROBUBBLE DETECTION DURING EXTRACORPOREAL CIRCULATION FOR OPEN HEART SURGERY

A thesis submitted for the degree of
Doctor of Philosophy in June, 1977
by A. Furness, B.Sc., M.Phil. C. Eng.,
M.I.E.E., University of Keele.

ACKNOWLEDGEMENTS AND DECLARATION OF PARTICIPATION

This thesis contains a report of the work completed in the W. E. Dunn Unit of Cardiology during the period November, 1973 to January, 1977. I, the author, am particularly indebted to Dr. G. Wright for his diligent, instructive and consistent supervision throughout the course of the project. His extensive knowledge and his forthright, friendly approach have been a constant source of encouragement and constructive criticism. I am also indebted to Dr. Wright for performing the surgery required in the in vivo studies and for assisting in the measurement of haematological parameters.

Throughout the project Mr. J. M. Sanderson, Senior Thoracic Surgeon, North Staffordshire Royal Infirmary, has provided advice, encouragement and constructive criticism which have been intellectually stimulating and of practical value. I am indebted to Mr. Sanderson for the interest he has taken in the study both as a surgeon specialising in open heart surgery and as a friend.

To Dr. V. S. Welsby, Reader in Acoustics, Birmingham University, I owe a debt of gratitude for introducing me to the subject of acoustics in a most agreeable manner and for his painstaking communication on his second harmonic technique for the detection of undissolved gas. The rejection of the technique for the application considered in this project in no way diminished his interest in the project or his encouragement to develop a pulsed ultrasound device.

I am grateful to Mrs. M. Riley, the Unit's only, but most capable technician, for assistance with the surgery during the in vivo studies and for the cell counts, blood gas analysis and blood smears performed throughout the study.

Mr. H. Wardell and his staff of the University Engineering Workshops are to be thanked for manufacturing the transducer mounting assemblies used in these studies.

Mr. A. Vickers, University Photographer, and Mr. G. Burgess, Chief Technician, Biology Department are to be thanked for producing the photographs contained in the thesis.

Professor A. R. Gemmell has provided the facilities of the Biology Department. Financial support for the project has been provided by a grant to the Unit by our benefactor the late Mr. W. E. Dunn.

For my part, I can claim that the critical review of the literature, the examination of microbubble detection techniques, the design, construction, calibration and use of a flow dependent microbubble detection system, and the design of experimental procedures are entirely my own work. I have also performed many of the analytical procedures involved in the blood damage studies, and microbubble investigations, assembled and interpreted the data and presented the results. In my review of the literature, the factors responsible for bubble formation, stability and elimination, and the techniques for microbubble detection I have endeavoured to be original, critical and accurate. I have also endeavoured to be original and critical in my discussions, even though the multidisciplinary nature of the project has presented considerable difficulties in attempts to integrate the facts and ideas from a variety of sources. Discussions with my colleagues within the W. E. Dunn Unit of Cardiology and members of the Association of Extracorporeal Technologists of Great Britain and Northern Ireland, actively involved in extracorporeal technology, have helped to ease these difficulties.

I thank Mrs. S. Tatton and Mrs. S. Cooper for typing the manuscript and last, but not least, I owe an enormous debt of gratitude to my wife, Ann, for her perseverence and understanding during this period of study.

ABSTRACT

In a review of the scientific literature clinical and experimental evidence is produced to implicate microbubbles as a source of brain damage during extracorporeal circulation for open heart surgery. Direct evidence of tissue damage and definitive, quantitative effects of microbubbles in vivo have yet to be determined.

The factors reported to be responsible for the formation and elimination of microbubbles during extracorporeal circulation are examined and consideration is given to the treatment of microbubbles as dynamic entities. An analysis is developed, in non-dimensional form, to relate bubble lifetime to system parameters appropriate to the extracorporeal circuit.

Reported techniques for detecting microbubbles during cardiopulmonary bypass are examined and found to be inadequate for quantitative measurements. Doppler and other continuous wave ultrasonic techniques are shown to be inherently less suitable for quantitative microbubble detection than pulsed ultrasonic methods.

A design for a flow dependent microbubble detector based upon a consideration of the limitations of previously used techniques and a consideration of physical principles is presented and the instrumentation discussed.

Calibration methods have been developed, applied and the flow dependent detector shown to be effective within defined limits. The results of calibration and evaluation tests are presented and discussed.

In vitro and in vivo applications of the flow dependent detector are presented and discussed. In particular the influences of blood flow rate, oxygen flow rate, oxygenator reservoir level and arterial line filtration upon microbubble liberation are investigated and the importance of quantification in extracorporeal microbubble studies examined.

Recommendations are presented for developing the microbubble detector and for reducing the volume of gas in the form of microbubbles pumped into the patient during cardiopulmonary bypass for open-heart surgery.

CONTENTS

INTRODUCTION

During the first fifteen years of open-heart surgery, temporary or permanent brain damage was a frequent post-operative problem (Ehrenhaft & Claman, 1961; Blachy & Starr, 1964; Gilman, 1965; Sachdev, 1967; Bass & Longmore, 1969; Hill et al., 1969; Javid et al., 1969; Tufo, Ostfield & Skekelle, 1970; Lee et al., 1971; Frank et al., 1972). The conditions ranged from slight psychological disturbances to gross cerebral damage characterised by excessive mental derangement and/or paralysis. In recent years, this problem has ameliorated, probably due to improvements in the design and manufacture of components for cardiopulmonary bypass, surgical and perfusion techniques, blood filtration and post-operative care. However a finite level of neurological deficit remains. The reported incidence of this varies from 7% to 15% depending upon the patient population, definition and methods of assessment (Branthwaite, 1973; Aberg, 1974; Branthwaite, 1975; Aberg & Kihlgren, 1976; Mats & Hane, 1976). In some cases, the deficit cannot be attributed to a specific feature of the operative period (Branthwaite, 1975).

Although other aetiologies have been considered, there is widespread opinion that the release of undissolved gas in the form of microbubbles may be an important factor (Starr, 1960; Groves & Effler, 1964; Fishman, Carlsson & Roe, 1969; Patterson & Kessler, 1969; Wright, 1971; Patterson et al., 1972; Fisk et al., 1972; Gallagher & Pearson, 1973; Patterson, Rosenfeld & Porro, 1976). Although considerable efforts have been made to establish the sources and consequences of microbubbles during extracorporeal circulation there has been no comprehensive, quantitative analysis of the factors responsible for their formation. Moreover it has never been unequivocally shown that circulating microbubbles can cause embolic tissue damage.

Gas microbubbles are distinct from particulate emboli in that their size and their possible consequences are dependent upon the rate at which

the gas phase is re-absorbed or dissolved following its appearance in the blood or body fluids (Yang et al., 1971). No reported study of extracorporeal bubble sources has considered the properties that determine bubble lifetime.

The identification of extracorporeal bubble sources has been performed using qualitative detection techniques. Without information concerning the size, number and rate at which microbubbles enter an extracorporeal system, conclusions concerning the embolic consequences are severely limited. Furthermore the evaluation of extracorporeal circuit devices as bubble sources or bubble sinks may result in misleading conclusions if quantification is ignored.

The object of this study is to (1) review the evidence for microbubble formation during extracorporeal circulation (2) establish the importance of considering bubble dynamics when undertaking studies of microbubbles during extracorporeal circulation (3) determine the validity of reported techniques for microbubble detection (4) establish the physical basis for a quantitative microbubble detection technique (5) design and construct a system for the quantitative analysis of microbubble populations arising during extracorporeal circulation and (6) investigate the significance of quantification in the study of microbubble formation during experimental extracorporeal circulation.

Chapter 1

FACTORS RESPONSIBLE FOR MICROBUBBLE FORMATION AND DISSOLUTION DURING EXTRACORPOREAL CIRCULATION

During extracorporeal circulation for open heart surgery, the blood gas composition varies considerably as a consequence of variations in lung ventilation before and after cardiopulmonary bypass and of variations in gas exchange in the oxygenator and body tissues during cardiopulmonary bypass. These variations may, under appropriate conditions, predispose the blood to the formation of bubbles as a result of counter diffusion (Graves et al., 1963; 1973) or exchange rate supersaturation (Quinn, Graves & Smock, 1974). Temperature variations (Donald & Fellows, 1959) and local pressure changes as a result of roller pump action (Willman et al., 1958; Bass & Longmore, 1969) may also initiate bubble formation as a consequence of their concomitant influence upon the rate of change of gas tensions. The conditions necessary within an extracorporeal circuit to promote bubble formation by these mechanisms have not been fully examined. In addition to the mechanisms of formation within the blood microbubbles may enter the patient's blood circulation as a result of bubble oxygenation (Jordan et al., 1958; Landew et al., 1960; Spencer et al., 1965; Selman, McAlpine & Ratan, 1967; Aronstam et al., 1968; Patterson & Kessler, 1969; Kessler & Patterson,1970; Fisk et al., 1972; Patterson et al., 1972; Gallagher & Pearson, 1973), cardiotomy suction (Spencer et al., 1969; Gallagher & Pearson, 1973) and various surgical manoevres (Nichols, Morse & Hirose, 1958; Spencer et al., 1965; Gallagher & Pearson, 1973).

While the majority of these mechanisms for bubble formation

appear to be confined to the cardiopulmonary bypass procedure exchange rate and counterdiffusion supersaturation mechanisms may also operate during the pre- and post-bypass stages. The exchange rate mechanism creates local and generalised supersaturation when blood containing slowly diffusing gases such as nitrogen is suddenly exposed to any influx of a more rapidly diffusing gas such as oxygen (Quinn, Graves & Smock, 1974).

The counterdiffusion mechanism creates the danger of micro-bubble formation as a result of supersaturation at a membrane boundary (Graves et al., 1963; 1973).

It is important to note that the only requirement for super-saturation is that the total gas tension exceeds the prevailing system pressure but it is not necessary for any gas to be present in excess of its equilibrium concentration.

Counterdiffusion Supersaturation

The counter directional diffusion of gases through a series of layers, or mass transfer resistances, is fundamental to the mechanism of counterdiffusion supersaturation. For a simple two layer system, such as a membrane-blood layer interface, through which a number of gases diffuse, the maximum supersaturation pressure, which exists at the interface between the two layers, has been defined by Quinn, Graves & Smock (1974) using the following analysis.

Considering a two-layer composite in which the layer thicknesses are X_1 and X_2 and the permeability (product of solubility α and diffusivity $\mathcal{D}$) to a given gas, i, are respectively K_{i1} and K_{i2}, the pressure at the interface may be determined once the partial pressures, P_{i1} and P_{i2} at the exterior boundaries of the composite are known.

In the steady state situation, the diffusing gas flux, J, is

constant throughout the composite. Consequently

$$J_{i1} = J_{i2} = J_i$$

By use of Fick's law of diffusion, incorporating Henry's law of partial pressures for dissolved gas concentrations, the flux may be defined as:

$$J_i = -K_{i1} \frac{(P_{i,12} - P_{i1})}{X_1}$$

$$= -K_{i2} \frac{(P_{i2} - P_{i,12})}{X_2}$$

where $P_{i,12}$ is the pressure at the layer interface. Solving for $P_{i,12}$:

$$P_{i,12} = \frac{\frac{K_{i1}}{X_1}}{\frac{K_{i1}}{X_1} + \frac{K_{i2}}{X_2}} P_{i1} + \frac{\frac{K_{i2}}{X_2}}{\frac{K_{i1}}{X_1} + \frac{K_{i2}}{X_2}} P_{i2}$$

By expressing permeability and layer thickness in the form of dimensionless ratios, $K_i^* = \frac{K_{i1}}{K_{i2}}$ and $X^* = \frac{X_1}{X_2}$, the interface pressure:

$$P_{i,12} = \frac{P_{i1}}{1 + \frac{X^*}{K_i^*}} + \frac{P_{i2}}{1 + \frac{K_i^*}{X^*}}$$

For situations in which simultaneous fluxes of n non-interacting gases exist, the total dissolved gas pressure at the layer interface, P_I, is obtained by summing the interface pressures derived for each gas:

i.e. $$P_I = \sum P_{i,12}$$

$$= \sum \left[\frac{P_{i1}}{1 + \frac{X^*}{K_i^*}} + \frac{P_{i2}}{1 + \frac{K_i^*}{X^*}} \right]$$

Solubility, α, and diffusivity, $\mathcal{D}$ are assumed to be constant in defining permeability ($K_i = \alpha_i \mathcal{D}_i$).

The extent to which counterdiffusion results in supersaturation depends upon the presence of additional gases and the elimination rates of gases present in solution but no longer present in the gas phase mixture. During cardiopulmonary bypass, nitrogen is particularly significant in this respect. Careful consideration of the nitrogen elimination rate is therefore important in estimating the effects of counterdiffusion.

Unfortunately difficulties may arise in estimating the prevailing levels of transient gases. This is because they depend upon composition of the mixture of gases to which the patient is exposed, the duration of exposure, the rate at which gases are eliminated from body stores, and the rate at which such gases are reintroduced.

The estimation of counterdiffusion supersaturation is further complicated by the fact that the effect will be different for different regions within the body and within the extracorporeal circuit. The exchange diffusion of nitrogen at a fatty tissue boundary, for example, may be expected to be greater than that at a boundary of a highly perfused tissue because of the higher solubility of nitrogen in fat.

Although the intracorporeal boundary conditions are virtually inaccessible for the measurement of the parameters necessary to calculate boundary pressures the conditions within the extracorporeal circuit are not. Quinn, Graves & Smock (1974) have calculated the worst and best case boundary pressure values for a commercially available membrane oxygenator (G.E. Dualung) under typical exit and entrance conditions and a range of X* values. The relationship between boundary pressure, P_{MB}, and the ratio of membrane thickness to blood film

thickness, X*, indicates that P_{MB} is a maximum for $k<X^*<10$ and that it is greater at the entrance of the oxygenator than at the exit. Over this range of X*, supersaturation is indicated and the formation of microbubbles is a distinct possibility. No specific, practical investigation has yet been reported concerning the formation of microbubbles in membrane oxygenators as a direct consequence of the counterdiffusion mechanism. However strong circumstantial evidence exists to suggest that counterdiffusion may cause microbubble formation in membrane oxygenators (Peirce, 1966; Kessler & Patterson, 1970; Ward & Zingg, 1972). Kessler & Patterson (1970) using a pulse ultrasound technique for microparticle detection observed echoes which they attributed to the presence of microbubbles within the blood emanating from the exit part of a membrane oxygenator. More convincingly Ward & Zingg (1972) observed visually the formation of bubbles at the membrane interface of a membrane oxygenator and followed the bubble growth photomicrographically.

Exchange rate supersaturation

Exchange rate supersaturation is a consequence of 'new' gases entering the blood or any body tissue faster than residual gases can be eliminated and may occur throughout the entire system.

During the procedure to perform open heart surgery, concentration of nitrogen in the blood may be an important determinant of counterdiffusion and exchange rate supersaturation (Quinn, Graves & Smock, 1974). For conditions in which the sum of the gas tensions within a selected region exceeds the prevailing system pressure, the predominant of these two mechanisms for supersaturation is the rate of gaseous exchange. When the simple sum of these tensions is less than the prevailing system pressure, supersaturation may only arise at tissue boundaries as a result of counterdiffusion (Quinn, Graves & Smock, 1974).

The period for which the conditions necessary for supersaturation prevail, by either mechanism, is considerably influenced by the rate at which nitrogen is eliminated from the circuit. Prior to bypass the cardiac output and respiratory minute volume have an obvious influence upon the elimination rate. Measurements of the nitrogen excretion rate in man at an estimated cardiac output of 5.4 $L.min^{-1}$ suggest that the total dissolved nitrogen content of the body is reduced by only 50% after 30 minutes of ventilation with a nitrogen free gas mixture (Jones, 1950).

During cardiopulmonary bypass, the nitrogen elimination rate may be significantly lower owing to the less efficient transfer characteristics of the artificial oxygenator compared with the alveolar membrane. Moreover the re-entry of nitrogen as a result of cardiotomy suction and of diffusion through the skin and through the tissues exposed within the open thorax may also reduce the overall elimination rate. Conditions for bubble formation by the exchange rate mechanism may therefore persist throughout the period of surgery.

In the case of respiratory support using veno-venous or veno-arterial circulation, Quinn, Graves & Smock (1974) suggest that the re-entry of nitrogen under conditions in which the patient breathes ordinary or oxygen enriched air while the oxygenator uses pure oxygen may be particularly hazardous if maintained for prolonged periods.

The 'washout' of anaesthetic gases may also promote bubble formation by the exchange rate supersaturation mechanism. The most likely agent in this respect is nitrous oxide. Contrary to the rates of gaseous uptake nitrogen elimination appears to be slower than nitrous oxide (Quinn, Graves & Smock, 1974). Consequently the conditions favouring supersaturation due to the presence of nitrous oxide are likely to be less persistent than the conditions dependent

upon nitrogen elimination. However the presence of nitrous oxide may promote an increase in the sizes of existing bubbles within the system due to its diffusion into the bubbles at a higher rate than the resident gas can diffuse out (Nunn, 1959; Tisovec & Hamilton, 1967).

Although supersaturation is generally a precursor to bubble formation a variation in temperature or turbulence may be necessary before bubbles are formed. Christoforides & Hedley-Whyte (1969) showed the effect of fluid disturbance upon an in vitro supersaturated solution of oxygen in blood. Human blood was equilibrated with oxygen at a tension of 101.3 kPa (760 mm.Hg) at $2^{o}C$. The tension was increased to 186.6 kPa (1400 mm.Hg) by raising the blood temperature to $37^{o}C$. Stirring the blood caused an immediate reduction in tension to 101.3 kPa and the rapid release of oxygen in the form of bubbles.

Extracorporeal bubble sources

The extracorporeal circuit may introduce microbubbles into the systemic circulation from various sources including the oxygenator, pump and cardiotomy reservoir. Bubble oxygenators in particular are capable of introducing microbubbles into the circuit as a consequence of direct, turbulent, blood-gas interaction. Friedman et al (1962) observed that 1.5 ml of air, or approximately 6 ml of oxygen per kilogram body weight, distributed in microbubble form (25-100 μm diameter bubbles) was uniformly lethal when injected into a carotid artery of normothermic dogs. Comparable quantities of oxygen in microbubble form may enter the systemic circulation during cardiopulmonary bypass if excessively high gas flows are used in conjunction with a low blood level in the arterial reservoir (Landew et al., 1960).

Other investigators have supported this claim although they have not made a quantitative evaluation of bubble populations (Maloney et al., 1958; Tepper et al., 1958; Patterson & Kessler, 1969; Fisk, et al., 1972; Gallagher & Pearson, 1973). Patterson & Kessler (1969) using a pulsed ultrasound technique for detecting bubbles, noted an increase in echo count in response to an increase in oxygenator gas flow rate (up to 9L min^{-1}) while perfusing an isolated canine lung. Fisk et al., (1972) investigated bubble formation in infant oxygenators (Temptrol Q 130 & Q110) at low blood flow rates. For the Temptrol Q130 operating at blood flow rates between 250 and 500 $ml.min^{-1}$, bubbles were observed under low power optical magnification whenever the gas flow was greater than $1L.min^{-1}$ and the reservoir level below maximum. However bubbles were not observed under the same conditions for the Temptrol Q110 pediatric oxygenator. Although the implication is that the Q110 oxygenator is less significant as a bubble source, the limitation of the bubble detection technique of observing only the surface of the oxygenator and the lack of

quantitative information of bubble size and number suggest that the basis for such a conclusion is unsound.

In the clinical situation the significance of high gas flows cannot be realised by increasing the gas flow above the level required for adequate oxygenation for ethical reasons. However, Gallagher & Pearson (1973) using a Doppler ultrasonic bubble detection technique noted an increase in the acoustic response toward the end of cardiopulmonary bypass during which the venous return was reduced and the gas flow was maintained at a constant level. This increase was attributed to the raised gas flow to blood flow ratio with a consequent increase in the release of microbubbles from the bubble oxygenator. Unfortunately the ratio of gas flow to blood flow as a guide to the propensity of bubble oxygenators to deliver microbubbles into the arterial line is misleading. An increase in blood flow for a given gas flow level, represented by a reduction in gas flow to blood flow ratio suggests a reduction in the outgoing bubble population. However an increase in outflow blood velocity may increase the population by reducing the settling time and the ability of bubbles below a specific velocity dependent diameter to settle out due to their natural buoyancy.

The influence of reservoir level on bubble population is undoubtedly a consequence of the relationship between reservoir blood volume and settling time. During pre-circulation of the oxygenator priming fluid Gallagher & Pearson (1973) noted that a low level of fluid in both Travenol and Rygg oxygenators was accompanied by an increase in acoustic response, suggesting an increase in bubble population. The absence of activity was noted only when the level of the priming fluid in the settling chamber reached the lower border of the defoaming chamber. They suggested that this was a consequence of reduced turbulence and increased settling time. The extent to which the prevailing dissolved gas conditions and the use of a whole blood prime would influence the bubble population has not

apparently been considered. Fisk et al (1972) reported that for oxygen tensions below 20 kPa (150 mm.Hg.) no bubbles could be observed within the oxygenator whilst maintaining the blood flow rate within the range 0.25 to 0.75 $L.min^{-1}$ and gas flow rates up to 4 $L.min^{-1}$. Once again, the limitations of the bubble detection technique suggest the need for caution in considering the implication of this statement. At low oxygen tensions (20 kPa) haemoglobin is unsaturated and oxygen bubbles are more readily dissolved than at higher oxygen tensions. The influence of prevailing gas conditions on bubble lifetime within the extracorporeal circuit requires further consideration.

Other factors that may influence the formation of bubbles within the settling chamber and the output line of a bubble oxygenator include splashing of reservoir additives such as additional blood or electrolyte solutions (Wright, 1971; Gallagher & Pearson, 1973) and agitation of the oxygenator promoting the release of bubbles adhering to the inner surfaces of the oxygenator reservoir (Patterson & Kessler, 1969). The oxygenator design may also exhibit a marked influence on the formation and elimination of microbubbles. Greater efficiency of oxygenation of flowing blood is achieved the greater the number of bubbles and the smaller their size, so increasing the surface area of the blood gas interface (Clark, 1958; 1959). The practical lower limit of bubble size is determined by the gas exchange characteristics for oxygen and carbon dioxide and the ability of the defoaming and settling chambers to remove excess bubbles (Clark, 1958; Rygg, 1972). Sparger designs having pore sizes of 120 μm have been shown to provide more efficient oxygenation than spargers having larger pore sizes (Ferguson, Burbank & Burford, 1967). Although Ferguson, Burbank & Burford (1967) claim that excess bubbles are completely eliminated from the perfusate, observations by Gallagher & Pearson (1973), on the basis of increased acoustic perturbation, suggest that this is not

so. However, in view of other features such as defoaming chamber and settling chamber design, conclusions concerning sparger design on the basis of observed 'carry through' of bubbles must be viewed with caution.

Comparisons of various types of oxygenator as bubble sources have been the subject of a number of investigations (Jordan et al., 1958; Spencer et al., 1965; Selman et al., 1967; Aronstam et al., 1968; Patterson & Kessler, 1969; Kessler & Patterson, 1970; Fisk et al., 1972; Gallagher & Pearson, 1973; Kayser, 1974; Pierce, 1974). The general conclusion from these studies is that bubble oxygenators liberate more bubbles than disc oxygenators and that both types liberate more than membrane oxygenators. Although this statement may be correct, the fact that none of these studies have provided quantitative information concerning bubble size distribution and numbers make any comparisons between oxygenators as bubble sources rather dubious. A smaller population of larger bubbles may, for example, be more offensive than a larger population of smaller bubbles. The rate at which bubbles enter the arterial line may also be important.

Increasing the temperature of the blood within the extracorporeal circuit following profound or mild hypothermia, may promote bubble formation following an increase in gas tension (Donald & Fellows, 1959; 1961; Drew et al., 1959; Gordan et al., 1960; Kaplan et al., 1962).

Donald & Fellows (1959) used an isolated canine lung preparation ventilated with pure oxygen and a specially constructed circuit for producing controlled temperature gradients to investigate the effects of sustained temperature differentials and the effects of rapid heating. In addition to temperature measurement, oxygen tension and hydrostatic pressure were measured and bubble formation was observed within a bubble trapping chamber. A sustained temperature differential of 17°C (20-37°C) creating an oxygen tension above that of the local hydrostatic

pressure consistently yielded a steady release of gas in the form of bubbles visible to the naked eye (Donald & Fellows, 1959; 1961). However, rapidly increasing the temperature of an isolated volume of circulating blood from 20°C to 37°C was not observed to be accompanied by a release of bubbles. Although no bubbles were observed during this procedure, it cannot be concluded that bubbles were totally absent. Under the conditions described a release of microbubbles could occur and be undetectable visually. Wright (1971) using a Doppler ultrasonic flow-meter and an in vitro circuit noted an increase in high amplitude Doppler activity, suggesting the formation of bubbles, following a rapid increase in blood temperature. Rapid localised temperature variations may similarly account for bubble formation as a result of adding cold blood to the oxygenator or cardiotomy reservoir (Gallagher & Pearson, 1973). More gradual increases in temperature ($0.5^{\circ}C.min^{-1}$) may avoid bubble formation (Wright, 1971).

Cardiotomy suction return has been considered to be a more hazardous source of microbubbles than those arising from the oxygenator during extracorporeal circulation (Miller & Allbritten, 1960; Baird & Mujagiohima, 1964; Spencer et al., 1965; Spencer et al., 1969; Gallagher & Pearson, 1973). The reason for considering this to be so is that the bubbles contain air rather than oxygen and the low solubility of nitrogen in blood together with its inability to combine chemically with blood cell constituents imply that bubbles containing nitrogen may persist for longer periods of time than correspondingly sized bubbles of oxygen. Observations by Friedman et al (1962) indicate that microbubbles of air are also potentially more lethal (total volume 1.5 ml) than oxygen by a ratio of approximately 4:1. Lawrence, McKay & Sherensky (1971) reported that the incorporation of a cardiotomy line filter reduced the liberation of microbubbles into the systemic circulation to insignificant levels. However,

since no quantitative assessment of the cardiotomy suction source of microbubbles or of the efficacy of the filter in removing them was made, the validity of the conclusion is dubious. Similarly the claim by Selman, McAlpine & Ratan (1967) that a cardiotomy reservoir is unnecessary when using a Travenol disposable oxygenator may be doubted on the basis of the non-quantitative (visual) assessment of bubble population.

Although the roller pumps used in extracorporeal circulation may appear to be unlikely sources of microbubbles, bubbles may form as a result of collapse cavitation (Willman et al., 1958; Bass & Longmore, 1969). The localised pressure drop on the venous side of the pump roller during compression of the cuff may be sufficient to cause cavitation and the release of gas from plasmatic solution. Depending upon the prevailing dissolved gas conditions bubbles of oxygen and/or nitrogen may form.

Surgical sources of bubbles

The potential hazard of systemic air embolism as a direct result of residual intravascular air following open heart surgery has been of concern for some time (Carrel, 1914). Exposure of the inner surfaces of the heart and subsequent closure may result in undissolved gas being trapped within the heart, even when adequate venting has been attempted, (Padula et al., 1971). Using intracardiac cinephotography, Padula et al (1971) observed that while most of the undissolved gas could be removed by aortic and ventricular venting, many small bubbles remained adherent to the endocardial surfaces.

During open heart surgery, air has been observed to collect in the aorta, ventricles and pulmonary veins depending upon the type of operation (Nichols et al., 1958; Gott & Lillehei, 1959; Groves et al., 1964; Jones et al., 1964; Anderson et al., 1965;

Spencer et al., 1965; Carlson et al., 1967; Fishman et al., 1969; Taber, Moraan & Tomatis, 1970; Lawrence, McKay & Sherensky, 1971; Gallagher & Pearson, 1973; Cleland & Ghadiali, 1976; Lemole & Pinder, 1976). Air collecting in this manner may inadvertently enter the circulation following the removal of an aortic clamp or following the restoration of effective heart function on completion of heart surgery (Gallagher & Pearson, 1973). Various surgical manoeuvres, such as cannulation of the aorta and right atrium and the performance of closed mitral valvotomy, may also allow air to enter the circulation (Gallagher & Pearson, 1973).

A number of procedures have been reported for removing air collecting in vessels during open heart surgery, including the use of vents (Miller et al., 1953; Groves & Effler, 1964) needle venting (Taber, Maraan & Tomatis, 1970) fibrillation during extracorporeal circulation (Senning, 1952; Nicks, 1969) and flooding of the operative field with carbon dioxide (Nichols, Morse & Hirose, 1958; Burbank, Ferguson & Burford, 1965). A more recent attempt to improve the removal of air involves partial aortic clamping combined with aortic, needle venting (Lemole & Pinder, 1976). In this technique partial aortic clamping is applied prior to the discontinuation of cardiopulmonary bypass to create a cupula into which the bubbles of air collect. A needle vent inserted into the cupula allows the gas to be aspirated. The clamp is left in position for up to 20 minutes following cardiopulmonary bypass and decannulation. Although this technique may offer some improvement over previous procedures it is doubtful whether the cupula would retain all of the bubbles that enter the circulation. Moreover the release of bubbles may persist for longer than 20 minutes. Gallagher & Pearson (1973) have observed high amplitude Doppler

activity, suggesting the presence of bubbles, whilst monitoring the carotid circulation for periods up to one hour following the restoration of effective heart function. No estimates of the quantity of undissolved gas entering the circulation from surgical sources have been reported.

Blood gas interface effects

Although microbubbles have been strongly implicated as agents of embolic damage by their ability to occlude vessels of the microcirculation products of blood gas interface reaction may also produce embolic damage (Lee et al., 1961; Lee & Hairston, 1971; Philp, Inwood & Warren, 1972). Lee et al (1961) observed that significant denaturation of plasma proteins occurs at the blood gas interface produced in disc, bubble, and screen oxygenators. Curvature related surface energy of the bubbles and the consequent exchange of energy during interaction by attachment with cell membranes may be responsible for inducing cell deformation and subsequent disruption (Philp, Inwood & Warren, 1972).

Secondary biochemical and physicochemical sequelae as a result of denaturation have been observed and reported (Lee & Hairston, 1971; Philp et al., 1972). Denatured protein, particularly fibrinogen, may adhere to viable blood cells and result in subsequent cellular aggregation, sludging and microthrombosis (Lee & Hairston, 1971). Release of lipids followed by coalescence to form larger embolic entities can also occur. Red cell membrane denaturation and subsequent haemolysis as a result of bubble interaction or blood contact with other foreign surfaces results in the release of adenosine compounds (DeWall et al., 1959; Bernstein, 1971) which in turn promote platelet aggregation and the release of further quantities of adenosine compounds (Stormorken, 1971).

Platelet adhesion and aggregation together with white cell adhesion and damage to the vascular endothelium as a result of a direct blood gas interface have been observed by Philp, Inwood & Warren (1972) using light and electron microscopy.

In addition to the release of adenosine compounds as a result of haemolysis disruption of platelets and leucocytes results in the liberation of vasoactive agents, histamine and serotonin which in turn may be responsible for particular aspects of hepatic and portal venous congestion and hypotension following prolonged bubble oxygenation (Hollenberg, Pruett & Thal, 1963).

The fission of microbubbles in plasma as a result of collision may be influenced by interfacial properties (Hills, 1974). Hills (1974) observed that microbubbles of 150-250 μm diameter may disintegrate upon collision in human plasma and surfactant solutions to yield a population of smaller bubbles 35-45 μm diameter. Bubbles greater than 300 μm in diameter were observed to coalesce. The fact that collisions in surfactant free solutions do not cause bubble fission suggests that the surface active properties of these substances are important. Irrespective of the mechanism for fission, the fact that it can occur in human plasma may have important physiological implications. The reduction in bubble size would be accompanied by a reduction in bubble 'lifetime' (the period for which it exists as a bubble) and smaller vessels would be the first occluded. Assuming that such vessel occlusions persisted long enough for resultant local ischaemia, focal lesions would be expected to occur. However the higher number of bubbles as a result of fission might also produce regions of ischaemia. More analytical information on fission and its significance in extracorporeal circulation is required.

Gas Bubble Dynamics

A bubble present in a liquid exhibits a natural tendency to increase or decrease in size depending on the prevailing conditions. In order to determine the stability of a bubble it is necessary to consider the dynamic relationship between the inertial force induced by the motion of the bubble surface and the forces due to pressure, surface tension and viscosity incident upon that surface. The relationship for a spherical bubble in whole blood or plasma is of the form presented by Yang & Yeh (1966).

$$\frac{d^2R}{dt^2} \cdot R + \frac{3}{2}\left(\frac{dR}{dt}\right)^2 = \frac{P_g(R) - P_\infty}{\rho} - \frac{2\sigma}{\rho R} - \frac{4\mu}{\rho R}\left(\frac{dR}{dt}\right)$$

where the terms on the left represent the inertial force induced by the motion of the bubble surface and the terms on the right represent the forces due to pressure, surface tension and viscosity respectively. R is the bubble radius at any time t, ρ the density of the liquid, $P_g(R)$ the gas pressure inside the bubble, P_∞, the system pressure, is the pressure in the liquid at a distance from the bubble, σ the surface tension tension, and μ the viscosity. The expression only applies to a stationary bubble but closely resembles the dynamic behaviour of a moving bubble (Yeh & Yang, 1968). The complete dynamic equation includes terms expressing the effects of liquid velocity, relative velocity between liquid and bubble and liquid acceleration. These effects are considered to be small under the extracorporeal conditions prevailing in a normal cardiopulmonary bypass (Tanasawa et al., 1970).

By inspection of the force equation it is evident that a bubble is in dynamic equilibrium if $\frac{dR}{dt} = 0$ and $f(R) = 0$ where $f(R) = P_g(R) - P_\infty - \frac{2\sigma}{R}$. The stability of the bubble may be determined from the

value of $\frac{df(R)}{dR}$ for a given radius, R; $\frac{df(R)}{dR} < 0$ indicates dynamic stability. As a result of this condition the bubble will dissolve through diffusion of gas out of the bubble. The range of equilibrium radii for which $\frac{df(R)}{dR} < 0$ is expressed by the identity $R_o < \frac{2\sigma}{P_{go} - P_\infty}$ where R_o is the initial radius and P_{go} the initial pressure of gas within the bubble.

The condition $\frac{df(R)}{dR} > 0$ indicates dynamic instability and a tendency for the bubble to increase in size. The identity $R_o > \frac{2}{P_{go} - P_\infty}$ signifies the range of radii for which $\frac{df(R)}{dR} > 0$.

Under conditions of dynamic stability the rate of dissolution of gas bubbles in whole blood is determined by the rate at which the gas can diffuse into the blood, the chemical reactivity of the gas and, in the presence of flow, a convective effect that enhances both the diffusion process and the process of chemical reaction where one is evident (Yang et al., 1971). The primary chemical reaction involved in the process of oxygenating blood, either naturally or during extracorporeal circulation, is the formation of oxyhaemoglobin. The oxygen contained within a bubble situated in whole blood diffuses across the bubble surface into the blood where it immediately combines with reduced haemoglobin to form oxyhaemoglobin. The amount of oxygen dissolving in the plasma during this process is minimal, since the reaction between oxygen and haemoglobin proceeds within a concentration boundary layer. In the absence of flow the concentration boundary layer increases in thickness over the bubble surface. As a result of the combined processes of diffusion and second order chemical reaction the uptake of oxygen from the bubble into plasmatic solution is expressed by a differential equation of the form (Forster, 1964):

$$\frac{\partial [O_2]}{\partial t} = \mathcal{D} \nabla^2 [O_2] + k' [HbO_2] - k'' [O_2][Hb]$$

where t is time, $\mathcal{D}$ the diffusion coefficient, ∇^2 the Laplacian operator, $[O_2]$ $[Hb]$ and $[HbO_2]$ the concentrations of oxygen, reduced haemoglobin, and oxyhaemoglobin respectively, k' the reaction velocity constant for the dissociation of oxyhaemoglobin and k'' the reaction velocity constant for the association of oxygen and haemoglobin.

Providing it can be assumed that whole blood is a homogeneous mixture of plasma and haemoglobin and that the reaction products are being continuously removed from the reaction boundary of a dissolving bubble the reaction may be considered to be restricted to the association of oxygen and haemoglobin. Such a condition may be considered to prevail where relative motion exists between the bubble and the blood due to flow and to the motion of the bubble surface as the bubble dissolves.

The rate of oxygen uptake into solution under these conditions may be defined by the expression (Yang, 1971):

$$\frac{D\,[O_2]}{Dt} = \mathcal{D}\nabla^2\,[O_2] - K\,[O_2]$$

where $\frac{D}{Dt}$ is the substantial derivative that represents both the local and convective effects on diffusion and $K = k''\,[O_2]$ The dissolved gas concentration, C, at a point in the liquid, distance, from the centre of the bubble is determined by this diffusion equation (Yang, 1971). By omitting the term encompassed by the substantial derivative, that relates to the effect of convection on the diffusion process the concentration rate equation may be expressed in the following manner (Yang, 1971):

$$\frac{\partial C}{\partial t} = \mathcal{D}\nabla^2 C - KC$$

The KC term within this expression signifies the existence of a

uniformly distributed sink. The greater the value of K the greater the sinking capacity with respect to time. This enhances the diffusion process and results in faster dissolution of gas bubbles.

While convection is important in ensuring the removal of reaction products from the reaction boundary layer and confines the reaction to one of association between oxygen and haemoglobin, the effect on the diffusion process may be omitted from the concentration rate equation providing the following assumptions can be made:

1) the concentration of dissolved gas within the liquid surrounding the bubble is much smaller than the density of the gas contained within the bubble, and
2) the region within the solution around the bubble through which the gas is diffusing becomes rapidly larger than the bubble (Yang, 1971).

Based on these assumptions and the application of the following initial and boundary conditions Yang (1971) has determined the concentration gradient at the bubble surface. Thus for the initial condition that the concentration of dissolved gas is uniform and equal to C_∞, $C(r,o) = C_\infty$ and boundary conditions $C(\infty,t) = C_\infty$ and $C(R,t) = C_s$ (where $C(R,t)$ is the concentration at the surface of the bubble, radius R and C_s the dissolved gas concentration for a saturated solution at constant temperature and pressure) the concentration gradient at the bubble surface is of the form:

$$\left(\frac{\partial C}{\partial r}\right)_{r = R} = (C_\infty - C_s)\left(\frac{1}{R} + \frac{e^{-Kt}}{\sqrt{\pi D t}} + \sqrt{\frac{K}{D}}\ \operatorname{erf}\sqrt{Kt}\right)$$

where erf $\sqrt{Kt}$ is the error function $\frac{2}{\sqrt{\pi}} \int_o^{\sqrt{Kt}} e^{-t^2}\, dt$. Knowing the concentration gradient it is possible to determine the rate of mass flow into the liquid, which in turn enables the rate of change of

bubble radius to be determined. Thus, the rate of mass flow into the liquid may be expressed as:

$$\frac{dm}{dt} = 4\pi R^2 \mathcal{D} \left(\frac{\partial C}{\partial r}\right) \quad r = R.$$

But the rate of mass flow into the liquid may also be expressed in terms of the gas density, ρ_g, and the rate of change of bubble radius, $\frac{dR}{dt}$

i.e. $$\frac{dm}{dt} = 4\pi R^2 \rho_g \frac{dR}{dt}$$

By equating the two expressions for rate of mass flow the bubble radius equation is derived:

i.e. $$\frac{dR}{dt} = \frac{\mathcal{D}}{\rho_g} \left(\frac{\partial C}{\partial r}\right) \quad r = R$$

$$= \frac{\mathcal{D}}{\rho_g} (C_\infty - C_s) \left(\frac{1}{R} + \frac{e^{-Kt}}{\sqrt{\pi \mathcal{D} t}} + \sqrt{\frac{K}{\mathcal{D}}} \operatorname{erf}\sqrt{Kt}\right)$$

In dimensionless form:

$$\frac{dR^*}{dt^*} = -C_\rho^* (1 - C_\infty^*) \left(\frac{1}{R^*} + \frac{e^{-K^*t^*}}{\sqrt{\pi t^*}} + \sqrt{K^*} \operatorname{erf}\sqrt{K^*t^*}\right)$$

where $R^* = \frac{R}{R_o}$; $C_\rho^* = \frac{C_s}{\rho_g}$; $C_\infty^* = \frac{C_\infty}{C_s}$; $t^* = \frac{\mathcal{D}t}{R_o^2}$; $K^* = \frac{KR_o^2}{\mathcal{D}}$

Integration of this expression provides the bubble radius-time relationship:

$$1 - (R^*)^2 = 2C_\rho^* (1 - C_\infty^*) \left((t^* + \int_o^{t^*} \frac{R^* e^{-K^*t^*}}{\sqrt{\pi t^*}} \, dt^* + \sqrt{K^*} \int_o^{t^*} R^* \operatorname{erf}\sqrt{K^*t^*} \, dt^*\right)$$

Using this expression Yang (1971) derived the bubble radius-time relationships for oxygen bubbles in plasma and whole blood corresponding to two distinct cases: $K^* = 0$ and $C_\infty^* = 0$ for plasma and $C_\rho^* = 0.025$

and $C_\infty^* = 0$ for whole blood. These two relationships are reproduced in Figs.1.1 & 1.2

By making appropriate assumptions concerning the magnitude of the terms within the above expression for rate of change of bubble radius the integration and subsequent solution for the bubble radius-time relationship can be considerably simplified. For large values of K^* and $t > 1$ second the $\frac{e^{-K^*t^*}}{\sqrt{\pi t^*}}$ term becomes negligible and the error function approximates to unity. Under these conditions the above equation may be simplified to the following form:

$$\frac{dR^*}{dt^*} = - C_\rho^* \ (1 - C_\infty^*) \left(\frac{1}{R^*} + \sqrt{K^*}\right)$$

$$\int \frac{R^* dR^*}{K^* R^* + 1} = -\int C_\rho^* \ (1 - C_\infty^*) dt^*$$

$$\int \left(\frac{1}{\sqrt{K^*}} - \frac{1}{\sqrt{K^* \ (\sqrt{K^*} R^* + 1)}}\right) dR^* = -\int C_\rho^* (1 - C_\infty^*) dt^*$$

$$\frac{R^*}{\sqrt{K^*}} - \frac{1}{K^*} \log_e \ (K^* R^* + \sqrt{K^*}) = - C_\rho^* \ (1 - C_\infty^*) t^* + A$$

where A is the constant of integration.

For $t^* = 0$; $R^* = 1$; $A = \frac{1}{\sqrt{K^*}} - \frac{1}{K^*} \log_e \ (K^* + \sqrt{K^*})$

$$t^* = - \frac{R^*}{\sqrt{K^* C_\rho^* \ (1 - C_\infty^*)}} + \frac{1}{K^*} \frac{\log_e \ (K^* R^* + \sqrt{K^*})}{C_\rho^* \ (1 - C_\infty^*)}$$

$$+ \frac{1}{\sqrt{K^* C_\rho^* \ (1 - C_\infty^*)}} - \frac{1}{K^*} \frac{\log_e \ (K^* + \sqrt{K^*})}{C_\rho^* \ (1 - C_\infty^*)}$$

Using this expression the bubble lifetimes for bubbles in whole blood may be estimated with reasonable accuracy. Thus the bubble lifetime t_L^* $(R^* = 0)$ is:

$$t_L^* = \frac{1}{K^*} \frac{\log_e \ (\sqrt{K^*})}{C_\rho^* \ (1 - C_\infty^*)} + \frac{1}{\sqrt{K^* C_\rho^* \ (1 - C_\infty^*)}} - \frac{1}{K^*} \frac{\log_e \ (K^* + \sqrt{K^*})}{C_\rho^* \ (1 - C_\infty^*)}$$

Values of t_L^* over the range of K^*, 0.1 - 1000 compare well with the values derived from the radius-time curves due to Yang (1971).

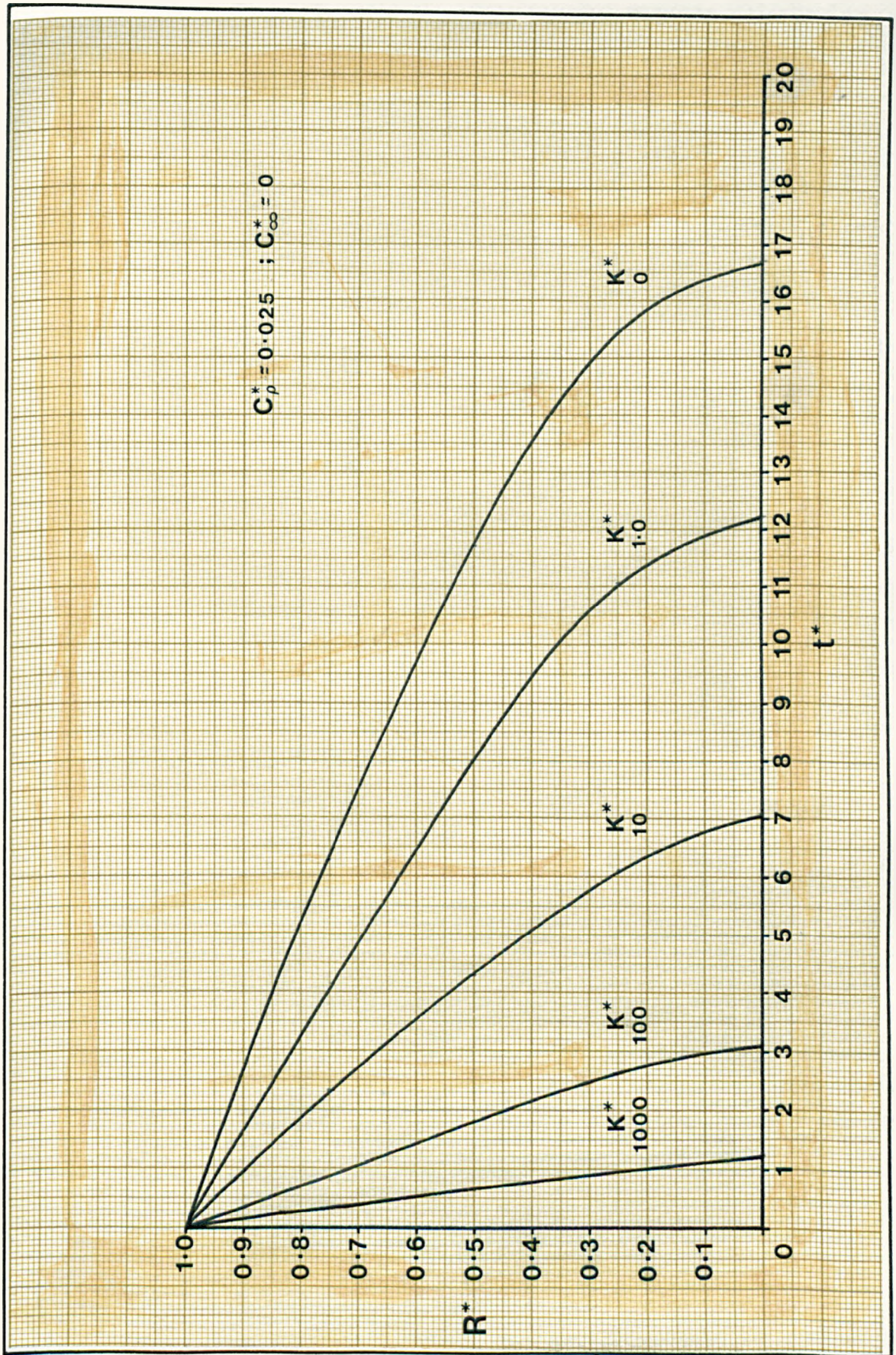

Radius time relationship for bubbles of oxygen dissolving in whole blood.
for $C_\rho^* = 0.025$ & $C_\infty^* = 0$
After Yang, 1971

Figure 1.1.

Referred to on pp 23, 27.

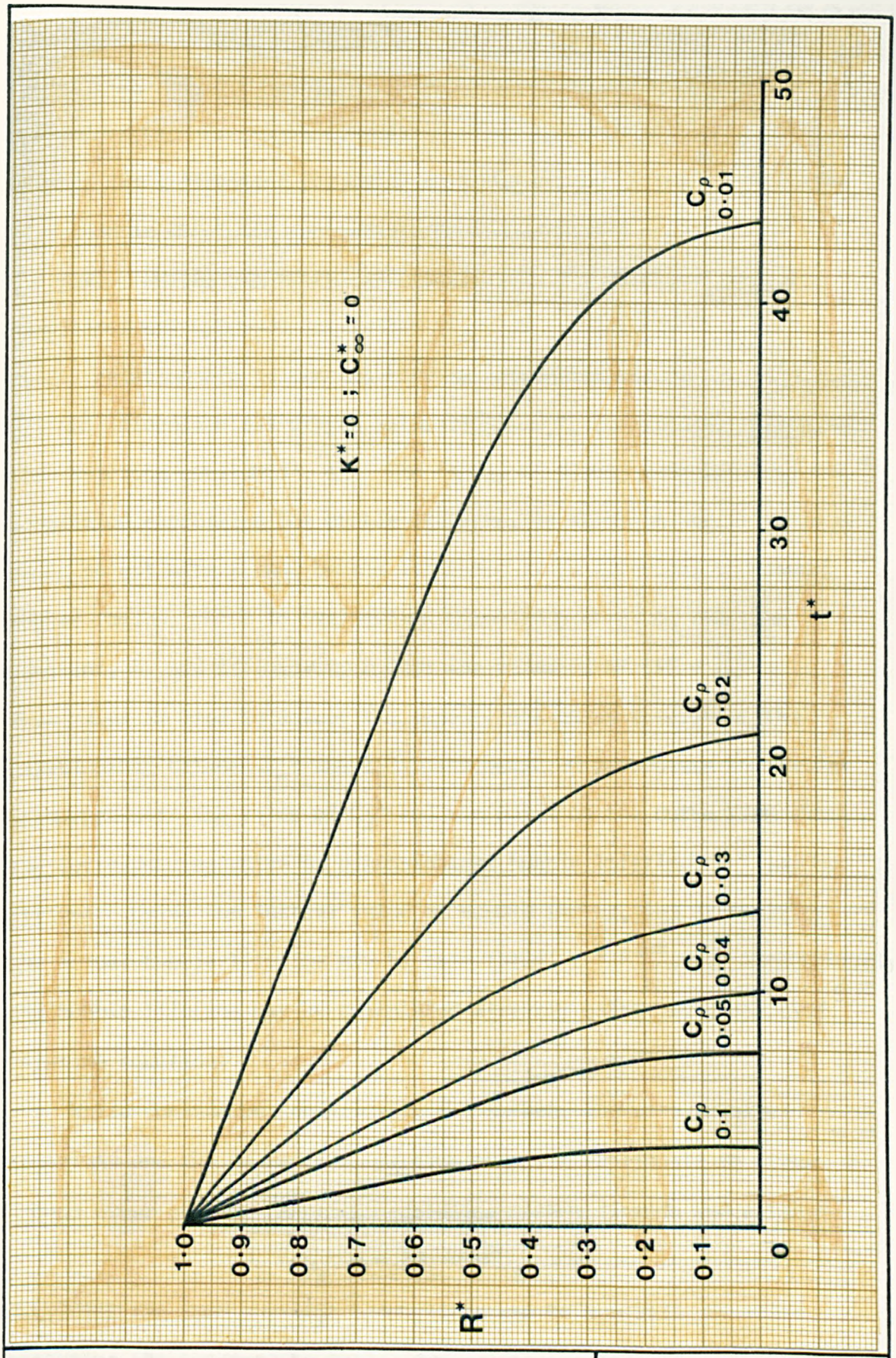

Radius time relationship for oxygen bubbles dissolving in plasma for $K^* = 0$; $C_\infty^* = 0$

After Yang, 1971

Figure 1.2

Referred to on p 23

The dimensionless radius-time relationship for oxygen bubbles in whole blood (Fig.1.1) provides a useful presentation of the dissolution characteristics of oxygen bubbles in whole blood (Yang, 1971). However the information presented in these curves relates only to the condition in which the concentration of dissolved oxygen is zero ($C_\infty = 0$). During extracorporeal circulation the dissolved oxygen conditions may approach saturation ($C_\infty = 1$). Consequently a more useful relationship is the one between 'dimensionless bubble lifetime', t_L^* and 'dimensionless oxygen saturation', C_∞^*, for various 'dimensionless reaction constants', K*. The family of curves computed from the simplified expression for bubble lifetime, is shown in Fig.1.3. In order to estimate actual bubble lifetime, it is necessary to measure bubble radius, which in conjunction with the prevailing reaction constant, K, and diffusivity D sets the value of K* $\left(K^* = \frac{KRo^2}{\mathcal{D}}\right)$. This value is used to select the appropriate curve describing the relationship between C_∞^* and t_L^*. The measured percentage saturation of oxygen sets the value of C_∞^* and the point on the curve from which the corresponding value of dimensionless bubble lifetime, t_L^* may be derived. Using the initial value of bubble radius, and diffusivity the actual bubble lifetime may be calculated $t_L^* = \frac{\mathcal{D}t}{Ro^2}$. Alternatively the bubble lifetime may be calculated directly using the simplified lifetime equation.

While considered specifically for oxygen, the mass transfer equations and the curves derived from them are applicable to other second order gaseous reactions including carbon dioxide and water;

$$CO_2 + H_2O \rightleftharpoons H_2CO_3 \rightleftharpoons HCO_3^- + H^+$$

providing the same physical assumptions can be applied. By substituting the appropriate values for reaction velocity constant, diffusivity, density and saturation the dimensionless parameters may be defined and bubble lifetimes calculated. The presentation of

data in dimensionless form enables the effects of physical conditions, such as temperature and pressure, to be accommodated without explicit inclusion in the lifetime characteristics.

For the situation in which a gas bubble is dissolving in plasma or whole blood without any chemical union being involved ($K^* = 0$) the expression for the rate of change of bubble radius with respect to time may be reduced to the following form. Assuming that sufficient time has elapsed for significant diffusion to have taken place, the exponential term within the mass transfer equation may be neglected thus;

$$\frac{dR^*}{dt^*} = - \frac{C_\rho^* (1 - C_\infty^*)}{R^*}$$

$$R^* dR^* = - C_\rho^* (1 - C_\infty^*) dt^*$$

$$\int R^* dR^* = - C_\rho^* (1 - C_\infty^*) \int dt^*$$

$$\frac{(R^*)^2}{2} = - C_\rho^* (1 - C_\infty^*) t^* + B$$

Where B is the constant of integration

For $t^* = 0$, $B = \frac{(R^*)_o^2}{2} = \frac{1}{2}$

$$\frac{(R^*)^2}{2} - \frac{1}{2} = - C_\rho^* (1 - C_\infty^*) t^*$$

$$t^* = \frac{1 - (R^*)^2}{2C_\rho^* (1 - C_\infty^*)}$$

Bubble lifetime $t_L^* = \frac{1}{2C_\rho^* (1 - C_\infty^*)}$, $(R^* = 0)$

The bubble lifetime curve, relating dimensionless lifetime to dimensionless saturation levels, was derived using this expression and is presented in Fig.1.3.

Epstein & Plesset (1950) obtained the solution to the complete mass transfer equation for the non-reactive dissolution of bubbles in water. This they did by noting that the equation is homogeneous and may be conveniently expressed in parametric form. The following

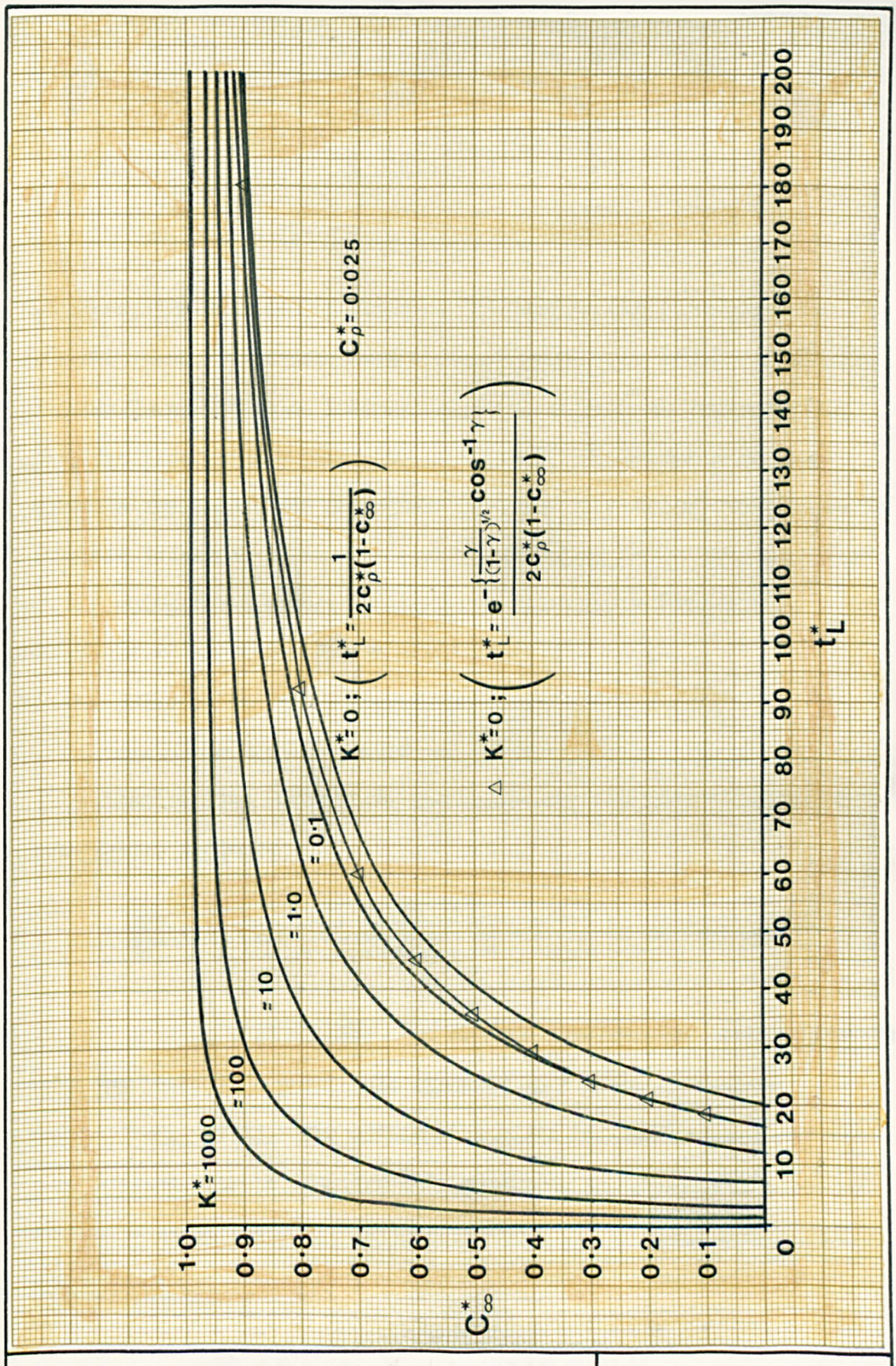

Saturation level-time relationship for oxygen bubbles in whole blood.

Figure 1.3

Referred to on pp 28, 30

expression was derived and may be applied to the dissolution of bubbles in plasma.

$$x = \exp\left\{ - \frac{\gamma}{(1 - \gamma^2)^{\frac{1}{2}}} \cos^{-1}\gamma \right\}$$

$$\text{Where } x^2 = 2t^* \, C_\rho^* \, (1 - C_\infty^*) \;\&\; \gamma = \left\{ \frac{C_\rho^* \, (1 - C_\infty^*)}{2\pi} \right\}^{\frac{1}{2}}$$

This expression has been confirmed and a plot of dimensionless lifetime with respect to dimensionless saturation levels derived (Fig.1.3). For comparison, the curve derived using the simplified expression for bubble lifetime is also presented in Fig.1.3. On the basis of this comparison the simplified expression provides a reasonable approximation for bubble lifetime, particularly for high values of C_∞^* and low values of C_ρ^*. Using these curves estimates of dissolution time may be derived for nitrogen bubbles in whole blood and plasma.

The analysis so far considered has neglected the effect of surface tension on both diffusion and bubble dynamics. By taking surface tension into account the expression for the rate of change of bubble radius becomes;

$$\frac{dR^*}{dt^*} = - \frac{C_\rho^* \, (\alpha^{1/n} - \rho^* C_\infty^*)}{\alpha^{1/n} \, (1 - \sigma^*/3R^* n\alpha)} \left\{ \frac{1}{R} + \frac{e^{-K^* t^*}}{\sqrt{\pi t^*}} + \sqrt{K^*} \, \text{erf} \sqrt{K^* t^*} \right\}$$

Where $\alpha = \rho^* + \frac{\sigma^*}{R^*}$; $\sigma^* = \frac{2\sigma}{RoPgo}$ (σ; surface tension; Pgo initial pressure within the bubble); n polytropic exponent (n = 1 for isothermal process) (Yang, 1971). The effect of surface tension on diffusion and bubble collapse may be examined by considering an approximation of the above expression. Thus for large times the $\frac{e^{-K^* t^*}}{\sqrt{\pi t^*}}$ becomes very small, the error function is close to unity and

$$\frac{dR^*}{dt^*} = - C_\rho^* \, \frac{1 - C_\infty^* + (\sigma^*/R^*)}{1 + 2/3(\sigma^*/R^*)} \left\{ \frac{1}{R^*} + \sqrt{K^*} \right\}$$

(Yang, 1971)

$$1-(R^*)^2 + \frac{2\sigma^*(1+2C_\infty^*)(1-R^*)}{3(1-C_\infty^*)} - \frac{2\sigma^*(1+2C_\infty^*)}{3(1-C_\infty^*)^2} \log_e \frac{\sigma^*+(1-C_\infty^*)}{\sigma^*+(1-C_\infty^*)R^*}$$

$$= 2\,C_\rho^*(1 - C_\infty^*)t^* \qquad \text{(Yang, 1971)}$$

Bubble lifetime t^*_L $(R^* = 0)$

$$t^*_L = \frac{1}{2C_\rho^*(1-C_\infty^*)} + \frac{2\sigma^*(1+2C_\infty^*)}{6C_\rho^*(1-C_\infty^*)^2} - \frac{2\sigma^*(1+2C_\infty^*)}{6C_\rho^*(1-C_\infty^*)^3} \log_e \frac{\sigma^*(1-C_\infty^*)}{\sigma^*}$$

Neglecting surface tension $\sigma^* = 0$

$$t^*_L = \frac{1}{2C_\rho^*(1 - C_\infty^*)}$$

The effect of surface tension is to shorten the time required for complete solution. In a saturated solution, $C_\infty^* = 1$, a bubble of any radius would appear to be stable against diffusion, unless the effect of surface tension is considered. In practise a bubble will tend to dissolve in a saturated solution due to the effect of surface tension. Solving the equation for rate of change of bubble size with respect to time for $C_\infty^* = 1$ and neglecting the $\sqrt{K}$ term yields the expression;

$$1 - (R^*)^3 + \sigma^*\left\{1 - (R^*)^2\right\} = 3\sigma^*C_\rho^*t^*$$

Thus the bubble lifetime in a saturated solution $(R^* = 0)$

$$t^*_L = \frac{1 + \sigma^*}{3\sigma^*C_\rho^*}$$

Since $\sigma^* = \frac{2\sigma}{RoPgo}$ it is clear that σ^* is greater the smaller the initial bubble size. The significance of this is that the surface tension effect becomes more important the smaller the bubble size, indicating that, as a bubble dissolves, the rate of dissolution increases as the surface tension effect becomes more prominent. The divergence in the values of bubble lifetime estimated with and without consideration of

surface tension also increases with saturation (C_∞*). Consequently the greatest error in the estimation of bubble lifetime, derived without considering surface tension occurs for conditions of complete or near saturation and small initial bubble size (Epstein & Plesset, 1950). The choice of equation for estimating bubble lifetime is thus determined by the measured population of bubbles and the degree of saturation.

A number of factors limit the application of lifetime estimates in a practical situation. Real time computation of bubble lifetimes for individually detected bubbles is limited by the time available between detected events, the capabilities of the computer and the availability of the appropriate parameter values. Currently available microprocessors rarely exhibit execution cycles of less than 2 μs. Even if the computation could be achieved in this time the spatial discrimination offered by a 2 μs processing time would be no better than 2.9 mm between bubbles, assuming the use of an ultrasonic detection technique and an ultrasonic propagation velocity in blood of 1450 ms^{-1}. However for a detection technique using discrimination levels that relate to ranges of bubble size, lifetime limits may be estimated for the prevailing conditions and the ranges specified.

The availability of parameter values presents a particular problem during extracorporeal circulation. To derive the K* value, for example, it is necessary to obtain values of the reaction constant, K, and mass diffusivity $\mathcal{D}$, appropriate for the prevailing conditions. Unfortunately, only limited data is available from measurements of reaction velocity constants for the association of oxygen and reduced haemoglobin, and for the reactions of carbon dioxide. Furthermore the values obtained experimentally vary considerably depending upon the method used to derive them (Tanasawa, et al, 1971). Tanasawa et al., (1971) observed that the reaction constants (K), derived by

solving the mass transfer equation for the diffusion of gas from a bubble into a liquid, compare favourably with the values derived by rapid reaction techniques, but are somewhat larger than the values derived using half-time reaction rate measurements. However the values determined by Tanasawa et al., (1971) relate to the reaction constant, K, which is the product of the reaction velocity constant k (for the association of reduced haemoglobin and oxygen) and the concentration of reduced haemoglobin. The assumption implicit in the definition of K is that the concentration of reduced haemoglobin within the region of the reaction is constant. Under conditions in which the concentration of reduced haemoglobin is small in comparison to the concentration of oxyhaemoglobin, and for conditions in which the microbubble population is large and the bubbles in close proximity to one another, this assumption may not be valid. For it to be a reasonable assumption, it is necessary to ensure a continuous, efficient supply of reduced haemoglobin to the reaction site together with an efficient, continuous removal of the reaction product, oxyhaemoglobin. Flow conditions and the natural shrinkage of the bubble surfaces as they dissolve favour the assumption providing sufficient reduced haemoglobin is available. Unfortunately Tanasawa et al., (1971) provide no reference to the haemoglobin concentration within the whole blood used to perform the experiments from which the K values were derived. Consequently the comparison of values with those derived from other sources must be considered with caution.

In addition to deriving values for specific conditions, difficulties also arise in attempting to accommodate changes due to variations in such parameters as temperature, pressure, density, pH, solubility, surface tension and haemoglobin concentration. Such considerations also apply to the derivation of mass diffusivity, and the estimation of the dimensionless quantities, including C_ρ^*, C_∞^* and σ^*.

Probably the greatest limitation to deriving estimates of bubble lifetime is the uncertainty concerning the contents of a bubble and the inability to discriminate bubbles of one gas from bubbles of another. Only in controlled perfusion experiments, in which a known population of bubbles is introduced into an experimental system can one be reasonably sure of the gas bubble contents and then only as they enter the system. In view of the uncertainty concerning the contents of gas bubbles and the gaseous exchange that can conceivably arise between dissolved blood gases and the gas within the bubbles, attempts at predicting the persistence of individual bubbles may be completely frustrated. However the consideration of dissolution characteristics may provide a useful insight into the conditions necessary for avoiding persistent microbubbles should such bubbles enter the systemic circulation as a result of extracorporeal circulation. It is evident from the $C_\infty^* - t^*_L$ relationship, for example, that as the concentration of dissolved gas increases so the bubble lifetime also increases. Moreover it is also evident that a small reduction in the degree of saturation, at high levels, can considerably reduce bubble lifetime. Consider for example the lifetime estimates for a bubble of oxygen of 100 μm diameter introduced into whole blood at a temperature of 19.5°C, the saturation level being 90% ($C_\infty^* = 0.9$). The density, gas concentration at saturation, diffusivity and reaction constant at this temperature are 1.38×10^{-3} g.cm^{-3}; 7.35×10^{-5} g.cm^{-3}; 7.47×10^{-6} cm.^{2}s^{-1}, and 24.2 s^{-1} respectively (Tanasawa et al., 1971). For $C_\infty^* = 0.9$, and Ro = 50×10^{-4} cm, $K^* = 81$, $C_\rho^* = 0.053$, and $t^*_L = 15.6$. The estimated lifetime of the bubble under these conditions is therefore approximately 52 s. (neglecting surface tension). Reducing the saturation level to 70% ($C_\infty^* = 0.7$) reduces the lifetime for the same size bubble to approximately 17 s, a reduction of 67%. For nitrogen bubbles under the same conditions of temperature and

saturation ($K^* = 0$, $C_\rho^* = 0.036$) the estimated bubble lifetimes are 276s ($C_\infty^* = 0.9$) and 41s ($C_\infty^* = 0.7$) respectively. Thus for nitrogen the reduction is better than 85%. The lifetime values of these bubbles may be critical since the occlusion of blood vessels for longer than 5 to 6 minutes has been observed to result in permanent damage to most neurones in the cerebral cortex at normal body temperatures (Greenfield & Meyer, 1963). However the minimum occlusion time to cause permanent damage is increased for lower temperatures (Greenfield & Meyer, 1963).

System pressure effect on bubble lifetime

The force balance on the surface of a bubble has been considered earlier. The system pressure and surface tension pressure components both influence in the same manner the rate at which a bubble will grow or collapse. Increasing either of these parameters increases the rate of bubble collapse. The mechanism for this effect may be considered as follows. An increase in system pressure results in a decrease in bubble volume, together with an increase in the surface tension pressure term. The resultant effect of the decrease in volume is an effective increase in density, ρ_g, and an increase in the saturation concentration, C_s, at the surface of the bubble. Although both C_s and ρ_g vary as a function of the instantaneous bubble size, their ratio, C_ρ^* is unaffected. Since the saturation concentration, C_s, is increased as a result of the pressure increase, the concentration gradient that determines the rate of mass transfer of gas from the bubble is also increased and the bubble therefore collapses more rapidly.

When a bubble contains a mixture of gases, the saturation concentration, C_s, at the surface of the bubble is determined by the sum of the partial pressures of the gases in the bubble and the

solubility of those gases in the liquid surrounding the bubble. The concentration gradient influencing the mass transfer of the gases being considered is determined by the saturation concentration, C_s and the concentration of gas in solution at some distance from the bubble, C_∞. The latter is a function of solubility and the tension of gas in solution.

Whilst the foregoing description relates to the net effect of a system pressure variation it neglects the consequences of the rate of change of system pressure. A bubble subjected to a step increase or decrease in pressure will oscillate about a mean radius, the oscillations decaying in time to zero in a non-inviscid fluid with the final bubble radius corresponding with the final system pressure (Chan & Yang, 1969). Providing the frequency of the system pressure variation is small relative to the natural frequency of the bubble, the expression

$$\frac{2\sigma}{R} = P_g - P(\infty)$$

may be used to determine instantaneous mean bubble radius (Chan & Yang, 1969). P_g is the instantaneous gas pressure, σ the surface tension, and $P(\infty)$ the instantaneous system pressure.

$$P_g = P_{go}\left(\frac{\rho_g}{\rho_{go}}\right)^n$$

Where P_{go} is the initial pressure within the bubble, ρ_g is the instantaneous gas density, ρ_{go} is the initial gas density and n is the polytropic exponent (n = 1 for an isothermal change).

For a step change in pressure the instantaneous system pressure $P(\infty)$ is the sum of the atmospheric pressure, the instantaneous amplitude of the blood pressure pulse, and the step change in external pressure. The bubble size determined using the radius expression including this term yields the bubble radius corresponding to the final system pressure. Chan & Yang (1969) having investigated the

effect of blood pressure pulsation on the dynamic behaviour of bubbles, concluded that for normal conditions of pulse rate and blood pressure pulse amplitude, the effects are negligible. The consideration of system pressure variations during extracorporeal circulation may therefore be confined to the variations encountered in perfusion pressure and their effect upon bubble size and saturation concentration in determining bubble lifetime.

Discussion

It is clear from the literature that microbubbles may enter the systemic circulation from both the extracorporeal circuit and from sites of surgical intervention during and following cardiopulmonary bypass. Bubbles may also arise throughout the systemic and extracorporeal circuit by mechanisms of counter diffusion and exchange rate supersaturation. No reports have yet been presented that fully quantify the population of bubbles entering the circulation from these various sources.

The suggestion, implicit in many of the investigations reported since 1960 (Patterson & Kessler, 1969; Spencer et al., 1969; Lawrence, Mckay & Sherensky, 1971; Lichti, Simmons & Almond, 1972; Gallagher & Pearson, 1973) that there is merit in recognising an increase in bubble numbers alone may be misleading. The assumption apparent in these investigations is that an increase in number is an increase in hazard. However the possibility must be considered that a small population of large bubbles may be more hazardous than a larger population of smaller bubbles. Therefore, it is important to measure bubble size as well as bubble numbers, especially since microbubbles have a propensity to fission or fusion upon collision with other bubbles (Hills, 1974).

Ideally it is necessary to measure;

1. The total number of bubbles in a given population.
2. The size of each bubble within the population.

and 3. The rate at which the bubbles are entering the circulation.

Any microbubble detection technique that does not satisfy these criteria must be considered unsatisfactory.

Complementary to the measurement of bubble population is the consideration of bubbles as dynamic entities. Because the physical and chemical properties of blood influence the rate at which bubbles dissolve it is necessary to take these into consideration when investigating the effects that bubbles may produce when introduced into the systemic circulation. Unfortunately the equations describing the dynamic relationship between bubble size and time, as illustrated for oxygen, are too complex for application in practical monitoring situations. Approximations of the form derived for oxygen in whole blood may be more readily applied, although the significance of deriving lifetime estimates for a measured population may be complicated due to limitations imposed by unpredictable influences. For situations in which the bubble content is a mixture of gases, such as air or nitrous oxide and oxygen, derivation of accurate bubble lifetimes may be indeterminate due to the uncertainty concerning the bubble content and the nature of the gaseous exchange. Consequently estimates of bubble lifetime can be used only as a guide to the subsequent period of existence of the bubbles once introduced into the circulation. The value of bubble lifetime estimates is further limited by the unpredictability of bubble collisions and their ability to coalesce or break up into smaller bubbles depending upon the energy constraints imposed by the collision.

Because of the dynamic nature of bubbles, greater accuracy should be obtained during controlled perfusion of a measured population of microbubbles into a selected vascular bed of an experimental animal than during cardiopulmonary bypass. During controlled microembolisation experiments the size, number and rate at which microbubbles are introduced into the vasculature may be regulated, the probability of collision may be reduced and the conditions that influence bubble

stability and lifetime may be more readily controlled.

Once it is clear to what extent microbubbles can be responsible for reversible and non-reversible tissue damage, the significance of extracorporeal and surgically induced bubble sources may be more readily appreciated. However this can only be achieved by performing quantitative analyses of these various bubble sources. This still remains to be done.

Chapter 2

TECHNIQUES FOR DETECTING MICROBUBBLES IN WHOLE BLOOD

Since it was first suggested that undissolved gas in the form of microbubbles may be responsible for cerebral damage following cardiopulmonary bypass, the development of a quantitative research technique for microbubble detection in whole blood has been a fundamental requirement for any study of the effects of microbubbles entering the systemic circulation. A number of techniques have been reported, but none have totally satisfied the need for a quantitative measurement of bubble population. In essence all the techniques reported have sought to detect or measure the perturbation phenomena produced by a bubble or population of bubbles when subjected to an incident source of energy. The limitations that have precluded the use of these various techniques as methods of deriving quantitative estimates of bubble populations have, in general, been the lack of actual measurement or the erroneous measurement of perturbation phenomena. In some cases little understanding or regard for the scientific basis for the technique has been evident and, in others, little regard for the manner in which the technique has been applied. Visible light (Jordan et al., 1958; Landew et al., 1960; Selman, McAlpine & Ratan, 1967; Emerson, Hempleman & Leatle, 1967), electrical energy (Spencer et al., 1969; Grulke, Marsh & Hills, 1973) and acoustic energy (Austen & Howry, 1965; Patterson & Kessler, 1969; Spencer et al., 1969; Lawrence, McKay & Sherensky, 1971; Lichti, Simmons & Almond, 1972; Gallagher & Pearson, 1973; Lubbers et al., 1974; Clarke, Dietz & Miller, 1975) have been variously used as the incident source of energy for extracorporeal microbubble detection techniques. The earlier

studies of the effects of intra-vascular microbubbles (Landew et al., 1960) and the significance of various extracorporeal circuit components as sources or sinks for microbubbles (Jordan, Tolstedt & Beretta, 1958; Donald & Fellows, 1961; Selman, McAlpine & Ratan, 1967) were based on the visual observation of bubble populations. Observation was achieved in these studies by the use of a shallow, flat surfaced observation chamber connected in parallel with the arterial line. Only a minor portion of the flow was directed through this chamber and by restraining this flow at periodic intervals, bubbles contained within sectioned and dimensioned regions of the chamber could be sized and/or counted. A low powered microscope was generally used to help facilitate these measurements. Based upon the sample measurements of both size and number considered for a known sample volume, together with a knowledge of the volume flow rate through the system, an estimate of total undissolved gas was considered possible (Landew et al., 1960). Tests involving the collection and volume measurement of undissolved gas using bubble traps have been used on one occasion to determine the effectiveness of the visual observation technique (Landew, et al., 1960). These tests revealed that the technique provided results that were consistently low by 30-50%. Little attempt appears to have been made by Selman, McAlpine & Ratan (1967) or by Jordan, Tolstedt & Beretta (1958) to quantify their results. While Selman, McAlpine & Ratan (1967) report that bubbles were both detected and counted, no actual bubble counts or sizing was reported. Similarly Jordan, Tolstedt & Beretta (1958) appear to have avoided any attempt at bubble sizing.

The limitations of the visual observation technique relate primarily to the relative opacity of the blood and the restriction of having to take measurements on a sample basis. Because the transmission of visible light through blood is so poor the observation

of bubbles in blood can be achieved only by using a shallow observation chamber. The sample volume may, in consequence, be quite small. Moreover, accurate sizing and counting may still be compromised by the poor transmission characteristic of blood to visible light. The combination of relatively small chamber volume and possibility of infrequent sampling will conceivably yield results that are unrepresentative of the total blood volume. Although the visual observation technique is subject to a number of limitations as a quantitative method of estimating bubble populations it has not been greatly surpassed by any in-line technique subsequently devised using instrumentational aids. However, the use of an electrical field has provided the basis for a successful method of counting and sizing particulate matter such as blood cells (Matten, Brackett & Olson, 1957) and has been applied to the problem of quantitative microbubble detection in an experimental situation (Grulke, Marsh & Hills, 1973).

The technique requires a controlled flow of a suitably diluted sample through an aperture across which a constant current density is maintained. The presence of particulate matter or undissolved gas causes a variation in the resistance to current flow. These variations in resistance are accompanied by variations in voltage that can be measured and related to particle size. Using a commercially available instrument, Coulter counter (Model FN), Grulke et al., (1973) have demonstrated that this technique may be used to detect and measure microbubbles from 20 to 250 μm in diameter. Bubbles for this study were produced using fine hypodermic needles (0.001, 0.002 and 0.003 in. internal diameter) through which gases could be passed at different pressures. Combinations of needle size, gas pressure, liquid surfactant content and liquid flow rate were used to derive different bubble sizes. The results determined for the Coulter counter correlated

well with terminal rise velocity and volume flow rate techniques for sizing bubbles. On the basis of this study it would appear that the Coulter counter provides an effective method of estimating quantitatively microbubble populations. Unfortunately the technique is unsuitable for on-line continuous measurement. Conventionally, particle sizing using this instrument requires a blood sample to be taken, diluted and then drawn through the detector head aperture. The nature of the detector head and the size of the aperture (50, 75, 100, 200 and 400 μm) would preclude its use for in-line detection of microbubbles contained in blood. For the measurement of microbubbles in blood the sampling and dilution procedures would also appear to be inadequate. Because bubbles are dynamic entities, their size being dependent upon prevailing conditions such as temperature, pressure, viscosity, solubility, and dissolved gas content, both the sampling and dilution procedure could influence the size of the sampled population. Consequently the estimate of total bubble population may be grossly unrepresentative of the actual in-line population.

Following a report by Austen & Howry (1965) on the use of pulsed ultrasound for detecting microbubbles during cardio-pulmonary bypass a number of studies were subsequently reported in which ultrasound was used as the basis for bubble detection during bypass and coronary investigations (Patteson & Kessler, 1969; Spencer et al., 1969; Edmonds-Seal & Maroon, 1969; Maroon, Edmonds-Seal & Campbell, 1969; Lawrence, McKay & Sherensky, 1971; Edmonds-Seal, Prys-Roberts & Adams, 1971; Lichti, Simmons & Almond, 1972; Gallagher & Pearson, 1973; Lubbers et al., 1974; Tinker et al., 1975; Clarke, Dietz & Miller, 1975).

Ultrasonic techniques have also been widely used as the basis for bubble detection in decompression studies (Gillis, Peterson & Karagianes, 1968; Gillis, Karagianes & Peterson, 1968; Spencer et al.,

1969; Smith & Spencer, 1970; Evans, Barnard & Walder, 1972; Nishi, 1972; Rubissow & McKay, 1971; Nishi & Livingstone, 1973; Spencer & Clarke, 1972; Powell, 1972; Powell, 1974; Hills & Grulke, 1975; Spencer, 1976; Balldin & Borgstrorn, 1976). The availability of ultrasonic Doppler flowmeters has led to the relatively widespread use of these devices for bubble detection (Edmonds-Seal & Maroon, 1969; Gillis, Karagianes & Peterson, 1969; Spencer et al., 1969; Edmonds-Seal, Prys-Roberts & Adams, 1971; Lawrence, McKay & Sherensky, 1971; Lichti, Simmons & Almond, 1972; Spencer & Clarke, 1972; Gallagher & Pearson, 1973; Tinker, et al., 1975). Unfortunately these devices exhibit certain limitations as microbubble detectors which have been largely unrecognised by those who have used them for this purpose. However, in most cases, they have been used only on a qualitative basis to demonstrate the presence of undissolved gas. This has usually been achieved by providing an audible presentation of the characteristic signal changes produced by a bubble or group of bubbles on passing the transducer head. Chirps, whistles, clicks and squeaks have been used to describe the various signal changes. Classification in this manner is clearly unsuitable for any attempt at a quantitative estimate of bubble population. Fundamental considerations of the Doppler principle and the nature and application of the ultrasound source further preclude the use of Doppler flowmeters as microbubble detectors. Doppler instruments specifically designed for bubble detection may largely avoid these limitations (Spencer & Clarke, 1972). The basis for bubble detection using these Doppler instruments would appear to be the magnitude of the perturbation associated with a bubble, with little or no relevance being attached to the Doppler shift information specific to bubbles in motion. Because of this, non-Doppler, continuous wave techniques can also be employed for bubble detection (Manley, 1969;

Manley & Cole, 1974; Tucker & Welsby, 1968). Discrimination and coincidence errors inherent in the use of continuous wave technique, together with stability and artefactual problems limit their use for the quantitative purposes of bubble counting and bubble sizing. It has been demonstrated that some of these limitations can be overcome by the use of pulsed ultrasound (Patterson & Kessler, 1969; Kessler & Patterson, 1970; Patterson et al., 1972). Unfortunately inadequate consideration of the physical basis for the technique and the manner in which it is applied introduce other limitations which similarly depricate its use as a quantitative tool.

Of the techniques used for microbubble detection, those involving the application of ultrasound would appear to provide the greatest sensitivity to undissolved gas in the form of microbubbles. A more detailed analysis of these techniques is therefore presented.

ULTRASONIC NON-DOPPLER CONTINUOUS WAVE TECHNIQUES

Introduction

A sound wave in propagating through a medium experiences a reduction in intensity related to the distance travelled. A number of factors may contribute to the attenuation of beam intensity including beam divergence, wave mode conversion, scattering and absorption. Sound waves incident upon a gas bubble contained within a liquid medium produce a forced vibration of the gas inside the bubble resulting in the scatter and absorption of acoustic energy. The presence of bubbles can considerably influence the degree of attenuation produced by these mechanisms. For this reason the measurement of attenuation has been used as the basis for several bubble detection techniques (Manley, 1969; Manley & Cole, 1974; Clarke et al., 1975) and has also provided the basis for a commercially available instrument specifically designed and marketed as a microbubble detector (Technique Laboratories). The literature describing these techniques contains claims in all cases that they enable the measurement of both bubble sizes and bubble numbers. However, all non-doppler continuous wave techniques exhibit limitations that prejudice their use for quantitative estimation of bubble population in continuous flow situations. An inherent limitation is the inability to discriminate and so count individual scatter sources contained within the volume of insonification. Amplitude variations due to the changing number and distribution of scatter sources entering the volume of insonification as a result of continuous flow may be considered a basis for effecting a count. However it would be difficult to interpret the significance of such a count since a bubble or group of bubbles represents a source of perturbation for

as long as it remains within the volume of insonification. Consequently the variation in amplitude in a densely populated flow situation may be insufficient to provide a representative count. A single response corresponding to the coincidence of two or more scatter sources within the volume of insonification would further prejudice an attempt at obtaining an accurate count.

Particle counting using a Coulter counter is similarly prejudiced by coincidence errors. However the Coulter counter results may be corrected for coincidence errors by use of a calibration curve relating actual count to true count. The curve is derived from counts taken at successive dilutions until coincidence is considered to be highly improbable. A similar estimate of coincidence loss for ultrasonic bubble detection techniques cannot be derived by dilution.

Bubble detection by measurement of attenuation

In principle the measurement of attenuation requires the measurement and comparison of the transmitted and received acoustic energy derived using a pair of diametrically opposed piezoelectric crystals, one acting as a transmitter and the other as a receiver. The choice of operating characteristics and crystal parameters together with the placement of the crystals with respect to the blood volume determine the effectiveness of the system as a bubble detector. Manley (1969) used the attenuation measurement technique as the basis for an instrument developed for the Wessex Cardio-thoracic surgical unit and subsequently known as the Wessex gas bubble detector. The crystal arrangement for this instrument is illustrated in Fig.2.1). The transmitter crystal is driven by a power amplifier the output of which is determined by a very stable oscillator and tuned to the fundamental harmonic. However a low system Q factor allows the crystal to be driven at other harmonics. The receiver crystal is coupled to a wide

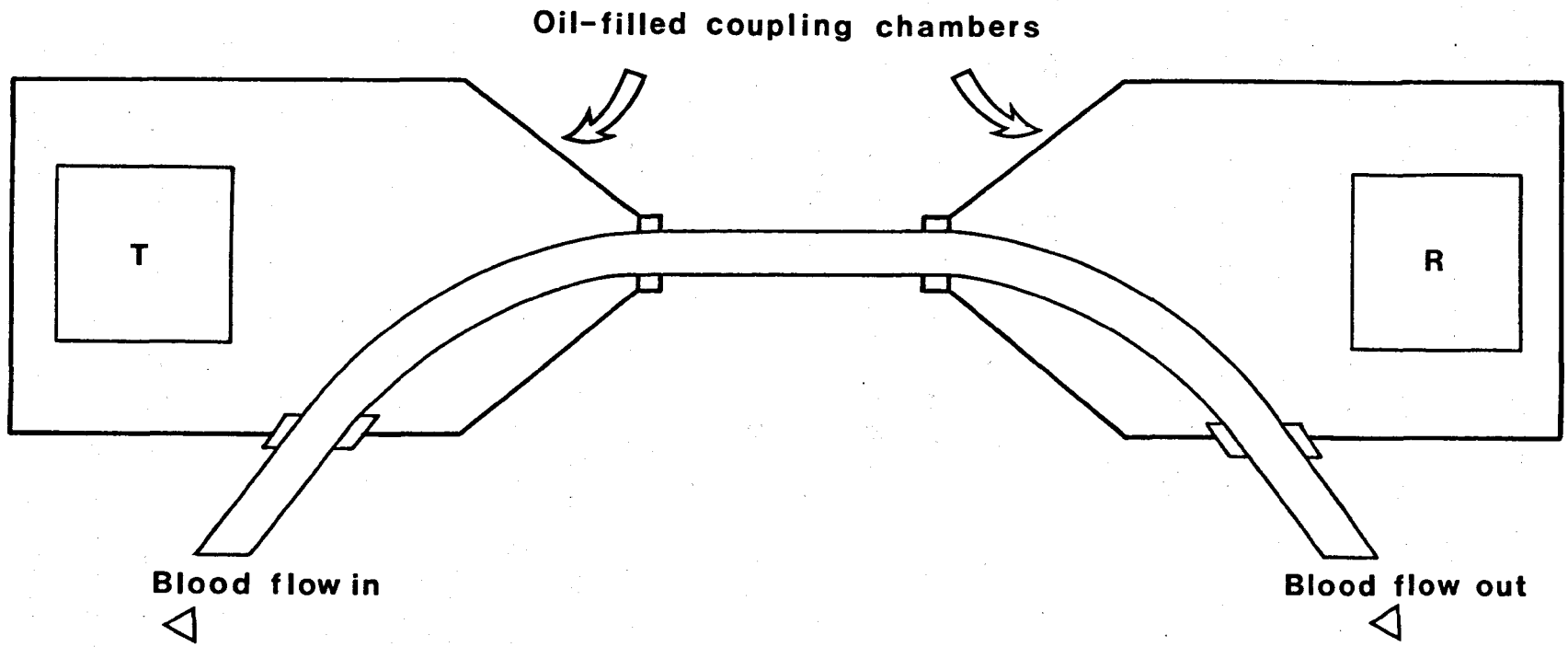

Wessex microbubble detector, transducer and mounting assembly

T: transmitter crystal R: receiver crystal

Figure 2.1

Referred to on p 48

band dc amplifier or a tuned amplifier and the output from this stage is coupled to an ac balancing circuit. In this section the received signal is mixed with the transmitter signal, after being phase shifted through 180^{o}, and the signal level adjusted to provide zero output for the condition in which bubbles are absent from the region of insonification. The attenuation produced by the presence of bubbles effectively modulates the transmitted carrierwave so leaving the amplitude variations corresponding to the bubble induced attenuations. In this form the bubble induced events are accessible for electronic detection and counting.

On the basis of a prototype study, using a fundamental operating frequency of 43 kHz and a harmonic of 130 kHz, Manley (1969) concluded that the instrument was capable of detecting bubbles and bubble clusters of the order of 100 μm in diameter. Although Manley (1969) has suggested that the amplitude variations are roughly proportional to bubble size, no rigorous evaluation of the sizing capabilities of this instrument is to be found in the published literature. However the choice of operating frequency would suggest a possible sizing limitation. The operating frequencies of 40 kHz and 120 kHz correspond to resonant bubble radii of 75 μm and 25 μm respectively. The signal amplitude/ bubble size relationships for bubble sizes below resonance differs from the relationship for bubbles above resonance. A distribution of bubble sizes above and below resonance would therefore preclude bubble sizing on the basis of signal amplitude alone. This has been confirmed in an independent evaluation of the Wessex detector by Winterton (personal communication). Winterton further revealed that each single bubble in water detected by the instrument produced a response characterised by between 17 and 24 peaks. This he attributed to the formation of a non-perfect standing wave within the region of insonification.

This was confirmed by reducing the flow through the detector and observing the bubble induced responses. The number of peaks remained unchanged, but the frequency of the peaks was found to have been reduced by the same factor that the flow rate had been reduced. Furthermore an analysis of the standing wave characteristic revealed that the number of antinodes spanning the region of insonification corresponded to the number of peaks observed in the bubble induced responses. The same affect was confirmed at both the fundamental (40 kHz) and harmonic driving frequencies (120 kHz). Bubble responses of this type would clearly prejudice attempts to achieve accurate bubble counts. In addition to these limitations the nature of the technique requires the electronics to be extremely stable in order to avoid artefacts due to oscillator variation and drift within the balancing circuit.

Subsequent development of the basic continuous wave technique has promoted the introduction of a range of instruments to cover a wide variety of applications (Manley & Cole, 1974) including an instrument specifically designed for cardiopulmonary bypass bubble detection studies. This instrument, manufactured and marketed by Technique laboratories, was evaluated as a tool for the quantitative estimation of bubble populations. The instrument was supplied with a clamp-on transmitter/receiver head designed for attachment to conventional extracorporeal tubing, so that the tubing is securely but gently sandwiched between a rectangular transmitter assembly and a rectangular receiver assembly. Both crystals are acoustically coupled to the tubing by means of a thin smear of acoustic coupling gel. The transmitter crystal is driven by an oscillator fed power amplifier operating at a frequency of 320 kHz. The receiver crystal is coupled to a tuned amplifier with automatic gain control operated

from a diode detector on the output of the final stage of the tuned amplifier. The detected signal from this stage is filtered, amplified and finally coupled to a comparator and counter configuration. A variable threshold facility on the comparator allows amplitude discrimination of the received signals. Monitoring of signal variations is facilitated by taking an output at the pre-comparator stage.

To evaluate the instrument a closed loop circuit consisting of a 2 m length of 9.5 mm internal diameter extracorporeal tubing attached to a 500 ml polycarbonate reservoir was assembled. The circuit was primed with 0.9% sodium chloride and flow within the circuit promoted using a De Bakey roller pump. A bipolar needle introduced into the line immediately adjacent to the detector head was used to generate bubbles electrolytically. Observations with this arrangement quickly revealed that the instrument was totally unacceptable for reliable sizing and counting of bubbles. Single bubbles passing the detector head consistently yielded multiple counts, ranging from 10 to 15 counts per bubble. The counter was also shown to be susceptible to extraneous electrical interference producing erratic and unpredictable additions to the recorded count. Switching on and off electrical equipment within the immediate vicinity was found to have a particularly marked effect in this respect. Sizing of bubbles based on the amplitude measurements of the pre-comparator signal source was found to be inconsistent and difficult to interpret because of the multiphasic character of the responses (Fig.2.2). Actual amplitude measurements were obtained using an oscilloscope (Tektronix 502A), but the responses illustrated in Fig.2.2 obtained using an ink jet recorder are representative of the responses observed on the oscilloscope. Below 2 $L.min^{-1}$ flow rate, bubbles of approximately 100 μm diameter were, on occasions, undetected and bubbles that were clearly different in size could not always be distinguished on the basis of the monitored response.

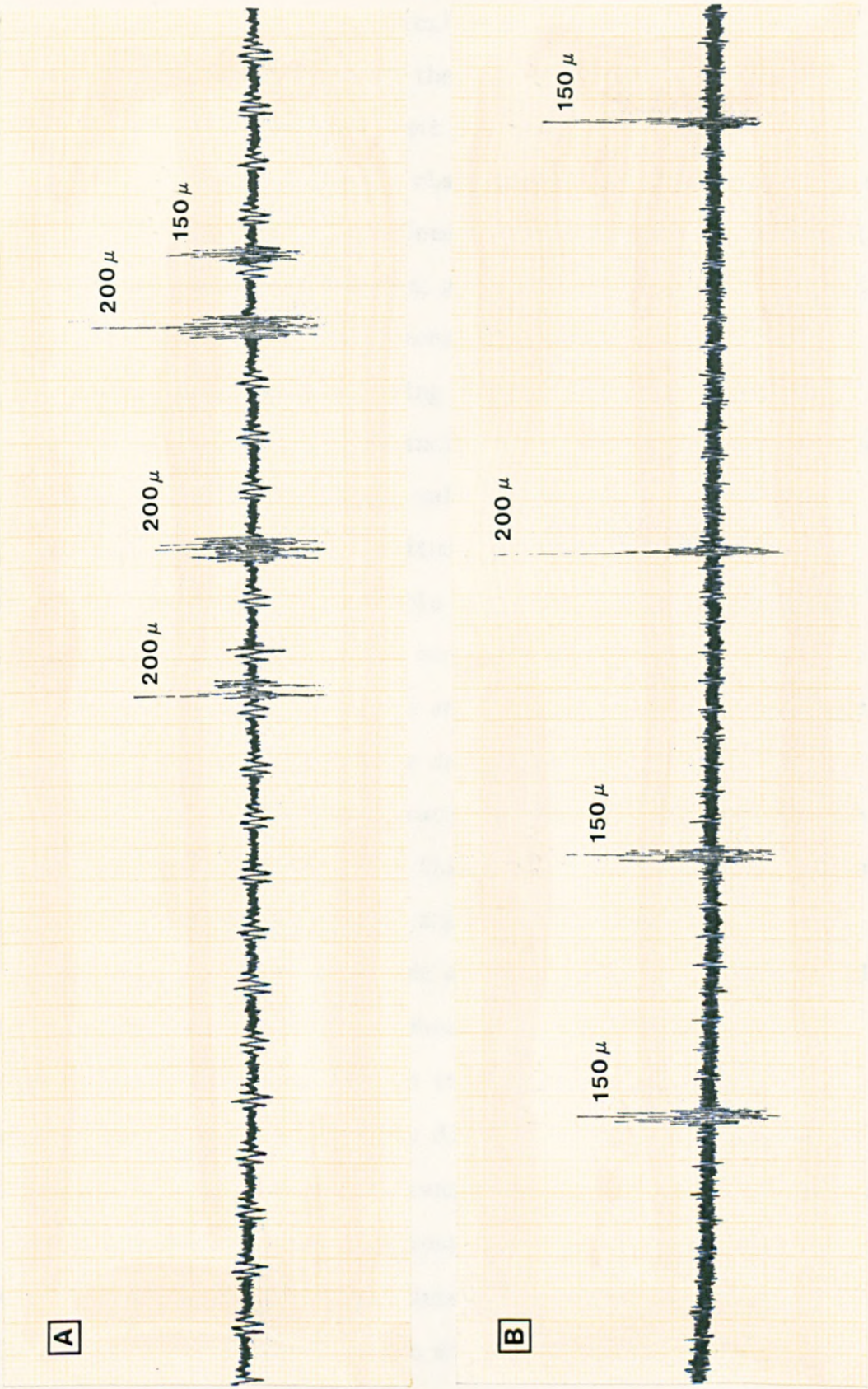

Technique laboratories microbubble detector: microbubble response recordings at 10 mms^{-1} from magnetic tape recordings at
A 7 $i.s.^{-1}$ and B 3.75 $i.s.^{-1}$

Figure 2.2

Referred to on pp 52, 54

Below 1 $L.min^{-1}$ bubbles up to approximately 500 μm in diameter were consistently undetected even with the instrument set at maximum sensitivity. On the assumption that the coupling of the detector head may have accounted for these observations the tests were repeated for several reattachments of the detector head to the circuit tubing, using differing amounts of coupling gel differing degrees of contact pressure. No appreciable improvements were noted.

A further limitation on sizing bubbles using the comparator facility was observed and is convincingly illustrated in Fig.2.2. The flow induced motion of the tubing wall is effectively detected as a wall motion artefact and the amplitude of these artefacts sets the lower limit on the detectable bubble size that can be discriminated using the signal comparator. The magnitude of the artefact is determined by the contact pressure and coupling between the detector head and the tubing and is further complicated by variations in the coupling with variations in flow rate. A specially designed in-line detector head would clearly avoid this particular problem, and on the basis of these observations would appear to be essential. However an in-line head would not avoid the multiple count problem and would not necessarily avoid the sizing inconsistency. The multiphasic response characteristic may be due to non-perfect standing wave formation or non-uniform intensity distribution or simply bubble vibrations. Unfortunately the transverse application of the source of ultrasound precludes the flow test for standing wave formation described earlier for the Wessex detector. However an estimate of four antinodes for a standing wave within the 9.5 mm cross-section of tubing suggests that the phenomenon was not due to a standing wave formation.

In addition to these observations in which single bubbles were

introduced into the flowstream, without any evidence of fission, observations were also made for situations in which groups of bubbles were introduced into the flowstream. Discrimination of bubble numbers on the basis of the recorded count could not be achieved. Amplitude discrimination corresponding to individual bubbles was likewise unobtainable. On the basis of the observations made, the Technique Laboratories instrument was rejected for use in quantitative studies of bubble populations during cardiopulmonary bypass.

A recent addition to the continuous wave techniques for microbubble detection during cardiopulmonary bypass has been provided by Clarke, Dietz & Miller (1975). Using a transmission oscillator ultrasonic spectrometer (TOUS) applied to two parallel piezoelectric crystals to produce a standing wave perpendicular to the blood flow, the authors claim that microbubbles may be both sized and counted by taking advantage of the extremely high sensitivity of the instrument to small changes in attenuation produced by microbubbles. The system was reported to have been calibrated over wide ranges of temperature, haematocrit, and protein content at 10 MHz, using 100 μm, 200 μm and 300 μm diameter microspheres. Subsequent results were reported to be highly consistent. Unfortunately, no further details concerning the technique were presented, thus making an appraisal of the technique somewhat speculative. However it is difficult to appreciate how bubble sizing and bubble counting could be accurately determined in a system using a standing wave formation. Erratic motion of bubbles through such a field could yield multiple counts per bubble. Signal amplitudes might be unrelatable to actual bubble size because of uncompensated variations in local intensity. Coincidence errors would further prejudice attempts at both sizing and counting. Although calibration of the instrument was reported to have been achieved using

plastic microspheres, no mention was made as to the significance attached to this method of calibration. For bubble detection purposes calibration using bubbles is essential, since no other material has identical acoustic properties.

Bubble detection by second-harmonic analysis

A fundamentally different continuous wave technique for microbubble detection to that of measuring attenuation involves the measurement of second harmonic distortion due to small bubble inclusions (Welsby, 1968, 1969; Welsby & Safar, 1969). The technique has been suggested as a tool for the detection of microbubbles in decompression studies (Tucker & Welsby, 1968) and for the detection of microbubbles in whole blood (Welsby, personal communication).

The strength of an acoustic source is, by definition, the time differential of the displaced volume. However the relationship between applied pressure and the resultant volumetric displacement is essentially non-linear. In consequence the response to a sinusoidal pressure source is a distorted waveform containing a second harmonic component in addition to the fundamental. The magnitude of the harmonic component in a bubble free medium is dependent upon the harmonic distortion due to the electro-acoustic transducers and the intrinsic non-linear distortion due to the liquid itself; the latter being a function of compressibility. An additional non-linear effect is introduced if the ultrasound source exhibits a travelling wave field. The harmonic components due to the background distortion of the liquid tend to add cumulatively as the wave progresses (Welsby, 1969). However it is possible to avoid this effect by establishing a standing wave field.

A bubble introduced into a liquid effectively increases the total compressibility of the liquid, the result being a consequential

increase in the harmonic content of the scattered waveform. A bubble in water is 10^8 times more effective as a generator of harmonics than the equivalent volume of water (Welsby, 1969). The absolute minimum bubble volume detectable within a 10 ml volume of water under ideal conditions is approximately 10^{-7} ml. In practice little better than 10^{-6} ml can be achieved (Welsby, personal communication) corresponding to a bubble radius of approximately 80 μm. This facility for measuring small volumes of undissolved gas within relatively large volumes of liquid is the basis of the Welsby technique of microbubble detection.

The harmonic response for a population of bubbles, derived for a selected point of observation, is a summation of the individual bubble contributions (Welsby & Safar, 1969). However the response may be complicated by the presence of other harmonic sources. Welsby & Safar (1969) defined the problem as one concerning the total output of a three dimensional array of point sources superimposed on a uniform source distribution used to represent the non-linear distortion of the liquid. In reality the situation is complicated by having a statistical distribution rather than a uniform distribution of spacings between individual bubbles and a statistical distribution of amplitudes and phase angles. However, provided the acoustic frequency is well below the natural resonant frequency of any of the bubbles present, a relatively simple solution is possible. Under these conditions the distorted waveforms will exhibit a fixed phase relationship to the main wave irrespective of size (Welsby & Safar, 1969). Moreover the effect of the small bubbles under these conditions depends entirely upon the total volume of undissolved gas, even when the average spacing between the bubbles is not small compared with the wavelength. At acoustic frequencies approaching bubble resonance phase angle variations

become evident and the total response is no longer the summation of the individual effects (Welsby & Safar, 1969). Thus, providing the acoustic frequency is kept well below the natural resonant frequencies of the bubbles to be encountered a quantitative estimate of total undissolved gas content is possible.

Although the initial studies of the detection technique were conducted using water the technique has also been demonstrated to work well in blood, in vitro, but has not been developed for use in extracorporeal studies (Welsby, personal communication). An important requirement in this respect would be a special in-line cell in which the transducer surfaces would be separated by parallel walls thin enough to permit adequate transmission of ultrasound. To attempt transmission and subsequent harmonic detection through conventional extracorporeal tubing would result in attenuation due to the losses imposed by overcoming the natural rigidity of the wall material and the internal frictional losses of the material.

The choice of operating frequency is primarily determined by the resonant frequency representative of the largest bubble size likely to be encountered. Initial studies by Welsby (1969) were conducted using a 16 kHz source corresponding to a resonant bubble radius of 200 μm, and later increased to 25 kHz, corresponding to a resonant bubble radius of 128 μm. The choice of operating frequency is particularly important since the presence of bubbles, greater in size than the limit suggested by the operating frequency may not even be detected. This is because the harmonic component decreases rapidly above resonance and actually passes through zero at a frequency that is approximately 1.5 times the resonant frequency (Welsby, personal communication). Assuming that bubbles greater than 250 μm radius are unlikely to be found within an extracorporeal circuit during a normal heart-lung bypass procedure, an operating frequency of approximately

12 kHz would be required. However a reduction in frequency favours an increase in harmonic distortion due to the transducer construction.

Ideally the transmitting transducer must be designed to have the lowest possible amount of intrinsic distortion. To achieve this it is necessary for the transducer to take the form of a mechanical filter, mechanically resonant at the fundamental frequency. Since mechnical resonance is a function of mass and compliance a reduction in frequency while maintaining constant mass requires an increase in compliance. Unfortunately this is not possible using a single piece of material. A bonded composite structure becomes necessary, which, because of the notoriously non-linear mechanical characteristics of the bonding materials, exhibits unacceptably large intrinsic harmonic distortion. An alternative method of reducing the operating frequency is to alter the mass. To effect a reduction in operating frequency by one half it is necessary to increase the mass by a factor of eight, thus doubling the linear transducer dimensions of the transducer. The face dimensions of the transducer together with the separation between transmitter and receiver transducers determine the active volume, which in turn sets the theoretical lower limit on the volume of undissolved gas that can be detected. For a fixed transducer separation an increase in the transducer face dimensions thus reduces this theoretical limit. Fortunately the separation must, in practice, satisfy the requirement of being small in comparison with the acoustic wavelength within the liquid, so allowing the active volume to be kept relatively small.

On the basis of these considerations it is evident that the technique could be effectively used for monitoring undissolved gas volume during extracorporeal circulation. However various other considerations have largely limited further consideration of the technique for extracorporeal purposes. The principal consideration

has been the fundamental need to determine the magnitude and distribution of undissolved gas in terms of bubble numbers and individual sizes. This is not seemingly possible using the harmonic technique.

Because of the need to ensure that the transducer separation is small in comparison with the acoustic wavelength within the blood an in-line cell would need to be shallow in depth, flat surfaced, and broad in width. Such a requirement presents a difficult design problem in order to avoid blood flow disturbances, including regions of stagnation, blood trauma and adequate coupling of the transmitter and receiver transducers.

In the absence of an ideal solution the harmonic analysis technique would be a valuable compromise. It would also provide a valuable complement to other techniques of microbubble detection.

ULTRASONIC DOPPLER TECHNIQUES

A scatter source contained within a volume of insonification produces a perturbation in the back scatter direction comprising a monopole term and a dipole term. Because the monopole term is proportional to the difference in compressibility of the scatter source and the surrounding medium, and because the dipole term is proportional to the difference in density, a bubble in blood is a far more efficient scatterer of acoustic energy than blood cells. The presence of microbubbles within a volume of blood subjected to a source of ultrasound is therefore characterised by an increase in the receiver signal strength. The relationships between the large amplitude fluctuations and the entry of microbubbles into the region of insonification is one of the principal reasons for the adoption of Doppler blood flowmeters as a means of microbubble detection during extracorporeal circulation for open heart surgery, neurosurgery (Maroon et al., 1968; Edmonds-Seal & Maroon, 1969; Gillis, Karagianes & Peterson, 1969; Maroon, Edmonds-Seal & Campbell, 1969; Spencer et al., 1969; Edmonds-Seal, Prys-Roberts & Adam, 1971; Gallagher & Pearson, 1973; Lubbers et al., 1974; Tinker et al., 1975; Lubbers & van den Berg, 1977), and for the detection of bubbles during investigations into decompression sickness (Gillis, Peterson & Karagianes, 1968; Gillis, Karagianes & Peterson, 1968; Spencer et al., 1969; Smith & Spencer, 1970; Rubissow & Mackay, 1971; Evans, Barnard & Walder, 1972; Nishi, 1972; Powell, 1972; Spencer & Clarke, 1972; Nishi & Livingstone, 1973; Powell, 1974; Hills & Grulke, 1975). In all cases it is the amplitude variation rather than any reference to a Doppler frequency shift that has been used to detect the presence of bubbles.

In addition to the pronounced amplitude variations, the presence of a bubble population within a volume of flowing blood may also be characterised by a broadening of the Doppler frequency spectrum. Gallagher & Pearson (1973) have reported the use of an electronic filter to supposedly discriminate bubble induced signals from those arising from the blood cell population. Lubbers et al (1974) have also reported the use of an electronic filter in order to restrict the conditioned signal source to signals arising from moving objects. Apart from these references to filter design, little significance appears to have been attached to the Doppler shift in either the extracorporeal or the decompression studies undertaken using Doppler instruments. Unless the Doppler shift is of significance in such studies with useful information being gained concerning the bubble population, then there would appear to be little advantage in using Doppler flowmeters for microbubble detection. A technique based upon the detection of scattered energy alone would be equally informative.

An analysis of the Doppler principle and the responses to be expected from a bubble population is presented in order to determine the basis for the observed spectral changes and to establish the relevance of Doppler techniques for bubble detection.

Doppler principle The frequency of an ultrasound signal reflected from a moving surface will differ from that of the transmitted signal by an amount determined by the velocity of the reflecting surface and the velocity of sound propagation within the medium in which the sound waves are travelling. The frequency shift will result in either an increase or decrease in frequency depending upon the direction of movement of the reflecting surface. Movement towards the transmitter/receiver assembly will yield an increase in frequency whereas movement away from the assembly will yield a decrease.

Analysis for transcutaneous arrangement of transducers

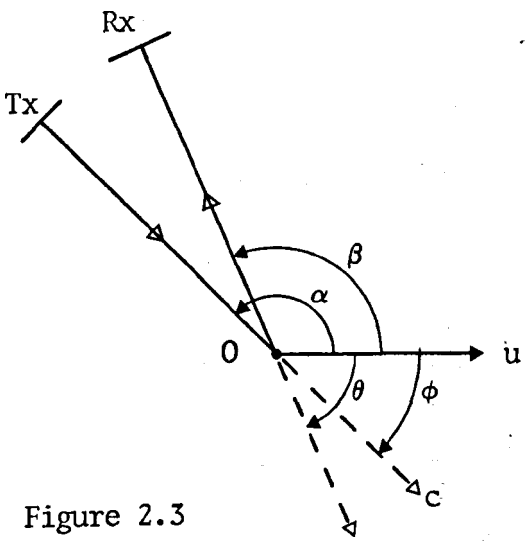

Figure 2.3

At the object O, (Fig.2.3) a decrease in frequency is observed due to the movement of the object away from the transmitter. This gives rise to a secondary source of ultrasound of frequency ω_{R1} such that:

$$\frac{\omega_{R1}}{\omega_T} = \frac{c - u\cos\theta}{c}$$

Where ω_T is the transmitted frequency, c the velocity of propagation of sound in the medium and u is the velocity of the object.

Now $\cos\theta = \cos(180-\beta) = -\cos\beta$

$$\therefore \quad \frac{\omega_{R1}}{\omega_T} = \frac{c + u\cos\beta}{c}$$

$$\therefore \quad \omega_{R1} = \left(\frac{c + u\cos\beta}{c}\right)\omega_T$$

With respect to the receiver the secondary source of sound is moving away from the receiver with a velocity of $u\cos\phi$. The resultant frequency ω_{R2} at the receiver as a result of this motion is related to the secondary source frequency ω_{R1} by the expression:

$$\frac{\omega_{R2}}{\omega_{R1}} = \frac{c}{c + u\cos\phi}$$

but $\cos\phi = \cos(180-\alpha) = -\cos\alpha$

$$\therefore \quad \frac{\omega_{R2}}{\omega_{R1}} = \frac{c}{c - u\cos\alpha}$$

$$\therefore \quad \omega_{R2} = \left(\frac{c}{c - u\cos\alpha}\right)\omega_{R1}$$

$$\therefore \quad \omega_{R2} = \left\{\left(\frac{c}{c - u\cos\alpha}\right) \times \left(\frac{c + u\cos\beta}{c}\right)\right\} \omega_T$$

$$= \left(\frac{c + u\cos\beta}{c - u\cos\alpha}\right) \omega_T$$

The change in frequency with respect to the transmitted frequency is:

$$\Delta\omega = \omega_{R2} - \omega_T$$

$$= \left(\frac{c + u\cos\beta}{c - u\cos\alpha}\right) \omega_T - \omega_T$$

$$= \left(\frac{c + u\cos\beta - c + u\cos\alpha}{c - u\cos\alpha}\right) \omega_T$$

$$\Delta\omega = \frac{u(\cos\alpha + \cos\beta)}{c - u\cos\alpha} \omega_T$$

For v>>u

$$\Delta\omega = \frac{u(\cos\alpha + \cos\beta)}{c} \omega_T$$

Now $\Delta\omega = \frac{2u}{c} \omega_T \cos\left(\frac{\alpha+\beta}{2}\right) \cos\left(\frac{\alpha-\beta}{2}\right)$

For a fixed mounting of the transmitter and receiver transducers $\cos\frac{\alpha-\beta}{2}$ is a constant K.

$$\therefore \quad \Delta\omega = \frac{2\omega_T}{c} Ku \cos\left(\frac{\alpha+\beta}{2}\right)$$

$u\cos\left(\frac{\alpha+\beta}{2}\right)$ defines a unit vector along the bisector of the angle between the transmitter and receiver axis (Fig.2.4) such that:

$$u\cos\left(\frac{\alpha+\beta}{2}\right) = \bar{u} \cdot \bar{k}$$

$$\therefore \quad \Delta\omega_i = \frac{2\omega_T}{c} (\bar{u} \cdot \bar{k})K$$

Where ω_i is the frequency component in the received signal due to an object having a velocity u_i.

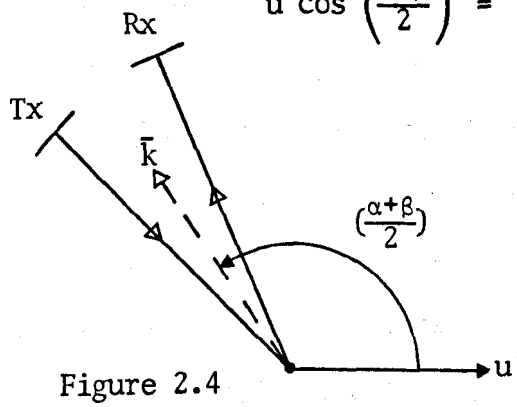

Figure 2.4

For blood flow purposes an average frequency difference $\Delta\omega_{av}$ may be defined, which represents the difference between the average angular frequency of the power density spectrum of the received signal and the angular frequency of the transmitted signal (Arts & Roevros, 1972).

Considering a volume, V, of blood within the beam, containing N particles (Fig.2.5).

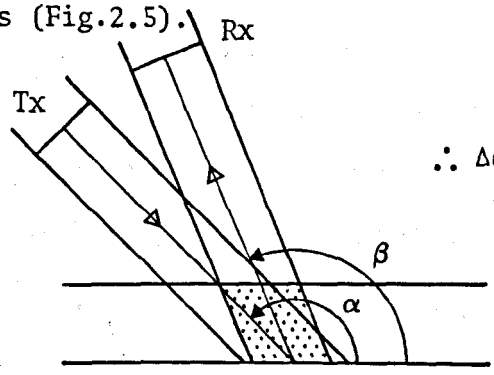

Figure 2.5

$$\therefore \Delta\omega_{av} = \frac{1}{N}\sum_{i=1}^{N} \Delta\omega_i$$

$$\Delta\omega_{av} = \frac{1}{N}\sum_{i=1}^{N} \frac{2\omega_T}{c} K(\bar{u}_i \cdot \bar{k})$$

$$= \frac{2\omega_T}{c}\left(\bar{k} \cdot \frac{1}{N}\sum_{i=1}^{N} u_i\right) K$$

The average velocity of the particles within the volume V:

$$u_{av} = \frac{1}{N}\sum_{i=1}^{N} u_i$$

$$\therefore \Delta\omega_{av} = \frac{2\omega_T}{c} (k \cdot u_{av}) K$$

If it is assumed that (i) the average velocity of the particles of the blood in the measured volume is the same as that measured along the cross-section of the vessel, (ii) the concentration is uniform throughout the whole volume considered, (iii) the velocity of the particles is equal to the velocity of the surrounding liquid, (iv) the centre of gravity of the cross-section of the blood containing vessel remains always in the same place and that (v) at any moment the blood containing vessel is cylindrical then

$$\Delta\omega_{av} = \frac{\omega_T}{c} u_{av} (\cos\alpha + \cos\beta)$$

The introduction of microbubbles into the flow stream will result in a broadening of the received frequency spectrum because of the variation in velocity and direction. The variations in velocity and direction are direct consequences of the bubble buoyancy in the fluid medium introducing a component of velocity in addition to that of forward flow, which can considerably alter the $(\bar{u}_i \cdot \bar{k})$ vector product.

Assuming that the bubble population is small and the contribution to the received frequency spectrum due to the blood particles is unaltered by the presence of the bubbles, the change in frequency due to both blood particles and the small population of bubbles may be defined by the expression

$$\Delta\omega_{av} = \frac{2\omega_T}{c} (k \cdot u_{av}) K \pm \frac{1}{N_b} \sum_{i=1}^{N} \frac{2\omega_T}{c} K (\bar{u}_{ib} \cdot \bar{k}_{ib})$$

Where $\bar{u}_{ib}$, $\bar{k}_{ib}$, and N_b relate to the population of bubbles. Depending on the nature of the flow, the movement of the bubbles under various conditions of flow and the inclination of the vessel through which they are flowing, the values of $(\bar{u}_{ib} \cdot \bar{k}_{ib})$ may range from 0 to $\bar{u}_{ib}$.

Possible errors, based on the assumptions, implicit in the derivation of the equation for average velocity include: (i) the radiation patterns of the transmitting and receiving crystals are generally such that they are not homogenous in the main beam, (ii) the acoustic properties of the vessel walls differ from the acoustic properties of the blood (this causes diffraction and reflection of ultrasound with the result that the sound intensity within the blood volume is non-homogeneous), and (iii) unequal power contributions to the received signal. With good beam properties these errors will not be too large. In addition to moving erythrocytes, all kinds of discontinuities, including microbubbles will contribute

to the power of the received signal. Contributions due to vessel wall movement will generally be small and close to ω_T in frequency but also dependent upon the values of α and β (Arts & Roevros, 1972).

Maximum frequency shift

By considering the Doppler frequency shift expression for a single bubble,

i.e. $$\Delta\omega = \frac{2\omega_T}{c} K u \cos\left(\frac{\alpha+\beta}{2}\right),$$

it is evident that the maximum theoretical change in frequency (for a given velocity) arises for the condition in which,

$$K \cos\left(\frac{\alpha+\beta}{2}\right) = 1 \quad \text{i.e. } \cos\left(\frac{\alpha-\beta}{2}\right) \cos\left(\frac{\alpha+\beta}{2}\right) = 1$$

The theoretical maximum shift in frequency is therefore $\frac{2\omega_T u}{c}$ max In practise $(\alpha-\beta)$ is always greater than zero since a finite angle exists between the transmitter and receiver crystals. Consequently, under this imposed constraint, $\cos\left(\frac{\alpha-\beta}{2}\right) \cos\left(\frac{\alpha+\beta}{2}\right)$ must be less than unity. For example, in the Doptone transducer $(\alpha-\beta)$ is 40^{o}. The maximum frequency shift for this arrangement is therefore,

$$\Delta\omega_{max} = 1.532\ \omega_T \cdot \frac{u_{max}}{c}, \quad \cos\frac{\alpha+\beta}{2} = 1$$

or $$\Delta f_{max} = 1.532\ f_T \cdot \frac{u_{max}}{c}$$

It is important to appreciate that the velocity, u_{max}, referred to in this expression is the maximum velocity in the direction corresponding to motion along the bisector of the angle between the normals subtended by the transmitter and receiver crystal surfaces (Fig.2.6). In a practical situation it is unlikely that the value of u_{max} will be as high as the peak velocity in the axial flow direction. Consequently the maximum frequency shift due to bubble motion in the non-axial direction may not exceed the maximum frequency shift due to motion in the axial direction. Therefore, broadening of the Doppler spectrum

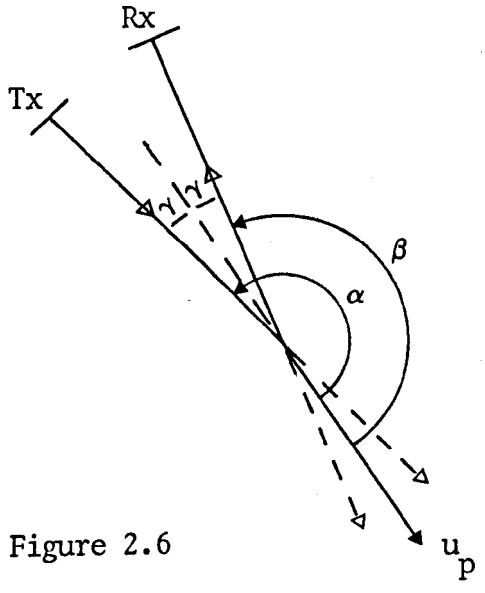

Figure 2.6

$$\beta = 180^{o} - \gamma \text{ and } \alpha = 180^{o} + \gamma$$

$$\alpha - \beta = 2\gamma \text{ and } \alpha + \beta = 360^{o}$$

$$\cos\left(\frac{\alpha + \beta}{2}\right) = \cos 180^{o}$$

$$= -\cos 0^{o}$$

$$= -1$$

due to the presence of bubbles may arise if the values of $K\, u \cos \frac{(\alpha+\beta)}{2}$ are greater in the non-axial direction than the value due to flow in the axial direction.

Influence of bubbles upon the Doppler spectrum

In order to investigate the influence of bubbles upon the Doppler frequency shifts a simple experiment was performed to record and analyse the frequency variations that may be attributed to the presence of bubbles in a flowing liquid and to compare these variations with theoretical estimates.

Materials and methods

A circuit was constructed using 1.8 m of 9.5 mm internal diameter tubing, a 400 ml polycarbonate reservoir and a 9.5 mm diameter cannulating flow probe (Nycotron). A Sarns roller pump was used to promote flow within the circuit. The circuit was primed with 0.9% sodium chloride. Bubbles were generated electrolytically using a unipolar myographical needle inserted into the flow line and an adjustable current source (Farnell, E30/1 Supply). The bubbles were

detected using a Doptone foetal blood flow detector, positioned at an angle of 43^{o} to the flow line in a perspex mounting head with the transducer coupled to the tubing using acoustic gel (Parkes Aquasonic). Flow recordings were obtained using a Nycotron type 376 electromagnetic flowmeter (50 hz band width) and a Mingograph 81 ink jet recorder.

Saline was chosen for the circuit prime in order to minimise background Doppler activity, and to permit observation of the bubble source and flow patterns using coalesced ink particles.

Recordings from the amplitude output of the Doptone were obtained with and without the presence of bubbles, at flow rates of 0.5 $L.min^{-1}$ (0.6 $L.min^{-1}$ peak), 1.0 $L.min^{-1}$ (1.25 $L.min^{-1}$ peak), and 1.5 $L.min^{-1}$ (1.75 $L.min^{-1}$ peak). The recordings of Doppler response obtained for subsequent frequency analysis were made onto magnetic tape using a Racal Store 7 instrumentation recorder operating at 60 ins per second (20 kHz recording capability). From these recordings sonograms were obtained using a Kay Sonograph (type R662B).

Theoretical estimates of frequency shift

In order to obtain an estimate of the Doppler frequency spectrum corresponding to motion in an axial flow direction, it is necessary to know the range and distribution of scatter source velocities. Since this information is inaccessible from electromagnetic flow data directly it is necessary to establish the nature of the flow velocity profile. In certain circumstances, such as the flow in an extra-corporeal circuit, it may be unreasonable to assume that the flow velocity profile is parabolic. For established pulsatile flow, the balance between viscous and inertial forces may be characterised by an expression, formulated by Womersley (1957), for each sinusoidal component of the observed waveform,

$$\xi = a\sqrt{\frac{W\rho}{\eta}}$$

Where a is the lumen radius, ρ is the density of the flow medium, η is the viscosity of the flow medium and w is the angular frequency of pulsatance. For ξ between 1 and 5 with reasonable forward flow, the velocity flow profile is theoretically a blunted parabola during diastole and flat during systole. For $\xi \geq 7$ the flow is plug-like. The maximum velocity for a parabolic flow profile is twice the average velocity across the tube ($u_m = 2\ \bar{u}$) whereas for plug-like flow, $u_m \simeq \bar{u}$. Thus for conditions of plug-like flow, the Doppler shift recordings would be expected to be dominated by one frequency corresponding to the average flow velocity. For the flow conditions produced by a roller pump, the waveforms may be considered to consist of a steady forward component combined with a forward, non-sinusoidal, pulsatile component (Fig.2.7). Moreover the waveforms may be considered to consist of sub-harmonics of the measured pulse frequency as well as harmonics. These sub-harmonics suggest that flow velocities greater than values corresponding to the average flow rate may be observed even during systole. For the flow rates considered in this investigation (0.5, 1.0, & 1.5 $L.min^{-1}$) $\xi \geq 8.2$ for the fundamental harmonic of each of the pulsatile components considered (derived using the Womersley expression and taking ρ for saline to be 1 and the viscosity, η, for saline to be 1.1×10^{-2} Poise). Whilst these values indicate that the flow would be plug-like for these harmonics alone, a blunted parabola may therefore be considered more reasonable for the flow velocity profile due to the combined contributions of harmonics and sub-harmonics.

Bearing in mind the discussion presented above, a worst case theoretical estimate of frequency shift has been based upon the assumption that the peak axial velocities, relevant to the flow conditions in this investigation, are twice the value of the velocities

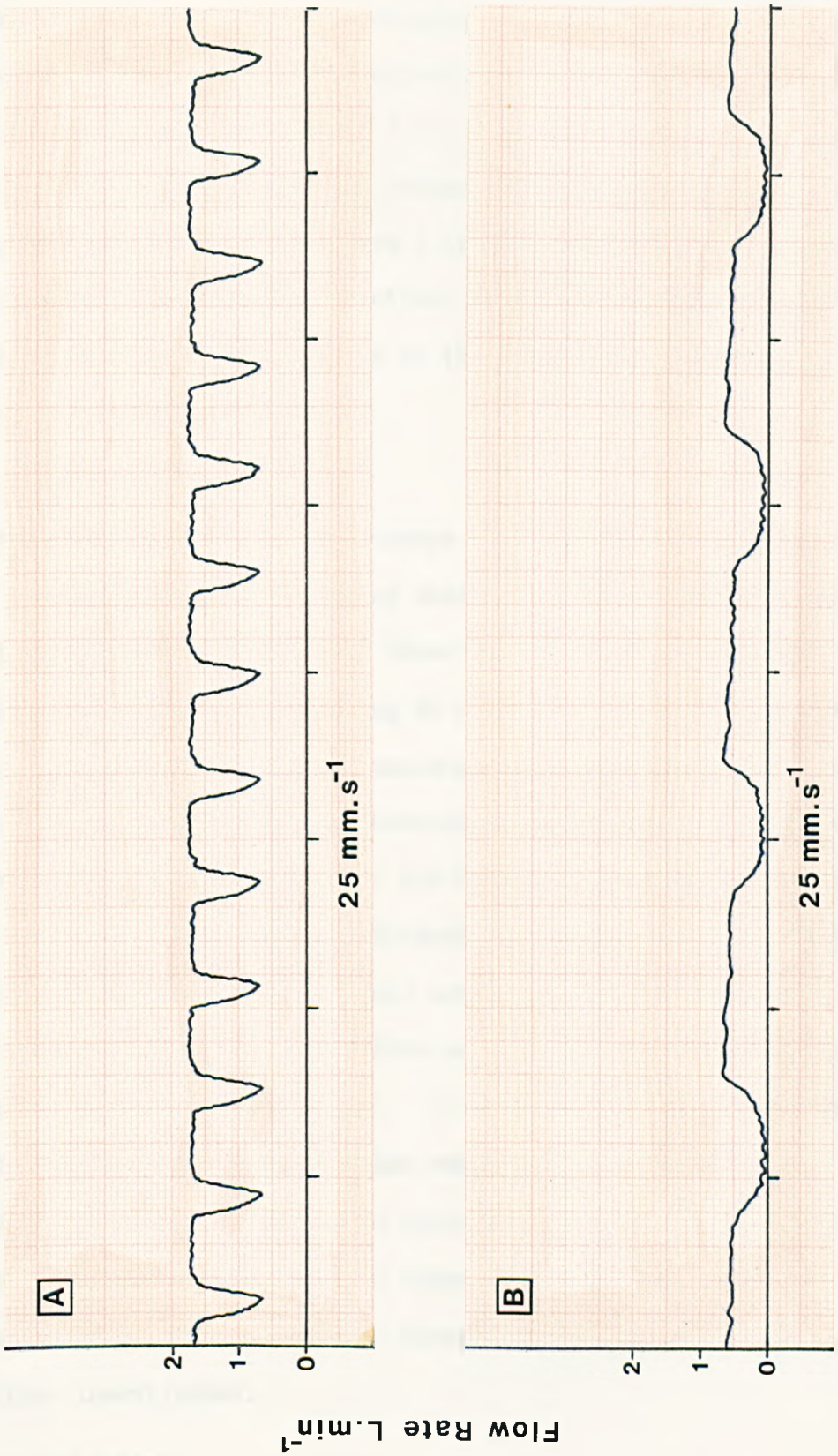

Roller pump flow waveforms for flow rates of 0.5 and 1L.min^{-1}

(High frequency cut off 50 Hz)

Figure 2.7

Referred to on p 70

derived directly from the observed peak flow rates (i.e. velocities corresponding to a parabolic flow profile). These velocities are 0.28 ms^{-1} (0.5 $L.min^{-1}$), 0.58 ms^{-1} (1.25 $L.min^{-1}$) and 0.82 ms^{-1} (1.75 $L.min^{-1}$). The theoretical frequency shifts, for the transducer arrangement considered earlier are 1.11 kHz, 2.30 kHz, and 3.22 kHz respectively. The maximum theoretical shifts corresponding to motion in the optimum direction relative to the transducer assembly are 1.51 kHz, 3.15 kHz, and 4.40 kHz.

Results and Discussion

Sonograms obtained at the average flow rates of 0.5, 1.0 and 1.5 $L.min^{-1}$ revealed maximum frequency shifts of 1.25 kHz, 2.8 kHz and 3.9 kHz respectively (Fig.2.8). These values are clearly larger than the estimated values corresponding to motion in the axial direction, but are less than the estimated maximum values corresponding to motion in the optimum direction. The observed frequency shifts may therefore be due to the non-axial motion of the bubbles. Even though the non-axial motion of the bubbles may account for broadening of the Doppler spectrum, it is clear that it would not be possible to completely discriminate bubbles from other flow entities by the use of electronic filtration of the received signal. It must also be considered that the non-axial motion of the bubbles observed in the experimental procedure could in part be due to turbulent flow, in which non-axial components could be expected from other flow entities. This consideration prompted an attempt to visualise the flow under the conditions investigated.

Flow visualisation

In order to achieve flow visualisation a proprietary black drawing ink (0.2 ml in 500 ml) was injected into the flow stream of the saline filled circuit. It was observed in this process that the electrolysis

Sonograms A 1.5L.min^{-1} B 0.5L.min^{-1}

Background: noise representative of bubble free flow

Figure 2.8

Referred to on p 72

used to generate a source of bubbles caused the ink particles to coalesce and in so doing yielded a more suitable flow visualisation medium. The mechanism causing the particles to coalesce may in part be due to charge imparted to them whilst electrolysis is proceeding. However they do not disperse following termination of electrolysis, but remain as stable coalesced entities (Fig.2.9).

Flow rates up to 1.5 $L.min^{-1}$ examined using this flow visualisation facility exhibited what may best be described as disturbed laminar flow according to the definition provided by Helps & McDonald (1954) and adopted by Yellin (1966). No evidence of vortex formation or gross non-axial motion of the particles was observed. Above 1.5 $L.min^{-1}$ visualisation of the flow became more difficult, but the condition of disturbed laminar flow appeared to persist up to reasonably high flow rates ($\simeq$ 4-5 $L.min^{-1}$). Bubbles introduced into the flow stream at low flow rates (0.5 - 1.5 $L.min^{-1}$) were seen to move erratically whilst the fluid flow as depicted by the movement of the coalesced ink particles appeared to remain laminar but slightly disturbed. These observations support the hypothesis that non-axial motion of bubbles is a principal contributor to the observed frequency shifts.

Figure 2.9 A

No flow situation showing the coalesced ink particles used as a flow visualisation medium

Figure 2.9 B

Flow situation showing the use of the coalesced ink particles as a flow visualisation medium

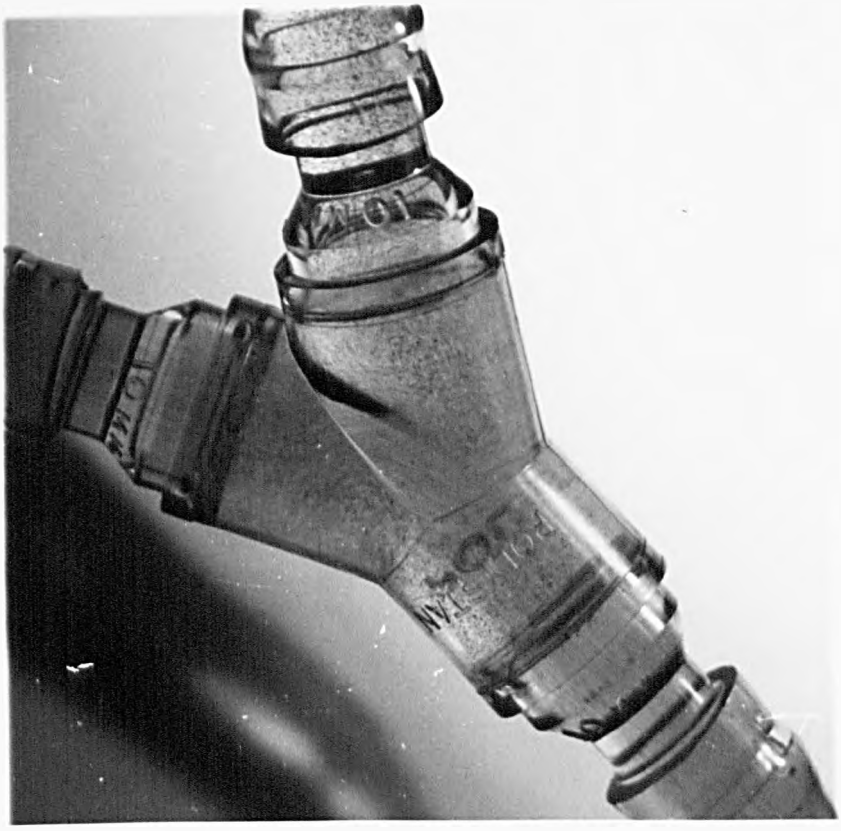

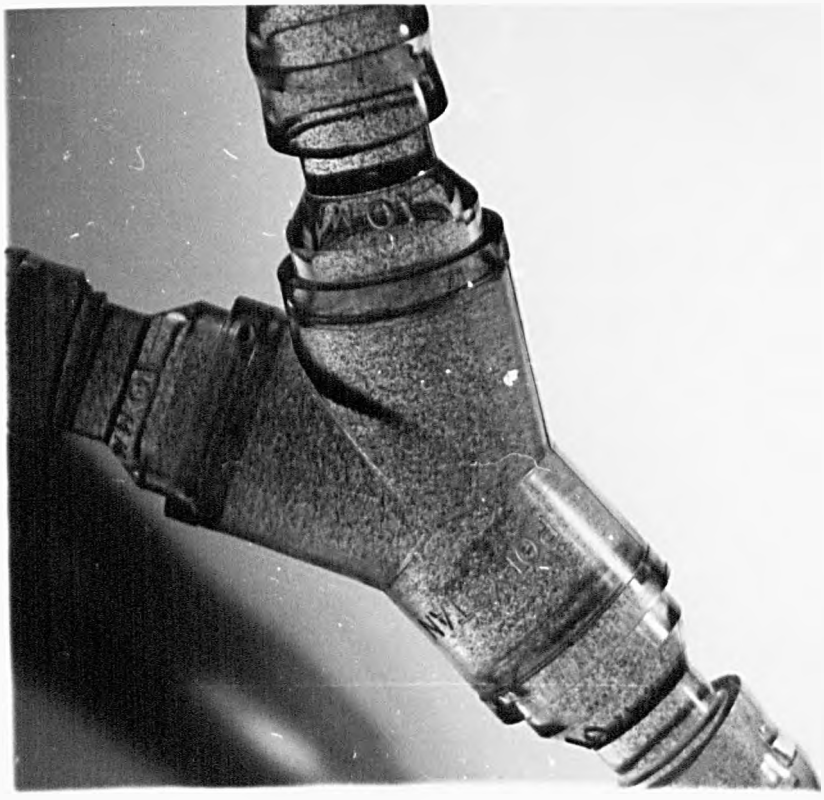

Significance of the Doppler spectrum

It is evident from the analyses presented that the measurement of the Doppler spectrum is of little use in estimating the magnitude of a given bubble population. The spectrum provides no information concerning bubble size and no accessible information concerning bubble numbers. The use of filtering in the manner described by Gallagher & Pearson (1973) would also appear to be of limited value. Analysis indicates that bubbles would, by virtue of their spiral motion, tend to contribute a wide range of Doppler shift components. High pass filtering would therefore remove signal components due to bubbles as well as signal components due to blood cells.

Widening of the Doppler shift spectrum at a given flow rate need not be due to the presence of bubbles. Sigel et al., (1970) demonstrated that the frequency spectrum from a Doppler flow detection system changes in response to a change from laminar to turbulent flow. Amplitude variations have also been observed due to the presence of particulate matter. Erythrocyte aggregation has been demonstrated to affect the output amplitude of Doppler flow meters (Thompson et al., 1970). Other particles such as aggregates of lipids and platelets have also been suggested as factors responsible for observed changes in the output of Doppler flow detectors (Nishi & Livingstone, 1973; Smith & Spencer, 1970). Because the magnitude of scatter is dependent upon the size and composition of the scatter source, variations in amplitude due to the presence of particular matter is to be expected. However the relative effectiveness of bubbles compared with blood cell and lipid aggregates as sources of scatter could well allow the discrimination of bubbles from particles. The procedure for achieving this is therefore one of amplitude discrimination, the Doppler shift having no relevance in this respect.

Signal amplitude and instrumentational limitations

In addition to output variations due to blood based conditions, the design criteria of commercially available Doppler blood flow meters may also limit their use in bubble detection. Inadequate high frequency response may introduce non-linearity into the input/output calibration curve (Gosling et al., 1969; Flax, Webster & Updike, 1973) and a low frequency gain that is higher than necessary can result in signal degradation by wall motion artefacts (Flax, Webster & Updike, 1973).

Gosling et al., (1969) have demonstrated that the audio-frequency response characteristics of the 5 MHz Doptone and 10 MHz Parks 802 flowmeters are far from linear above 2.4 kHz and 1.7 kHz respectively.

In the case of the Doptone flowmeter the cut off frequency of 2.4 kHz would correspond to an average velocity in excess of 0.6 $m.s^{-1}$. Departure from the theoretical average velocity/Doppler shift frequency characteristic suggests the need to determine the characteristic practically in order to determine the velocity corresponding to a particular frequency shift. The loss of linearity above 2.4 kHz imposes a serious limitation upon the use of the Doppler output for quantitative bubble detection purposes.

While signal degradation due to wall motion artefact may be eliminated by the use of high pass filtering, this inevitably results in the loss of uniform sensitivity throughout the frequency range. Bubble detection sensitivity is also dependent upon bubble velocity. Hills & Grulke (1975) have demonstrated that a commonly used Doppler device for bubble detection (Sonicaid foetal heart monitor) is capable of detecting single bubbles of 150 μm diameter under static

conditions but this value is reduced to 50 μm in diameter under flow conditions depending upon bubble velocity. This result could be due to a non-linearity in the high pass filter characteristic.

Count and sizing capabilities

Although a Doppler flowmeter may exhibit variations in output due to the presence of undissolved gas in the form of microbubbles, a count of the number of such variations is not necessarily representative of the number of bubbles passing the transducer head. Because of the nature of the signal conditioning within a Doppler instrument, an envelope detector would be necessary to recognise the Doppler shift components specific to a particular perturbation and so derive a single count per perturbation. In the absence of such a detector, a counter attached to the output could count each cycle within the Doppler shifted signal. Spencer et al., (1969) purposely effected a cycle by cycle count of the Doppler shifted signals by using a zero crossing detector followed by a frequency to voltage convertor having a meter output. The significance that Spencer et al., (1969) attached to the recordings so derived is unclear, although reference is made to "bubble counts". If such counts are based upon zero crossing measurements, they are clearly erroneous, since it is the Doppler shift frequency that determines the zero crossing count and not the number of bubbles. Even assuming that adequate envelope detection is possible, a single response would not necessarily correspond to a single bubble.

Coincidence between two or more bubbles within the volume of insonification would result in a single overall variation in signal amplitude and reduce the count. Furthermore, the continued perturbation associated with a bubble, or group of bubbles, while present within the region of insonification may preclude the

detection of incoming bubbles.

In contrast to the low count introduced by coincidence errors, a variation in the intensity of the ultrasound field due to interference, focusing effects and transducer characteristics (Marini & Rivenez, 1974) may result in multiple counts per bubble during its passage through the field. Limitations such as these would seemingly preclude any meaningful measurement of bubble count using Doppler flowmeters.

Sizing of bubbles using Doppler flowmeters is equally difficult. It has been suggested by Gallagher & Pearson, (1969) that bubble signals may be distinguished from blood flow signals by using electronic filtering and so discriminate bubble information making it more amenable for analysis. The theoretical and practical evidence provided earlier indicate that such discrimination is not possible on the basis of frequency alone. Furthermore, the coincidence of bubbles within the volume of insonification would preclude discrimination, and therefore sizing, on the basis of signal amplitude. Any variations in beam intensity would also mitigate against bubble sizing, on the basis of signal amplitude even in the absence of coincidence.

Spencer et al., (1969) have suggested that the development of a swept-frequency Doppler technique could possibly allow sizing of bubbles by recognising the resonant frequency characteristic of each bubble. This statement cannot be derived from the Doppler principle. A swept-frequency Doppler system would unnecessarily complicate the bubble sizing procedure since the signal conditioning facility within a Doppler instrument is designed to derive the Doppler shift frequency components rather than the amplitude variations that would be of prime importance in a resonant bubble

sizing technique. However a swept-frequency source of ultrasound and measurement of amplitude attenuation could conceivably allow bubble sizing by recognition of resonant frequency variations, providing that only one bubble was present within the volume of insonification, and providing that the resonant peaks were sufficiently pronounced for consistent discrimination. Even assuming that the resonance characteristic could be utilised in this manner, the scanning or sweep time that would be necessary to effect an analysis would probably limit continuous sizing at the extracorporeal blood flow rates used in open-heart surgery.

Doppler flowmeters or foetal heart monitors were quite clearly never designed for quantitative microbubble detection. In view of the severe criticism presented above, the low cost and availability that have apparently made them popular for bubble detection purposes are poor criteria for selecting such instruments for studies requiring a quantitative technique of bubble detection.

PULSED ULTRASOUND TECHNIQUES

The use of pulsed ultrasound for the detection of bubbles during extracorporeal circulation was first reported by Austen & Howry in 1965. Using a standard Sperry Products, 2 MHz, ultrasonic flow detector, Austen & Howry (1965) demonstrated that bubbles of various sizes could be detected and the sizes roughly determined from the amplitudes of the detected echoes. To evaluate the bubble detection capabilities of the instrument Austen & Howry (1965) constructed a closed loop bypass circuit which was then filled with water to enable visualisation and photographic recording of bubbles introduced into the flow stream proximal to the ultrasound transducer. Although no direct mention was made of the bubble sizes introduced the scaled oscilloscope derived photographs indicate that bubble sizes between 1 mm and 4 mm diameter were observed. Bubbles below 1 mm were introduced and detected but they were not photographed. In the absence of a rigorous analysis of bubble size-received signal amplitude relationship or bubble count capability an estimate of accuracy for the technique is unobtainable. The manner in which the transducer was applied to the line in this study, at the centre of a T-junction and range gated to detect bubbles in blood flowing directly toward the transducer, suggests particular limitations both in sizing and counting bubbles. The same limitations, relating to the coincidence of bubbles within the gated volume and signal attenuations due to non-gated bubble population, also apply to a more recent technique (Patterson & Kessler, 1969) which is to be discussed in detail.

Following this preliminary assessment of the instrument as

a bubble detector, Austen & Howry (1965) performed five cardiopulmonary bypass experiments using dogs as the experimental animals. Each dog was placed on total cardiopulmonary bypass for a period of 1 hour. Bubbles similar in size to those introduced into the water filled circuit were introduced into the arterial line, again proximal to the transducer. Measurements of serum haemoglobin and platelet count were obtained for the five animals on bypass with ultrasonic bubble detection being performed and for a control group of five animals also on bypass but without ultrasonic bubble detection. On the basis of these experiments, Austen & Howry (1965) concluded that the signal variations due to bubbles in water were identical to those observed from bubbles in blood for a similar range of bubble sizes. Unfortunately no detailed analysis has been presented to substantiate this conclusion. Based on the measurement of serum haemoglobin and platelet count, Austen & Howry (1965) also concluded that ultrasound had no apparent ill effects upon the blood. However this statement is clearly only applicable to low intensity levels of ultrasound (Hill, 1968).

Since the report by Austen & Howry (1965) the use of pulsed ultrasound for microbubble detection has featured in a number of extracorporeal studies (Patterson & Kessler, 1969; Kessler and Patterson, 1970; Brennan, Patterson & Kessler, 1971; Patterson & Twichell, 1971; Patterson, Kessler, & Bergland, 1971; Carlson, et al., 1972, 1973; Patterson et al., 1972; Simmons et al., 1972; Patterson, Wasser & Porro, 1974). With the possible exception of Simmons et al., (1972) all these studies have incorporated the microbubble detection technique initially described by Patterson & Kessler (1969). Simmons et al., (1972) did not describe the pulsed ultrasound technique used to quantify by number extracorporeal based

bubble populations, although reference was made to the technique of Patterson & Kessler (1969).

Patterson and Kessler Technique

Of all the ultrasonic techniques that have been used for the detection of microbubbles during cardiopulmonary bypass, the technique attributed to Patterson & Kessler (1969) has been the most widely quoted. Unfortunately the technique is subject to a number of limitations that have been ignored in clinical studies of embolic tissue damage and neurological dysfunction associated with cardiopulmonary bypass. In view of the emphasis that has been placed upon the results provided by this technique a careful analysis of its limitations was considered necessary in order that the validity of the conclusions derived on the basis of these results could be appropriately tested.

Construction and operation of the microbubble detector

The detection chamber and transducer assembly for the Patterson-Kessler technique is illustrated in Fig.2.10. The chamber consists of a divided 9.5 mm diameter ($\frac{3}{8}$ inch diameter) blood flow channel contained within a rod of nylon, 50 mm wide and 123 mm in length. Stainless steel fittings couple the chamber to the tubing of the extracorporeal circuit. The transducer (Sperry products SIL transducer) is located, by means of a threaded union at the lower end of the chamber in line with the blood outflow tract. It operates in both transmission and receiver modes. In the transmission mode, the transducer crystal provides a pulsed 5 MHz source of ultrasound at a pulse repetition frequency of 650 pulses per second (Patterson & Kessler, 1969). However the pulse repetition was later increased to 750 pulses per second supposedly to provide a higher count capability (Kessler & Patterson, 1970; Patterson et al., 1972). As soon as a pulse has been transmitted,

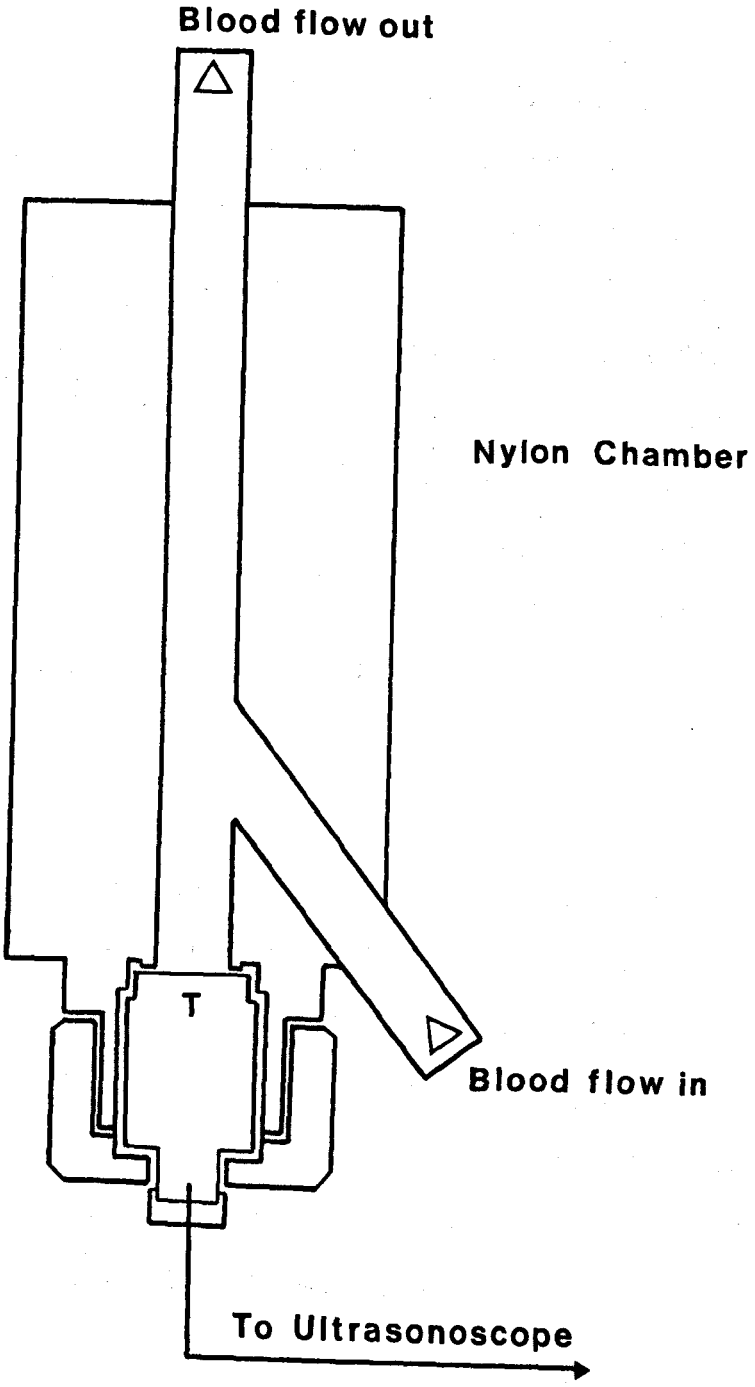

Patterson technique: transducer and mounting assembly

T: transducer

Figure 2.10

Referred to on p 83

the pulse duration being less than 4 μs (Kessler & Patterson, 1970; Patterson et al., 1972), the transducer crystal is switched to a receiver mode. In the receiver mode the received pressure variations incident on the transducer surface are translated to an electrical analogue signal and processed electronically (UCD Reflectoscope, Sperry products) to provide display and gated counter impulses. The electronic gate facility allows only echoes from a selected region of the chamber to be counted. This function is illustrated in Fig.2.11. A pulse of ultrasound propagates through the blood at an approximate velocity c of 1450 $m.sec^{-1}$ and is scattered according to the number and types of particles present within the blood. Bubbles provide a very effective source of scatter. Echoes from particles present within the path of propagation are received at the transducer at a time, t, following pulse emission such that:

$$t = \frac{2d}{c}$$

Where d is the distance of the scatter source from the transducer. The electronic gate is a switch facility that passes signals received within a selected time interval $(t_2 - t_1)$ following pulse emission. Providing the propagation velocity is constant the time interval $(t_2 - t_1)$ corresponds to a region of observation $c(t_2 - t_1)/2$ mm in width (where c is expressed in $mm.s^{-1}$). Gating used in the Patterson-Kessler technique consists of a gate 2 mm in width located 80 mm from the transducer surface (Kessler & Patterson, 1970).

Particle resolution

Echoes received at the transducer simultaneously cannot be resolved as individual echoes. At the transducer surface, the spatial pressure variations are effectively summated and so elicit a single electrical response. Consequently any particles contained within the

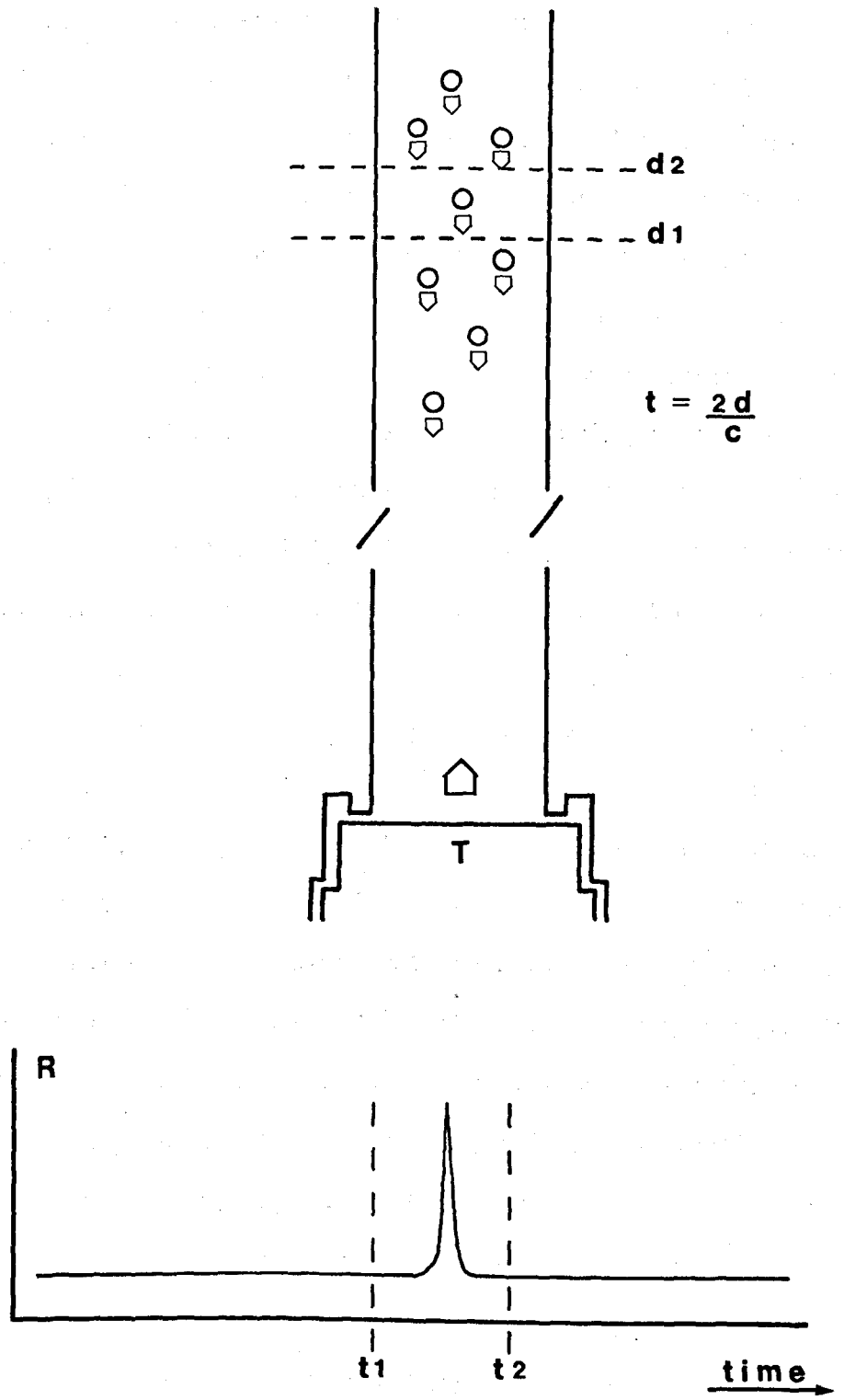

Patterson technique: signal response to a single bubble within the gated region (d2 - d1) of the field

T: transducer R: signal response

Figure 2.11

Referred to on p 85

same cross-sectional plane of the Patterson-Kessler detector cannot be individually resolved. A single response is all that can be expected for any in-plane population of particles, whether they are bubbles or any other efficient source of scatter, (Fig.2.12).

The duration of the response is related to the duration of the incident pulse of ultrasound. Since a source of scatter will continue to scatter energy for as long as it is subjected to an incident source of energy the echo response duration will not be less than the effective duration of the pulse of ultrasound. The pulse duration used in the Patterson-Kessler technique is quoted as being less than 4 μs (Patterson et al., 1972). Since the pulse propagation time through the 2 mm wide gate is approximately 1.4 μs (assuming a propagation velocity in blood of $1450 m.s^{-1}$), it is clear that none of the scatter sources contained within the gated volume of insonification can be individually resolved, unless, of course, only one is present. However, in general, only one response per pulse can be expected using the Patterson-Kessler arrangement, irrespective of the content of the gated volume of insonification (Fig.2.13). These observations substantiate the report made by Patterson & Kessler that the maximum number of echoes per second that can be counted using their instrument is equal to that of the pulse repetition frequency (Patterson & Kessler, 1969; Kessler & Patterson, 1970; Patterson et al., 1972). The implication of this observation does not appear to have been appreciated with respect to the resolution of particles within the gated volume.

On the basis of these observations alone, as a quantitative means of estimating bubble population, the technique is seriously in error. Even for a fairly wide distribution of microbubbles, for example one per microlitre (0.1 volume per cent) the count would be a factor of at least 10^2 too low.

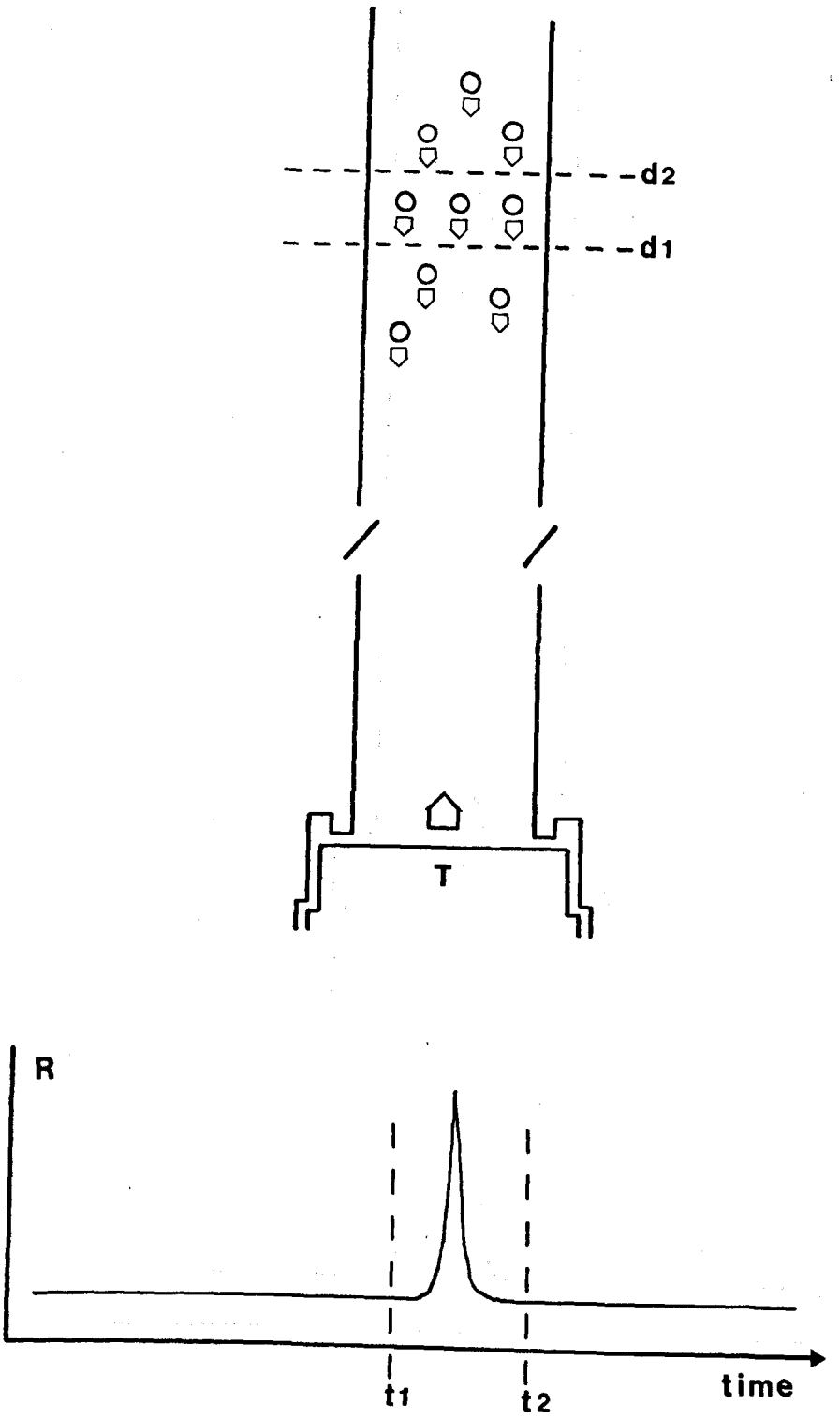

Patterson technique: signal response for in-plant distribution of microbubbles within the gated region (d2 - d1) of the field

T: transducer R: signal response

Figure 2.12

Referred to on p 87

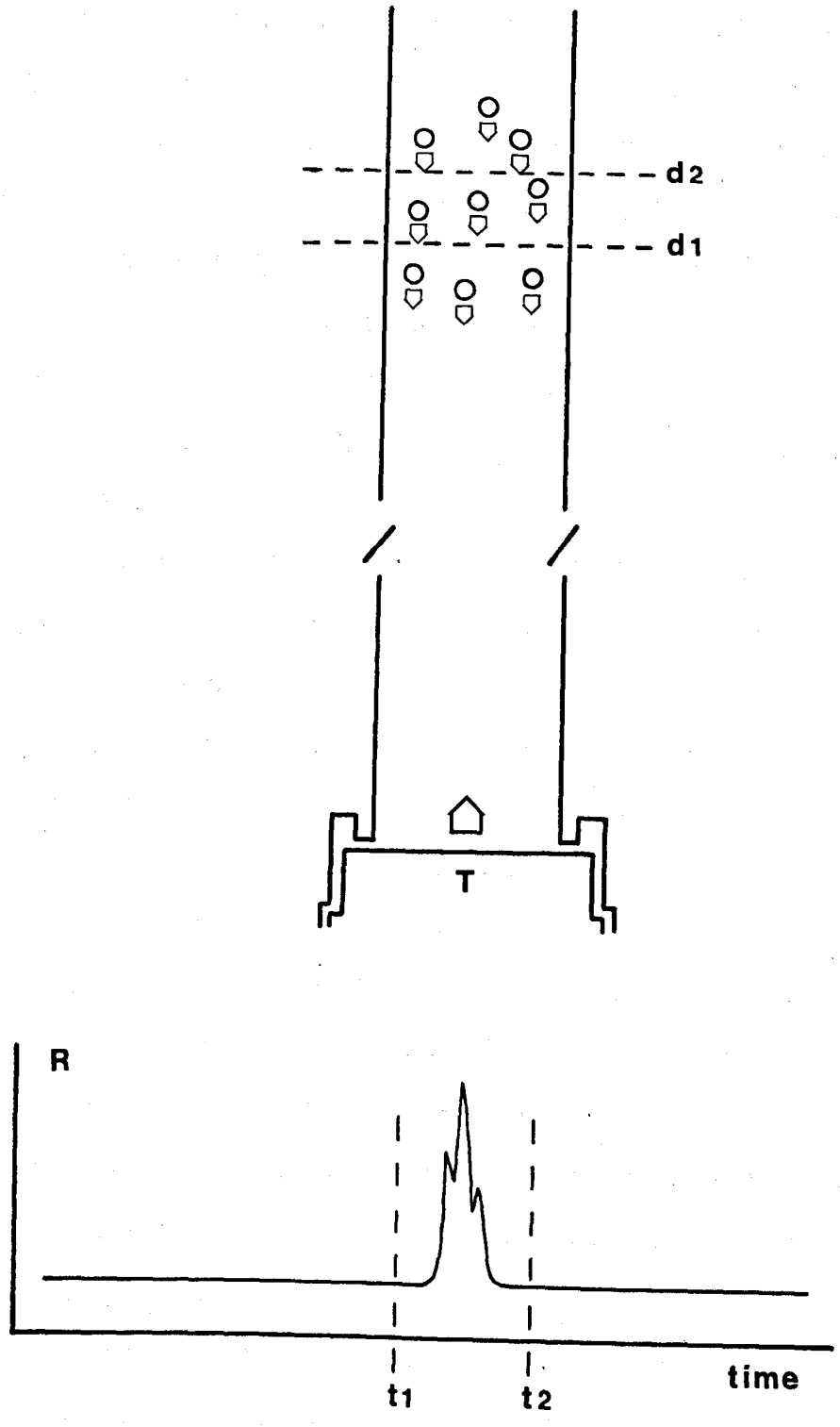

Patterson technique: signal response for a staggered population of bubbles within the gated region (d2 - d1) of the field

T: transducer R: signal response

Figure 2.13

Referred to on pp 87,99

Flow dependent count error

Patterson & Kessler (1969) in a discussion of their technique have stated that at the usual rates of flow employed in cardiopulmonary bypass the detector is likely to count each particle more than once during the time taken to traverse the 2 mm electronic gate (Patterson & Kessler, 1969; Patterson et al., 1972). Unfortunately they have failed to recognise the importance of considering flow as an integral part of the particle detection technique. The reason for this is an erroneous conclusion based upon a test that is non-representative of the cardiopulmonary bypass circuit. Patterson & Kessler (1969) state that although each particle may be counted more than once during the time taken to traverse the gate, several particles may give rise to a single echo. They concluded that although the number of echoes may not represent the exact number of particles passing the gate per unit time, the echoes are proportional to the concentration of particles. The apparent justification for this conclusion is provided by tests in which plastic microspheres were circulated around a saline filled closed loop circuit of tubing. They observed that as the flow rate was increased the number of counts tended to remain constant. This they explained by stating that a doubling in flow rate propels twice as many particles through the gate per unit time, but because the transit time is halved the count remains constant. While these tests do indeed suggest that the system provides a measure of concentration irrespective of flow, it must be stressed that it is a special case and totally unrepresentative of the cardiopulmonary bypass circuit. Yet the same argument has been quoted on a number of occasions and implied that it is applicable to the cardiopulmonary bypass circuit (Patterson & Kessler, 1969; Kessler & Patterson, 1970; Brennan et al., 1971; Patterson

et al., 1971; Patterson et al., 1972).

Both the limitations of the closed loop tests and the importance of considering flow as part of a particle detection technique may be appreciated by analysing the closed loop test using the source-sink model. As a result of one test in which a single plastic microsphere was circulated within a closed loop the relationship for echoes per minute and rate of flow as illustrated in Fig.2.14 was obtained (Patterson & Kessler, 1969). At low flow rates (3 $L.min^{-1}$) variation in flow rate is shown to be accompanied by a variation in echo frequency (Fig.2.14 continuous line). Above 3 $L.min^{-1}$ the echo frequency is observed to be reasonably constant.

Analysis of the particle count for a closed loop system containing one detectable particle

Assuming the flow through the circuit to be constant, the time taken for a particle to pass through the electronic gate; the gate transit time $t = \frac{d}{v}$ where d is the gate width and v the particle velocity. The circuit transit time $T = \frac{L}{v}$ where L is the length of the circuit.

The count per particle per unit time = t.f

where f is the pulse repetition frequency of the ultrasound source.

The number of circuit transitions per unit time = $\frac{1}{T}$

Hence the total count per particle per unit time = $\frac{t.f}{T}$

Since $t.f = \frac{f.d}{v}$ and $\frac{1}{T} = \frac{v}{L}$,

the total count per particle per unit time = $\frac{f.d}{v} \times \frac{v}{L}$

Now since for this system f, d and L are constant the count per particle per minute is constant and therefore independent of particle velocity. But this is only so for this special case in which the

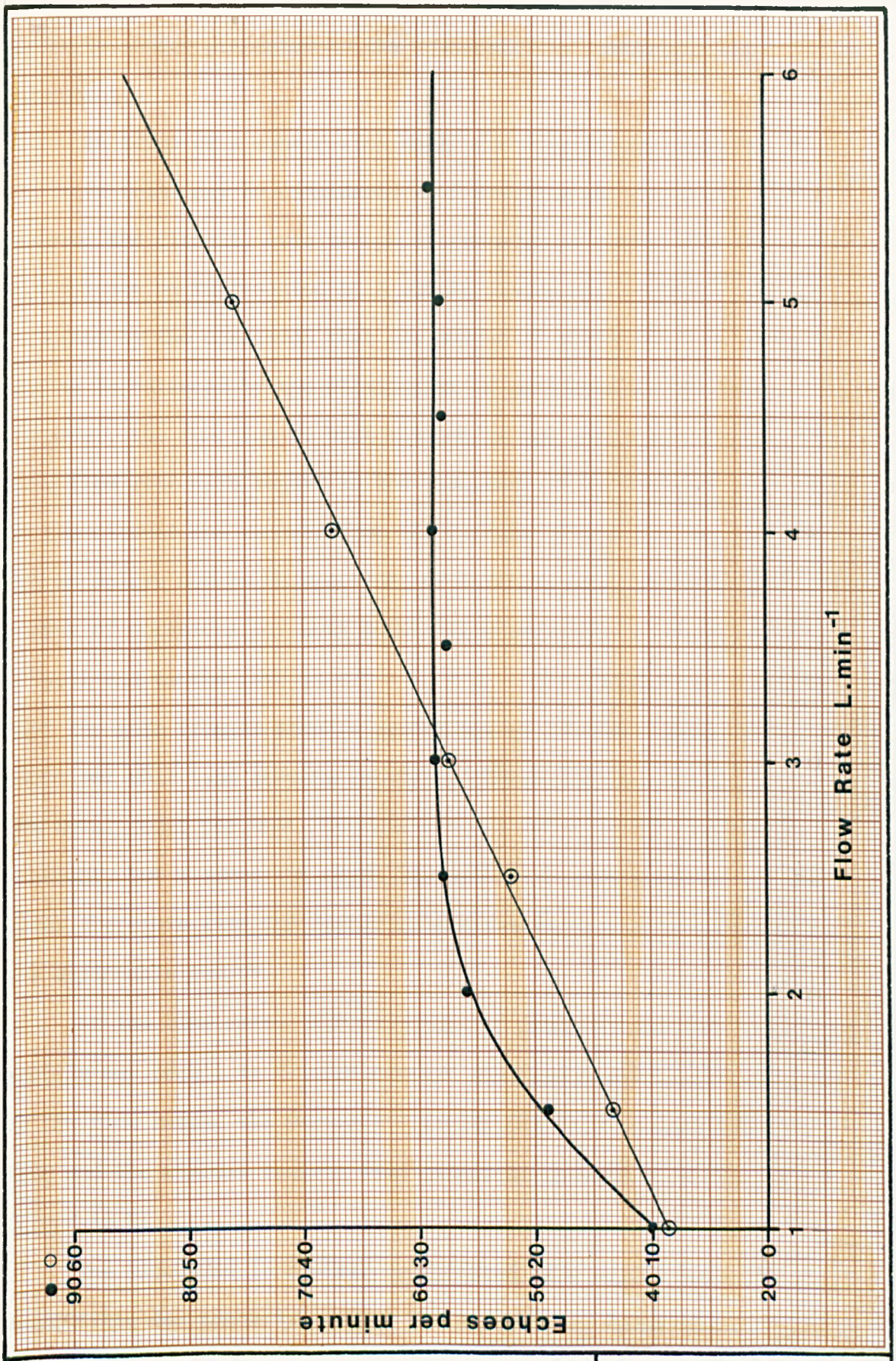

Echo rate - flow relationship after Patterson & Kessler, 1969

As reported
Flow corrected

Figure 2.14

Referred to on pp 91, 97

particle source presented to the transducer is completely flow dependent.

In terms of a source-sink model the closed loop circuit used in these tests may be considered as containing an unsinkable source. However the circuit, even though it contains no sinks, may for convenience be represented by a single source and a single sink constrained by the condition that the output of particles from the source is balanced by the elimination of particles by the sink. Moreover, the function of both the source and sink are solely dependent upon flow rate with regard to the frequency at which they are presented to the circuit and removed from the circuit (Fig.2.15). Assuming there are no delays due to obstructions or velocity profile influences the number of occasions per unit time that a particle is presented to the circuit and to the gate is $v/L = S_o = S_i = Kv$. Because it is assumed that the gate transit time is determined by the same velocity v, the count per unit time remains constant. For a system containing n particles the total count per unit time would also, under these conditions, be constant, but n times the count derived for a single particle. The model therefore fits the foregoing derivation of count frequency for the unsinkable source.

At low flow rates, the influence of obstructions and velocity profile may result in alinear circuit and gate transit times. Hence at low flow rates, the particle velocity determining the gate transit time and the circuit transit time cannot be assumed to be the same (Fig.2.15 B).

The situation is further complicated if a roller pump is responsible for promoting flow. The movement of fluid under roller pump conditions is by no means constant and while it may be reasonable to calculate the circuit transit time by using the mean particle

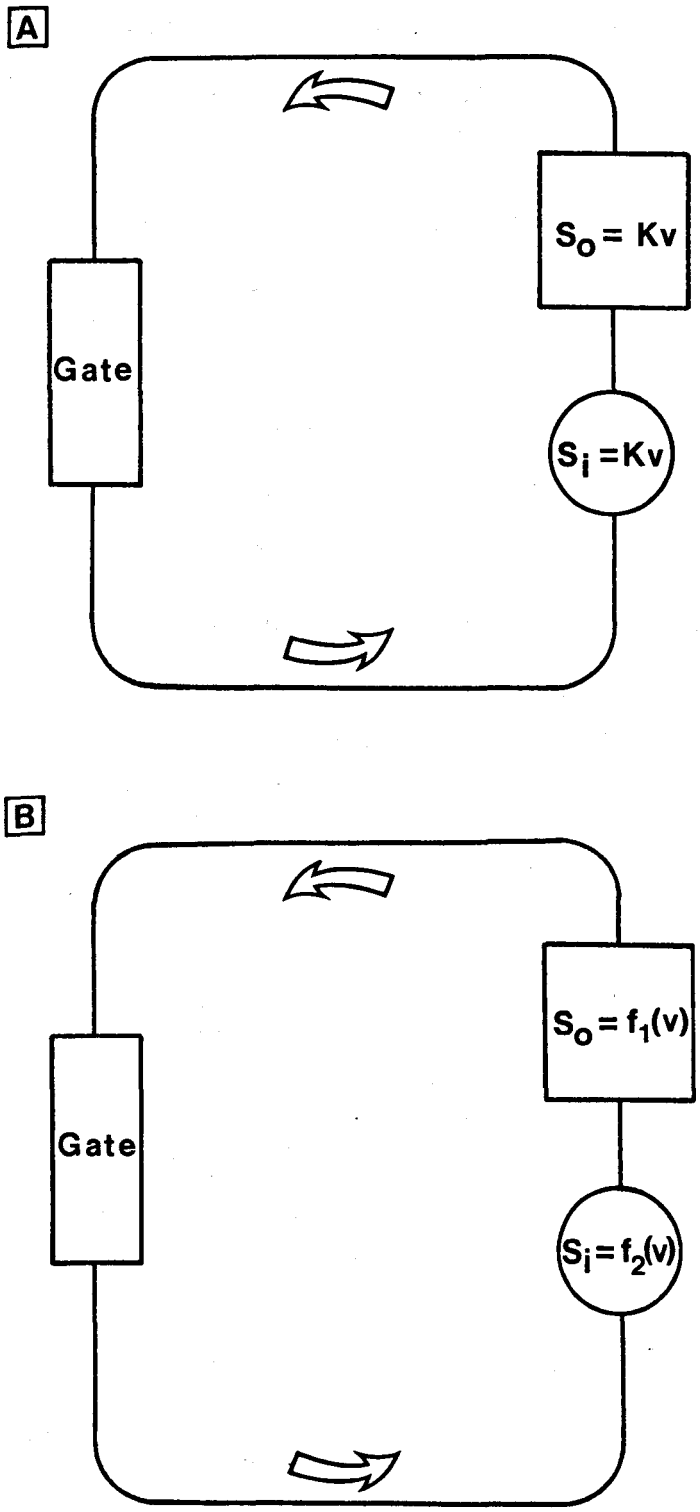

Source sink analysis of echo counts
A source constant B source variable
K is constant, v the partile velocity

Figure 2.15 A & B

Referred to on p 93

velocity v_m (i.e. $T = \frac{L}{v_m}$) the mean particle velocity cannot be used when calculating the gate transit time. The actual velocity within the volume of insonification is necessary for determining this value (i.e. $t = \frac{d}{v_i}$ where v_i is the velocity while passing through the gate).

Under these conditions, the average circuit transit time

$$T_a = \frac{1}{N} \sum_{i=o}^{N} T_i$$

and the average gate transit time t_a

$$= \frac{1}{N} \sum_{i=o}^{N} t_i$$

Where N is the number of cycles of the circuit per unit time. If the latter is influenced only by the prevailing velocity

$$t_a = \frac{1}{N} \sum_{i=o}^{N} \frac{d}{v_i} = \frac{d}{N} \sum_{i-o}^{N} \frac{1}{v_i}$$

The average count per particle per unit time:

$$C_{av} = \frac{\frac{f.d}{N} \sum_{i=o}^{N} \frac{1}{v_i}}{\frac{1}{N} \sum_{i=o}^{N} T_i} = \frac{f.d \sum_{i=o}^{N} \frac{1}{v_i}}{\sum_{i=o}^{N} T_i}$$

Because obstructions such as drag imposed by the tubing wall increase the transit time, T_i, it is clear that a departure from the constant count frequency observed at the higher flow rates is inevitable. Such conditions would account for the downward trend in count frequency observed by Patterson and Kessler (1969) in their circulation tests using microspheres suspended in saline.

Practical circuit representation

The analysis and source-sink representation for the closed loop circuit containing plastic microspheres provides an explanation for the observed frequency count-flow relationship. However the most important result of the analysis is the indication it provides for the requirements that must be satisfied by the sources and sinks in order that the particle velocity may be ignored as part of the particle detection technique. These requirements are that the actual sources and sinks be linear and equal functions of velocity. In a practical cardiopulmonary bypass situation the sources and sinks need not be linear or equal functions of flow velocity or, indeed, functionally dependent upon flow velocity. Where such sources and sinks are present in a circuit, the circuit transit time no longer has any significance as far as the particle count is concerned. However the rate at which the particle population is passed through the volume of insonifcation will be dependent upon particle velocity. For these reasons it is imperative that the particle count be flow related so that only a single count per particle is derived for a population of particles passing through the volume of insonifcation. This is achieved by making the interval between pulses, $t_p = d/v_i$, the gate transit time. Since the count per particle = t.f, then under these conditions the count per particle $C_p = t_p.f$

$$C_p = t_p.f = \frac{d.f}{v_i}$$

but $f = \frac{1}{t_p}$

$$\therefore C_p = \frac{d}{v_i} \times \frac{v_i}{d} = 1$$

The error implicit in neglecting the particle velocity as part of a particle detection technique may be derived by comparing the gate transit time to the pulse to pulse interval. The ratio of

gate transit time to pulse to pulse interval provides the flow dependent count error in terms of the count per particle for one passage through the gate. The count-flow relationship is parabolic in form (Fig.2.16) and may be described by the equation for the count per gate transit time, $C = \frac{6}{F}$ where F is the flow rate in litres per minute.

It is interesting to note that in applying this count-flow relationship to the Patterson & Kessler single microsphere test curve (Patterson & Kessler, 1969) an approximate straight line relationship is obtained (Fig.2.14 o thin line). This would suggest that at low flow rates the frequency with which the microsphere presented to the gate was no longer a linear function of flow velocity. Such a condition is more representative of a practical situation.

Bubble Sizing Limitations

In an attempt to quantify their technique Patterson & Kessler have used plastic microspheres to determine the sensitivity of the detector and the manner in which it is applied (Patterson & Kessler, 1969; Kessler & Patterson, 1970; Patterson et al., 1971). Unfortunately the use of plastic microspheres only provides a measure of the instrument sensitivity to plastic microspheres and the results cannot be directly extrapolated to estimate the sizes of particles of other types. The degree of scatter from a particle is dependent upon the the compressibility and density of the constituent particle material so that the amplitude of the received signal is in some measure determined by the nature of the material. In their communications describing the technique, the interpretation of signal amplitudes was made by relating them to equivalent signal amplitudes received

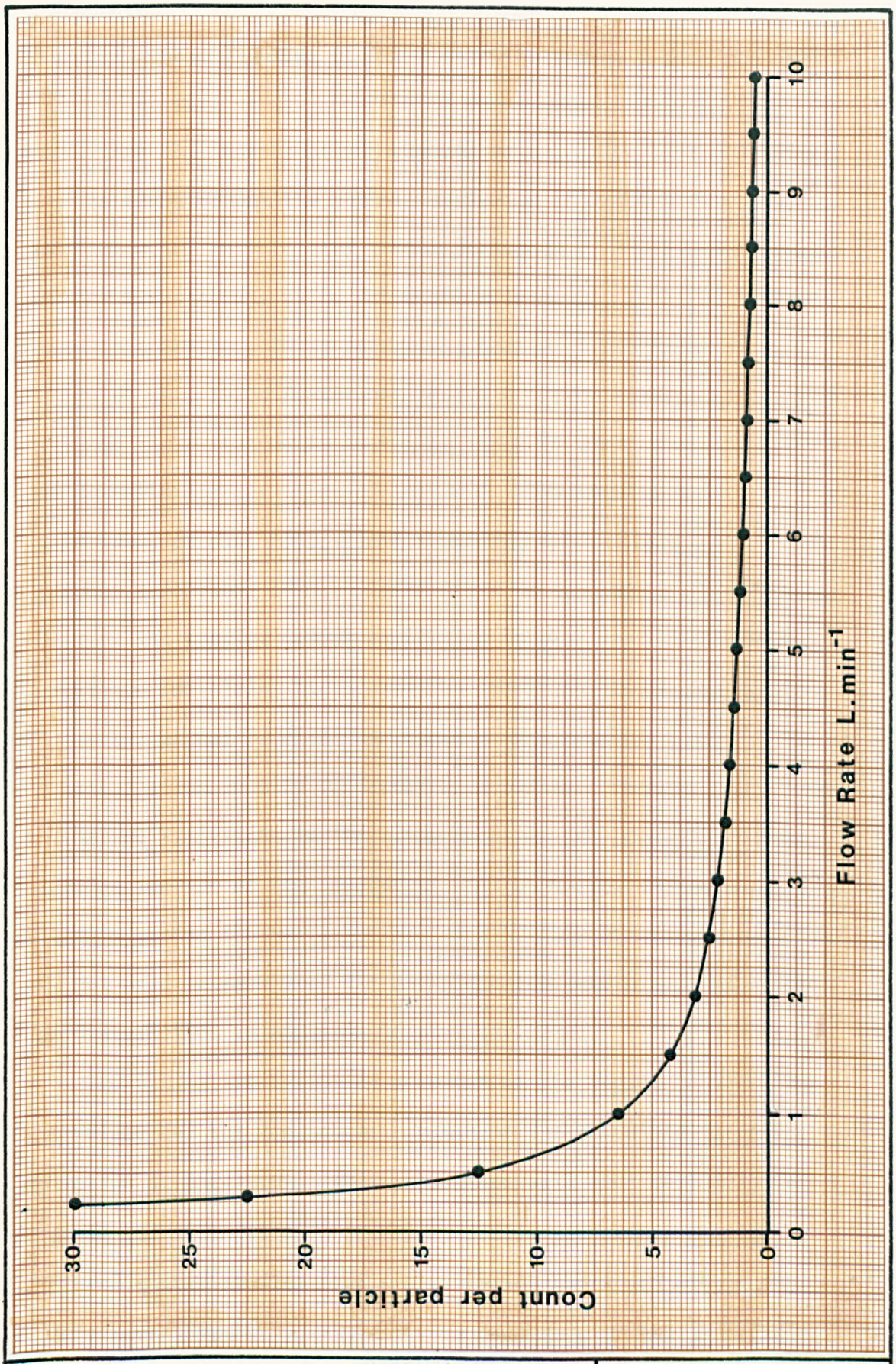

Count-flow rate relationship for a pulsed detection system having a fixed pulse repetition frequency

Figure 2.16

Referred to on p 97

from plastic microspheres of known size (Patterson & Kessler, 1969; Patterson et al., 1972). However in other communications it was stated that the instrument was capable of detecting particles above 50 μm in diameter but the authors neglected to mention that this size limitation only relates to the detection of plastic microspheres (Kessler & Patterson, 1970; Patterson & Twichell, 1971; Brennan, Patterson & Kessler, 1971; Patterson, Kessler & Bergland, 1971; Carlson et al., 1973; Patterson, Wasser & Porro, 1974). In some instances these statements have been taken to imply that the calibration is valid for all types of particle, when in fact this is not so (Carlson, et al., 1972; Clark & Weldon, 1972; Simmons et al., 1972; Gallagher & Pearson, 1973). Calibration in the manner described by Patterson and Kessler (1969) would also suggest that the technique is suitable for sizing microparticles according to the amplitude of the scatter signal received and capable of providing a measure of the distribution in size of detected particles. However there exists an inherent limitation in the arrangement of the transducer that precludes the use of the instrument for meaningful sizing of microparticles within the gated volume. Fortunately Patterson & Kessler have not used or advocated the technique for determining particle size distribution in addition to particle count.

The sizing limitation is a result of the region between the gate volume and the transducer containing the immediate incoming population of particles. This population will most certainly be variable and will act as a secondary source of scatter for the scattered energy arising from the particles contained within the gated volume (Fig.2.13). Similarly the amplitude of the propagating pulse of ultrasound will be attenuated by the presence of the incoming population of particles. The received signal amplitude cannot,

therefore, be reliably related to the size of the particles detected within the gate.

Discussion

The analysis has revealed that for the absolute quantitative measurement of bubble population in terms of both sizes and number, the Patterson-Kessler technique is severely limited. Fortunately the nature of the bypass studies in which this technique has been generally applied have been such that the limitations have been largely avoided or diminished as far as their influence upon the conclusions are concerned.

In studies, such as the comparative study of oxygenators (Kessler & Patterson, 1970) or microembolic studies related to cerebral blood flow and metabolism (Brennan et al., 1971) where the blood flow in the extracorporeal circuit is maintained fairly constant, comparative measurements of particle count are acceptable even though they are not absolute. Such studies avoid the flow dependent count limitation. However this limitation has not been universally avoided. Patterson, Wasser & Porro (1974) have reported a slow rise in particle count over a three hour bypass period amounting to a total 1.5 fold increase. Although the blood flow rate was maintained at 1.5 to 2 $L.min^{-1}$ a reduction to 1.5 $L.min^{-1}$ over the period of bypass would be sufficient to account for this 1.5 fold increase on the basis of the flow dependent count relationship alone. This once again illustrates that the limitation was not even appreciated.

Although plastic microspheres have been used to supposedly calibrate the instrument for sizing purposes no attempt appears to have been made to determine the particle size distributions in any of the reported studies undertaken using this technique. While such

an omission avoids erroneous conclusions based upon non-representative particle sizing, it must also introduce some doubts concerning the validity of conclusions supposedly based upon quantitative estimation of bubble populations. A comparative study of oxygenators (Kessler & Patterson, 1970; simmons et al., 1972), for example, is incomplete without an estimation of particle size distribution. Studies of micro-embolic encephalopathy (Brennan et al., 1971; Patterson et al., 1971; Carlson et al., 1972, 1973; Patterson et al., 1974) are similarly incomplete without an estimation of particle size distribution.

In studies where extracorporeal filters have been evaluated as devices for removing microparticles (Patterson & Twichell, 1971; Patterson, Kessler & Bergland 1971; Patterson, Wasser & Porro, 1974) the count error limitation is effectively diminished because of the observed wide differences in count before and after the filters considered. Similarly in comparisons of bubble and membrane oxygenators as sources of microparticles (Carlson et al., 1972, 1973) the large differences between the counts observed indicate that the count errors involved would not substantially alter any conclusions made concerning the relative magnitude of the microparticle populations released. However, even though the count error limitation may be reduced in such studies, the evaluation is still incomplete without an estimate of size distribution.

Chapter 3

FLOW DEPENDENT DETECTOR DESIGN: PHYSICAL CONSIDERATIONS

The review of existing techniques suggests, despite the recognised shortcomings, that the perturbation of an ultrasound field by a bubble is sufficiently discernable from the small perturbation due to formed elements of the blood to provide an effective basis for microbubble detection. It is unfortunate that the limitations inherent in all the techniques considered have prevented the use of any one of these techniques per se.

By recognising the significance of the limitations observed and the importance of establishing sound physical principles, an attempt has been made to develop an effective quantitative technique for microbubble analysis in whole blood during extracorporeal circulation.

A number of considerations favour the use of pulsed ultrasound for microbubble detection. The principal considerations are:

1. the pronounced, measurable perturbation produced by bubbles compared with that of the formed elements of the blood. Pulsed ultrasound is potentially the most sensitive.
2. the relative transparency of blood to ultrasound compared with electromagnetic radiation within the visible spectrum.
3. the absence of demonstrable damage to whole blood or tissues by diagnostic intensity levels of ultrasound.
4. the facility for establishing flow related measurements by using pulsed ultrasound.

Ultrasound incident upon a gas bubble contained within a liquid produces a forced vibration of the gas within the bubble leading to a dissipation of energy by scattering and absorption. Measurement of back scattered energy is the basis of the flow related technique. For bubbles of radius R > 10 μm the acoustic properties may be derived without considering the viscous and thermal losses which exhibit such significant effect on both scatter and absorption below 10 μm radius. The following analysis assumes that the viscous and thermal losses are negligible.

Scattering of ultrasound by a suspension of elastic spheres

A source of ultrasound ($P = P \exp j(wt-k_x)$) incident upon a volume of blood will experience scattering due to the formed elements of the blood. The presence of microbubbles within the volume would considerably enhance the components of scattered energy. Considering a beam of ultrasound of intensity I_o, incident upon a volume of blood containing microbubbles a reduction in intensity would result due to both absorption and scatter. If n(x) is a function describing a linear distribution of microbubbles along the incident beam, the decrease in the incident intensity δI over a distance δx may be defined for the bubble population by the expression:

$$\delta I = -\alpha I n(x) \delta x \qquad (\alpha: \text{attenuation factor})$$

Where δI represents the total reduction in intensity due to absorption and scatter by the population of bubbles. A similar expression may be defined for the reduction in intensity due to the population of blood cells. However it is assumed that the attenuation due to the blood cell population is small in comparison with the attenuation due to the presence of microbubbles.

Since $\delta I = -\alpha I n(x) \delta x$

$$\frac{\delta I}{I} = -\alpha n(x) \delta x$$

Integrating $$\int \frac{dI}{I} = -\int_o^d \alpha n(x) dx$$

Where it is assumed that d is the diameter of a cylindrical vessel in which the blood is situated.

$$\log_e I = -\alpha \int_o^d n(x) dx + C$$

For $x = o$, $C = \log_e I$:

$$\therefore \log_e \frac{I}{I_o} = -\alpha \int_o^d n(x) dx$$

$$\therefore I = I_o \exp \left[-\alpha \int_o^d n(x) dx \right]$$

For a square section volume of insonification

$$I = I_o \exp -\alpha n(x) L$$

Where L is the linear dimension of the square section.

For the situation in which the bubbles are small in comparison with the wavelength of the incident source of ultrasound, the local pressure P_1 and the particle velocity of the incident wave may be assumed to be uniform within its vicinity. Under these conditions the bubbles may be considered as a source of secondary spherical waves. These waves interfere with the incident beam to produce scattered waves, the amplitude of which exhibit an angular distribution. If it can be assumed that the sources of scatter exhibit no preferred orientations then, to a first approximation the sources of scatter may be treated as flexible spheres that pulsate elastically under the influence of the alternating pressure.

The decrease in intensity due to scatter from a population of bubbles in a rectangular section of blood

$$I_{xs} = \sigma I \exp\left[-\alpha n(x) L\right]$$

Where σ is the coefficient of scattering.

By applying particular boundary conditions Rschevsky (1963) has demonstrated that the scattered intensity per unit solid angle, produced by a flexible sphere is defined by the expression:

$$I_s = I \frac{k^4 R^6}{9r^2} \left[\frac{\rho_2 c_2^2 - \rho_1 c_1^2}{\rho_2 c_2^2} + \frac{3(\rho_1 - \rho_2)\cos\theta}{2\rho_2 + \rho_1} \right]^2$$

Where θ is the angle between the incident and scattered wave, I the intensity of the wave of ultrasound incident upon the sphere, R the radius of the sphere, r the distance of the point of observation from the sphere, $\rho_2 c_2^2$ the adiabatic bulk modulus of the sphere determined by its density ρ_2 and acoustic velocity of propagation of sound c_2, $\rho_1 c_1^2$ the adiabatic bulk modulus of the suspending medium, ρ_1 the density of the sphere, ρ_2 the density of the suspending medium and k the propagation constant which is a function of wavelength λ of the incident source of ultrasound, i.e. $k = \frac{2\pi}{\lambda} = \frac{\omega}{c}$ (ω, the radial frequency and c the acoustic velocity of propagation).

For $\theta = 180^o$, $\cos\theta = -1$.

$$\therefore \quad I_s = \frac{Ik^4 R^6}{9r^2} \left[\frac{\rho_2 c_2^2 - \rho_1 c_1^2}{\rho_2 c_2^2} - \frac{3(\rho_1 - \rho_2)}{2\rho_2 + \rho_1} \right]^2$$

$$\therefore \quad \frac{I_s}{I} = \frac{k^4 R^6}{9r^2} \left[\frac{\rho_2 c_2^2 - \rho_1 c_1^2}{\rho_2 c_2^2} - \frac{3(\rho_1 - \rho_1)}{2\rho_2 + \rho_1} \right]^2$$

Acoustic intensity $I = \frac{p^2}{2\rho c}$ where P is the acoustic pressure, ρ the density of the medium in which the sound is propagating and c the acoustic velocity of propagation of the sound within the medium,

the perturbation may also be expressed in terms of acoustic pressure.

$$\text{Thus} \quad \frac{I_s}{I} = \frac{P_s^2}{P^2} = \frac{k^4 R^6}{9r^2}\left[\frac{\rho_2 c_2^2 - \rho_1 c_1^2}{\rho_2 c_2^2} + \frac{3(\rho_1 - \rho_2)}{2\rho_2 + \rho_1}\cos\theta\right]^2$$

$$\therefore \quad \frac{P_s}{P} = \frac{k^2 R^3}{3r}\left[\frac{\rho_2 c_2^2 - \rho_1 c_1^2}{\rho_2 c_2^2} + \frac{3(\rho_1 - \rho_2)}{2\rho_2 + \rho_1}\cos\theta\right]$$

For $\cos\theta = -1$

$$\frac{P_s}{P} = \frac{(kR)^2}{3}\left\{\frac{R}{r}\right\}\left[\frac{\rho_2 c_2^2 - \rho_1 c_1^2}{\rho_2 c_2^2} - \frac{3(\rho_1 - \rho_2)}{2\rho_2 + \rho_1}\right]$$

This term is only valid for $kr \gg 1$ and $kR \ll 1$. In order for the expression to be valid for all values of kr volumetric resonance and the reactive component of acoustic impedance must be taken into consideration. Volumetric resonance is taken into account by multiplying the compliance $\left[\frac{\rho_2 c_2^2 - \rho_1 c_1^2}{\rho_2 c_2^2}\right]$ by a resonance factors of the form $\left[1 + \frac{j}{Q}\left\{\frac{\omega}{\omega_o}\right\} - \left\{\frac{\omega}{\omega_o}\right\}^2\right]^{-1}$ where Q is termed the Q factors and $\frac{1}{Q}$ represents the damping of the resonant system. ω_o is the resonant frequency.

Since $\frac{(kR)^2}{3} = \left\{\frac{\omega}{\omega_o}\right\}^2 \frac{\rho_2 c_2^2}{\rho_1 c_1^2}$ substituting for kR in the $\frac{P_s}{P}$ expression and including volumetric resonance factor

$$\frac{Ps}{P} = -\left\{\frac{R}{r}\right\}\left\{\frac{\omega}{\omega_o}\right\}^2 \frac{\rho_2 c_2^2}{\rho_1 c_1^2}\left[\frac{\rho_2 c_2^2 - \rho_1 c_1^2}{\rho_2 c_2^2}\right]\left[1 + \frac{j}{Q}\left\{\frac{\omega}{\omega_o}\right\} - \left\{\frac{\omega}{\omega_o}\right\}^2\right]^{-1}$$

$$+ \left\{\frac{R}{r}\right\}\left\{\frac{\omega}{\omega_o}\right\}^2 \frac{\rho_2 c_2^2}{\rho_1 c_1^2} \frac{3(\rho_1 - \rho_2)}{2\rho_2 + \rho_1}\cos\theta$$

Substituting now for $\frac{(kR)^2}{3} = \left\{\frac{\omega}{\omega_o}\right\}^2 \cdot \frac{\rho_2 c_2^2}{\rho_1 c_1^2}$

$$\frac{Ps}{P} = -\left\{\frac{R}{r}\right\}\left[\frac{\rho_2 c_2^2 - \rho_1 c_1^2}{\rho_1 c_1^2}\right]\left[\frac{\left\{\frac{\omega}{\omega_o}\right\}^2}{1 + \frac{j}{Q}\left\{\frac{\omega}{\omega_o}\right\} - \left\{\frac{\omega}{\omega_o}\right\}^2}\right]$$

$$+ \left\{\frac{R}{r}\right\} \cdot \frac{(kR)^2}{3} \cdot \frac{3(\rho_1 - \rho_2)}{2\rho_2 + \rho_1} \cos\theta$$

In order to include the reactive component of acoustic impedance it is necessary to multiply the dipole pressure term $\frac{(\rho_1 - \rho_2)}{2\rho_2 + \rho_1}\cos\theta$ by

$$\left[\left\{\frac{R}{r}\right\}(kR)^2 - j\left\{\frac{R}{r}\right\} kR\right] \quad \text{rather than} \quad \left\{\frac{R}{r}\right\}(kR)^2$$

$$\therefore \frac{Ps}{P} = -\left\{\frac{R}{r}\right\}\left[\frac{\rho_2 c_2^2 - \rho_1 c_1^2}{\rho_1 c_1^2}\right]\left[\frac{\left\{\frac{\omega}{\omega_o}\right\}^2}{1 + \frac{j}{Q}\left\{\frac{\omega}{\omega_o}\right\} - \left\{\frac{\omega}{\omega_o}\right\}^2}\right]$$

$$+ \left[\left\{\frac{R}{r}\right\}(kR)^2 - j\left\{\frac{R}{r}\right\} kR\right]\frac{(\rho_1 - \rho_2)}{2\rho_2 + \rho_1}\cos\theta$$

This expression is now valid for any homogeneous sphere, for all values of kr but limited to values of $kR \ll 1$. For a gas sphere $\rho_2 \ll \rho_1$ and $\rho_2 c_2^2 \ll \rho_1 c_1^2$

Hence $$\frac{Ps}{P} = -\left\{\frac{R}{r}\right\}\left[\frac{\left\{\frac{\omega}{\omega_o}\right\}^2}{1 + \frac{j}{Q}\left\{\frac{\omega}{\omega_o}\right\} - \left\{\frac{\omega}{\omega_o}\right\}^2}\right]$$

$$+ \left[\left\{\frac{R}{r}\right\}(kR)^2 - j\left\{\frac{R}{r}\right\} kR\right]\cos\theta$$

When $kr \gg 1$

$$\frac{P_s}{P} = -\left\{\frac{R}{r}\right\} \left[\frac{\left\{\frac{\omega}{\omega_o}\right\}^2}{1 + \frac{j}{Q}\left\{\frac{\omega}{\omega_o}\right\} - \left\{\frac{\omega}{\omega_o}\right\}^2} - (kR)^2 \cos\theta \right]$$

At frequencies well above resonance the volumetric resonance factor tends to unity

$$\therefore \quad \frac{P_s}{P} = \left\{\frac{R}{r}\right\} \left[1 - (kR)^2 \cos\theta\right]$$

and for a wide range of kR values $\frac{P_s}{P} \alpha \left\{\frac{R}{r}\right\}$. At resonance:

$$\frac{P_s}{P} = Q \left\{\frac{R}{r}\right\}$$

Well below resonance the dipole pressure terms tends to zero and

$$\frac{P_s}{P} \simeq \left\{\frac{R}{r}\right\} \left\{\frac{\omega}{\omega_o}\right\}^2$$

$$= \left\{\frac{R}{r}\right\} \cdot \frac{(kR)^2}{3} \cdot \frac{\rho_1 c_1^2}{\rho_2 c_2^2}$$

Relating the perturbation pressure ratio to bubble size, it is evident that for values of kr>>1 and kR<<1, well above resonance, $\frac{P_s}{P} \alpha R$, the radius of the bubble and well below resonance $\frac{P_s}{P} \alpha R^3$. For values of kR>>1, the assumption that the incident field is uniform over the surface of the sphere is no longer valid. Non-uniformity of field may be taken into account by the introduction of an infinite series of spherical harmonics within the expression for the perturbation pressure ratio. The monopole term, independent of θ, and the dipole term, proportional to $\cos\theta$, represent the first two terms of such a series. Because of the spherical nature of the scatter source the subsequent terms of this series are not merely cosines of θ harmonics but functions of $\cos\theta$, termed Legendre polynomials and

denoted by the expression $P_n(\cos\theta)$

where $P_o(\cos\theta) = 1$

$P_1(\cos\theta) = \cos\theta$

$P_2(\cos\theta) = \frac{1}{2}(3\cos\theta^2 - 1)$

$P_3(\cos\theta) = \frac{1}{2}(5\cos\theta^3 - 3\cos\theta)$

thus for $kR \gg 1$

$$\frac{Ps}{P} = -\left\{\frac{R}{r}\right\}\left[\frac{\rho_2 c_2^2 - \rho_1 c_1^2}{\rho_1 c_1^2}\right]\left[\frac{\left\{\frac{\omega}{\omega_o}\right\}^2}{1 + \frac{j}{Q}\left\{\frac{\omega}{\omega_o}\right\} - \left\{\frac{\omega}{\omega_o}\right\}^2}\right] P_o(\cos\theta)$$

$$+ \left[\left\{\frac{R}{r}\right\}(kR)^2 - j\left\{\frac{R}{r}\right\}^2 kR\right]\frac{\rho_1 - \rho_2}{2\rho_2 + \rho_1} P_1(\cos\theta) + \ldots\ldots$$

when $kR \gg 1$ the perturbation pressure ratio at the surface of the sphere ($r = R$) is asymptotic to a value of 0.5 (Hickling, 1962). The implication of this statement is that the pressure at the surface of the sphere is half that of the incident pressure. In practice this is not so, since under these conditions, the pressure distribution over the surface would not be completely uniform. However it is possible to consider the back scatter source as the product of a perturbation pressure, $\frac{P}{2}$ uniformly distributed over the surface of the sphere and the effective surface of scatter. The total radiated power intensity is, under these conditions ($kR \gg 1$):

$$I_s = \frac{P^2}{4\rho_1 c_1} \times 4\pi R^2 = \frac{P^2 \pi R^2}{\rho_1 c_1}$$

and is therefore proportional to the square of the radius. Consequently the received pressure and the detector signal amplitude are proportional to the radius of the sphere. Clearly the effective scattering cross-section corresponds to the actual geometrical cross-section of the

sphere (πR^2). At resonance the scattering cross-section may be considerably greater than the geometrical cross-section. However in a well damped system the scattering cross-section may not be substantially different from the geometrical cross-section.

If each bubble can be assumed to scatter sound independently of the others and interference between scattered wavelets, multiple scattering and absorption are neglected, the scattering intensity, I_{ST}, due to all of the bubbles within the volume of insonification, V, is related to the perturbation intensity ratio for a single bubble, by the expression:

$$\frac{I_{ST}}{I} = NV \left| \frac{I_s}{I} \right|$$

where N is the number of bubbles per unit volume.

Interference between wavelets results in a modification of the angular distribution of the scattered wave, reducing it in the forward direction while augmenting it in the backward and side directions. Consequently, for a population of bubbles each of radius R, the intensity ratio takes the following form (Morse & Ingard, 1969):

$$\frac{I_{ST}}{I} = NV \left| \frac{I_s}{I} \right| \sqrt{\frac{2\pi}{8}} \left| \frac{k_R}{k} \right|^4 \left(k_R R \sin \frac{\theta}{2} \right)^2 \exp\left(-2k_R^2 R^2 \sin^2 \frac{\theta}{2} \right)$$

where $k_R = \frac{\omega}{c_R}$ the wave number for the bubble containing medium.

For $\theta = 180^o$, $\sin^2 \frac{\theta}{2} = 1$

$$\therefore \frac{I_{ST}}{I} = \sqrt{\frac{2\pi}{8}} NV \left| \frac{I_s}{I} \right| \left| \frac{k_R}{R} \right|^4 \left(k_R^2 R^2 \right) \exp\left(-2k_R^2 R^2 \right)$$

This expression is valid providing the region of insonification is small, or is so sparsely populated with scatter sources that the total scattered energy is a small fraction of the incident energy.

If $k_R \simeq k$:

$$\frac{I_{ST}}{I} = \sqrt{\frac{2\pi}{8}}\ NV \left[\frac{I_s}{I}\right] (k^2R^2)\ \exp\left[-2k^2R^2\right]$$

$$= \sqrt{\frac{2\pi}{8}}\ NV \left[\frac{I_s}{I}\right] (kR)^2\ \exp\left[-2(kR)^2\right]$$

$$\exp\left[-2(kR)^2\right] = 1 - 2k^2R^2 + \frac{(2k^2R^2)^2}{2!} - \frac{(2k^2R^2)^3}{3!} + \ldots$$

$$\therefore \frac{I_{ST}}{I} = \sqrt{\frac{2\pi}{8}}\ NV \left[\frac{I_s}{I}\right] (kR)^2 \left\{1 - 2k^2R^2 + \frac{(2k^2R^2)^2}{2!} - \frac{(2k^2R^2)^3}{3!} + \ldots\right\}$$

$$= \sqrt{\frac{2\pi}{8}}\ NV \left[\frac{I_s}{I}\right] \left\{(kR)^2 - 2(kR)^4 + \frac{4(kR)^6}{2!} - \ldots\right\}$$

For $kR<1$ (<25 μm radius for 10 MHz source).

$$\frac{I_{ST}}{I} = \sqrt{\frac{2\pi}{8}}\ NV \left[\frac{I_s}{I}\right] (kR)^2$$

For the situation in which the population of bubbles is heterogeneous in size, the total intensity ratio may be considered as the summation of the perturbations associated with each group of equally sized bubbles.

Thus $$\frac{I_{ST}}{I} = \sqrt{\frac{2\pi}{8}}\ V \left\{N_{R_1} \left[\frac{I_s}{I}\right]_{a1} (kR_1)^2 + N_{R_2} \left[\frac{I_s}{I}\right]_{a2} (kR_2)^2 + \ldots\right\}$$

Providing each bubble within the volume of insonification can be individually resolved using a pulsed technique, the magnitude of the perturbation and the number of perturbations of equal magnitude may be readily derived using a system of amplitude discrimination and counting. In this manner it may be possible to derive a quantitative estimate of the bubble population.

So far it has been assumed that absorption and multiple scattering may be neglected. However, in traversing the volume of insonification, energy will be lost from the incident beam due to both absorption and

scatter so that the intensity of the beam, I, incident upon each scatter source will be different depending upon the distance into the volume of insonification.

i.e. $I_{xs} = \sigma I \exp\left[-\alpha n(x)L\right]$ described earlier.

Providing that $\alpha n(x)L$ is small compared with unity the assumption that the incident beam intensity I is constant, is reasonable. However if this is not so, multiple scattering will be important and will considerably complicate the analysis.

Turbulence

Ordinarily in a turbulent region the fluctuations in compressibility and density are proportional to the square of the Mach number. Turbulence can therefore give rise to large variations in scatter and the directionality of scatter from the turbulent region (Morse & Ingard, 1969).

Scatter from formed elements of the blood

All of the formed elements of the blood scatter ultrasound. However the total scatter from platelets and leucocytes is generally considered to be negligible compared with that from erythrocytes because of the relatively small number of these cells.

If the orientation of the red cells is assumed to be random then each cell can be treated as a non-rigid sphere even though the erythrocytes are actually biconcave discs (Thompson, Mennel & Joyner, 1970). The intensity of scatter from a single blood cell can thus be determined using the theory of scatter for non-rigid spheres. Using a 5 MHz source and back scattered intensity measured at 60^{o} angle to the incident beam, 10 mm from the source of perturbation, Nishi and Livingstone (1973) reported a figure of 4.2×10^{-15} for the intensity ratio I_s/I corresponding to a single erythrocyte. If each erythrocyte is assumed to scatter sound independently of the others, and if interference between scattered wavelets, multiple scattering and absorption are neglected, the intensity of scatter is proportional to the number of erythrocytes within the volume of insonification.

Considering a sample volume of 0.5 ml (500 mm^3) containing blood, the total intensity of scatter relative to the incident beam intensity for an erythrocyte count of 5×10^6 per mm^3 is $(500 \times 5 \times 10^6 \times 4.2 \times 10^{-15}) \approx 1.05 \times 10^{-5}$ (assuming the intensity ratio for a single erythrocyte to be 4.2×10^{-15}). Well above resonance, the scattered intensity due to a sphere of gas is defined by the expression:

$$\frac{I_s}{I} = \left[\frac{R}{r}\right]^2 \left[1 + (kR)^2 \cos\theta\right]^2$$

considered earlier. For a single bubble comparable in size to that of an erythrocyte (7.5 μm dia.) the scattered intensity due to a 5 MHz source of ultrasound and measured at angle of 60^{o} to the incident beam 10 mm from the source of perturbation is

$$\frac{I_s}{I} \simeq 1.4 \times 10^{-7}$$

considered relative to the incident beam intensity.

For the situation in which pulsed ultrasound is used the effective background scatter that must be exceeded in order to distinguish individual bubbles is determined by the number of blood cells within the volume of insonification defined by the transducer face dimensions and the 'pulse width'. The latter is the product of pulse duration and the velocity of propagation of ultrasound within the medium. By suitable choice of transducer dimensions and the pulse duration, individual bubbles comparable in size to that of a single erythrocyte may be distinguished. However the presence of cellular aggregates within the same volume would diminish the degree of discrimination possible for single bubbles. For $kR \ll 1$ the intensity of scatter increases as the sixth power of the radius of the source (Morse & Ingard, 1969). Thus a blood cell aggregate of 30 μm diameter, for example, will exhibit a perturbation 10^4 times greater than a single erthrocyte.

The presence of aggregates within a volume of blood continuously circulated and oxygenated within an extracorporeal circuit have been reported on several occasions (Allardyce, et al., 1966; Ashmore, et al., 1968 and 1972; Rittenhouse, et al., 1972). However Wright and Sanderson (1975) have demonstrated that aggregation does not occur if the blood is collected into acid citrate dextrose (ACD) or citrate

phosphate dextrose (CPD) and heparin then added to the circuit prime. For blood collected directly into heparin alone and circulated at 1 $L.min^{-1}$ with oxygenation set at 3 $L.min^{-1}$ through the venous reservoir compact aggregates of both platelets and leucocytes, 35 - 108 μm diameter, were noted. By use of ACD and CPD preparations it would appear that aggregation within the extracorporeal circuit may be avoided and the background scatter minimised.

Bubble Resonance

The resonant frequency, ω_o, of a pulsating bubble is defined by the expression:

$$\omega_o = \left\{\frac{1}{R_o}\right\}\left\{\frac{3\gamma P_o}{\rho}\left[1 + \frac{2\sigma}{P_o R_o}\left(1 - \frac{\varepsilon}{3\gamma}\right)\right]\right\}^{\frac{1}{2}}$$

where R_o is the equilibrium radius of the bubble, P_o the static pressure within the liquid in which the bubble is situated, σ the surface tension of the liquid, γ the ratio of the specific heats of the gas, ρ the density of the liquid and ε a parameter varying from 1 to γ depending upon-the thermal conduction within the gas (Devin, 1959). The expression does not describe ω_o as an explicit function of R_o since ε is a function of both frequency and radius.

If the bubble is very small (R_o < 1μm) the compression and expansion of the gas contained within the bubble is isothermal ($\varepsilon = \gamma$) and the resonant frequency expression becomes:

$$\omega_o = \left\{\frac{1}{R_o}\right\}\left\{\frac{3P_o}{\rho}\left(1 + \frac{4\sigma}{3P_o R_o}\right)\right\}^{\frac{1}{2}}$$

For large bubbles (R_o> 100 μm) the pulsation of the bubble is adiabatic (ε = 1), the surface tension term is negligible and the resonant frequency expression simplifies to the following form:

$$\omega_o = \left\{\frac{1}{R_o}\right\}\left\{\frac{3\gamma P_o}{\rho}\right\}^{\frac{1}{2}}$$

Based on the general expression for resonant frequency, the relationship between bubble size and computed resonant frequency may be derived (Fig.3.1A). For blood at a temperature of 37°C and atmospheric pressure, the constants required for computing resonant frequency are:

$\gamma = 1.4$; $\rho = 1056\ \text{Kgm}^{-3}$, $\tau = 0.06\ \text{N.m}^{-1}$ $\varepsilon = 1 \rightarrow \gamma$

A more generalised expression for bubble resonance, often considered sufficient for most purposes is:

$$\omega_o = \frac{3.28\ (2\pi)}{R} \quad \text{MHz}$$

where R is the bubble radius in microns. Providing R is not less than 5 μm the effects of surface tension can be neglected and the expression is reasonably accurate.

System Damping

Because of the resistive and viscous properties of a liquid, the propagation of sound through a liquid will always be accompanied by a loss of energy and a decay in the amplitude of the beam with time as the energy is lost (Morse & Ingard, 1969). The loss of energy may be defined in terms of a system quality factor Q

$$Q = \frac{\text{energy stored per cycle}}{\text{energy lost per radian of angular frequency}}$$

$$= \frac{2\pi \text{ x energy stored per cycle}}{\text{energy lost per cycle}}$$

The reciprocal of the system quality factor relates to the system's acoustic damping and is termed the total damping constant, δ. For a liquid containing bubbles, the total damping constant may be resolved into three components, δ_{th}, the thermal damping constant due to the thermal conduction between the gas within the bubble and the surrounding liquid, δ_{rad}, the damping of sound radiation, and δ_{vis} the viscous

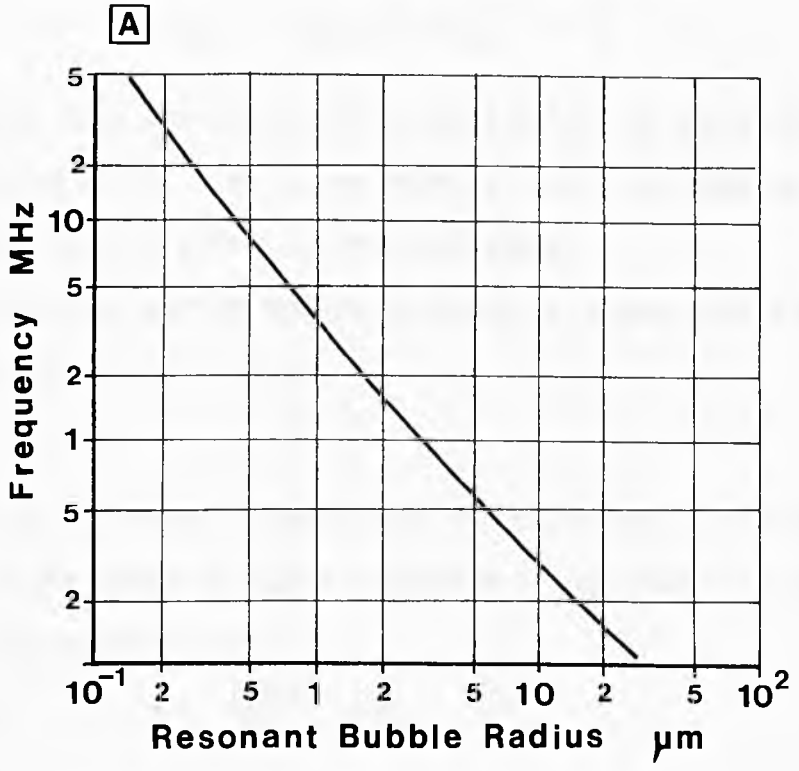

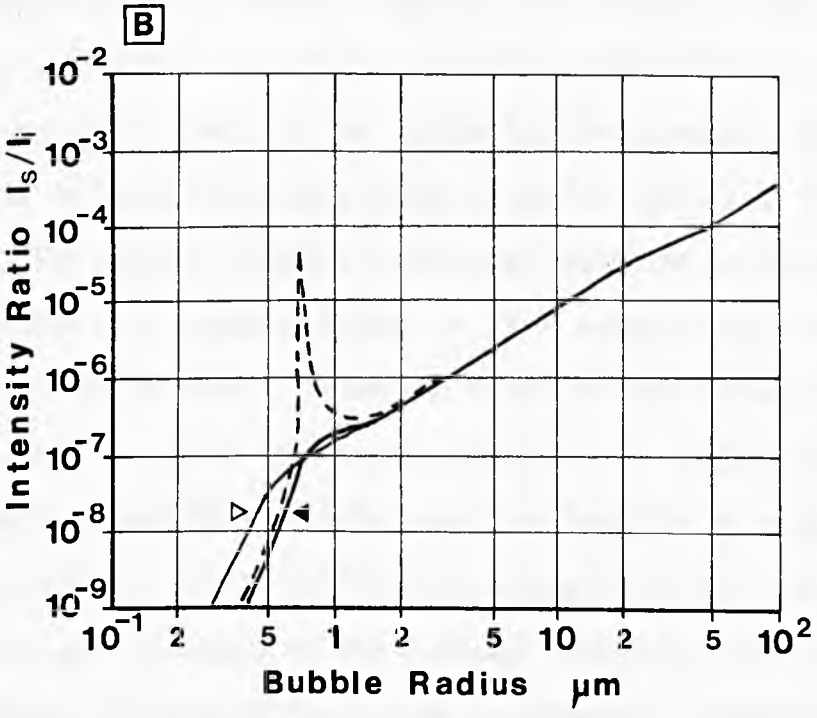

A Resonant frequency as a function of bubble radius

B Back scatter at 1 cm as a function of bubble radius for air in blood at 5 & 10MHz
▷ 10MHz ▶ 5MHz --- Undamped response

Figure 3.1 A & B

Referred to on pp 116 (A) 119 (B)

damping due to viscous forces at the gas-liquid interface.

$$\delta = \delta_{th} + \delta_{rad} + \delta_{vis} = \frac{1}{Q}$$

The damping terms are considered in more detail by Devin (1959) and Kapustina (1970). For large bubbles, kR>1, the damping terms and surface tension effect become negligible.

In relating system damping to decay of signal amplitude the following expression is used:

$$\delta = \frac{\pi}{\eta}$$

where η is the natural logarithmic decrement and is directly related to the decay in signal amplitude A, for free vibrations at a given resonance frequency:

$$\text{i.e.} \qquad \eta = \frac{2.303}{n} \log_{10} \frac{A_o}{A_n}$$

where A_o is the initial amplitude of the incident vibration and A_n is the amplitude value after n complete oscillations. This offers a practical approach to deriving a value for system damping.

Nishi (1972) computed the scattering cross-sections for an air bubble in blood (viscosity taken to be 0.03 Poise) at a temperature of 37°C. The results showed a pronounced reduction in the scattering cross-section of a resonant bubble in blood compared with that of a resonant bubble in water. Below the resonant bubble size, the scattering cross-section was shown to decrease rapidly. The higher viscosity of blood compared with that of water was considered to be responsible for these effects. Nishi (1972) also demonstrated that the damping terms have less influence on the resonant scattering cross-section as the static pressure of the system is increased. Within the physiological pressure range, the peaking of the scattering cross-section-bubble radius characteristic would appear to be negligible.

Pronounced peaking comparable with that of a bubble in water was observed only when the static pressure was raised to 10 atmospheres. The same form was demonstrated in the scattering intensity-bubble radius relationship (Fig.3.1B) for an air bubble in blood (Nishi & Livingstone, 1973).

The peaking at resonance is also strongly influenced by the frequency of the ultrasound used. The higher the frequency the smaller the peak response (Nishi, 1975). At 1 MHz, the peak response in blood is clearly pronounced, while at 5 MHz it is diffuse and at 10 MHz it is barely perceptible (Nishi, 1975).

On the basis of these observations, the above resonance characteristic using a 10 MHz source frequency, could be reasonably used as the basis for a pulse technique for detecting and sizing bubbles present in whole blood without introducing sizable errors that would be inherent in a bubble in water situation or at a lower operating frequency due to under-damping at resonance.

Pulse echo characteristics

The incident pulse characteristic commonly used in pulsed ultrasound applications is generally of the form:

$$\begin{aligned} P(t) &= 0 \qquad t < -\Delta t \\ &= \exp(-j\omega t), \quad -\Delta t < t < \Delta t \\ &= 0 \qquad t > \Delta t \end{aligned}$$

where ω is the angular frequency of the ultrasound and $2\Delta t$ is the pulse duration (Hickling, 1964). The incident pulse duration may also be expressed in a non-dimensionalised form $\Delta\tau = \frac{c\Delta t}{R}$ which also relates pulse length $2c\Delta t$ to the radius of the scatter source, R. For $\Delta\tau = 1$, the pulse length is equal to the scatter source diameter.

It is useful to express pulse duration in this manner since the echo structure can be significantly altered when the incident pulse length becomes greater than the scatter source diameter. For short incident pulses, the echo structure is practically unaffected by small changes in the dominant frequency x_o (where $x_o = \frac{\omega_o R}{c} = kR$). This is because the frequency spectra for such pulses are broadly distributed relative to variations in the steady state function of the echo. When the incident pulse length, $\Delta\tau$ is greater than 1 the echo structure is strongly dependent upon the dominant frequency (kR). The principal effect would appear to be the interaction of secondary with primary echoes as the pulse length is increased. In general, the first part of an echo corresponds to a rigid body reflection while the remainder corresponds to vibrations induced within the sphere. Where short incident pulses are used ($\Delta\tau < 1$), the secondary echoes due to vibrations within the sphere are separated from the primary echo due to rigid body reflection. For long incident pulses ($\Delta\tau > 1$), the secondary echoes interfere with the primary echo, the result being either constructive or destructive. The extremes correspond to high and low points in the steady state echo functions f_∞, where f_∞ is defined by:

$$P = \left\{\frac{P_o R}{2r}\right\} f_\infty \exp\left\{jk(r-ct)\right\} \quad \text{(Hickling, 1964)}.$$

The nature of the primary echo due to rigid body reflection is dependent upon the thickness of the sphere's enclosing shell. As the shell thickness is decreased the incident waves interact more strongly with the interior surface and the flexural waves so produced become more prominent while the surface waves due to the rigid body reflections become less prominent.

In the limit as the shell thickness tends to zero the echo attains the form of that received from a free-surface sphere. Where

as the echo intensity from a fluid-filled sphere can vary quite erratically (Hickling,-1964), the echo intensity from a free surface sphere is almost constant. To what extent a gas sphere or bubble in blood may be considered as a free-surface sphere is unknown, but it would seem reasonable to consider it to be a good approximation. Although such a bubble has a thin proteinaceous skin (Lee & Hairston, 1971) it is not expected to give rise to prominent surface waves. On this basis the pulse echoes from bubble inclusions should be the result of a flexural response, well defined and consistent in intensity. The kR variation in steady state function for bubble inclusions should be sufficiently small to allow the use of long pulse lengths ($\Delta\tau > 1$) without significantly influencing the echo structure.

Frequency dependence of propagation velocity

The velocity of propagation, and the corresponding value of k, for ultrasound within a liquid is dependent upon the physical conditions prevailing within the liquid. In blood, the propagation velocity is also influenced by physiological conditions. The extent to which these conditions influence propagation velocity must be considered.

Cartensen and Schwan (1959) have observed a frequency dependent dispersion of propagation velocity for ultrasound in haemoglobin solutions. A rough analysis of the data for haemoglobin at a concentration of 0.165 $mg.ml^{-1}$ (15°C) indicates that the relationship between velocity dispersion and absorption is linear over the range 1 to 10 MHz.

i.e. $c_{10} - c_1 \simeq 10\ \alpha_{f_1}$

where c_{10} and c_1 are the velocities of propagation ($m.s^{-1}$) at 10 and 1 MHz respectively and α_{f_1} is the absorption coefficient ($dB.cm^{-1}$) at 1 MHz. The measured velocity at 10 MHz in haemoglobin (0.165 $mg.ml^{-1}$ @ 15°C) was 1530.4 $m.s^{-1}$ while the velocity at 1 MHz under the same

conditions was 1529.3 $m.s^{-1}$. This result was verified by Bradley & Sacerio (1972) for propagation velocity measurements in whole blood.

Influence of physiological parameters on propagation velocity

Bradley & Sacerio (1972) have reported investigations into the influence of frequency, distance, temperature, total protein content and haematocrit on the propagation velocity of ultrasound in human blood (ACD bank blood). The influence of frequency and flow velocity on the velocity of propagation of ultrasound was found to be negligible. The variations found were for temperature 1.48 $m.s^{-1}.C^{o-1}$, for total protein content 1.69 $m.s^{-1}.gm^{-1}.100\ ml^{-1}$ and for haematocrit, 0.59 $m.s^{-1}$ per unit of haematocrit. The maximum range of normal variation for ultrasonic propagation velocity as determined by the haematocrit is, on the basis of these studies, 1550 $m.s^{-1}$ to 1585 $m.s^{-1}$, a difference of 35 $m.s^{-1}$ between the minimum and maximum values quoted. This corresponds to an error or approximately 1% of the haematocrit is ignored in calculating the propagation velocity.

Effects of ultrasound on whole blood

The disruptive influence of collapse cavitation on blood cells as a direct consequence of high frequency insonification has long been established (Weissler, 1960). The intensity threshold above which the mechanism occurs is markedly higher than the levels generally encountered in diagnostic applications of ultrasound. Consequently collapse cavitation as a mechanism for cellular damage in diagnostic applications would appear to be extremely remote. However this is not the only mechanism whereby cellular damage may occur.

Hill (1968), in a review of the possible hazards of ultrasound, distinguished three biophysical modes of action for ultrasound, in addition to collapse cavitation, that may account for cellular damage

as a result of insonification. These are thermal effects as a result of absorption or mode conversion, stable cavitation due to the presence of microbubbles, and direct mechanisms of induced molecular stresses and enhanced diffusion.

The absorption of ultrasound and the subsequent rise in temperature, either locally or within the bulk of the medium is dependent upon the beam characteristics, the absorption and scattering properties of the medium, and the efficiency of thermal dissipation.

In situations where pulsed ultrasound is used for diagnostic purposes, the pulse is usually of microsecond duration and the pulse repetition rate is rarely greater than one thousand pulses per second. The ultrasound source is generally between 1 and 10 MHz. Although the average intensities for such a configuration may be very low ($\sim$ 0.1 $mW.mm^{-2}$), the instantaneous local intensities are substantially greater (0.014 - 0.96 $W.mm^{-1}$; Hill, 1972). These values exceed the intensity thresholds generally observed for tissue damage when ultrasound is applied in a continuous manner. However the low rate of energy delivery largely precludes the incidences of thermal damage. Moreover, the short duration of the pulses avoids the damage of collapse cavitation (Hill et al., 1969).

In continuous beam applications for diagnostic purposes, intensity levels of about 0.5 $mW.mm^{-1}$ are used. A considerable margin of safety would appear to be provided by such low levels, the actual margin depending upon the frequency of the ultrasound used. The higher the frequency the higher the intensity threshold for collapse cavitation (Howkins & Weinstock, 1970; Taylor & Dyson, 1972). Above 1 MHz, intensities greater than 1 $W.mm^{-2}$ are necessary to achieve cavitation.

While a cursory consideration of diagnostic beam intensities may indicate that cavitation or thermal thresholds are unlikely to be

exceeded, the manner in which a beam is used may, in some situations, result in the beam being focused so producing localised increases in beam intensity (Hill, 1968).

Using a controlled intensity, 1 MHz beam having a maximum unfocused intensity of 0.024 $W.mm^{-2}$, Howkins & Weinstock (1970) investigated the effects of focused ultrasound on human blood. When focused at the blood-air interface (fresh human blood contained in an inverted Erlenmeyer flask and maintained at a temperature of 23°C) no changes in plasma haemoglobin or osmotic fragility were observed for an estimated focal intensity of 0.05 $W.mm^{-2}$ until the period of insonification exceeded one hour. Increasing the focal intensity to approximately 0.2 $W.mm^{-2}$ produced a fountain effect of fine blood droplets and a 3% increase in plasma haemoglobin concentration over a period of 5 minutes. Above 0.2 $W.mm^{-2}$ the blood was observed to be rapidly haemolysed. By positioning the focal point 50 mm below the blood-air interface, much higher intensities were found to be necessary to produce blood cell damage. Under these conditions no damage could be detected over a period of 30 minutes using an estimated focal intensity of 0.25 $W.mm^{-2}$ (Howkins & Weinstock, 1970).

The importance of the blood-air interface and mechanical agitation in determining the extent of blood cell damage at a given intensity would appear to be well demonstrated. Howkins & Weistock (1970) suggest that a similar mechanism may be responsible for blood cell damage observed to occur in a specimen of blood containing micro-bubbles when subjected to a low intensity field (Connoly, 1963). Connolly (1963) observed that damage could occur in a low intensity field even though the bubbles were not of resonant size and further observed a degree of correlation between the amplitude of the second harmonic scattered waveform and the extent of the cellular damage.

The second harmonic component may be considered to provide an indication of bubble vibration and surface wave phenomenon. It is the formation of surface waves on a vibrating air bubble that Howkins & Weinstock (1970) suggest is analogous to the fountain effect, particularly if the population of microbubbles is large and so effectively increases the surface area of the blood-air interface.

Bubble vibration may also be considered to contribute to the incidence of cellular damage by a process termed "stable cavitation" to distinguish it from that of "collapse cavitation" (Hill, 1968). Under the action of moderate field intensities, microbubbles have been observed to increase in size. On reaching resonant size the vibrational amplitude may become sufficiently large to induce small localised patterns of fluid movement or 'microstreaming' that are capable of introducing shear and tensile stresses high enough to disrupt molecular bonds and cell membranes (Hughes & Nyborg, 1962).

In addition to undissolved gas in the form of microbubbles, the prevailing blood gas conditions may also influence the extent of cellular damage during insonification. Hypoxia has been observed to increase tissue sensitivity to integrated dose time damage (Taylor & Dyson, 1972). An arterial PO_2 of 6.7 kPa (50 mm.Hg) has been observed to reduce the dose time required to produce tissue damage by 40%.

In view of the enhanced possibility of blood cell damage as a result of microbubbles being present within a region of insonification, an assessment of the damage attributable to an ultrasonic technique of microbubble detection is of considerable importance, particularly if it is envisaged to use the technique in a clinical situation.

Discussion

The physical considerations presented provided important guidelines both in the choice of operating characteristics for the detector source of pulsed ultrasound and in the choice of tests required to establish the safety of the technique in terms of cellular damage.

The analysis of scatter from bubbles contained in whole blood, based upon the theory of scatter for non-rigid spheres, suggests that two working ranges, of practical value, may be distinguished in which the scattered pressure variations are proportional to bubble radius. For kR values $<<1$ and above resonance the perturbation pressure ratio can be practically independent of kR and equal to $-\left\{\frac{R}{r}\right\}$ for quite a wide range of kR values. Below resonance the ratio becomes proportional to bubble radius cubed. This is clearly less attractive as the basis for a bubble detection technique requiring bubble sizing over a reasonably wide range.

For kR values $>>1$ the pressure ratio at the surface of the bubble is asymptotic to a value of 0.5 and the back scattered power or intensity is proportional to the cross-sectional area of the bubble. Consequently the scattered pressure variation is proportional to the bubble radius, providing the bubble size is well above the resonant bubble size.

In order for either of these, above resonance ranges to be quantitatively useful, the resonance peaking must be sufficiently damped to ensure that the measured signal amplitude for a given perturbation cannot be related to both a bubble size above resonance and one at or close to resonance. Fortunately the damping observed in blood is considerably greater than that observed in water and would therefore seemingly satisfy the above requirement for an ultrasound source within the megahertz range.

Since the system damping is greater the higher the frequency, the choice of a high megahertz frequency is to be preferred. Such a choice favours the working range defined by kR values >>1. The upper limit generally considered for diagnostic purposes is 10 MHz. This was also considered to be a reasonable choice for the detector source. The resonant bubble size in blood at this frequency is approximately 0.3 μm and the selected working range commences, for kR >>1 at a radius of approximately 10 μm.

Although a reasonably linear relationship between the scattered pressure waveform and bubble size may be expected for single bubbles contained within the volume of insonification the presence of more than one bubble within this volume at any instance in time may, as the analysis indicates, complicate the relationship. Such a problem is difficult to resolve, particularly as the size and distribution of bubble populations arising during extracorporeal circulation are unknown. However the problem may in some measure be reduced by making the volume of insonification as small as is reasonably possible. In bubble perfusion studies in which a known bubble population is introduced into an experimental model, the problem may be completely avoided simply by controlling the distribution of the bubbles introduced.

A small volume of insonification is also necessary in order to minimise the background scatter due to blood cells and so define the minimum bubble size that can be readily detected. Assuming that the effective volume of insonification at any instance in the pulse propagation is the product of pulse width and the active surface area of the transducer, the use of a short pulse duration allows a greater freedom of choice in selecting transducer face dimensions and minimises the possibility of inconsistent echo structures. A 1 μs pulse duration, yielding a pulse width of approximately 1.5 mm in whole blood, fulfils this requirement.

The possibility of blood cell damage as a result of microbubbles being present within a low intensity field of insonification suggested the need to test for cellular damage as part of the detector evaluation procedure. Tests to assess cellular damage are described and discussed in Chapter 5.

Chapter 4

FLOW DEPENDENT DETECTOR DESIGN: INSTRUMENTATION

Based upon the foregoing considerations of existing techniques and the physics of ultrasound perturbation by bubbles, the following design criteria have been selected;

1. incident intensity level sufficiently low to avoid cellular damage by direct and prolonged insonification,
2. ultrasound source frequency that will permit a practically useful relationship between bubble size and measured perturbation,
3. pulse mode operation in order to achieve higher sensitivity to bubble induced perturbation and better discrimination of bubbles compared with continuous wave techniques,
4. flow dependent pulse repetition frequency in order to achieve 1:1 bubble count relationship,
5. orthogonal placement of the transducer with respect to the direction of flow in order to allow the use of flow dependent pulse triggering and avoid attenuation of incident and scattered energy by bubbles outside the volume of insonification,
6. small volume of insonification in order to improve sensitivity by minimising background perturbation due to formed elements of the blood,
7. uniform beam intensity in order to avoid variations in signal amplitude for bubbles of equal size within different regions of the volume of insonification,
8. signal gating to eliminate crystal and wall induced artefacts, and
9. signal processing to provide bubble count, bubble size, and bubble rate.

As a basis for an experimental instrument an ex-demonstration 'Ekoline 20' diagnostic ultrasonoscope (Smith Kline Instruments Inc.) was purchased and modified. The transducer for use with the modified instrument was manufactured

to specification by Smith Kline Instruments Inc.

The Ekoline 20

The 'Ekoline 20' diagnostic ultrasonoscope is a pulsed ultrasonic transmitter-receiver system designed specifically for medical applications. The essential constituents of the 'Ekoline 20' are the timing circuit, pulse generator, transmitter-receiver transducer, signal amplifier and oscilloscope display (Fig.4.1).

The timing circuit executes a timing cycle corresponding to a fixed rate frequency of one thousand Hertz. At the end of each cycle an electrical trigger pulse is generated and delivered to the transducer crystal causing it to oscillate at a frequency determined by its physical and dimensional characteristics. With the Ekoline 20 frequencies in the range 1-11 MHz can be accommodated. The duration of the acoustic pulse is determined primarily by the duration of the trigger pulse (1 μs) but it is also influenced by the time that the crystal continues to 'ring' after the initial pulse has been delivered. A damping control effectively regulates the 'ringing' influence upon the form of the transmitted pulse. The damping control also regulates the power delivered to the transducer by controlling the amount of the initial pulse voltage applied to the transducer. The average acoustic power delivered by the Ekoline 20 cannot exceed 25 mW.

Following the transmission of a pulse of acoustic energy, the transducer acts as a receiver for echoes (perturbations of acoustic energy) and continues to function in this mode until the next pulse is initiated. The echo-induced electrical signals are amplified and presented as an amplitude modulated A-mode oscilloscope display in which the echoes appear as vertical, localised displacements of the horizontal, time base generator trace. Each delivered pulse triggers the horizontal sweep so that the echoes can be related to both time and distance from the transducer surface.

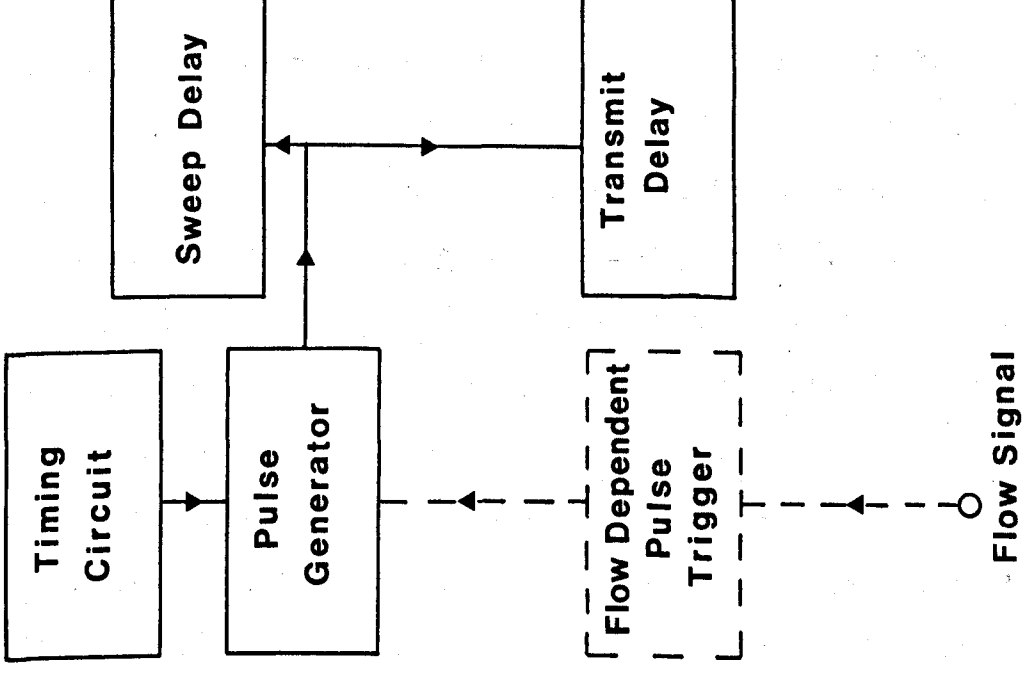

Schematic diagram of detector assembly

Figure 4.1

Referred to on p 130

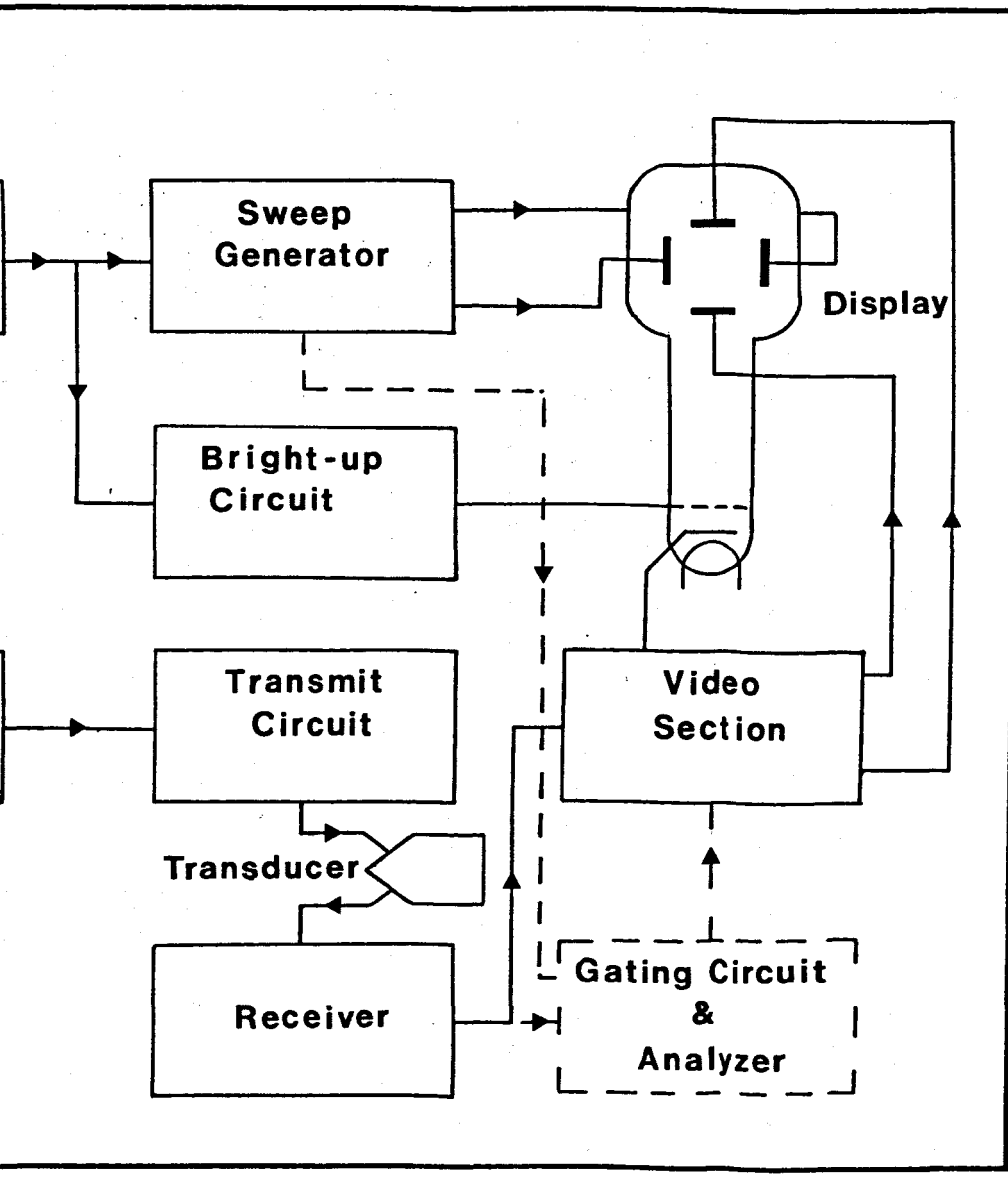
Sweep Generator
Display
Bright-up Circuit
Transmit Circuit
Video Section
Transducer
Receiver
Gating Circuit & Analyzer

Transducer design considerations

The transducer design has been influenced by both acoustic and physical considerations. With the transducer orientation perpendicular to the blood flow axis the volume of insonification has to be cuboidal and the active surface of the transducer has to be rectangular. Use of a cylindrical volume of insonification such as a section of tubing within the extra-corporeal circuit would result in the echoes arising from sources distal to the mid-line plane, parallel to the active surface of the transducer, being obscured by reflections from the natural curvature of the distal wall (Fig.4.2a). The use of a rectangular section in the flow line avoids this problem (Fig.4.2b).

The rectangular shape of the active surface of the transducer is required for a flow dependent technique and for the avoidance of repeated or unpredictable insonification of any one volume of blood. The principle of the flow dependent detection technique is that a pulse of acoustic energy is delivered to the volume of insonification when required and the echoes arising from that pulse are analysed. The time delay between pulses is derived from the electromagnetic blood flow data to allow the complete replacement of the volume of blood within the volume of insonification. Providing the flow profile is not parabolic, multiple counts per bubble are thus avoided. Since the velocity of propagation for sound in blood is very high compared with any practically encountered blood flow velocity, errors due to changes in the contents of the volume of insonification during the period of echo analysis are negligible.

It is necessary to ensure that the boundaries of the volume of insonification are flat in order to avoid repeated or inadequate analysis of the blood flowing past the transducer. This source of error would be inevitable with a circular-faced transducer (Fig.4.3). A parabolic flow profile would introduce limitations similar to those arising with a cylindrical volume of insonification, the actual coverage of the blood volume being determined by the pulse to pulse inverval setting.

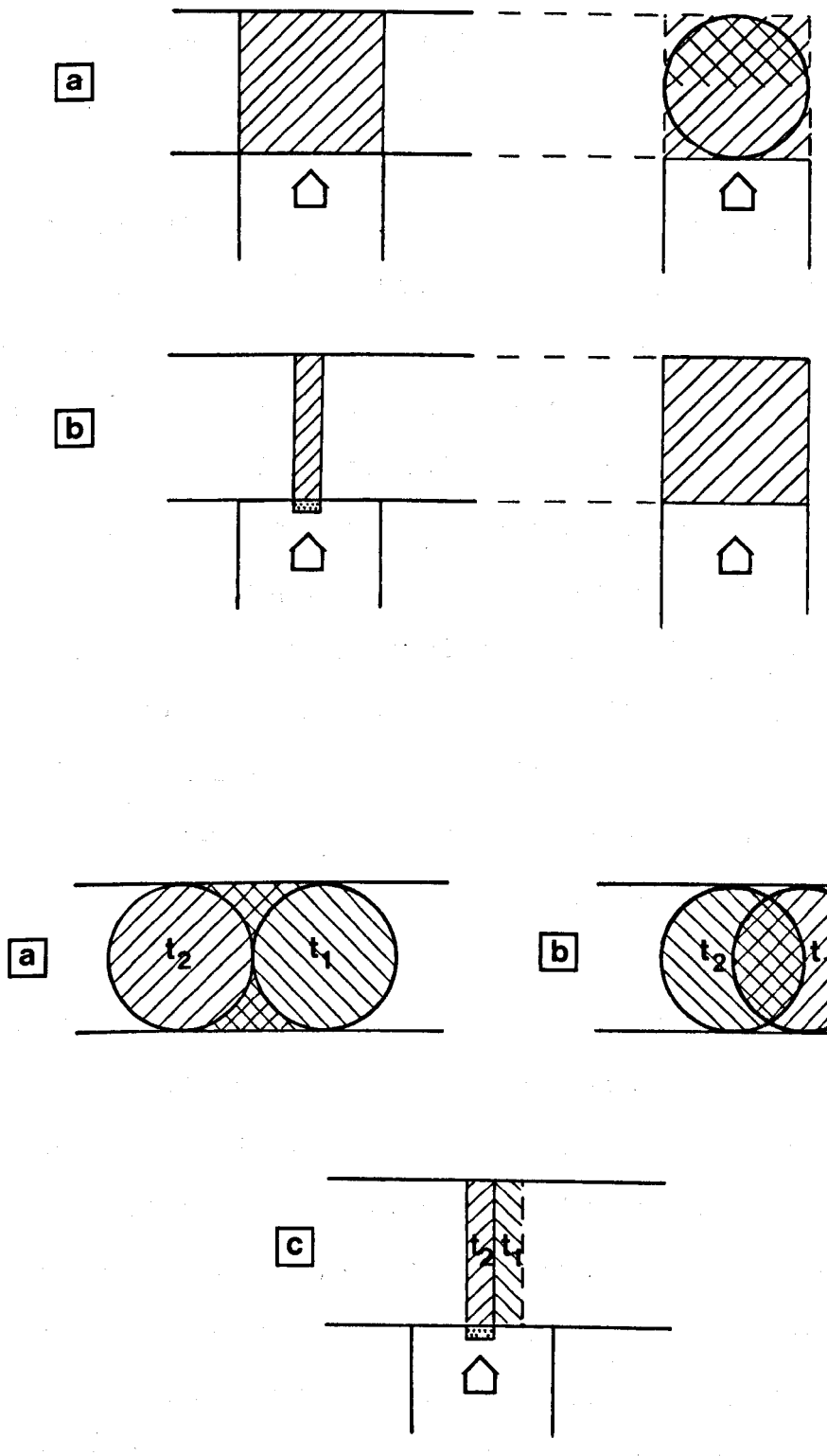

Volumes of insonification for circular and rectangular transducers
Errors due to overlap or inadequate coverage of the field by using circular transducer

Figure 4.2 a & b
Referred to on p 131
Figure 4.3 a, b & c
Referred to on p 131

Flow visualisation using coalesced carbon particles in 0.9% saline showed that at flow rates between 1 and 4 $L.min^{-1}$, produced by a Sarns roller pump in 9.5 mm internal diameter tubing the flow is best described as disturbed laminar and the profile more plug-like than parabolic (see section on Doppler frequency shift).

Further limitations that relate to the dimensional and structural definition of the volume of insonification include velocity gradients close to the walls during laminar, plug-like flow and the back-scattered energy from targets both within and immediately adjacent to the volume of insonification. The first of these limitations may be avoided by careful use of signal gating whilst accepting that total coverage of the blood volume for echo analysis is not quite possible. The second limitation is a consequence of multiple scattering and while the incidence of this cannot be accurately predicted in a monitoring situation, it may be reduced by using a transducer with a small active surface area. If the bubble population is small and well dispersed problems due to multiple scattering should be diminished even further.

Knowledge of the pressure or energy distribution for the field of an ultrasonic transducer is essential for the interpretation of the signal amplitude derived from a reflected or scattered source of acoustic energy. Both the pressure and the energy at a selected point in an acoustic field may be determined theoretically by summing the pressure or energy contributions from segmental elements of the transducer surface. To simplify the analysis, certain assumptions are necessary. In order to derive a general expression for computing the field strength distribution of rectangular transducers Marini & Rivenez (1974) used the assumptions that (i) the system being considered is representative of plane wave scattering by an aperture, (ii) every point upon the surface of the transducer vibrates at the same phase and amplitude, (iii) energy radiated is sufficiently low to avoid prominent non-linear propagation

phenomena, and (iv) the propagation is continuous and within an isotropic medium. Based upon this analysis, they were able to demonstrate that the intensity function for a transducer of rectangular section is a series of maxima and minima for distances measured normal to the transducer surface up to values corresponding to

$$\frac{b^2}{2.88\lambda} \text{ and } \frac{a^2}{2.88\lambda}$$

(a and b being the dimensions of the active surface of the transducer and λ the wavelength of ultrasound used.). Beyond these distances the intensity function exhibits a uniform decrease with distance.

Because the intensity is proportional to the product of the squares of two sets of Fresnel integrals, the position of the last maximum is difficult to determine. However it is possible to distinguish three characteristic zones. Close to the transducer and not exceeding $\frac{a^2}{2.88\lambda}$ (where $a < b$), the acoustic field is very complicated. This region is termed the 'very near field'. In the second and intermediate zone, 'the near field', the intensity is less irregular and extends to a distance not exceeding $\frac{b^2}{2.88\lambda}$ (where $b > a$). The third zone or 'far field' is characterised by a gradual decrease in intensity with respect to distance from the transducer.

For a square transducer ($a = b$) the field is distinguished by only two zones the near field and far field with the transition being defined at a distance $\frac{a^2}{2.88\lambda}$. The fields arising from circular transducers are similarly characterised by two zones. The intensity function is more readily resolved that the function for a square or rectangular transducer, and by being a sine squared function of wave number, distance and transducer diameter considerable variability in intensity may be expected close to the surface of such transducers.

The complexity of the acoustic fields of both rectangular and circular transducers has been well demonstrated practically as well as

theoretically, particularly within the near field (Marini & Rivenez, 1974). Such evidence emphasises the need to exercise considerable care in the choice of transducer for studies in which echo responses are to be interpreted as a measure of the scatter source or reflector size. Moreover, it is necessary to consider to what extent the continuous field analysis relates to the field arising during insonification using a pulsed regime.

During pulse emission the transient acoustic field differs from the theoretical continuous wave field for points which are very near to the transducer and for points that are far from the axis of propagation (Marini & Rivenez, 1974). Unfortunately the transient acoustic field characteristics cannot be readily computed (Stepanischen, 1970). However the transient field may be similar to the continuous field for pulse emissions containing several cycles per pulse (Freedman, 1970).

A 10 MHz ultrasound source delivered in a pulse mode probably generates an acoustic field similar to that arising during a continuous wave mode. However, in choosing such a high frequency the use of the more regular characteristics of the far field is precluded because of the large physical distance that the transducer would have to be away from the blood volume when using an active surface configuration of even reasonable dimensions. A transducer having an active surface configuration of 10 mm by 4 mm (10 mm corresponding to the internal flow path diameter in 10 mm tubing) for example, would require that the active surface be positioned approximately 0.23 m away from the blood volume in order to use the far field.

In view of the impracticality of using the far field and of the uncertainty concerning the characteristic of the very near field, it was decided to investigate the uniformity of the field arising within 20 mm of a transducer having active surface dimensions of 15 mm by 3 mm and an operating frequency of 10 MHz. The ultrasound was pulsed

at a repetition frequency of 1000 Hz. The 15 mm dimension was chosen to allow coverage of a 15 mm square section flow path within a perspex transducer mounting assembly. By restricting the other face dimension to 3 mm the active volume of insonification could be made reasonably small.

Transducer mounting assembly

In order to accommodate a rectangular volume of insonification within an extracorporeal line a transducer mounting assembly was necessary that allowed a smooth flow transition from a circular (10 mm diameter) section to a square (15 mm) section and back to a circular section for an acceptable range of blood flow rates (0 - 5 $L.min^{-1}$). Moreover it was considered necessary to avoid abrupt changes in profile in order to minimise blood trauma and regions of stagnation in which blood clots could form.

A number of problems were encountered in the design and construction of the mounting assembly. Initially it was envisaged that the change in profile from circular to square section should take the form of a gentle upward gradient to the square section flow path and a corresponding downward gradient for the transition from square to circular section at the opposite end of the assembly. However difficulty was encountered by the commercial concern (Stanley Plastics Ltd., Sussex) commissioned to manufacture the assembly, an attempt having been made to cast such a profile using casting resins, and mandrels supplied by the University workshops. The initial design was therefore rejected and a compromise design adopted that could be readily machined in perspex using the University workshop facilities. The compromise design of the transducer mounting assembly is shown in Fig.4.4.

The essential difference between initial and compromise designs is in the transition from the circular to square section. In the compromise design the 10 mm diameter section is coned up to 30 mm diameter section and then coned down to the 14 mm square section, the total transition being

Figure 4.4

Transducer mounting assembly.
Transducer in situ on left hand side. The observation port is immediately opposite on the right hand side.

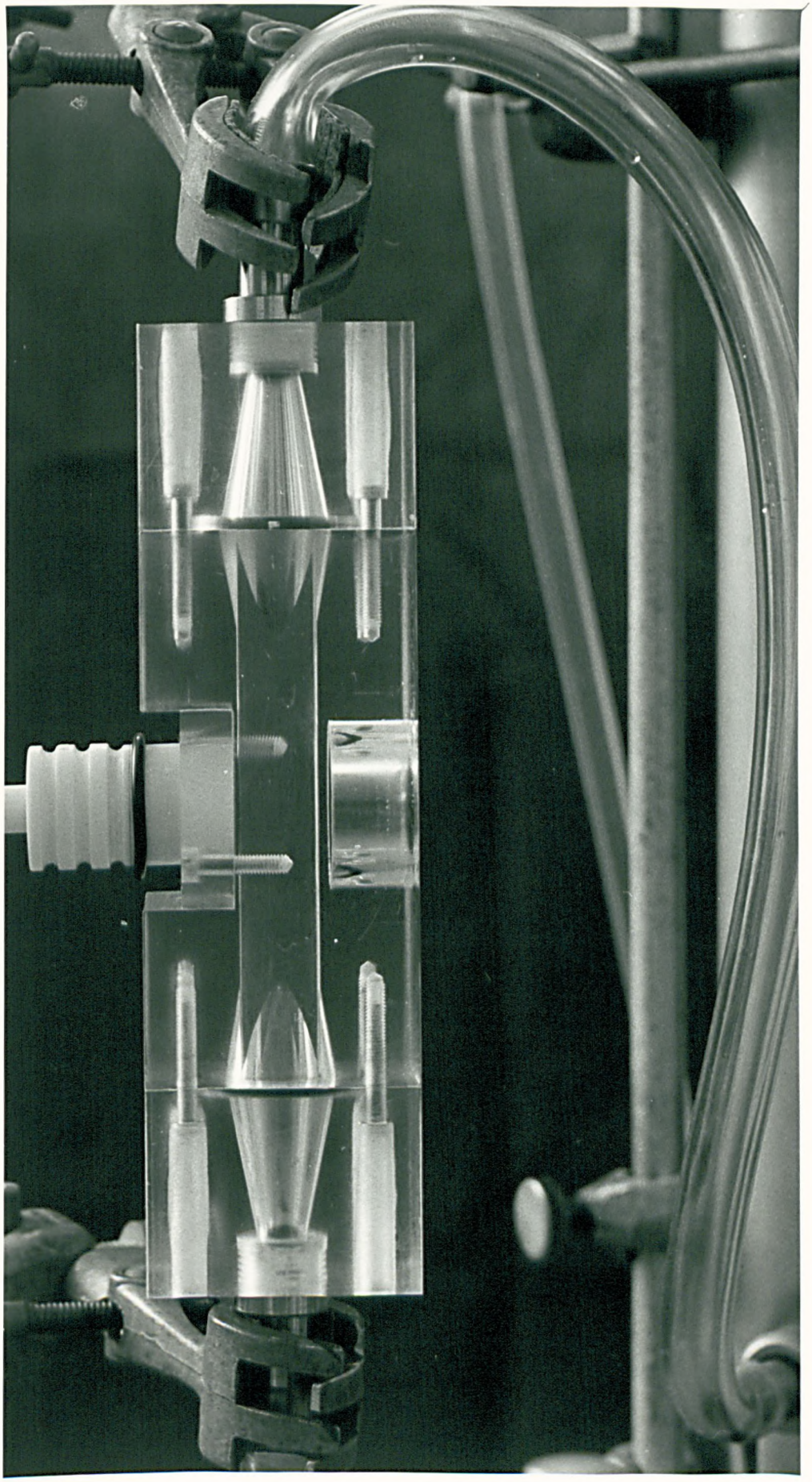

accommodated over a distance of 60 mm. The two coned end sections may be separated from the centre section for cleaning. An observation port is recessed into the centre section to allow close microscopic observation of the contents during calibration using an optically clear solution. Opposite the observation port is a second recess in which the transducer is mounted as shown in Fig.4.4.

The choice of position for the transducer surface with respect to the blood flow channel presented a problem. To avoid possible deletrious effects due to discontinuities within the acoustic transmission path it was initially envisaged that the transducer surface should be in direct contact with the blood. However the complex intensity variations observed to be present very close to the transducer surface (see following chapter on calibration) would, if used in this manner, reduce the useable volume of insonification for analytical purposes. In addition to this particular limitation the possibility of using the detector in a clinical procedure precludes the use of direct contact with the blood because of the inability to autoclave the transducer and the inferiority of other sterilization methods that are readily available.

The use of a thin perspex window (1 mm thick) and the application of acoustic coupling gel (Aquasonic 100 - Parker Laboratories Inc.) just sufficient to ensure effective coupling between the transducer surface and the window avoids transducer contact with the blood without introducing substantial irregularities. A reasonably uniform acoustic field within the volume of insonification may be achieved using this arrangement. Moreover, providing the amount of acoustic gel used for coupling is kept to a minimum, consistent uniformity of field may be achieved (discussed in detail in the following chapter).

The choice of a thin transducer window section was directed primarily by the need to avoid reverberations from the window boundaries and the transducer surface. With a relatively thick window section

the longer time intervals between window boundary reflections can result in the appearance of reverberation artefacts within the period of blood volume analysis. By moderating the acoustic source intensity, the effective reverberation time may be reduced. By also reducing the window thickness the propagation of reverberation artefacts well into the blood volume analysis time may be effectively avoided.

Predictability of the flow characteristics for the transducer mounting assembly described is difficult. A general formula for Reynolds number for a channel of any shape (Goldstein, 1938) is;

$$Re = \frac{4\ m\ u\ \rho}{\mu}$$

Where m is the mean hydraulic depth and is defined as the cross-sectional area divided by the channel perimeter, u the average velocity across the flow path, ρ the density of the liquid and μ the absolute viscosity.

Applying this formula to the square section flow channel of the mounting assembly at a flow rate of 5 $L.min^{-1}$, Re = 1267 (ρ = 1.05 $g.cm^{-3}$ and $\mu = 4.6 \times 10^{-2}P$). Whilst controversy exists concerning the critical figure for Reynolds number to indicate the onset of turbulence, a figure of 2000 is generally considered standard for conditions in which the contents of the reservoir are disturbed (McDonald, 1974). Much higher figures may prevail in less disturbed conditions. Taking the critical value to be 2000 the blood flow through the transducer mounting assembly should be laminar up to at least 5 $L.min^{-1}$. During extracorporeal circulation the blood is diluted to about 50% with Ringer-lactate. This may reduce the absolute viscosity to about $2 \times 10^{-2}P$. Consequently a more realistic value for Reynolds number for the mounting assembly for these conditions is 2917. Turbulence may therefore be expected above 4 $L.min^{-1}$.

The expression used to derive Reynolds number assumes that the flow is steady. The flow promoted by a roller pump may not be so.

Moreover the changes in the shape of the channel at the input and output of the mounting assembly may make any estimates of the square channel flow characteristic meaningless. Practical evaluation of the flow characteristics were therefore attempted and these are presented in chapter 5.

Flow dependent pulse triggering

The pulse repetition frequency of the Ekoline 20 ultrasonoscope is determined by the master oscillator (Fig.4.5) the output of which triggers the horizontal sweep of the oscilloscope display and the 'main bang delay' circuit. Following a delay of 150 μs, the 'main bang delay' circuit delivers a 1 μs pulse to the transducer pulsing circuit.

In order to effect a flow dependent triggering regime it was necessary to design a flow related pulsing circuit. The output line of the pulsing circuit is connected to one of the two selection contacts of a two way switch, the other selection contact being connected to the output of the master oscillator. The selector arm is connected to test point TP02 as illustrated in Fig.4.5. Applied in this manner the horizontal sweep sequence, main bang delay, and the transmit-receive sequence are retained and the pulse mode can be switched to either flow dependent trigger or master oscillator.

The circuit for flow dependent triggering is shown diagrammatically in Fig.4.6. The input consists of an invertor and adjustable attenuator. This allows the appropriate input level to be applied to the linear integrator in order to achieve the correct pulse to pulse interval for a given flow rate and transit time for the volume of insonification. The input signal causes the integrator output to ramp toward its maximum positive voltage level, the rate being determined by the input and feedback components of the integrator and the input voltage. When the output level exceeds the comparator reference level the

Pulse trigger modification

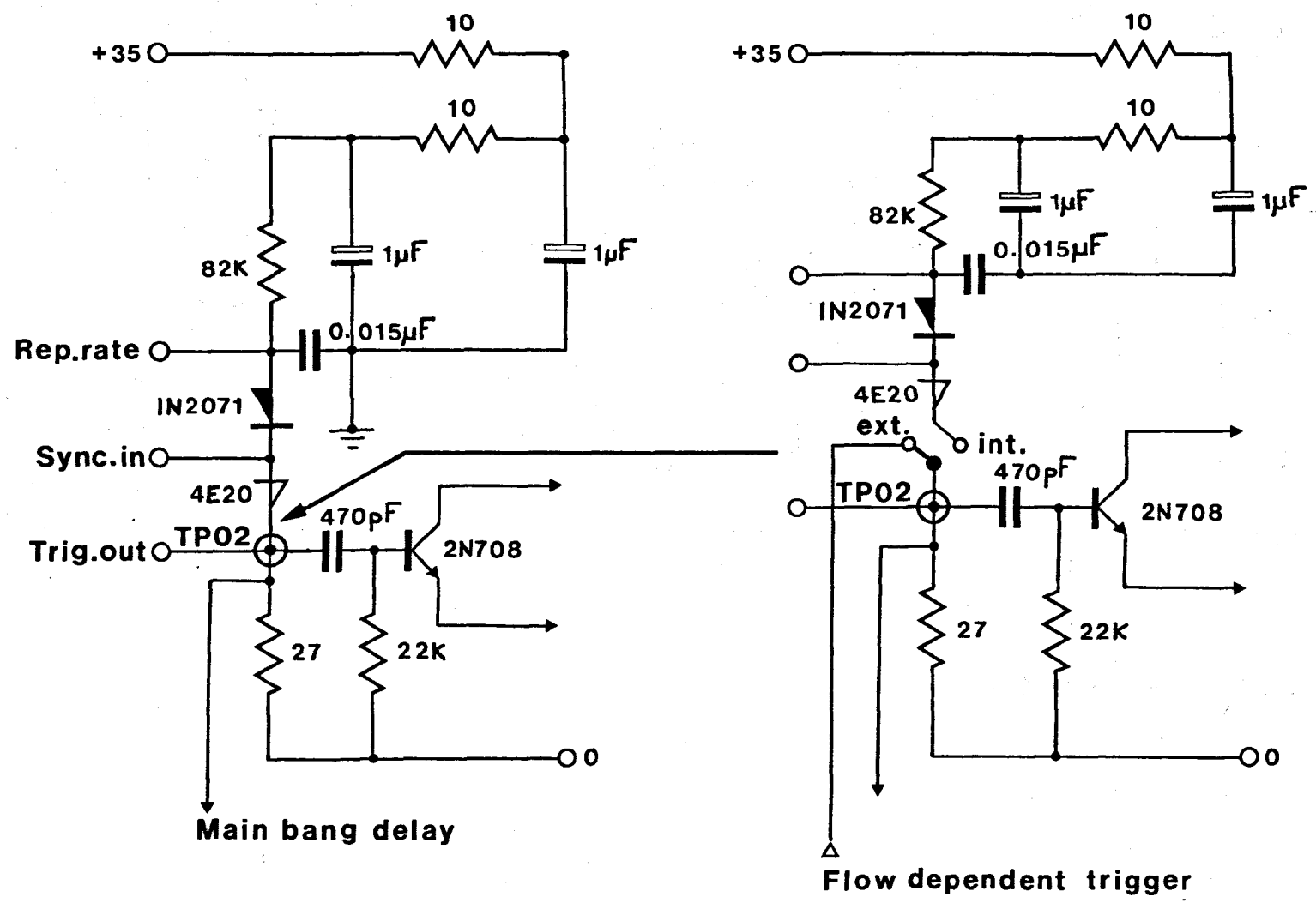

Figure 4.5

Referred to on p 141

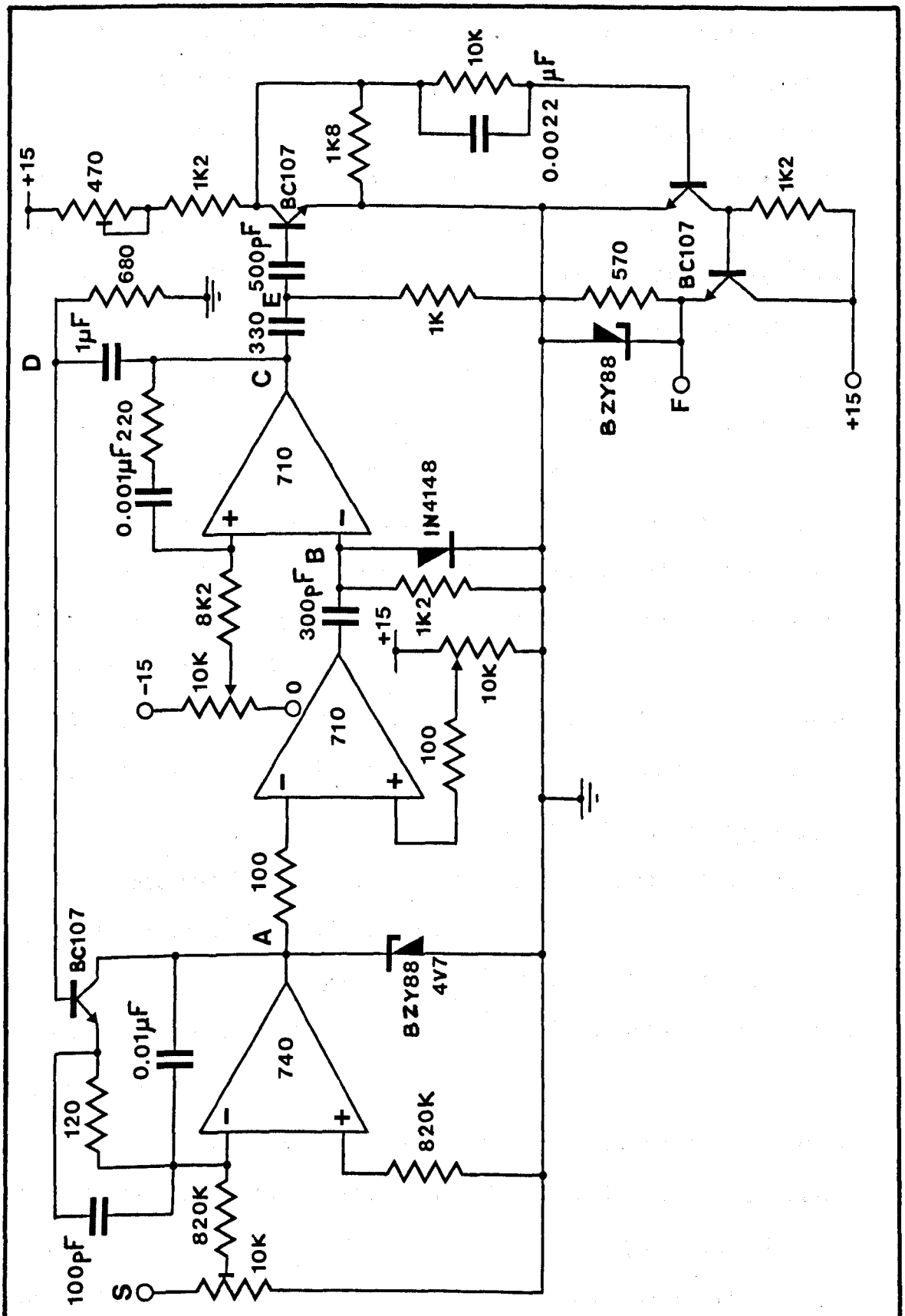

Flow dependent trigger circuit
Waveforms for A F see figure 4.7

S: Signal input from electromagnetic flowmeter

Figure 4.6

Referred to on p 141

comparator output falls rapidly from +3.1 volts to -0.5 volts. A simple differentiator allows a negative going pulse to be derived from this excursion which in turn triggers the monostable circuit. The monostable output pulse, which may be up to 25 μs in duration, activates the integrator reset circuit and the main bang delay trigger pulse circuit. In both cases the monostable output is differentiated to provide positive directed pulses appropriate to each circuit. The reset pulse is approximately ten times the duration of the pulse delivered to the main bang delay trigger circuit in order to ensure complete discharge of the integrator capacitor and to introduce a trigger circuit refractory period. The pulse delivered to the main bang delay trigger circuit is shaped and amplified, the output being a 10 volt rectangular pulse of 1 μs duration. The waveform sequence for the trigger circuit is shown in Fig.4.7.

In order to set the correct operating mode a flow rate is selected and the flow velocity within the volume of insonification is estimated;

i.e. $v = \frac{F}{A}$ where v is the flow velocity, F is the flow rate and A is the cross-sectional area of the flow path within the region of insonification.

Knowing the width of the volume of insonification in the direction of flow, the time taken for a complete change in the contents may be determined;

i.e. $t = \frac{d}{v}$ where t is the transit time and d is the effective width of the volume of insonification in the direction of flow. This value of t represents the required pulse to pulse interval and by monitoring the output pulses using an oscilloscope the attenuator may be adjusted to obtain the appropriate pulse repetition frequency. Once set for a selected flow rate any subsequent variations in flow are accompanied by a corresponding change in pulse repetition frequency. Fig.4.8 illustrates the relationship between

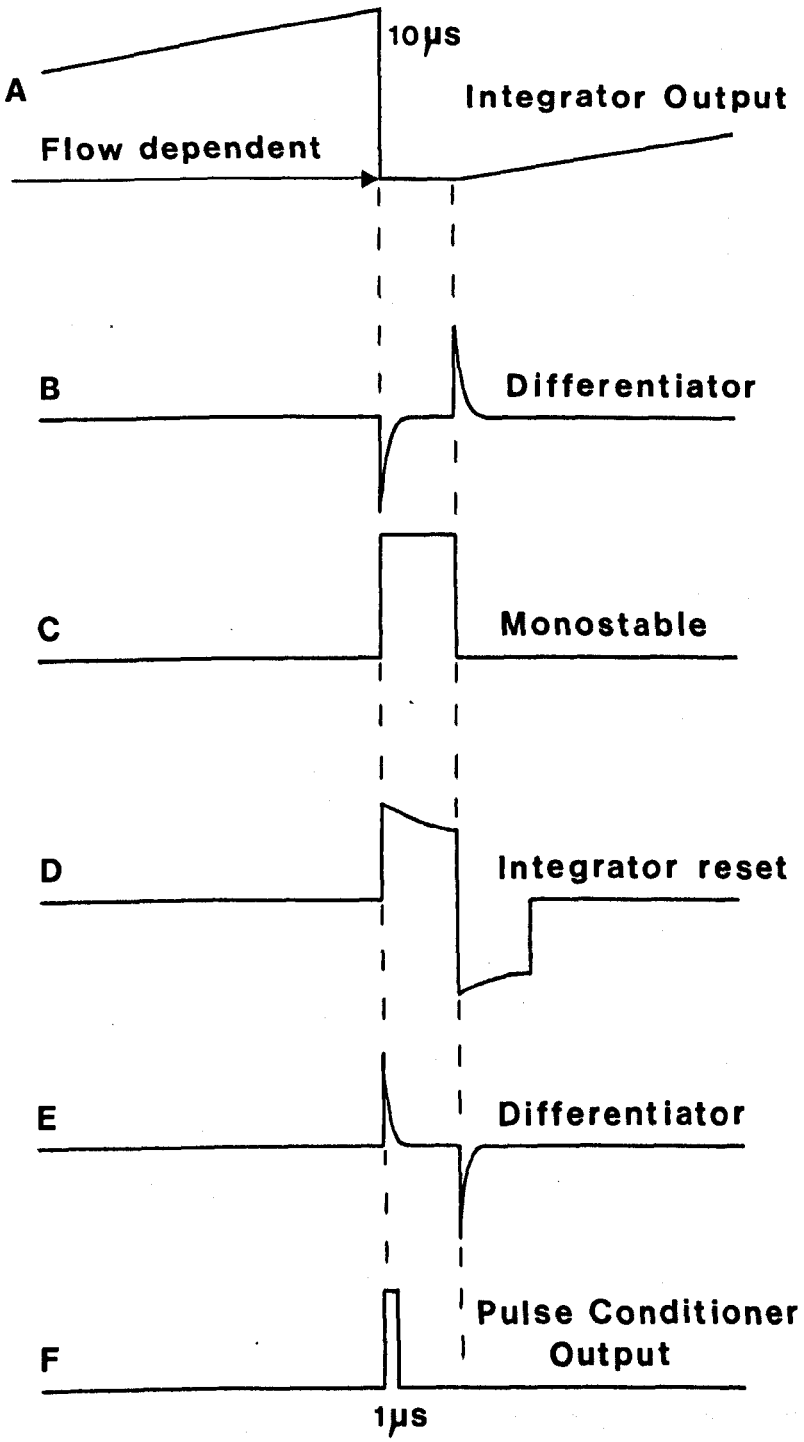

Flow dependent trigger circuit waveforms

Figure 4.7

Referred to on p 144

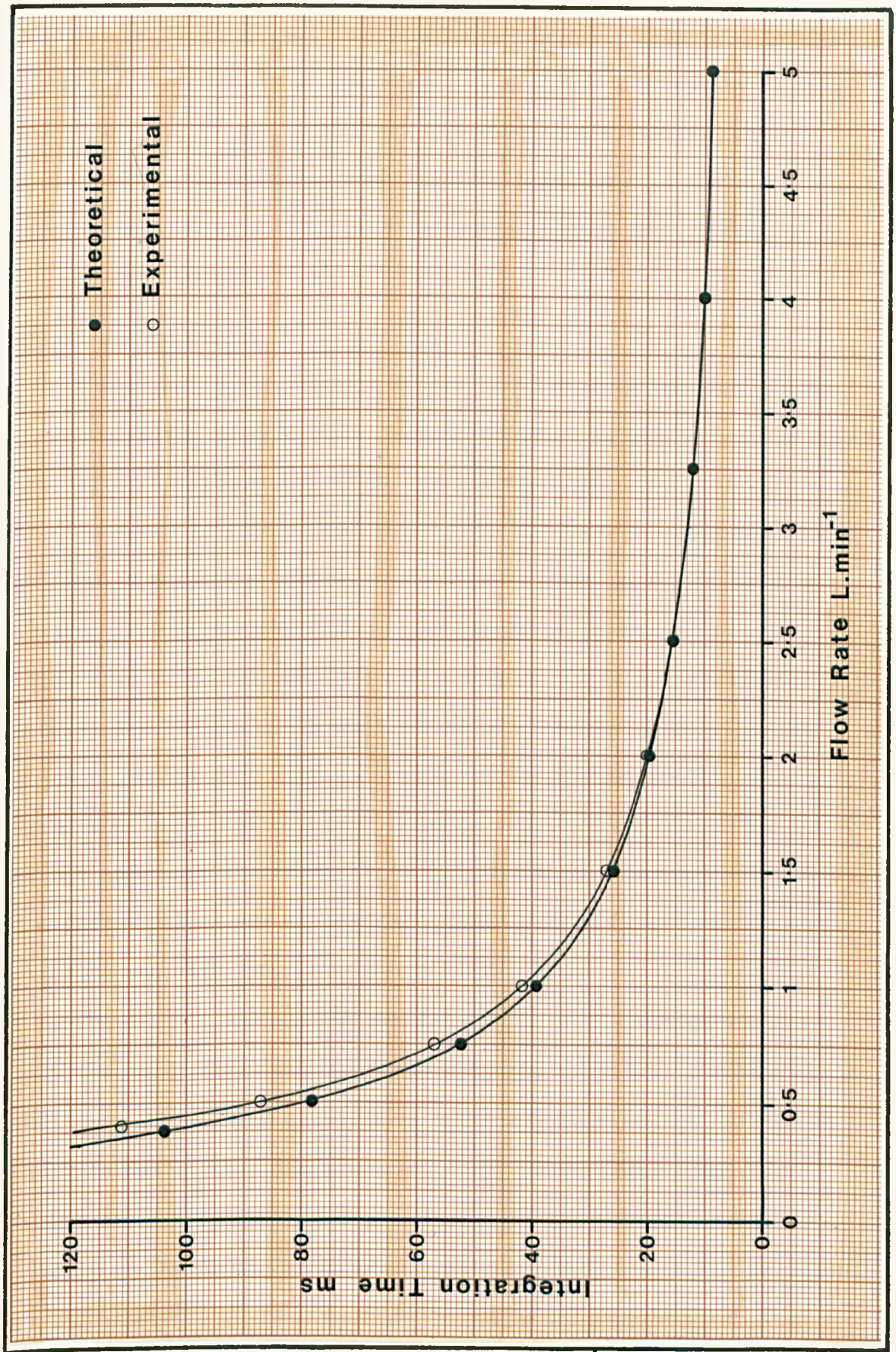

Integration time-flow rate relationship

Figure 4.8

Referred to on pp 144, 147

integration time and pulse repetition frequency vs flow rate for both theoretical and observed conditions. The slight discrepancy at very low flow rates is attributed to the fluctuating flowmeter output levels (Nycotron flowmeter type 376 with 9 mm internal diameter cannulating probe) due to irregular roller pump action (Sarns Inc.) at low rotor speeds.

Signal gating circuit

The signal gating circuit may be considered in two parts, an analogue gating section and a section designed to generate the pulses that effectively open and close the analogue gate.

In order to achieve both positional and timing reference for the gate pulse generator circuit, the Ekoline sweep generator waveform derived from test point TP04 of the horizontal sweep circuit was used (Fig.4.9). With the Ekoline depth control turned fully counter clockwise a minimum sweep duration of 25 μs is achieved. This was found to be the most useful display setting for microbubble detection using the transducer mounting assembly discussed earlier. However it is not necessary to retain the depth control in this position since the gating pulses may be adjusted relative to the onset of the sweep sequence and with respect to one another.

The circuit diagram for generating the gating pulses is illustrated in Fig.4.10. The sweep generator waveform is presented to the buffered input of the gate pulse generator and attenuated in order to ensure that the maximum voltage level at the comparator input does not exceed 5 volts. The comparator threshold setting determines the levels at which the output transitions occur relative to the leading and trailing edges of the sweep generator waveform (Fig.4.11). An invertor and a simple differentiator follow the comparator. These components allow a negative directed pulse to be derived from the trailing edge of the comparator output transition.

Sweep generator

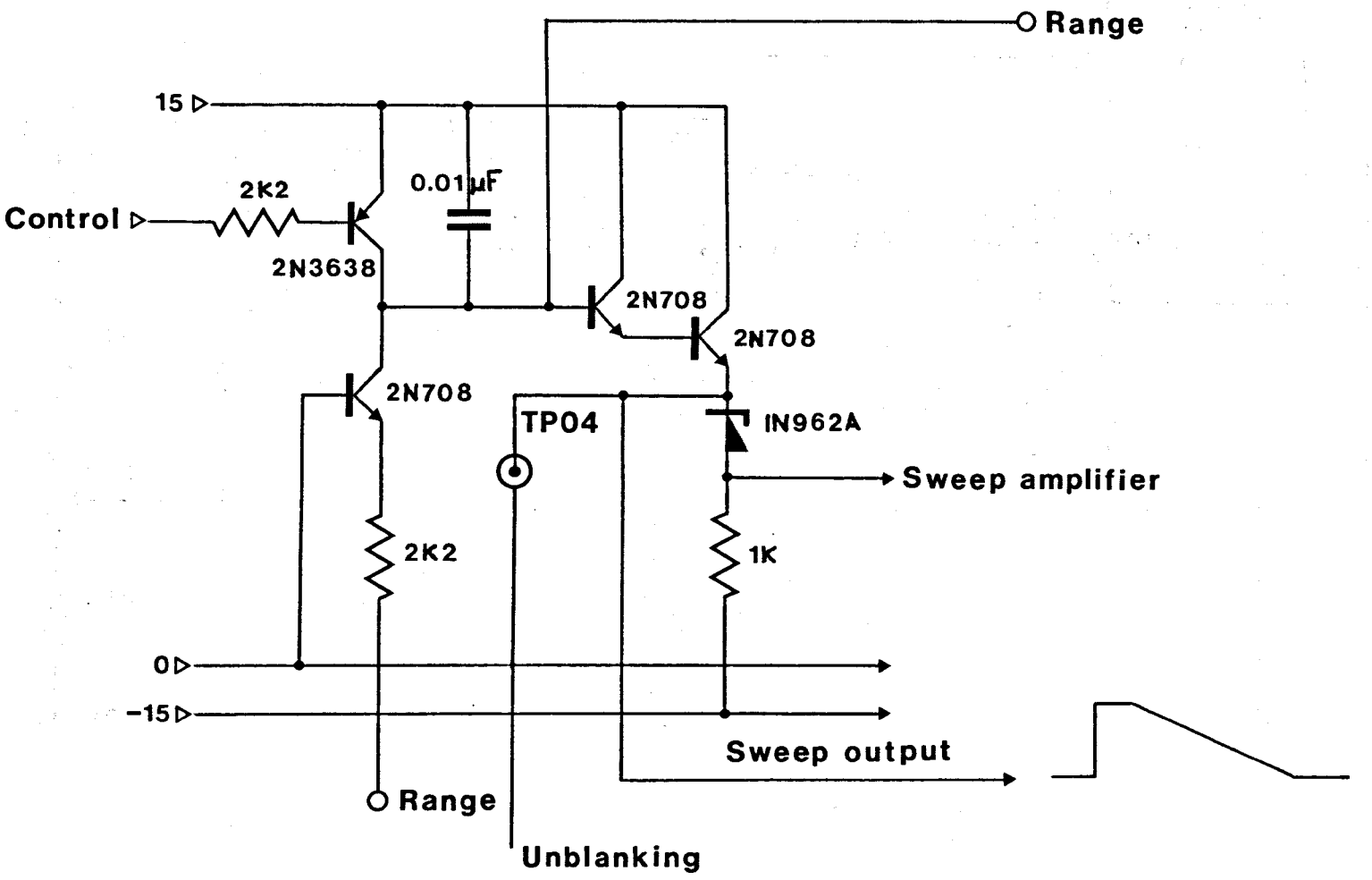

Figure 4.9

Referred to on p 147

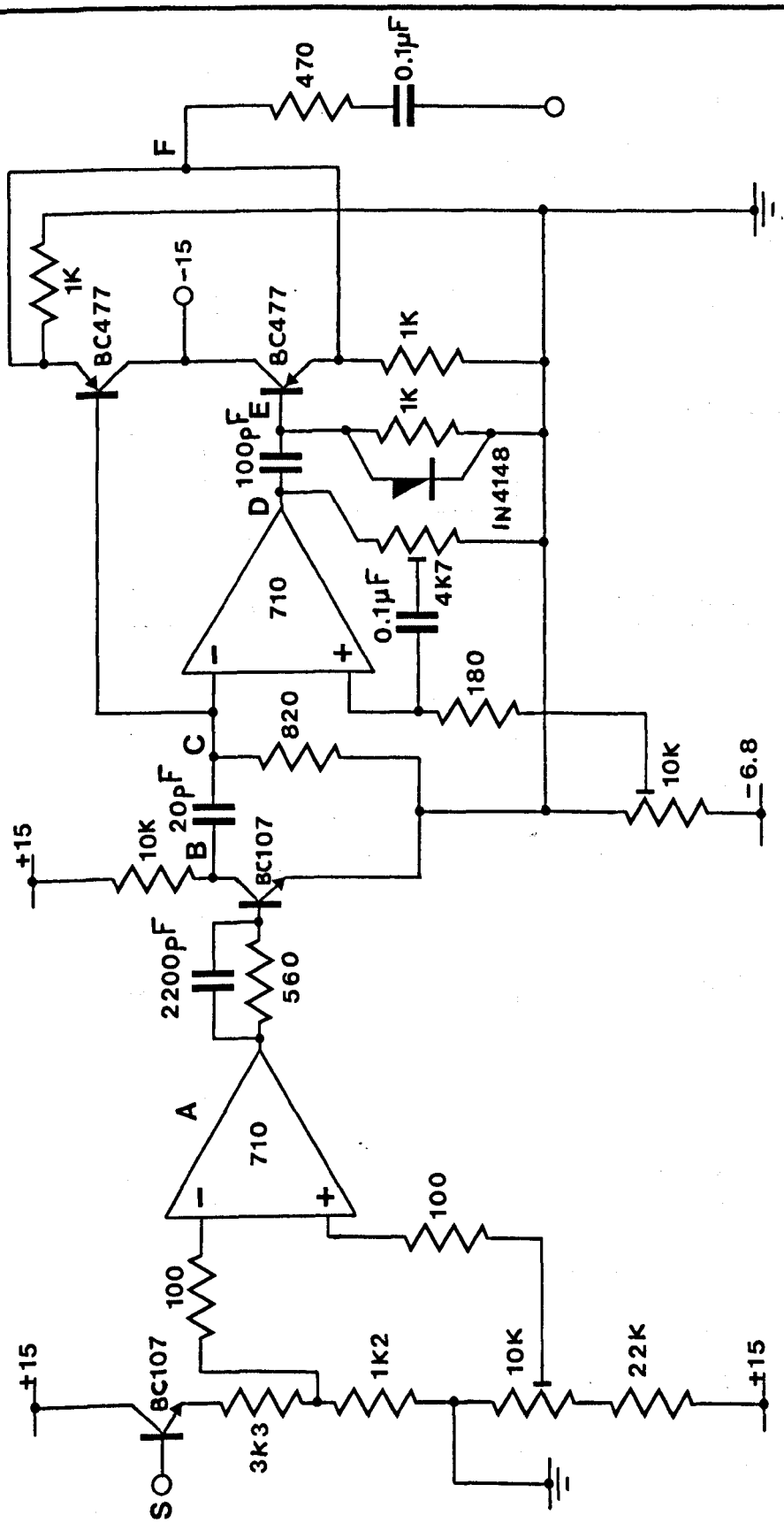

Gating pulse generator
Waveforms at A, B, C, D, E & F see figure 4.11

Figure 4.10

Referred to on p 147

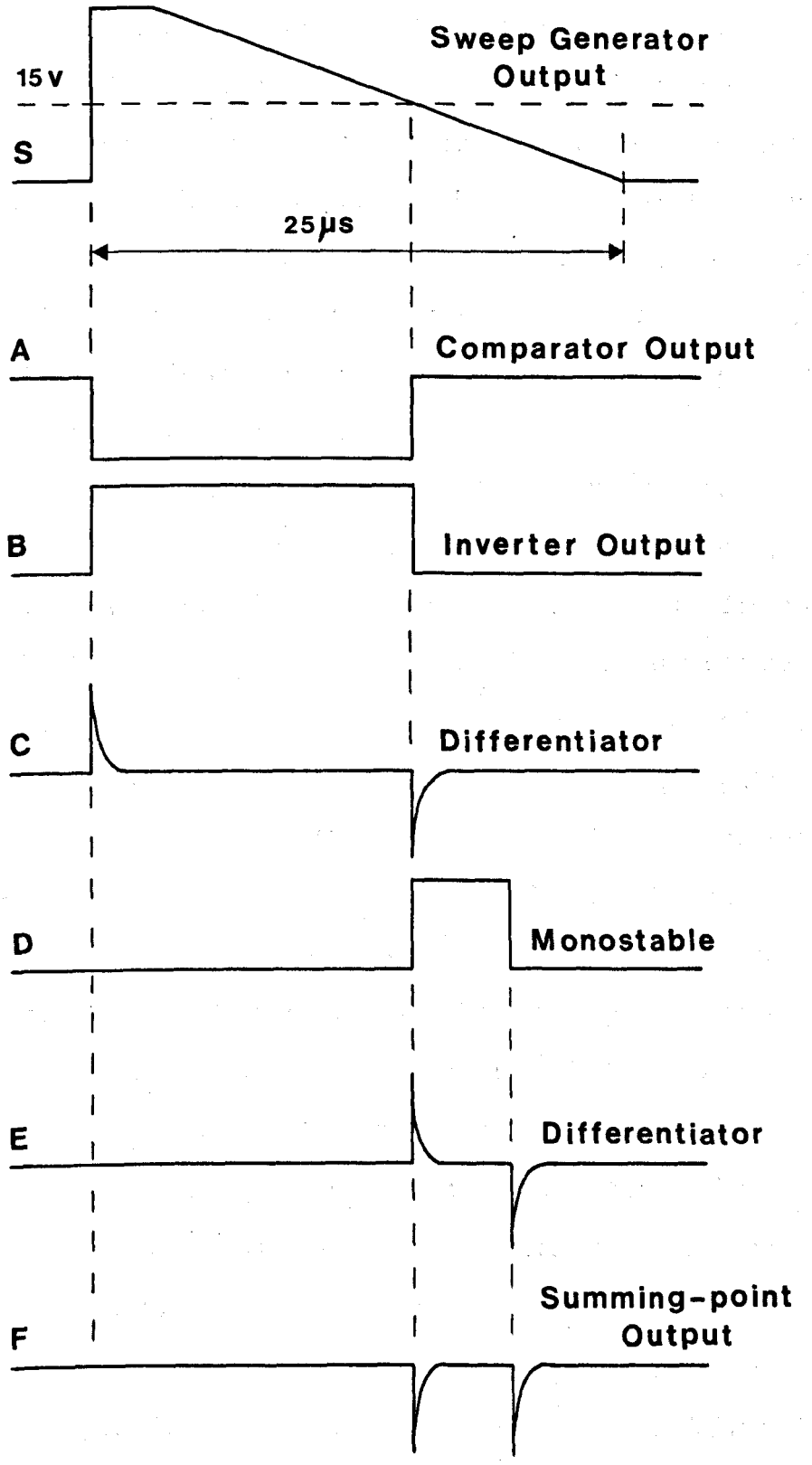

Gating pulse generator waveforms

Figure 4.11

Referred to on p 147

This pulse is used to trigger the monostable circuit whilst also being conditioned as the first gating pulse. After being buffered by an emitter follower the gating pulse is delivered to the output summing point. The triggered monostable circuit delivers an output pulse, the duration of which is determined by the non-inverting input components and the components in the monostable feedback path. This pulse is also differentiated and the negatively directed pulse derived from the trailing edge is buffered using an emitter follower prior to being routed to the output summing point.

In response to the input sweep generator waveform, two output pulses of approximately 1 μs duration are generated. By reducing the comparator threshold level, the pair of gating pulses may be delayed relative to the leading edge of the sweep waveform. By increasing the threshold the delay is reduced. Variation of the monostable feedback resistor value causes a change in the duration of the output pulse. Since this pulse is triggered by the first gating pulse and the second gating pulse is derived from the trailing edge the facility is introduced for positioning the second gating pulse relative to the first.

The ability to vary the positions of the gating pulses offers considerable flexibility in selecting the region of the display required for analysis. By means of a switch the gating pulses may be displayed on the oscilloscope for the purpose of setting the interval for analysis. For this purpose the pulses are directed to test point TP04 of the Ekoline video section (Fig.4.12).

The analogue gating section of the signal gating circuit is illustrated in Fig.4.13. An input comparator is used to redefine the gating pulses. These are then inverted in order to operate the bistable circuit. In response to the first gating pulse the bistable output switches from zero to + 12 volts. This in turn causes the analogue gate to present a low resistance pathway for the processed receiver

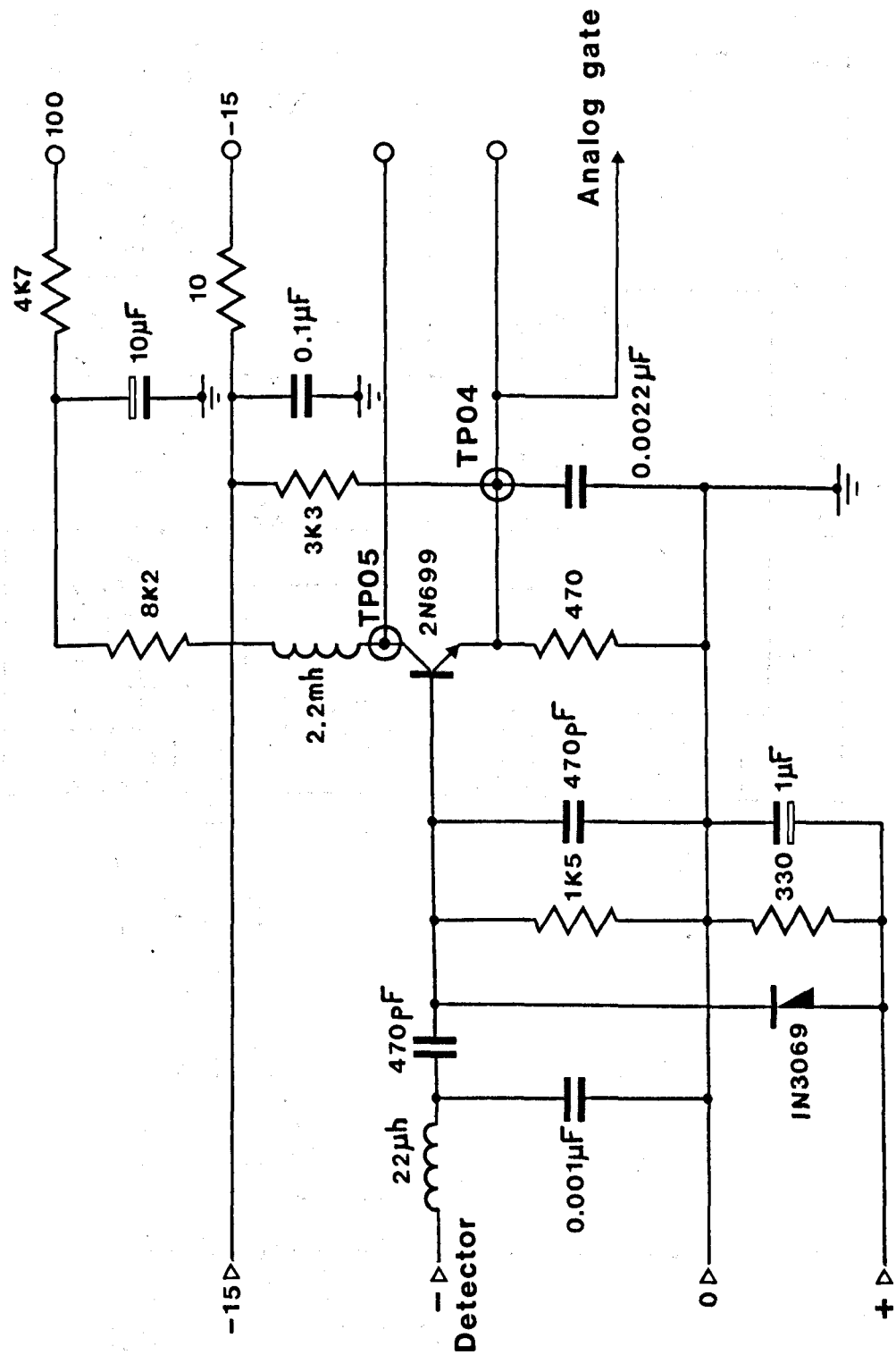

Video driver circuit

Figure 4.12

Referred to on pp 151, 154

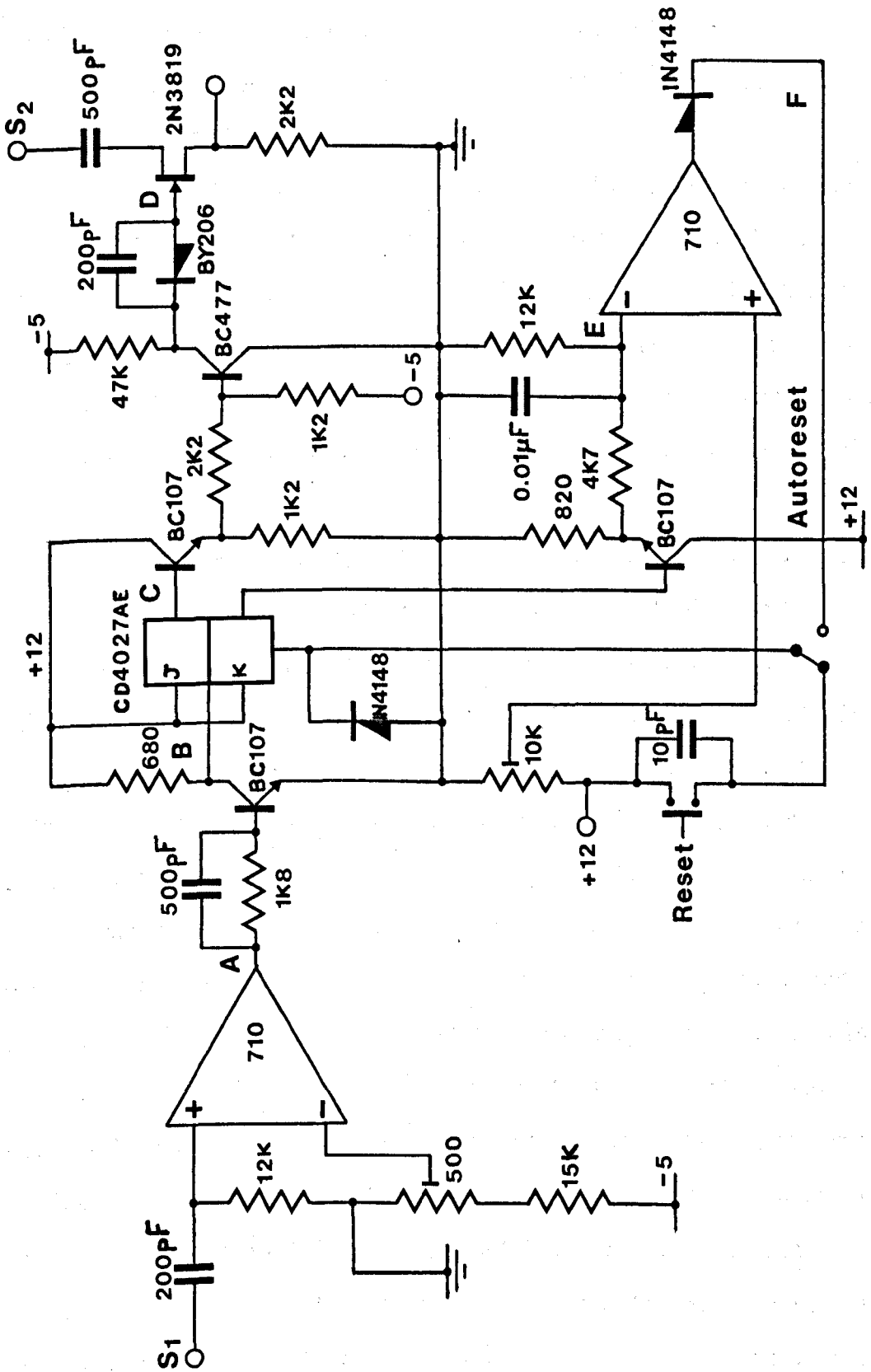

Analog gating circuit
Waveforms for A F see figure 4.14

S_1 Gating pulses S_2 Signal input from detector

Figure 4.13

Referred to on p 151

signals derived from test point TP04 of the Ekoline video section (Fig.4.12). The use of a field effect device for this purpose ensures that no offset voltages are introduced to limit the transmission of low amplitude signals.

The second gating pulse triggers the bistable to return to zero and in so doing causes the analogue gate to present a very high resistance to the passage of input signals. Using the field effect device the increase in resistance in the switch off mode is sufficiently high to effectively eliminate any evidence of input signals on the output side. Transducer crystal and wall artefacts can therefore be eliminated from the analysis.

To accommodate and correct the possibility of a missed trigger response or a premature trigger response at the bistable due to extraneous interference, a simple autoreset circuit has been included in the design. The complementary output of the bistable circuit is connected to a simple leaky integrator which is in turn connected to the inverting input of a comparator. When the bistable gate source output is zero the complement output is high (+ 12 volts). This sets the comparator output to - 0.5 volts. When the bistable is triggered, the gate source output goes high and the complement returns to zero. This enables the capacitor connected to the comparator input to discharge and when the input level to the comparator falls below the reference level set by the voltage at the non-inverting input, the output switches to + 3.1 volts. Since the output of the comparator can be manually switched to the set facility of the bistable, in the autoreset mode, the output is coupled to the set terminal of the bistable causing the gate source output to return to zero. The complement output returns to + 12 volts and the set level to zero. A 50 μs delay is imposed by the autoreset circuit following a switch in the gate source output to + 12 volts before a set level is initiated.

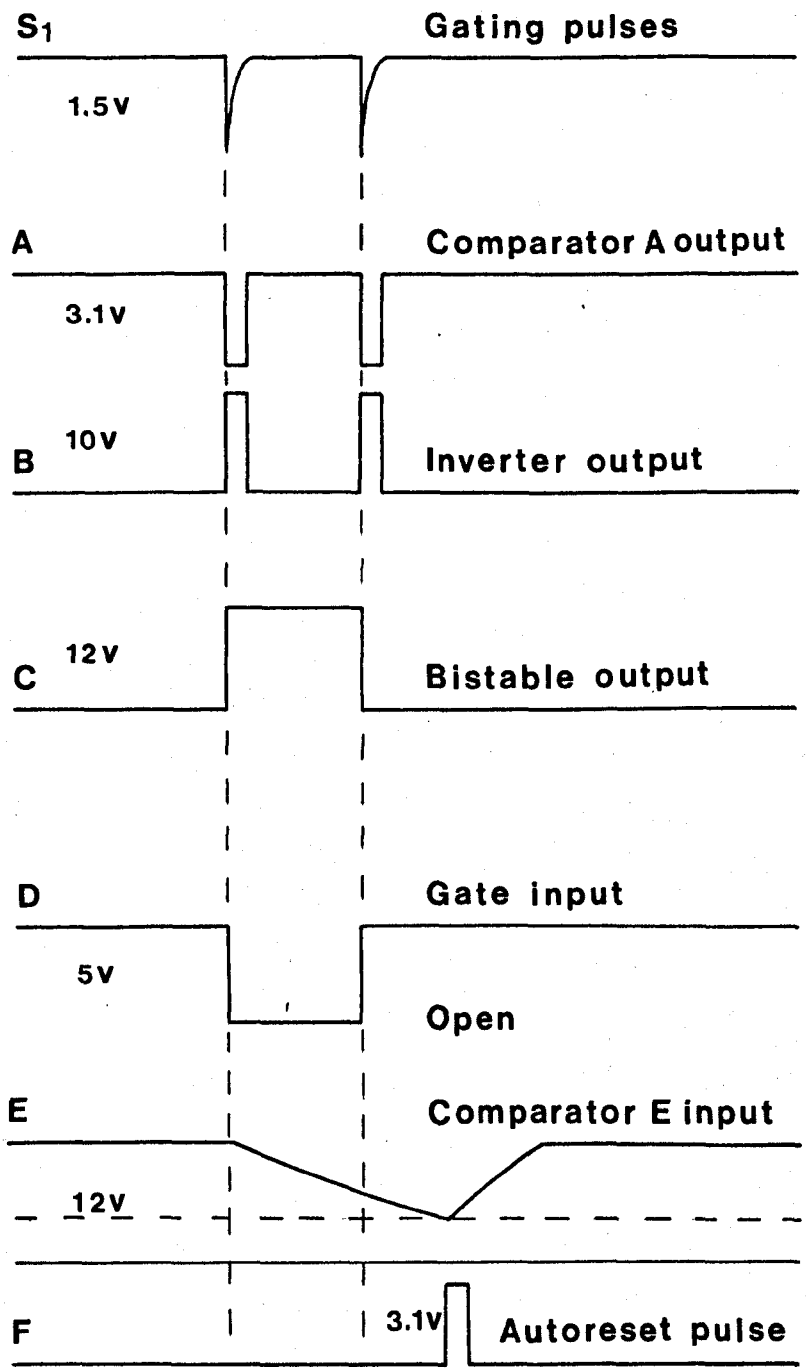

Analog gating circuit waveforms	Figure 4.14 Referred to on p 156

Considering a pair of gating pulses, if the first pulse successfully triggers the bistable whilst the second fails to trigger, the autoreset returns the bistable to the correct state in readiness for the next gating pulse of the following pair. A slight count error may arise in this situation by the inclusion of a wall reflection artefact in the analysis. However the reset prevents this from being perpetuated by the loss of synchronisation in subsequent analyses.

If the first pulse fails to trigger, but the second succeeds a small error is again incurred due to the inclusion of wall reflection artefact in the analysis period, determined in this situation by the 50 μs autoreset delay. Again the condition is prevented from perpetuating by correction of the output states prior to receiving subsequent gating pulses.

In practice it has rarely been necessary to use the autoreset facility, consistent triggering having been observed over typical operating periods of three and four hours. In addition to the autoreset facility a manual reset has also been included in the form of a push button switch which when depressed connects a positive voltage level to the bistable set terminal.

The waveform sequence for the analogue gating section is illustrated in Fig.4.14. For convenience and in order to use the internal power supplies of the Ekoline 20, both the flow dependent pulse triggering circuit and the gating pulse generator circuits were constructed as a module to fit into the rack system of the Ekoline 20. This module is shown in situ in Fig.4.15. Outputs for the gating signals and the Ekoline processed receiver signals are obtained from the adjacent module as shown, the top socket providing the gating pulses and the lower socket the signal output. The socket on the circuit module is the input for the flow waveform.

Figure 4.15

Analogue gating section incorporated into the Ekoline 20.
The two inner modules constitute the analogue gating and output lines for the gating pulses (top socket, right hand module) and conditioned receiver signals (lower socket, right hand module). The socket on the left hand module is the input for the flow waveform.

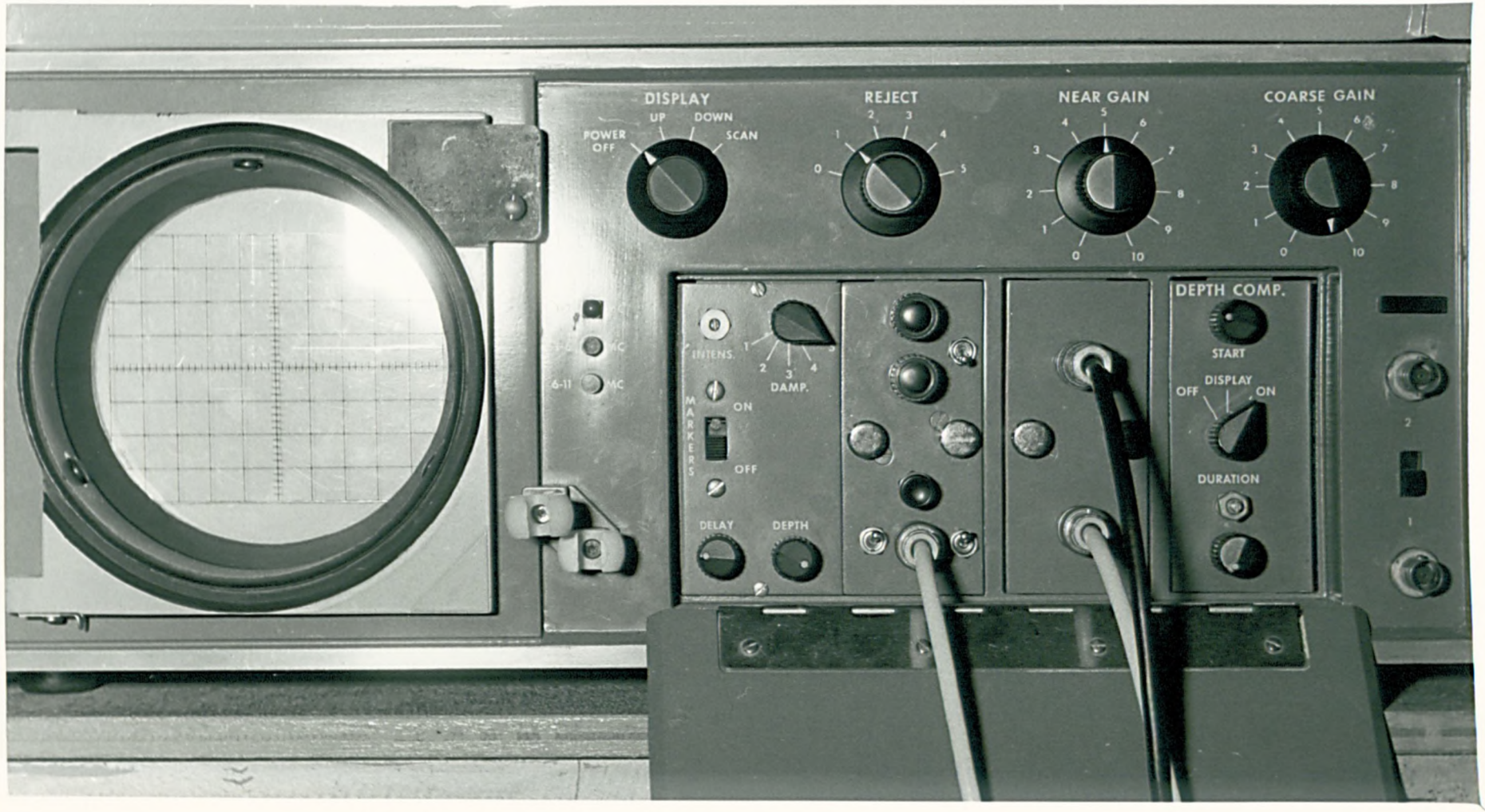
DISPLAY
UP
DOWN
POWER OFF
SCAN
REJECT
NEAR GAIN
COARSE GAIN
DEPTH COMP.
START
DISPLAY
OFF
ON
DURATION
INTENS.
DAMP.
MARKERS
ON
OFF
DELAY
DEPTH
6-11
MC

Amplitude discriminator circuits

In order to avoid excessive costs in the design of a high frequency amplitude discriminator to size input signals and relate them to bubble diameters, a prototype ten channel instrument was designed and constructed based upon a principle previously described by Daigle, Morgan & Budak (1973). Each channel is of the form illustrated in Fig.4.16. Upper and lower threshold limits applied to the input comparators determine the range over which a signal peak will elicit an output response from the circuit monostable.

Considering a single channel, if an input signal exceeds the lower threshold (LT) but is below the upper threshold (UT) the output of comparator 1 changes from - 0.5 volts to + 5 volts whilst the output of comparator 2 remains at - 0.5 volts. The signal delivered to the input of the Schmitt trigger (level detector with hysteresis) due to the output transition of comparator 1 is insufficient to trigger the circuit owing to the attenuation produced by the resistor combination (R_1, R_2 & R_3) and the output condition of comparator 2. Consequently the output of the Schmitt trigger remains at + 5 volts. A potential divider ensures that the voltage level at the inverting input of the monostable is greater than 5 volts (5.3 volts) thus allowing the output to remain at - 0.5 volts until triggered. The trigger source facility is provided by a simple differentiator formed by the potential divider and a capacitor connected between the centre connection of the divider and the output of comparator 1. The negative going pulse derived from the differentiated output pulse of comparator 1 triggers the monostable by momentarily reducing the voltage level at the inverting input below that of the non-inverting input. An output pulse is thus generated in response to a signal peak occurring between the upper and lower threshold levels for the channel considered, the duration of which (1 μs) is determined by the monostable feedback

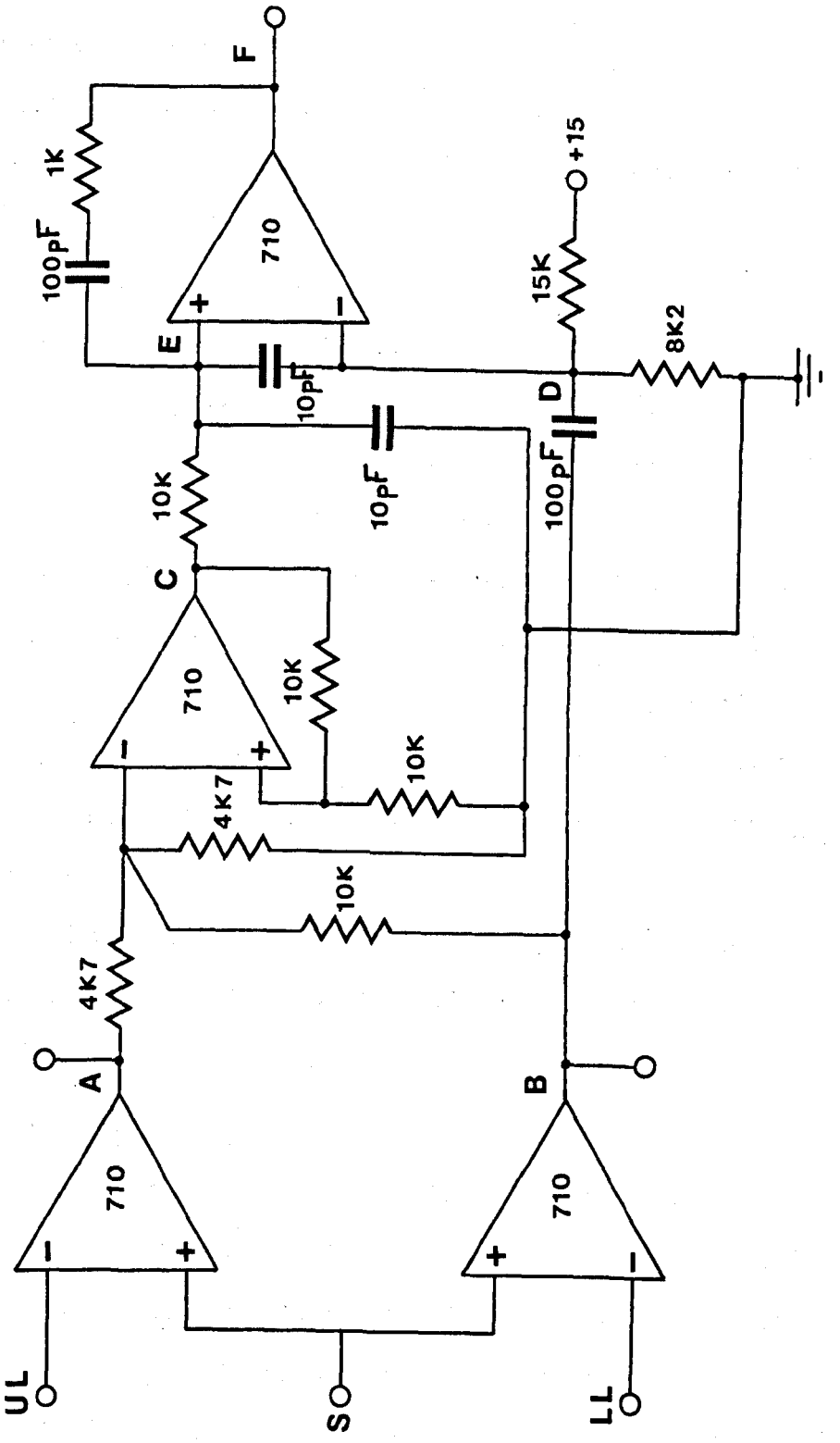

Amplitude discriminator stage
UL Upper threshold level
LL Lower threshold level
S Signal input from analog gate
A & B connected to upper & lower channels

Figure 4.16

Referred to on p 158

components. For the situation in which the input signal peak exceeds both the lower and upper threshold levels of the channel considered, both input comparator outputs switch from - 0.5 volts to + 5 volts, the combined output conditions being sufficient to cause the Schmitt trigger output to switch to - 0.5 volts. This in turn suppresses the response of the monostable to the negative trigger pulse derived from the output of comparator 1.

The waveform sequence for a single channel discriminator is illustrated in Fig.4.17. In order to achieve ten levels of discrimination, circuits were coupled together as illustrated in Fig.4.18, with the upper thresholds of one stage serving as the lower threshold of the stage to which it is coupled. Channel 10 was derived as the output response of comparator 10 in channel 9. The threshold levels were all derived from a + 15 volt stabilized supply rail using the potential divider circuits illustrated in Fig.4.19, each of the variable resistances being 10 turn potentiometers in order to achieve fine setting of each threshold level.

Using 1 μs duration rectangular input pulses, the ten channel discriminator is capable of accommodating pulse repetition frequencies up to 0.5 MHz.

Counters and count display

To obtain a pulse count for each output of the ten amplitude discriminator channels, a system was designed and constructed using conventional transistor - transistor logic (TTL). This system is illustrated in Fig.4.20. Each channel is accommodated by six serially connected 7490 decade counters providing a maximum count capability of 999,999. A common reset to zero facility is incorporated for reseting all channels simultaneously.

The twenty four outputs from each channel (six, four bit binary coded decimal outputs) are connected to the inputs of each of twenty

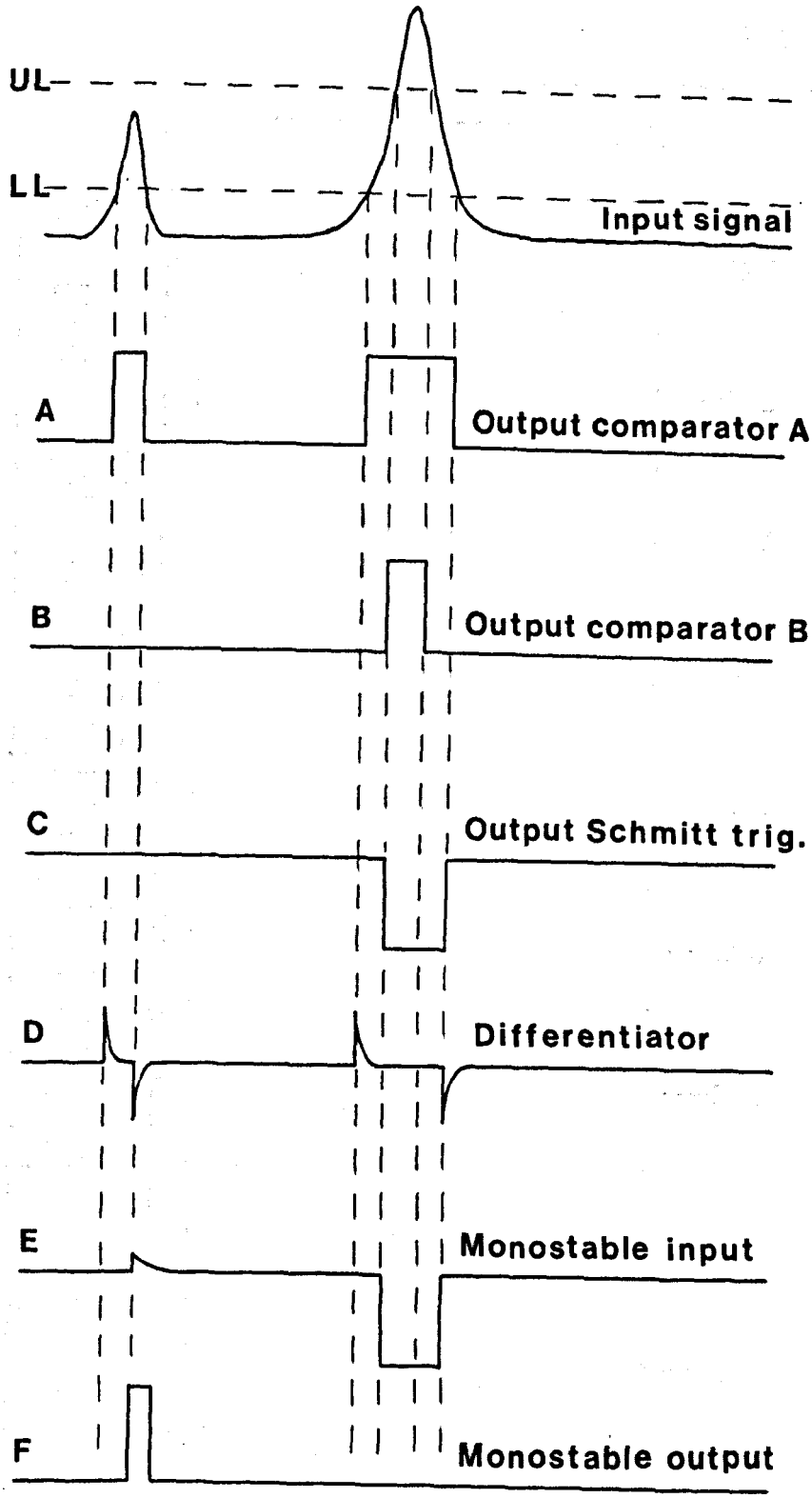

Amplitude discriminator waveforms
UL Upper threshold for stage considered
LL Lower threshold for stage considered

Figure 4.17

Referred to on p 160

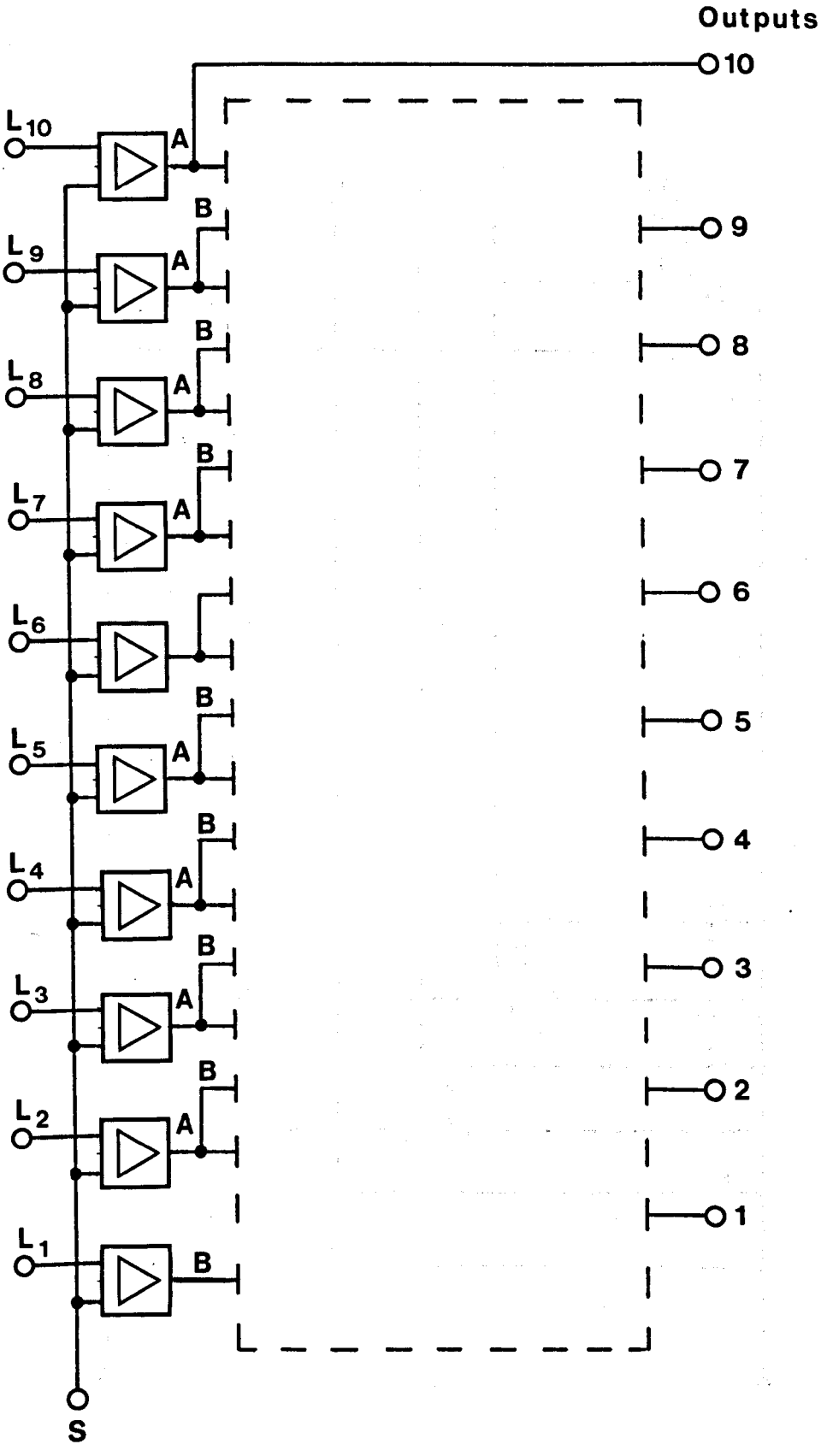

Amplitude discriminator schematic
LI-LIO Threshold levels; S: Signal input
A & B Points indicated on diagram for single stage (figure 4.16)

Figure 4.18

Referred to on p 160

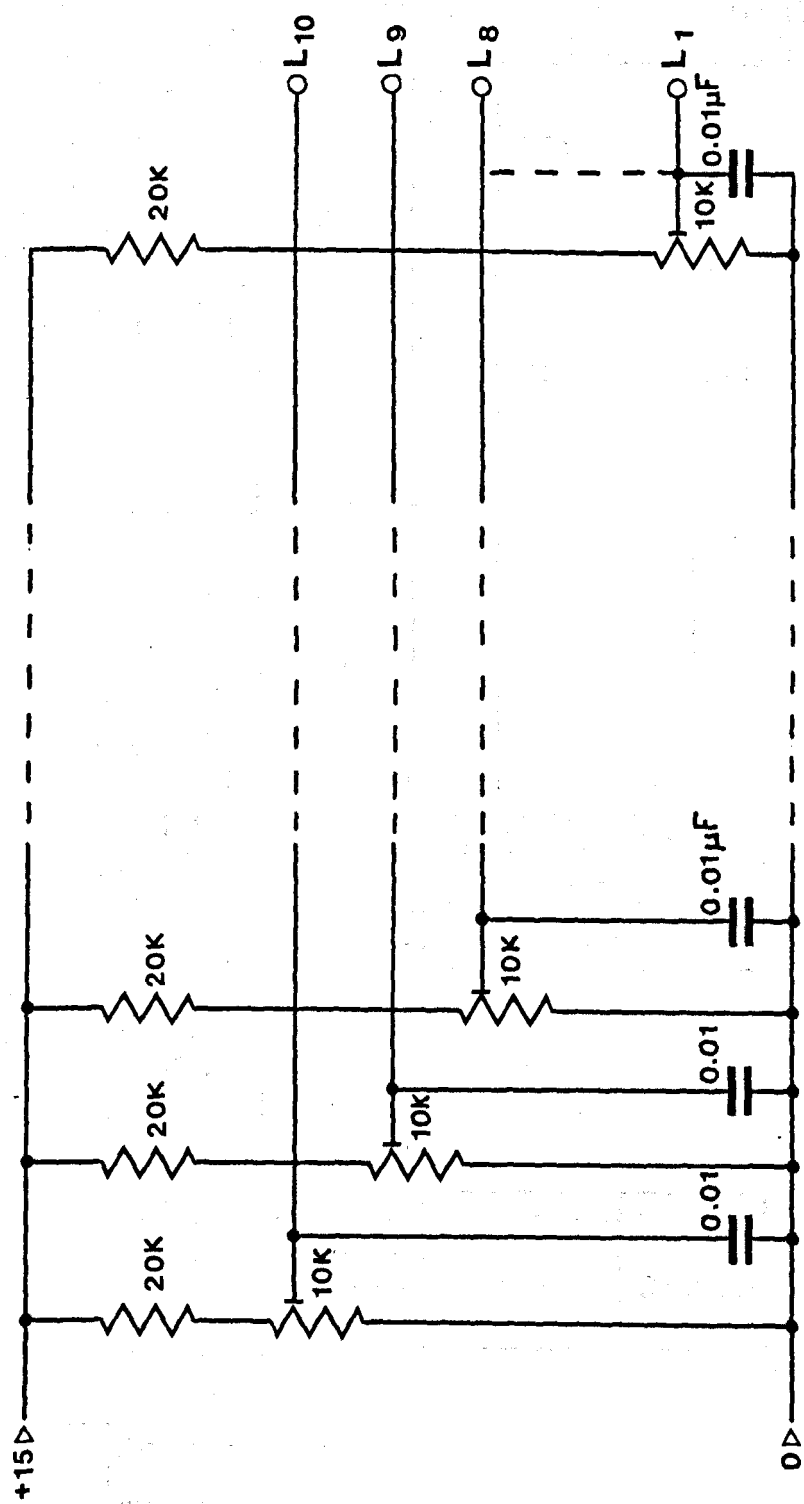

Circuit for deriving voltage thresholds for the amplitude discriminator LI-LIO (figure 4.18)

Figure 4.19

Referred to on p 160

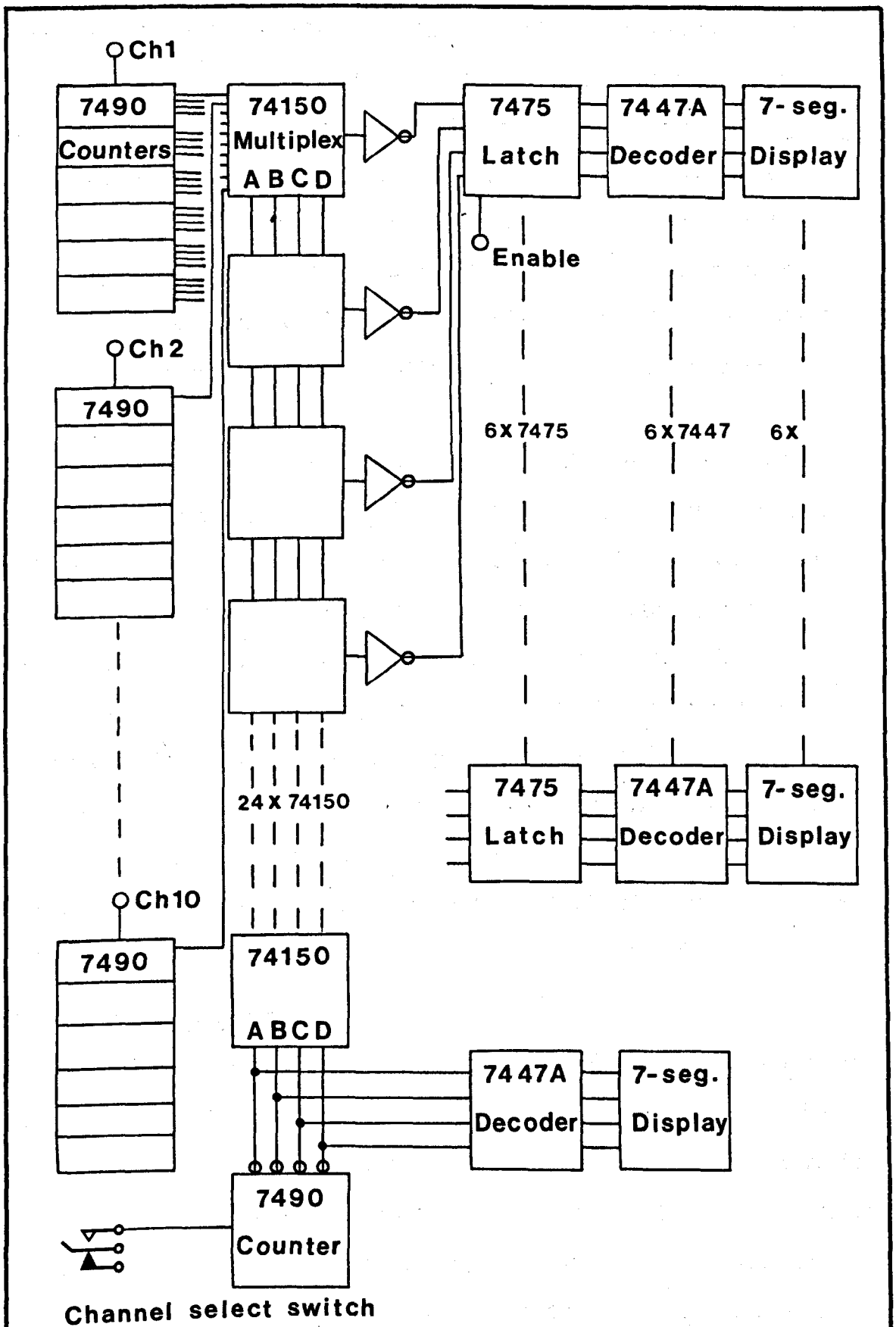

Counters, multiplexer, display & channel select system (TTL logic)

Figure 4.20

Referred to on p 160

four 74150 digital multiplexers. In accommodating ten channels, ten of the sixteen inputs for each of the twenty four multiplexers are used. A common BCD code applied to the input select section of the multiplexers allows each input for the channel selected to be presented at the multiplexer outputs. By multiplexing in this manner it is necessary to have only one six digit, latch, decoder-driver and seven segment light emitting diode display. Indexing the BCD code applied to the multiplexer input select allows each channel count to be displayed in turn.

The multiplexer index facility is achieved by using a manual spring return lever switch to apply a + 5 volt level to the input of a 7490 decade counter. A simple NAND gate latch circuit is used to avoid spurious counts due to contact bounce, thus allowing a count increment of one for each depression of the switch. In order to accommodate the input select power requirements for the total complement of multiplexers, the BCD output of the decade counter is buffered using 7437 quad, two-input NAND buffers. The BCD output is also decoded using a 7447A BCD to seven segment decoder-driver and displayed on a seven segment light emitting diode display, the channel select thus being identified as a number between 0 and 9.

Frequency to Voltage converter

For the purpose of measuring the rate of bubble detection a pulse frequency to voltage converter has been included in the system, the source frequency being derived from an amplitude discriminator circuit of the type described earlier in the section on amplitude discrimination. The circuit diagram for the converter, including the discriminator is shown in Fig.4.21. By setting the discriminator threshold levels to accommodate the complete range of bubble sizes to be detected (assumed on the basis of signal amplitude) the rate for the complete population may be recorded. Conversely the discriminator threshold may be adjusted

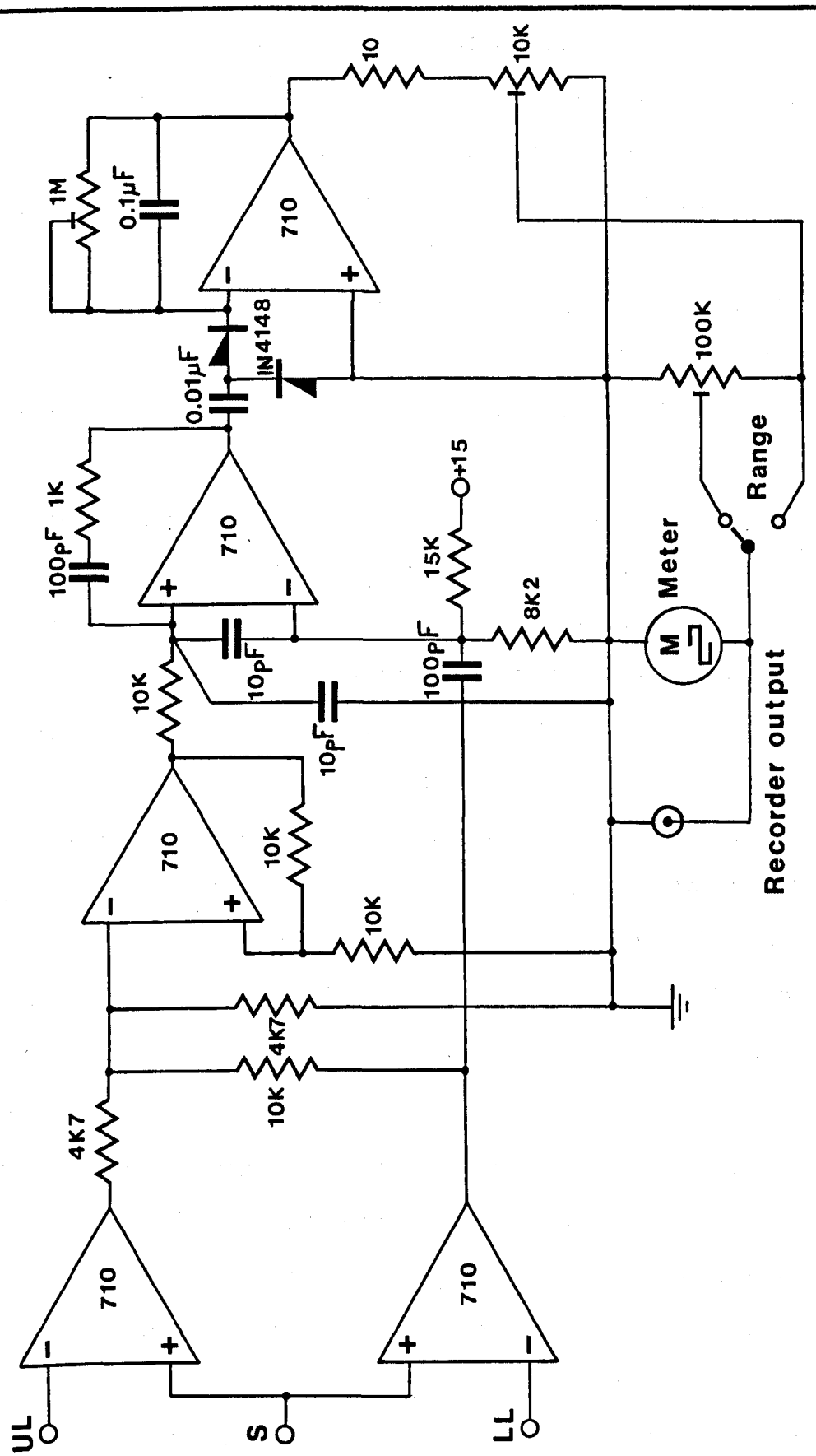

Frequency to voltage converter

UL Upper Threshold level
LL Lower threshold level
S Signal input from analog gate

Figure 4.21

Referred to on p 165

to provide a measure of rate for a particular size range.

The converter circuit is basically an ac coupled integrator used to linearise the output of a simple diode pump circuit. The resultant current produced by the transfer of charge is directed through the resistance in parallel with the feedback capacitor in order to determine the output voltage (the product of frequency, feedback resistance and capacitance, and input voltage). The input capacitor ensures that the circuit is responsive only to an ac signal source and the diode connected to ground ensures that the input is effectively maintained at zero potential in the absence of an input signal.

In operation, the input capacitor charges through the diode connected to ground on the negative going edge of each input pulse and discharges through the input diode on the positive going edge, transferring the charge to the integrating capacitor. This transfer of charge produces a current through the feedback resistance which in turn determines the output voltage. Providing the input pulses are of consistent amplitude, the output voltage is proportional to the applied pulse frequency. A linear response has been observed for this circuit up to one thousand five hundred pulses per second using a square wave test input (Fig.4.22).

Power Supplies

Three power supplies were constructed for individually powering the amplitude discriminator, the digital counters and the frequency to voltage converter. The flow dependent pulse triggering circuit and the gate pulse generator circuit are powered from the existing supplies within the Ekoline 20.

Modular construction of the discriminator, counter and frequency to voltage converter circuits together with separate power supplies both simplify testing and maintenance and enables their use for other applications should they arise. All three power supplies have

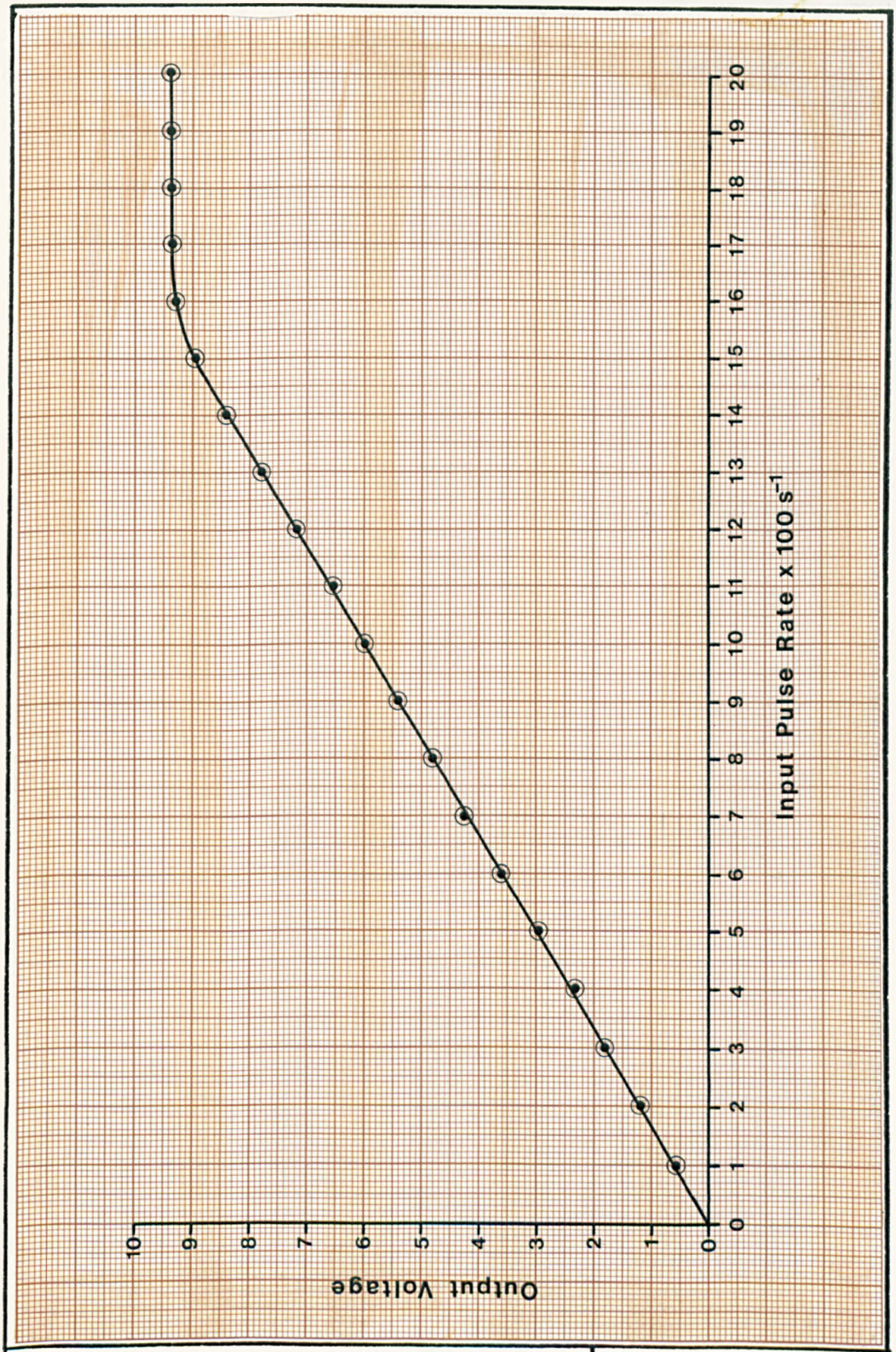

Frequency to voltage converter response characteristic

Figure 4.22

Referred to on p 167

conventional circuit configurations and provide voltage stabilised outputs with load regulation of better than 4% and 100 Hz ripple rejection greater than 60 dB.

The modular construction of the detector, incorporated into a 19 inch rack system is shown in Fig.4.23.

Figure 4.23

Complete electronic instrumentation for the flow dependent microbubble detector. The modified Ekoline is situated at the bottom of the rack. Immediately above is the power supply for the logic system. Above this is the amplitude discriminator showing the level check meter on the left and the threshold level setting potentiometers (row on lower right). Above the discriminator is the counter and display module and above that the frequency to voltage converter or rate meter.

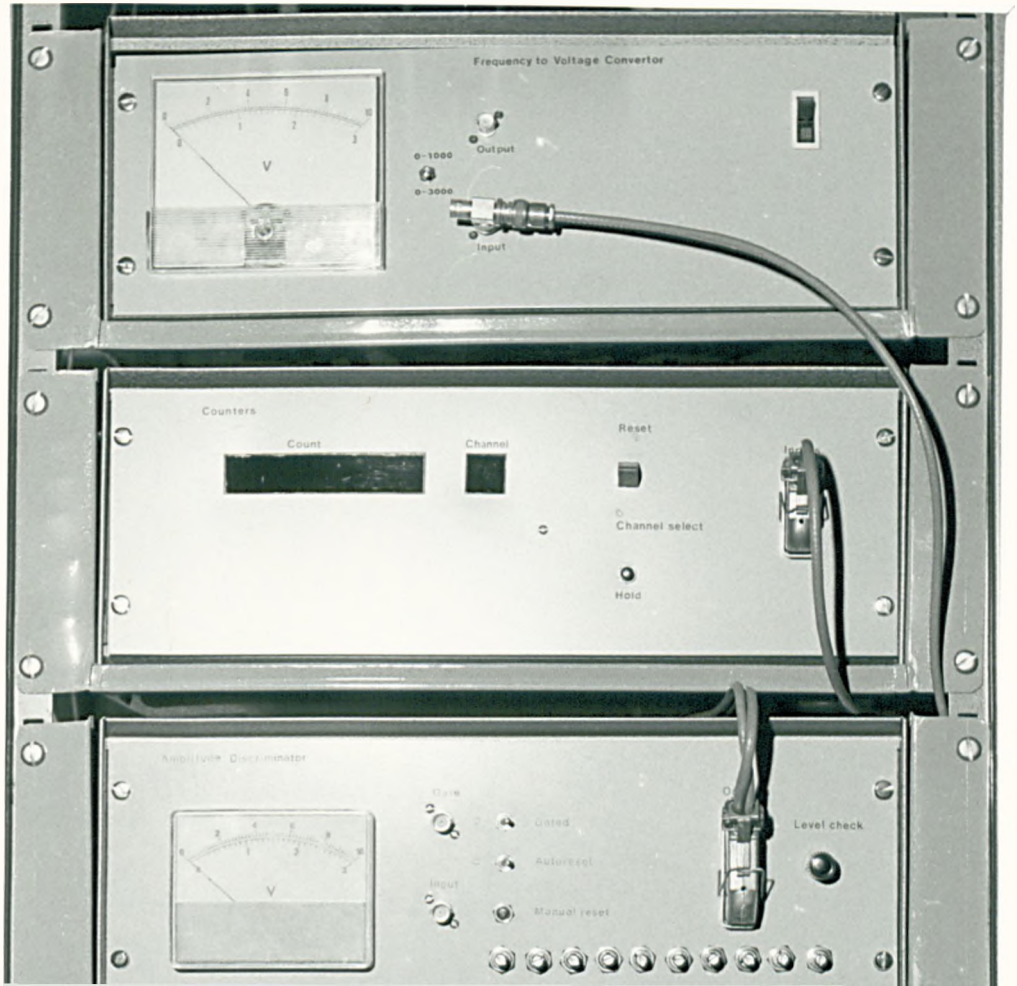
Frequency to Voltage Convertor
V
Output
0-1000
0-3000
Input
Counters
Count
Channel
Reset
Channel select
Hold
Level check
Manual reset

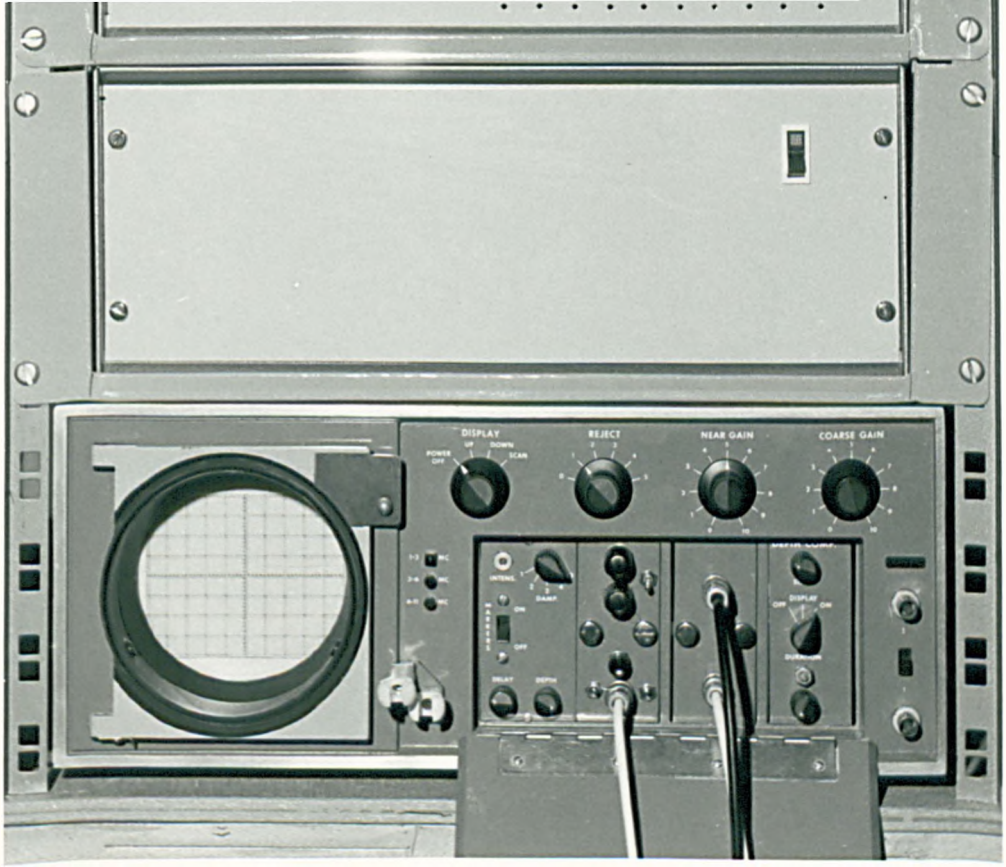
DISPLAY
REJECT
NEAR GAIN
COARSE GAIN
POWER OFF
UP
DOWN
SCAN
INTENS.
DELAY
DEPTH

Chapter 5

CALIBRATION AND SYSTEM ASSESSMENT

Introduction

Before attempting to obtain quantitative results with the ultrasonic bubble detector it was necessary to evaluate the following characteristics:-

1. the intensity distribution within the volume of insonification,
2. the relationship between bubble size and received signal amplitude, including the significance of transducer coupling variations,
3. the flow profile within the transducer mounting assembly,
4. the flow dependent signal response,
5. the resolution of the detector, and
6. the safety of the instrument in a practical application.

These characteristics appear to have been largely ignored in previous reports on microbubble detectors for use in decompression and extracorporeal circulation studies (Gillis, Karagianes & Peterson, 1969; Patterson & Kessler, 1969; Carlson et al., 1972; Clark & Weldon, 1972; Simmons et al., 1972; Gallagher & Pearson, 1973; Lubbers et al., 1974; Patterson, Wasser & Porro, 1974; Hills & Grulke, 1975). This is surprising since techniques for measurements of acoustic power and for the measurement of spatial and temporal distribution of acoustic energy have been reported for bio-medical applications (Hill, 1970; Robinson & Kossoff, 1972). In attempts to size particles the emphasis has been placed upon obtaining a relationship between particle size and received signal amplitude without considering the intensity distribution.

Plastic microspheres have been used as a source of scatter in many attempts to determine instrument sensitivity (Patterson & Kessler, 1969; Kessler & Patterson, 1970; Patterson & Twichell, 1971; Brennan, Patterson & Kessler, 1971; Patterson, Kessler & Bergland, 1971;

Carlson et al., 1973; Patterson, Wasser & Porro, 1974). Although plastic microspheres are convenient for calibration the results cannot be directly related to microbubble signals, since the density and compressibility of bubbles are different from those of plastic microspheres. It is certainly incorrect to assume that calibrations based upon signals derived from plastic microspheres are valid for both particulate and gaseous inclusions (Carlson et al., 1972; Clark & Weldon, 1972; Simmons et al., 1972; Gallagher & Pearson, 1973).

For the calibration of microbubble detectors a microbubble target source is clearly preferable. Hills & Grulke (1975) have reported the use of carefully measured microbubbles as targets for evaluating ultrasonic microbubble detectors. Unfortunately the evaluation neglected to include intensity distribution and signal processor characteristics, thus making comparisons between instruments somewhat dubious. The two instruments considered by Hills & Grulke (1975) were both Doppler devices. The ability of these instruments to size bubbles is subject to the limitations discussed in chapter 2. Moreover the transducer crystals for both instruments were of square section and as such could be expected to exhibit bizarre intensity distributions within the 'focal' regions of the devices (Marini & Rivenez, 1974). This clearly illustrates the need to consider circuit response and beam characteristics in addition to the relationship between bubble size and received signal amplitude.

Calibration bubble source

A method of producing microbubbles suitable for calibration purposes has been described by Grulke, Marsh & Hills (1973). The bubbles are formed by injecting a selected, dust free, gas through a fine hypodermic needle (25, 50 or 75 μm internal diameter) into a suitable surfactant solution. By varying the combination of needle

aperture, gas pressure, liquid surfactant content and liquid flow rate a range of bubble sizes (20 - 250 μm diameter) may be obtained. The bubbles so produced have been reported to exhibit a very narrow size distribution (80% of the bubbles falling within ± 2 μm and 99% within ± 4 μm of the mean radius) and may be generated at relatively constant rates.

Lubbers & van den Berg (1977) have also described a bubble source to calibrate an ultrasonic detector. The gas bubble generator consists of a capillary tube (0.1 mm internal diameter) incorporated in the side arm of a T-connector, through which saline is pumped using a motor driven syringe. The bubbles are produced electrolytically within the saline filled tube, a copper wire (0.12 mm diameter) forming the cathode and a silver wire (0.22 mm diameter, 10 mm in length) forming the anode. Using a constant current source, Lubbers & van den Berg (1977) reported that hydrogen bubbles of 100 - 300 μm diameter could be obtained at the cathode, the actual size depending upon the infusion rate of saline. The rate of bubble formation was determined by the strength of the electrical current source. Bubbles down to 20 μm diameter could be obtained by the addition of detergent to the infusion source of saline. No bubbles were reported to form at the anode, suggesting that oxygen was moving rapidly into solution.

A microscope with an eyepiece calibrated at a magnification of 90-times was used to observe the bubbles as they left the cathode. Lubbers & van den Berg (1977) assume that the bubbles so generated experience a negligible change in size between leaving the generator and entering the volume of insonification. It is difficult to accept this assumption for a non-uniform field within the volume of insonification since the signal variation due to position within the field may preclude accurate sizing. Considerable scatter was observed

in the pulse heights of detected glass spheres (410 $\pm$ 22 μm dia.). In any case, the measurement of pulse height distribution is subject to the limitations inherent in the Doppler technique (see Chapter 2).

In spite of these criticisms the bubble generator and calibration technique described by Lubbers & van den Berg (1977) was an interesting attempt to solve the difficult problem of calibration under flow conditions.

A modified form of the method described by Grulke, Marsh & Hills (1973) has been used as the basis for deriving the bubble size - signal amplitude relationship and for investigating the uniformity of the field of insonification. Glass micropipettes were made from 1 mm internal diameter chemically clean tubing using a Palmer microelectrode puller. The tips of these pipettes were reduced in length of achieve selected aperture diameters (10, 15, 20 & 25 μm internal diameter) by 'bumping' against the end of a rack mounted glass rod fixed to the stage assembly of a Prior microscope and illuminated with blue light to improve tip definition. A calibrated eyepiece enabled measurement of the aperture during the 'bumping' procedure.

Microbubbles for calibration were generated with a 25 μm aperture diameter micropipette, a 2% solution of Teepol (sodium dodecyl benzenosulphonate) in distilled water, and a 100% oxygen source, filtered to remove oil and dust by using a Pall ultipor gas line filter. The observation chamber shown in Fig.5.1 was used to investigate the bubble source, measurement of bubble size being achieved directly by means of a Swift traversing microscope and a Reichart calibrated eyepiece.

Prior to connecting the source of oxygen, a small quantity of the Teepol solution was drawn into the micropipette. After connecting the oxygen source the pressure within the pipette increased to 1 $Kg.f.cm^{-2}$ and the solution was displaced. Thereafter a stream of

Figure 5.1

Observation chamber and manipulator assembly for calibration.

Referred to on p 174.

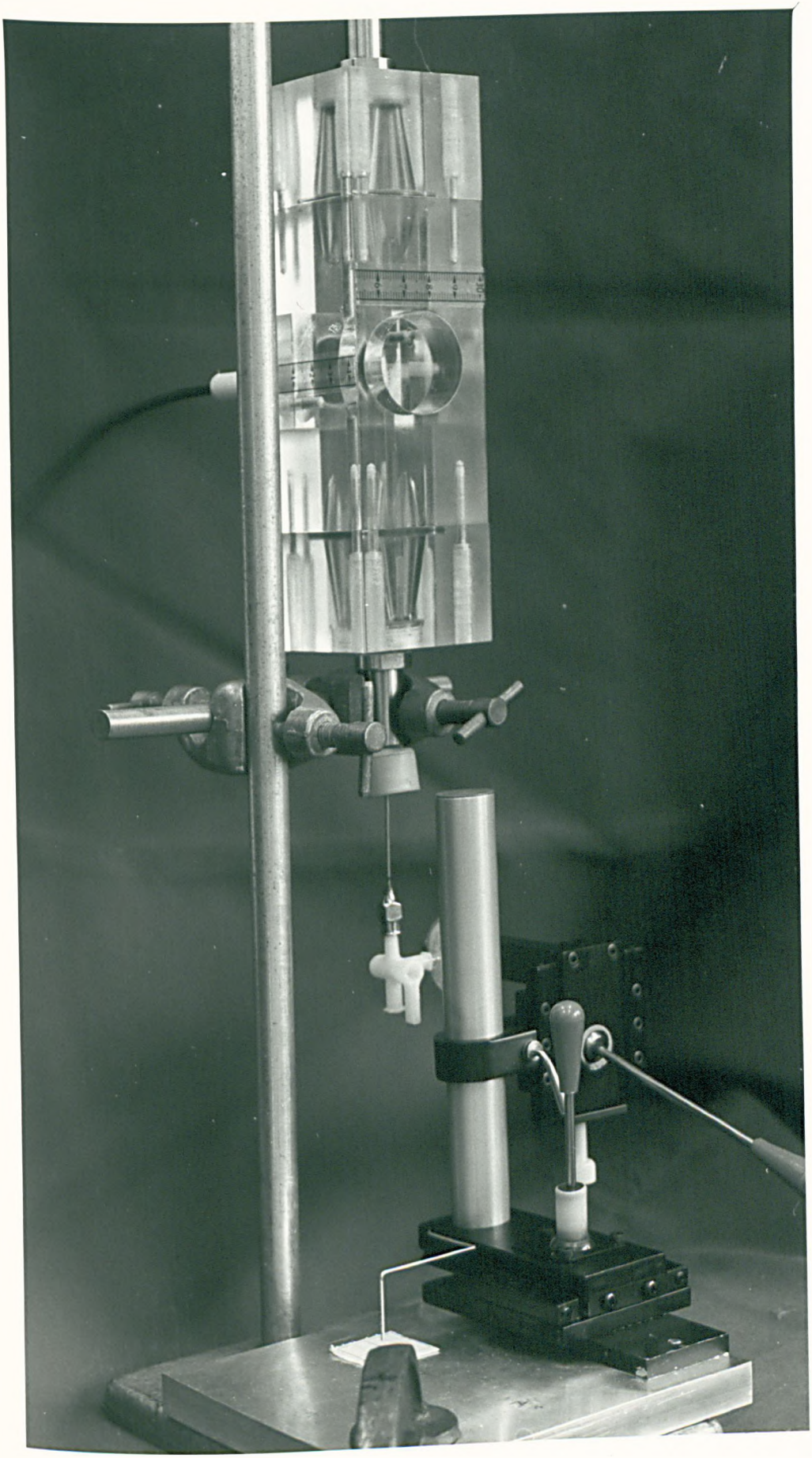

nominal dimensions were also found to affect bubble formation. However, so long as the bubbles are measured optically the technique is useful for the production of a range of bubble sizes for calibration. Only the production of very small bubbles (10 μm diameter and less) has presented a problem. These were produced in the manner described, but they invariably formed in clusters of three or four bubbles rather than individually. With a 10 μm aperture micropipette, careful manipulation of pressure and a reduced surfactant concentration individual bubbles as small as 10 μm diameter were produced. The very high pressures necessary to promote bubble formation precluded the use of micropipettes with aperture sizes less than 10 μm diameter.

Measurement of field uniformity

The objective in determining the spatial distribution of acoustic energy in this particular application was to indicate how the position of a bubble within the field of insonification would influence the amplitude of the received signal. Conventionally the spatial distribution of unfocused, low intensity, acoustic energy is measured with a small piezoelectric detector capable of providing a sensitivity of at least one volt per bar ($10^5 Nm^{-2}$) (Hill, 1970). Whilst such devices are simple in principle and are easy to use, the measurement of acoustic pressure throughout the volume of insonification does not completely fulfil the stated objective. However, the availability of a uniform bubble source enables this objective to be achieved in total.

Materials and Methods

Using the bubble source described earlier advantage was taken of the consistent source of 320 μm diameter bubbles produced after prolonged gas flow through the micropipette.

The micropipette was coupled to a long metal hypodermic needle

(120 mm in length, 1 mm internal diameter) by means of a silicone rubber tube and a PVC sleeve to provide a more rigid arrangement. Prior to coupling the micropipette to the hypodermic needle, the needle was passed through the centre of a rubber cap inserted into the lower part of the observation chamber (Fig.5.1). The flexibility of the rubber membrane through which the shaft of the needle was passed provided a simple pivot for positioning the bubble source to any region of the observation chamber by adjusting the position of the lower end of the needle. The arrangement is shown diagrammatically in Fig.5.2. By attaching a micromanipulator to the lower end of the needle via the three way tap and syringe attachment, the position of the bubble source could be effected smoothly and accurately. A pointer attached to the rack assembly of the micromanipulator and a grid fixed to the base plate provided a convenient method of locating the bubble source within the chamber, the ratio of the needle lengths above and below the rubber membrane having been adjusted to allow meaningful indexing.

The tip of the micropipette was positioned immediately below the volume of insonification. This was done to reduce the possibility of any significant change in bubble diameter between the time of release from the micropipette and entry into the field. The chamber was filled with 2% Teepol in distilled water solution and the temperature of the solution measured directly using a mercury in glass thermometer.

The transducer was coupled to the observation chamber by means of a thin layer of Aquasonic 100 transmission gel (Parker Laboratories Inc.), care being taken to avoid bubble inclusions. By observing from the opposite side of the chamber the correct orientation of the active element of the transducer was accomplished, two marker lines inscribed on the edge of the transducer housing and the transducer retaining port of the observation chamber being used to ensure correct

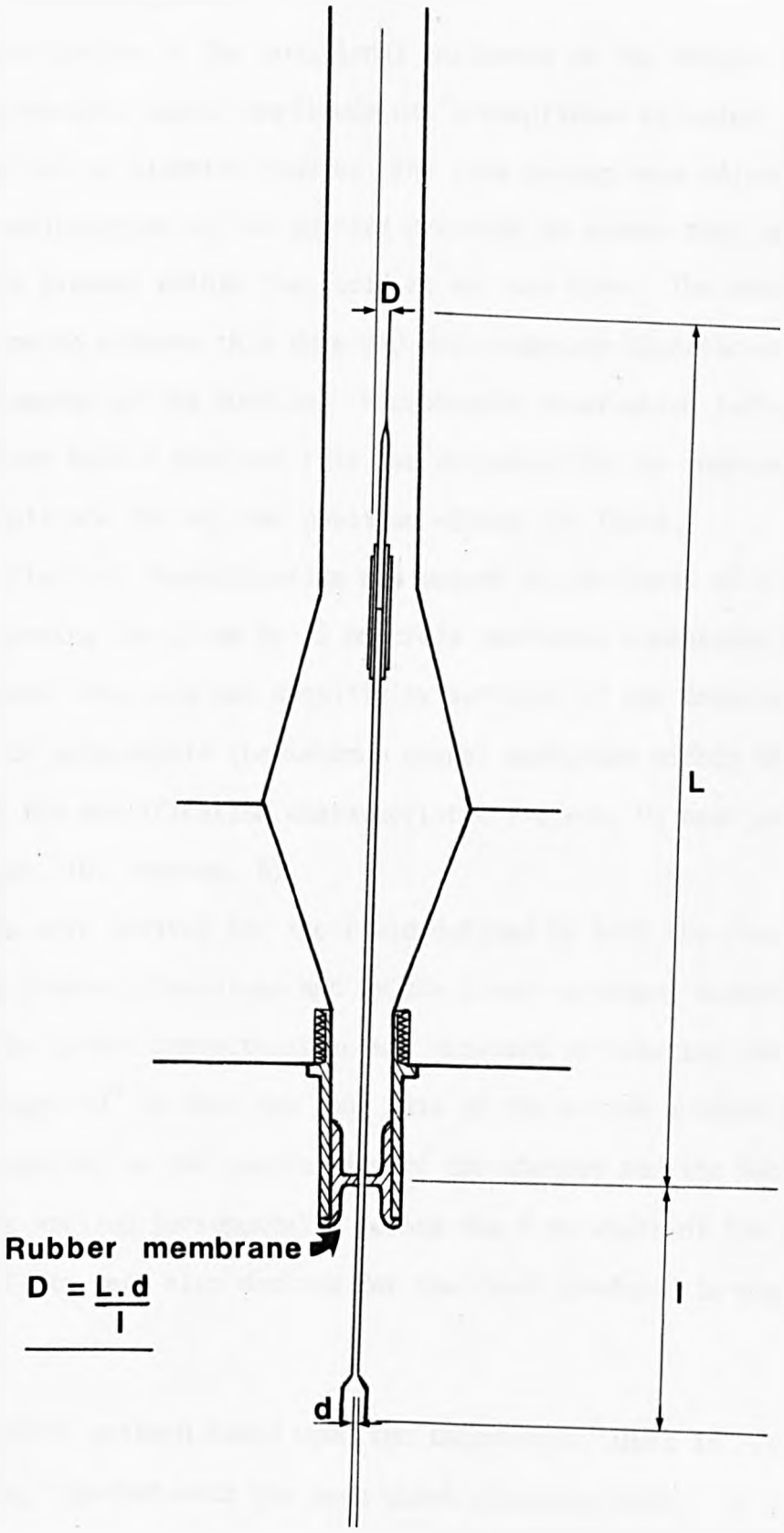

Schematic of the micropipette assembly for use in the measurement of field uniformit

Figure 5.2

Referred to on pp. 178, 187

and consistent alignment.

Investigation of the positional influence of the bubble source upon the receiver signal amplitude was accomplished by using a stream of 320 μm diameter bubbles, the rate having been adjusted by careful manipulation of the applied pressure to ensure that only one bubble was present within the field at any one time. The manipulation of pressure to achieve this rate did not cause any significant change in the diameter of the bubbles. Microscopic observation indicated a consistent bubble size and this was supported by the constancy of signal amplitude for any one position within the field.

The field of insonification was mapped on the basis of a 9 by 9 matrix covering the 15 mm by 15 mm cross sectional dimensions of the chamber. The gain and sensitivity settings of the detector were adjusted to accommodate the maximum signal amplitude within the linear region of the amplification characteristic (reject, 0; near gain, 2; course gain, 10; damping, 5).

Plots were derived for the field defined by both the cross sectional chamber dimensions and by the cross sectional acoustic field. The latter characteristic was obtained by rotating the transducer through 90^{o} so that the long axis of the active surface was aligned parallel to the centre line of the chamber and the bubble source was applied incrementally across the 4 mm width of the active region. Plots were also derived for the field produced in pig blood.

Results

The field pattern based upon ten independent plots is illustrated in Fig 5.3A, together with the beam width characteristic. It is clearly apparent from these characteristics, that the field close to the transducer is non-uniform and exhibits a pronounced gradient up to and into the centre of the field. Within the distal region of the field,

Plot of field uniformity

SD Standard deviation ; SE Standard error

Figure 5.3A

Referred to on pp. 180, 185

(0.59)	(0.40)	(0.63)	(0.44)	(0.11)	(0.57)	(0.58)	(0.29)	(0.58)
2.14	4.50	4.19	4.36	3.99	4.11	4.13	4.66	2.12
(0.65)	(0.35)	(0.26)	(0.24)	(0.11)	(0.24)	(0.26)	(0.39)	(0.27)
2.00	4.34	4.16	4.11	3.96	4.10	4.16	4.3	1.78
(0.49)	(0.36)	(0.26)	(0.24)	(0.29)	(0.24)	(0.26)	(0.39)	(0.28)
1.73	4.30	4.15	4.10	3.88	4.10	4.16	4.30	1.6
(0.36)	(0.37)	(0.26)	(0.21)	(0.11)	(0.18)	(0.26)	(0.34)	(0.28)
1.75	4.34	4.15	4.10	3.85	4.08	4.15	4.35	1.6
(0.28)	(0.37)	(0.31)	(0.34)	(0.35)	(0.33)	(0.31)	(0.44)	(0.29)
1.94	4.30	4.08	4.0	3.71	3.96	4.09	4.28	1.77
(0.29)	(0.43)	(0.35)	(0.40)	(0.53)	(0.38)	(0.30)	(0.47)	(0.92)
1.65	3.79	3.83	3.68	2.88	3.65	3.85	3.63	2.02
(0.37)	(0.53)	(0.40)	(0.49)	(0.65)	(0.35)	(0.38)	(0.32)	(0.61)
1.49	2.96	3.16	3.21	2.18	3.1	3.14	2.75	2.07
(0.67)	(0.95)	(0.92)	(0.76)	(0.88)	(0.82)	(1.01)	(0.96)	(0.85)
1.65	1.14	1.11	1.0	0.9	1.0	1.51	1.58	1.5
(0.93)	(0.45)						(0.28)	(0.92)
0.78	0.23	0	0	0	0	0	0.53	0.95

Mean and standard error values for the complete field of insonification

Figure 5.3B
Referred to on
p. 180

SE	(0.40)	(0.63)	(0.44)	(0.11)	(0.57)	(0.58)	(0.29)
	4.50	4.19	4.36	3.99	4.11	4.13	4.66
P	0.0125	0.45	0.15 - 0.1	0.0005	0.45 - 0.4	0.45	0.0005
SE	(0.35)	(0.26)	(0.24)	(0.11)	(0.24)	(0.26)	(0.39)
	4.34	4.16	4.11	3.96	4.10	4.16	4.3
P	0.1 - 0.05	0.48 - 0.49	0.35 - 0.3	0.0005	0.3 - 0.25	0.48	0.2 - 0.15
SE	(0.36)	(0.26)	(0.24)	(0.29)	(0.24)	(0.26)	(0.39)
	4.30	4.15	4.10	3.88	4.10	4.16	4.3
P	0.15	0.497	0.3 - 0.25	0.01 - 0.005	0.3 - 0.25	0.475	0.2 - 0.15
SE	(0.37)	(0.26)	(0.21)	(0.11)	(0.18)	(0.26)	(0.34)
	4.34	4.15	4.10	3.85	4.08	4.15	4.35
P	0.1	0.497	0.25 - 0.2	0.0005	0.15 - 0.1	0.497	0.1 - 0.05
SE	(0.37)	(0.31)	(0.34)	(0.35)	(0.33)	(0.31)	(0.44)
	4.30	4.08	4.0	3.71	3.96	4.09	4.28
P	0.15- 0.1	0.25	0.15 - 0.1	0.0005	0.1 - 0.05	0.3 - 0.25	0.25- 0.2

Mean, standard error, and P values for the selected region of insonification

SE Standard error

Figure 5.3C
Referred to on p. 180

									5.14	
									Δ	
								4.26	4.18	
								Δ	Δ	
							4.16	4.00	4.16	
							Δ	Δ	Δ	
						4.12	4.06	4.16	4.16	
						Δ	Δ	Δ	Δ	
					4.56	3.86	4.05	4.16	4.16	
					Δ	Δ	Δ	Δ	Δ	
				4.22	4.16	4.11	4.15	4.16	4.44	
				Δ	Δ	Δ	Δ	Δ	Δ	
			4.84	4.16	4.15	3.81	4.05	4.16	4.16	
			Δ	Δ	Δ	Δ	Δ	Δ	Δ	
		4.52	4.17	4.16	4.07	4.15	4.15	4.15	4.44	
		Δ	Δ	Δ	Δ	Δ	Δ	Δ	Δ	
	4.44	4.16	4.16	4.16	4.16	4.15	4.15	4.15	4.44	
	Δ	Δ	Δ	Δ	Δ	Δ	Δ	Δ	Δ	
4.52	4.16	4.16	4.14	4.14	4.05	4.05	4.05	4.16	4.16	
Δ	Δ	Δ	Δ	Δ	Δ	Δ	Δ	Δ	Δ	
4.16	4.16	4.14	4.14	4.16	4.05	3.62	4.05	4.16	4.16	
									4.54	
									Δ	
								4.16	4.16	
								Δ	Δ	
							4.15	4.14	4.16	
							Δ	Δ	Δ	
						4.09	4.01	4.16	4.16	
						Δ	Δ	Δ	Δ	
					4.15	3.61	4.05	4.14	4.16	
					Δ	Δ	Δ	Δ	Δ	
				4.16	4.15	4.09	4.15	4.16	4.54	
				Δ	Δ	Δ	Δ	Δ	Δ	
			4.52	4.16	4.15	3.61	4.05	4.14	4.16	
			Δ	Δ	Δ	Δ	Δ	Δ	Δ	
		4.44	4.16	4.14	4.05	4.15	4.15	4.15	4.44	
		Δ	Δ	Δ	Δ	Δ	Δ	Δ	Δ	
	4.44	4.16	4.16	4.14	4.05	4.15	4.15	4.15	4.44	
	Δ	Δ	Δ	Δ	Δ	Δ	Δ	Δ	Δ	
4.44	4.16	4.16	4.01	4.14	3.85	3.28	3.77	4.03	4.16	
Δ	Δ	Δ	Δ	Δ	Δ	Δ	Δ	Δ	Δ	
4.16	4.16	4.01	4.01	4.16	3.85	3.28	3.77	4.03	4.16	

Confidence limits for the selected region of insonification

Figure 5.3D
Referred to on p. 180

peaks can be distinguished within 1 mm of each side wall ($\bar{x}$ = 35 dB, with respect to system noise level; σ = 15.4 dB). The response is attenuated by 3 dB within 0.5 mm of these peaks followed by a more gradual attenuation into the centre of the field (0.8 dB over a distance of 6 mm). For the purpose of sizing bubbles, the most consistent region of the field was taken to be the distal half, 1 mm in from the side walls. This region was tested for uniformity by evaluating probability values for each point based upon the use of the unpaired Student-t test. Confidence limits were also computed for each point. The results of these computations presented in Fig.5.3 indicate that the field is reasonably uniform except for a narrow region within the centre. By confining measurements to perturbations arising from within this region of the field an error of approximately 15% may be expected. Including the sidewall peaks in the region of analysis increases the uncertainty in sizing to approximately 50%.

The beam width characteristic (Fig.5.3) also indicates that the most uniform part of the field is confined to the distal half of the volume of insonification, but it also indicates that the field contour is parallel and exhibits sharp attenuation within 1.5 mm of the centre line (18 dB within 0.5 mm).

Plots derived with pig blood within the volume of insonification indicated no discernible differences from those derived with the 2% Teepol solution. However the bubble source was observed to be less stable in the blood than the Teepol solution which made the analysis more difficult. The signal variations that marked this lessened stability were considered to be due to surface active agents within the blood and the result of collisions with particulate matter rather than intrinsic transient variations in field intensity. A 500 μm diameter wire target introduced into the field yielded a signal of constant amplitude, which would seemingly obviate the possibility of

transient field variations.

The noise level observed when using blood was consistently no greater than 6 dB compared with the noise level observed when using 2% Teepol solution even when the blood samples contained large numbers of cellular aggregates producing screen filtration pressure values (Swank, 1961) greater than 80 kPa(600 mm Hg).

Discussion

The bizarre contours of the field distribution plots for the volume of insonificatin show that it is important to evaluate the field characteristic prior to any investigation requiring quantitative interpretation of perturbation measurements. By accepting measurements from the whole of the field, the error in measurement of bubble sizes would be well in excess of 100%. However this assumes that it is possible to restrict the measurements to those arising from perturbations within the distal part of the field without including the peaked regions that border the flow path. By range gating, the distal half of the field may be conveniently accepted for analysis whilst the proximal half is rejected.

Eliminating signals from the peak regions (50% error in the measured size) is more difficult. Unless these regions are avoided by the bubbles as they pass through the volume of insonification, the error cannot be reduced. Bubbles, because of their natural buoyancy may move in a convoluted manner. Consequently, little can be said about the actual position of a bubble in the flow path even when the velocity flow profile is known for all flow conditions likely to be encountered. However it is likely that under the flow conditions encountered the bubbles experience a centripetal force component directing them toward the centre of the flow path, in which case the possibility of bubbles entering the peak regions would be reduced.

Alternatively, such problems might be overcome by averaging several echo responses from adjacent synchronised detectors.

In view of the small variations of propagation velocity for ultrasound in blood with respect to frequency, distance, flow velocity, temperature, haematocrit, and total protein content (Bradley & Sacerio, 1972) and the variations of density and compressibility over the range of parameter variations encountered in extracorporeal procedures, the investigation of field uniformity under various conditions was not at this stage considered necessary. Clarke, Dietz and Miller (1975) have reported consistent sizing of plastic microspheres over wide ranges of temperature, haematocrit and protein content using a 10 MHz source frequency.

Bubble size-signal amplitude relationship

Materials and methods

Using the arrangement described for the evaluation of field uniformity (Fig.5.2) and the technique for generating a wide range of bubble sizes, a relationship between bubble size and signal amplitude was established. The initial rate of bubble release was adjusted to approximately one per second, the final bubble sizes being achieved after a period of about 30-40 minutes. Measurements were achieved by one operator estimating the bubble size by means of a Swift traversing microscope and Reichert calibrated eyepiece as the bubbles were released whilst a second operator noted the amplitude of the signal response on the oscilloscope display.

Bubble size-signal amplitude relationships were established for various gain settings and repeated (x 10) following decoupling and recoupling of the transducer to the transducer mounting assembly. Attempts were made to repeat the measurements in whole blood, estimates of bubble size being obtained using a modified terminal velocity

measurement based upon the number of counts recorded as a bubble passes through an acoustic field pulsed at a fixed rate of 1000 Hz. Again the amplitude of the signal response was noted. The obvious limitations of the indirect technique of sizing together with the same instability phenomenon observed during the evaluation of field uniformity in blood suggested the need for caution in accepting such results in the absence of other information. As in the procedure for measuring field uniformity a wire target introduced into the blood indicated a stable response, thus suggesting the instability was related to bubbles and not a transient field effect.

Results

The relationship between bubble size and signal amplitude for a bubble source in 2% Teepol solution (over a temperature range 20-35^{o}C) are shown in Fig.5.4, for gain settings that provide acceptable dynamic ranges and signal to noise ratios. Within the linear range of amplification the measured relationship is also linear and as such conforms with the theoretical relationship for perturbation pressure ratio and bubble size. In all measurements the course gain was set at maximum (37 dB), damping at maximum and rejection at zero. The near gain facility exhibits a non-linear characteristic. For this reason bubble size-signal amplitude relationships were selected for fixed values of near gain that offered potentially useful dynamic ranges.

The variations attributable to changes in acoustic coupling did not appear to be appreciable, particularly if measurements were confined to the measurement of small bubble sizes. Upper and lower limits illustrated in Fig5.4 indicate the range of variation encountered.

Discussion

The measured relationships for bubble size and signal amplitude provide a practically useful working characteristic. Although the

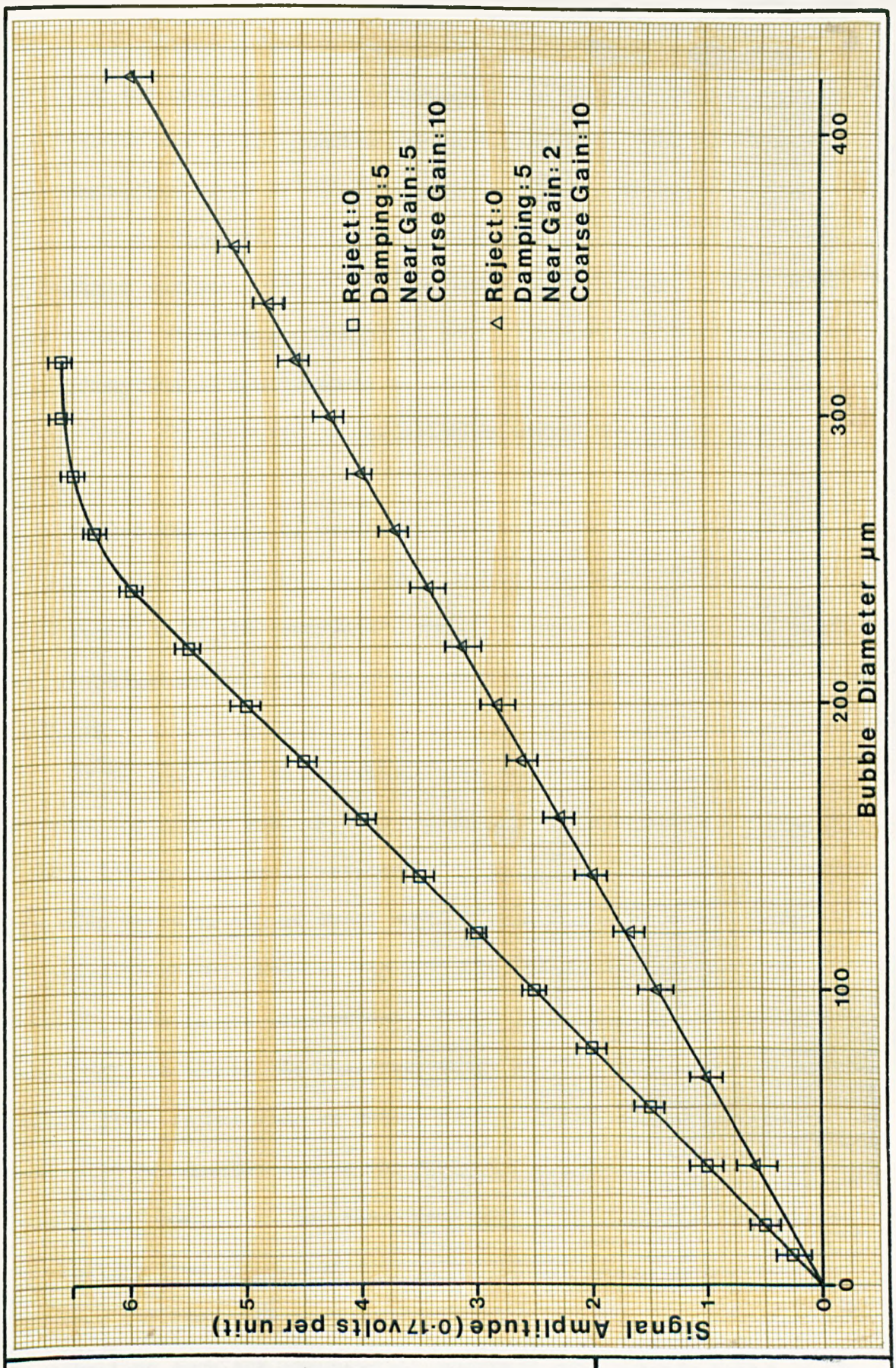

Bubble size - signal amplitude relationship for single bubbles

Figure 5.4
Referred to on
p. 188

theory of scatter indicated that such a characteristic was to be expected for measurements at some distance from the transducer, some uncertainty was to be expected for measurements derived for scatter sources within 15 mm of the transducer. However the measurements have been confined to perturbations arising within 7 to 15 mm of the transducer surface. Since the wavelength of ultrasound in both water and blood (0.15 mm at 10 MHz) is small compared to these distances, the assumption of measurements at some distance would appear to be justified. The measured characteristics appear to support this assumption.

Whilst the range of variation due to acoustic coupling was not great, a rigorous attempt at bubble sizing requires calibration for each mounting of the transducer, and preferably both before and after an investigation in order to detect any time related change in coupling.

It is important to appreciate that the characteristics were derived for single bubbles. In the absence of multiple scattering and bubble interaction it is reasonable to assume that the characteristics may also apply to two or three bubbles contained within the volume of insonification. However the characteristics must be used cautiously, with larger populations. Under such conditions it is more reasonable to accept the characteristics as a guide to the most likely bubble sizes rather than as actual measurements. The possibility must also be considered that the measured perturbations arise from clusters of bubbles rather than from single bubbles. Discrimination of clusters from single entities is at present unavailable. A facility for analysing echo profiles could possibly provide a means of effecting such discrimination. Certainly the echo profiles from 250 μm diameter plastic microspheres are markedly different from those of 250 μm diameter bubbles as well as being of different amplitude.

Flow characteristic of the transducer mounting assembly

The measurements of field uniformity and bubble size-signal amplitude response so far reported have been performed under static fluid conditions. Investigations under flow conditions require an assessment of the flow characteristics of the transducer mounting assembly. Flow visualisation together with a measurement of the pressure-flow relationship at various flow rates was attempted in order to establish these characteristics.

Materials and methods

A circuit was constructed using 1.8 m of 9.5 mm internal diameter tubing, a 400 ml polycarbonate reservoir and the transducer mounting assembly. A 9.5 mm diameter cannulating flow probe (Nyoctron) was introduced into the circuit just proximal to the transducer mounting assembly and a 9.5 mm cannulating sampling port just distal to the mounting assembly. A Sarns roller pump was used to promote flow within the circuit; which was primed with 0.9% sodium chloride. A short (150 mm, 3 mm internal diameter) PVC tube was connected to the Luer sampling connector of the sampling port and coupled to a Bell & Howell (4-422-0001-1-B4MS) pressure transducer (0-75 mm Hg range). A proprietory black drawing ink (0.2 ml in 500 ml) was injected into the saline. Coalescence of the ink particles, in order to derive a useful flow visualisation medium, was induced by circulating the saline at $1 L.min^{-1}$ whilst maintaining electrolysis for twenty minutes at 15 volts, applied to a unipolar myographic needle inserted into the tubing. The polarity of the applied voltage was reversed after ten minutes.

Having established an acceptable flow visualisation medium, the flow through the assembly was observed at flow rates up to $5 L.min^{-1}$ and mean pressure and flow measurements were obtained at each flow

rate setting in 0.5L.min^{-1} steps.

Results

Up to 2.5L.min^{-1} the flow through transducer mounting assembly appeared to be "disturbed laminar flow" (Helps & McDonald, 1954). No evidence of vortex formation was observed within the central region of the assembly or the inlet and outlet regions. Fig.5.5 is representative of the flows observed up to 2.5L.min^{-1}. Above 2.5L.min^{-1} the flow appeared to become more turbulent, particularly within the inlet and outlet regions of the assembly. This observation is supported by the transition in the mean pressure-flow relationship above 2.5L.min^{-1} (Fig.5.6)

Discussion

The limited facilities for analysing non-steady state flow characteristics have somewhat precluded a rigorous assessment of the flow conditions imposed by the transducer mounting assembly. However the absence of visible vortex formations, the overall impression obtained from the flow visualisation medium, and the relationship between pressure and flow strongly indicate that the flow is disturbed laminar up to at least 2.5L.min^{-1}. McDonald (1975) suggested that measurement of the pressure-flow relationship is an effective method of determining the onset of turbulence. Accepting that this is so the indication for laminar flow up to 2.5L.min^{-1} may be accepted with some confidence. For a more viscous diluted blood prime, the onset of turbulence undoubtedly occurs at a higher flow rate.

The assessment of flow profile was more difficult to obtain. On the basis of flow visualisation the flow profile appeared to be more plug-like than parabolic during the principal phase of the pump cycle and flow rates greater than 0.5L.min^{-1}. This being so the desired flow characteristic for the transducer mounting assembly has been achieved. Further study is necessary to establish if they are

Figure 5.5

Flow visualisation through the transducer mounting assemply.

Referred to on p. 192

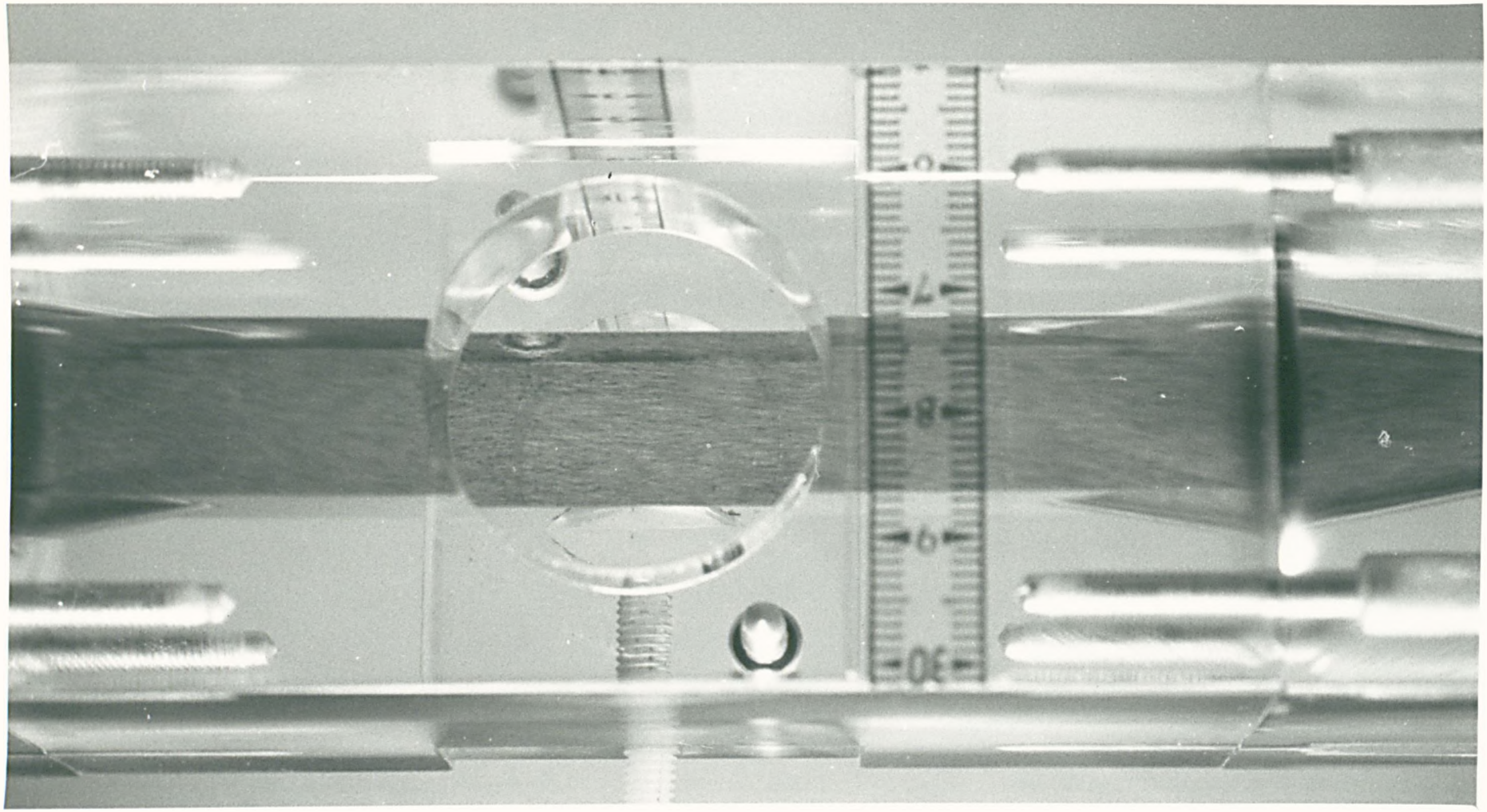
7
8
9
30

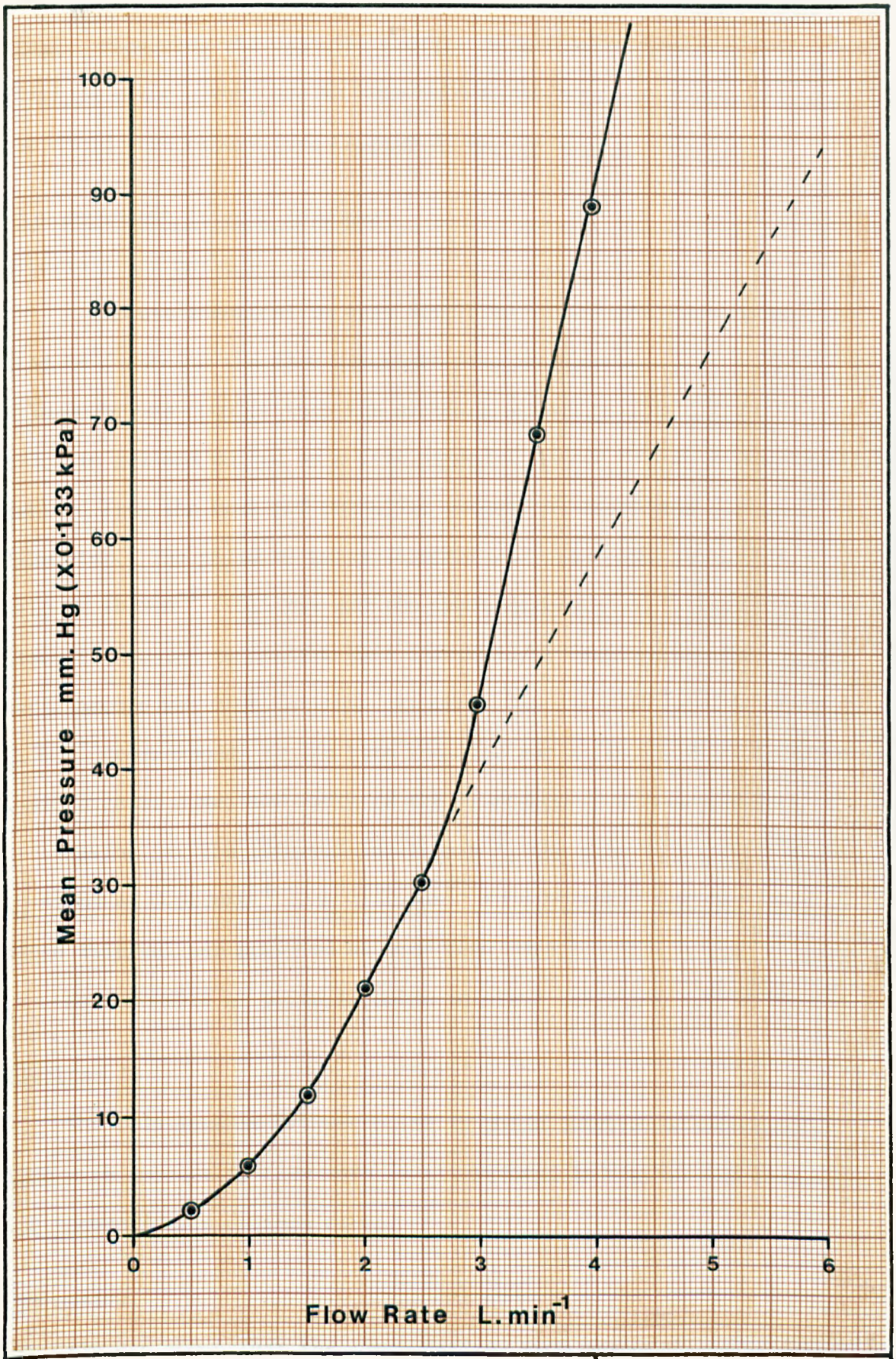

Test for the onset of turbulence

--- estimated non-turbulent relationship

Figure 5.6
Referred to on
p.192

ideal. Providing the velocity profile is not fully parabolic the multiple count errors due to some bubbles moving more slowly through the field than others (see Chapter 4) may be largely avoided.

Flow dependent trigger response

Materials and methods

A circuit identical to that described in the previous section was used to determine the flow dependent trigger response. The acoustic transducer was coupled into the mounting assembly using Aquasonic acoustic gel and pulsed on a flow dependent basis, the flow signal being derived from the mean and pulsatile outputs of a Nycotron (type 376) flowmeter. The pulse to pulse interval was calculated for a mean flow rate of $1L.min^{-1}$ (40.5 ms) and the input attenuator of the pulse trigger circuit adjusted to achieve this interval. A Tecktronix (type 502A) oscilloscope was used for this purpose. The interval of 40.5 ms at $1L.min^{-1}$ corresponds to the time required for a flow entity to traverse a distance of 3 mm, the width of the transducer's active surface.

Having set the interval for $1L.min^{-1}$, the flow rate was adjusted in steps of $0.5L.min^{-1}$ from $0.5L.min^{-1}$ to $4.5L.min^{-1}$ and the pulse to pulse interval was measured at each flow rate.

Measurements of pulse to pulse interval variation were noted.

Results

The relationship between pulse to pulse interval or integration time with respect to flow rate is illustrated in Fig.5.7 together with the theoretically derived curve.

Discussion

Fig.5.7 shows that the curve derived from measurements of flow and pulse to pulse interval compare favourably with the theoretical curve. The observation that interval variation for pulse triggering followed the pulsatile waveform indicates that the pulse triggering

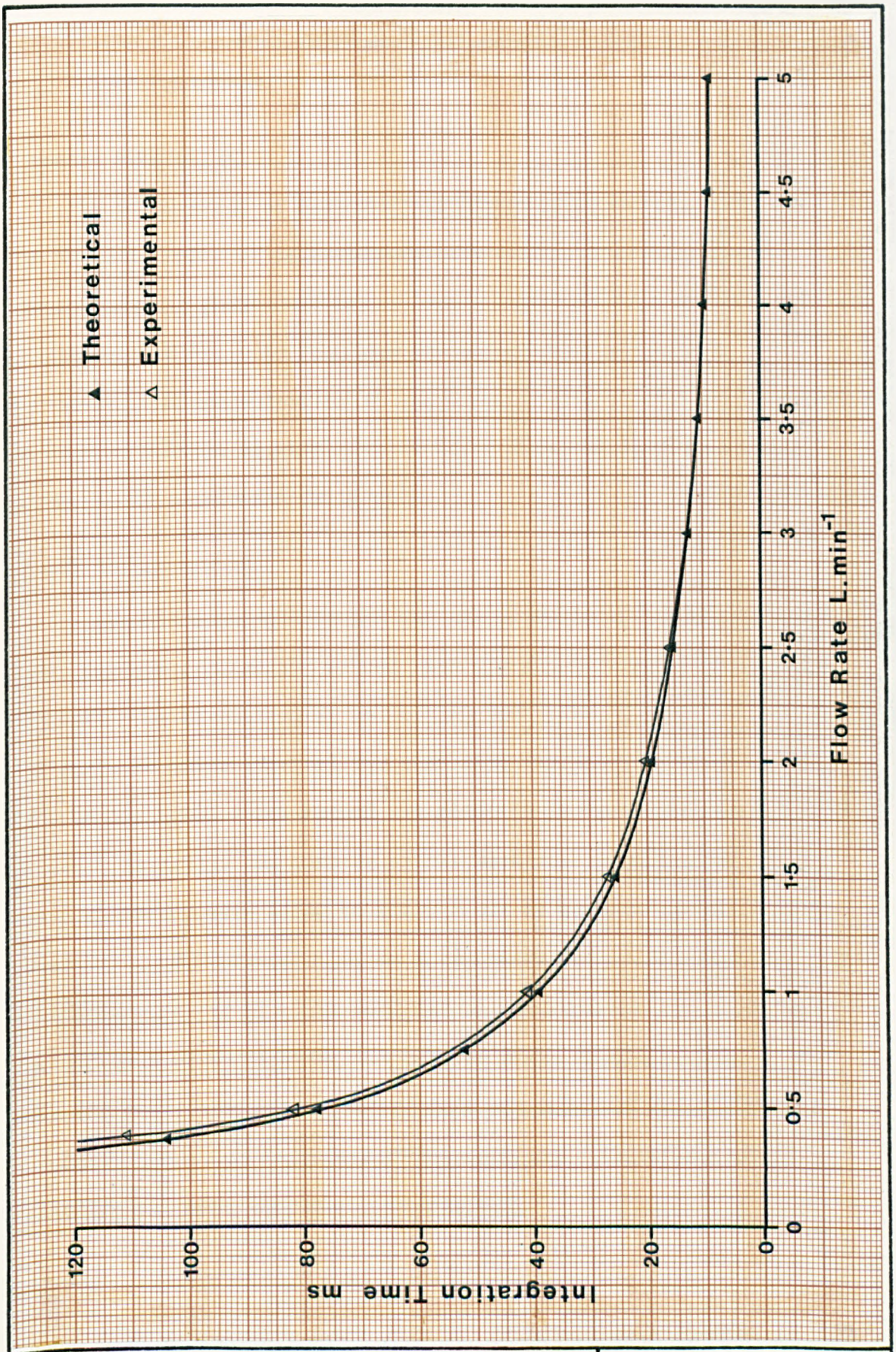

Integration time - flow rate relationship

Figure 5.7
Referred to on
p. 195

circuit can effectively respond to the pulsatile flow changes for the flow rates considered.

Detector resolution

The measurement of detector resolution requires an estimate of the maximum number of perturbations that can be discriminated for a single acoustic pulse delivery to the volume of insonification. To obtain such an estimate requires the use of dimensionally stable targets, the number and concentration of which can be conveniently adjusted. Carbonised plastic microspheres of 250 $\pm$ 40 μm diameter (3M Nuclear Products) were selected as targets.

Materials and methods

A circuit identical to the one described for the flow visualisation study was constructed and primed with 500 ml of 0.9% sodium chloride. The prime was circulated at an initial flow rate of 1.5 $L.min^{-1}$, and the pulse to pulse interval for this rate was measured as 26 ms. A rate of 1-2 bubbles per second was noted to be the background level of activity following ten minutes of circulation. Microspheres (250 μm $\pm$ 40 μm diameter) were added to the circuit in batches of 200 up to a total of 2,400, corresponding to a concentration of approximately 5 microspheres per ml. The addition of microspheres was achieved with the aid of a glass pipette, the spheres being carefully introduced into the reservoir. The detector rate was measured approximately 5 minutes after each addition of microspheres. The effect of flow variation on count rate was also observed.

Results

A plot of the mean count rate vs number of microspheres is presented in Fig.5.8 together with a theoretical estimate of the count rate to be expected for each addition of microspheres. The latter

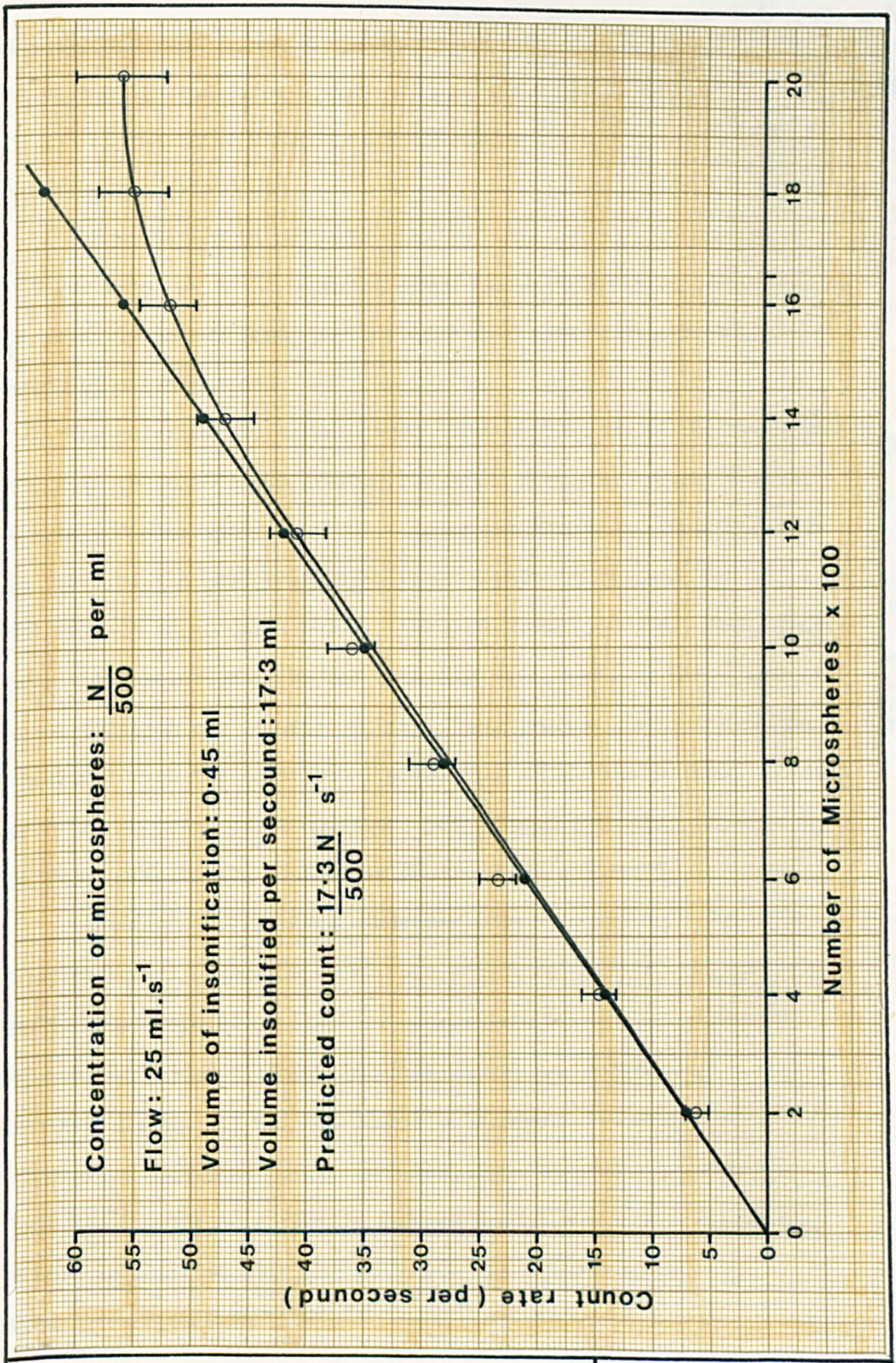

Detector resolution - Relationship between microsphere concentration and count rate

Figure 5.8
Referred to on
pp. 197, 199

was derived from values of circuit prime volume (500 ml), flow rate ($1.5L.min^{-1}$), the gated volume of insonification (0.45 ml corresponding to 2/3 of the total volume), and the number of microspheres for each addition (see Fig.5.8).

The variation in measured rate was considerable (Fig.5.8). However this was to be expected since the distribution of microspheres was clearly non-uniform, particularly just after the addition of each batch of microspheres.

The relationship between mean count rate vs number of microspheres suggests reasonable proportionality up to a concentration of approximately 3 microspheres per ml. Since the volume of insonification is 0.675 ml the mean resolution would appear to be about two for each delivery of an acoustic pulse. The peak values of count rate suggest that the resolution is better than four perturbations per volume of insonification per acoustic pulse. These values are in reasonable agreement with the theoretical prediction of spatial resolution based upon the acoustic pulse duration, propagation velocity, and spacing between perturbation sources as discussed in chapter 3.

Variation of flow rate, smoothly from 0 to $5L.min^{-1}$ indicated a proportional change in count rate whilst maintaining the previously established resolution limit of approximately three microspheres within the volume of insonification during the delivery of a single acoustic pulse. It was not possible to repeat the procedure of successive additions of microspheres, for flow rates greater than $1.5L.min^{-1}$ owing to a rapidly induced predominance of signals from bubble inclusions. Fig. 5.9 indicates the maximum count rates for flow rates from 0 to $5L.min^{-1}$, based upon the above resolution limit.

Discussion

Measurements of detector resolution are notable by their absence

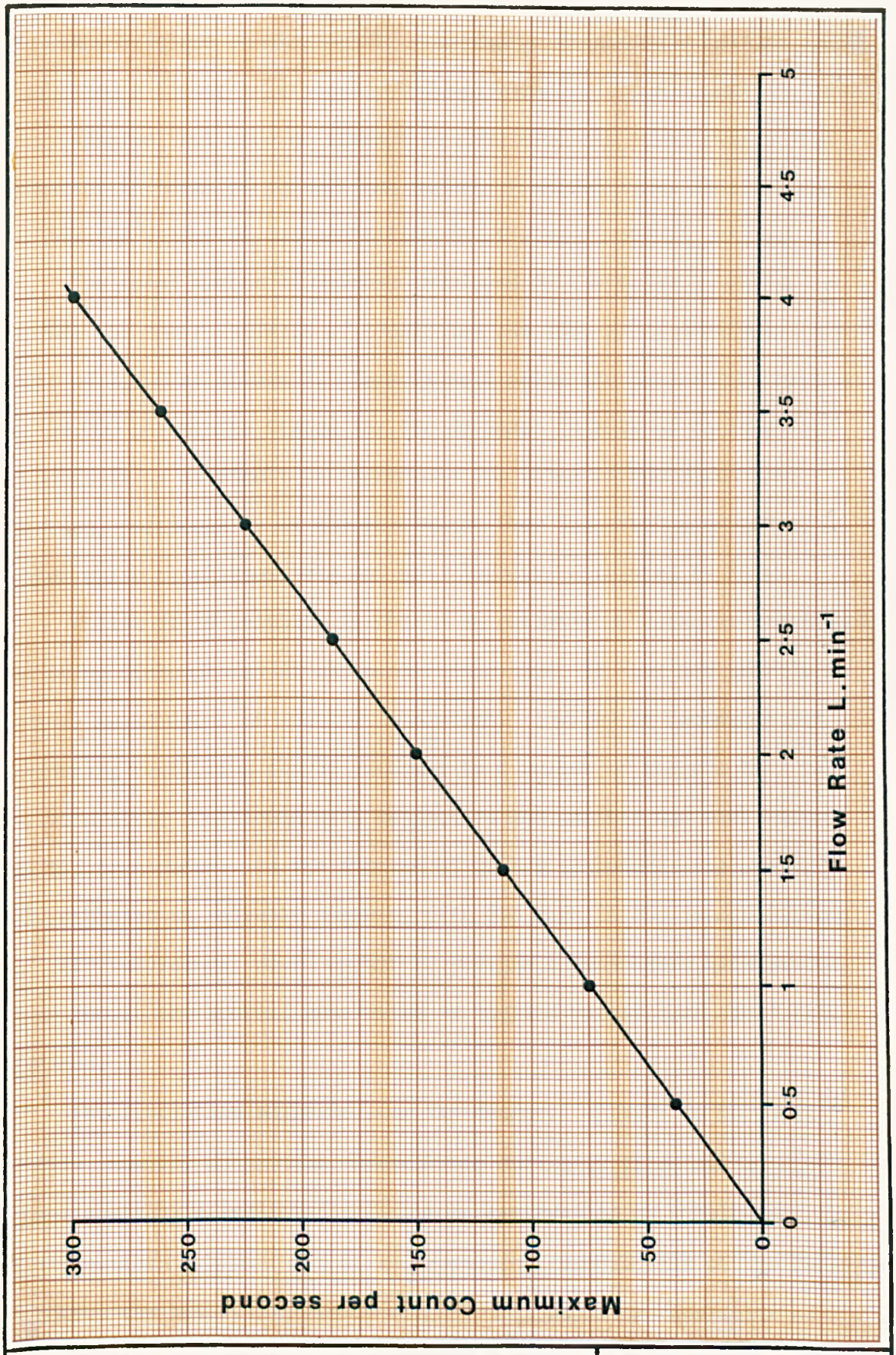

Detector resolution - Maximum count rate-flow rate relationship (estimated from microsphere analysis)

Figure 5.9
Referred to on p. 199

in communications on microbubble detection. Patterson & Kessler (1969) indicated a linear relationship between count rate and number of plastic microspheres, but made no attempt to determine the resolution of the detector in terms of the maximum number of microspheres detectable within the volume of insonification for a single acoustic pulse.

The total number of mcirospheres used by Patterson & Kessler (1969) for their estimate of resolution was 100, which provided a count rate of 2,400 at 3L.min^{-1}. This is well below the theoretical maximum of 39,000 per minute stated for the device. In view of these observations it is difficult to appreciate the value of the curve they derived, particularly as the instrument they described operated at a fixed pulse repetition rate and was therefore unrelated to flow.

Whilst it is possible to obtain an estimate of detector resolution by using microspheres in the manner described, it does not provide an actual measurement of spatial resolution. Ideally, a technique for measuring resolution should incorporate a number of targets that can be accurately positioned with respect to one another and with respect to the transducer. In the absence of such a technique, the use of microspheres in suitable numbers, with due care in the interpretation of rate recordings, would appear to provide a reasonable alternative, even though the spatial resolution is implied rather than explicitly defined.

The resolution suggested for the detector appears to be quite small. However subsequent observations during <u>in vitro</u> and <u>in vivo</u> experiments have indicated that the concentrations of bubbles and their distributions are well within the resolving capabilities of the detector. Whenever the bubble population exceeds the resolving capability of the detector the oscilloscope provides a convenient indication, a thick grass like display being prominent when bubbles are in excess.

Under conditions in which the spatial separation between significant

sources of scatter is too small to allow discrimination, the summation of signal levels, inherent in continuous wave techniques must be recognised. However, in contrast to continuous wave techniques, the effective discrimination offered by the flow dependent pulse technique may be considerably enhanced by reducing the acoustic pulse duration and by reducing the width of the volume of insonification.

Assessment of cellular damage

In a discussion on the margin of safety for diagnostic ultrasound Taylor & Dyson (1972) stated that the low average intensities that are usually quoted for sonar systems (about 0.1 $mW.mm^{-2}$) have little meaning when considering the possible deletrious effects of pulsed ultrasound, since the instantaneous point values of intensity may be substantially higher (0.014 - 0.96 $W.mm^{-2}$) than the average values. Whilst the high transient intensities exceed the thresholds for damage established for continuous mode delivery for a variety of experimental models, under a variety of conditions, the low duty cycles and short pulse durations characteristic of pulsed diagnostic equipment preclude thermal damage and reduce the possibility of collapse cavitation. However this does not eliminate the possibility of other mechanisms for producing cellular damage some of which have been presented in the discussion on the effects of ultrasound in chapter 3 . For these reasons it was considered necessary to determine whether the flow dependent detector and its mounting assembly were likely to produce significant cellular damage under normal operating conditions.

Materials and methods

The protocol for assessing cellular damage was to examine various cellular degradation parameters related to the conditions prevailing whilst the ultrasonic transducer was energised. Had significant damage been observed under these conditions the same measurements would

then have been repeated for conditions in which the transducer was not energised. This would have allowed the distinction to have been made between the circuit and the ultrasonic field as the principal agent of cellular damage.

In each of six investigations two circuits were constructed, each containing a polycarbonate reservoir (400 ml), a stainless steel sampling port and an electromagnetic cannulating flow probe (Nycotron). The circuit components were coupled together using 9.5 mm internal diameter extracorporeal tubing (1.6 m). To accommodate differences in flow probe and sampling port diameters (9.5 mm internal diameter and 6.4 mm internal diameter), Polystan coupling connectors (9.5 mm to 6.4 mm diameter) were introduced into the circuit and arranged so that the size variations within each circuit were matched. The transducer mounting assembly was included in one circuit and 0.56 m of tubing was removed to compensate for the priming volume of the assembly (42 ml). The flow in each circuit was promoted by a Sarn's roller pump. Fresh porcine venous blood was collected into acid citrate dextrose solution (ACD 'A'). Initially a ratio of 75 ml ACD to 250 ml of blood was used but evidence of cellular aggregation and clots during collection indicated that the quantity of ACD was inadequate and was subsequently increased to 100 ml ACD to 250 ml of blood. The blood was filtered using a Swank micropore filter type 1L-200 and 250 g introduced into each of the circuits together with 12.5 mg of sodium heparin.

The blood was circulated at a flow rate of $1 L.min^{-1}$ for 3 hours. Five millilitre samples were obtained at half hourly intervals. The ultrasonic transducer was energised on a flow dependent basis ($\simeq$ 25 pulses per second). As the procedure progressed, the removal of blood samples led to a significant variation in the blood-air interface within the reservoir with the result that the blood became well oxygenated. Increased oxygenation was accompanied by a notable increase

in the bubble population.

The tests selected for assessing cellular damage were as follows;

(i) Osmotic fragility. The resistance of erythrocytes to osmotic haemolysis may be quantitatively assessed by subjecting them to a graded series of hypotonic sodium chloride solutions, and measuring the plasma haemoglobin concentration at each sodium chloride concentration. Since mechanical disturbances can damage cellular membranes, a measurement of osmotic fragility was considered important for assessing the effect of disturbances produced by ultrasonic perturbations. The method Dacie & Lewis (1968) was used for measuring osmotic fragility.

(ii) Plasma haemoglobin concentration. Estimates of plasma haemoglobin concentration were taken as a measure of cellular disruption resulting in the release of haemoglobin. The benzidene method of Crosby & Furth (1956) was used for this purpose. For reference purposes total haemoglobin was also determined, using the cyanmethoxyhaemoglobin method described by Dacie & Lewis (1968).

(iii) Cell counts. Erythrocyte, platelet and leucocyte counts were determined according to standard methods using formal citrate solution for the erythrocyte preparation, procaine hydrochloride solution for the platelet preparation, and 2% acetic acid coloured with gentian violet for the preparation of leucocytes. Packed cell volume was measured in capillary tubes using a Gelman-Hawksley haematocrit centrifuge.

(iv) Cellular aggregation. Platelet and leucocyte aggregation was evaluated on the basis of screen filtration pressure measurements (Swank et al., 1964) and blood smears.

Results

The results of the osmotic fragility tests are presented graphically in Fig.5.10. There were no significant differences between the control

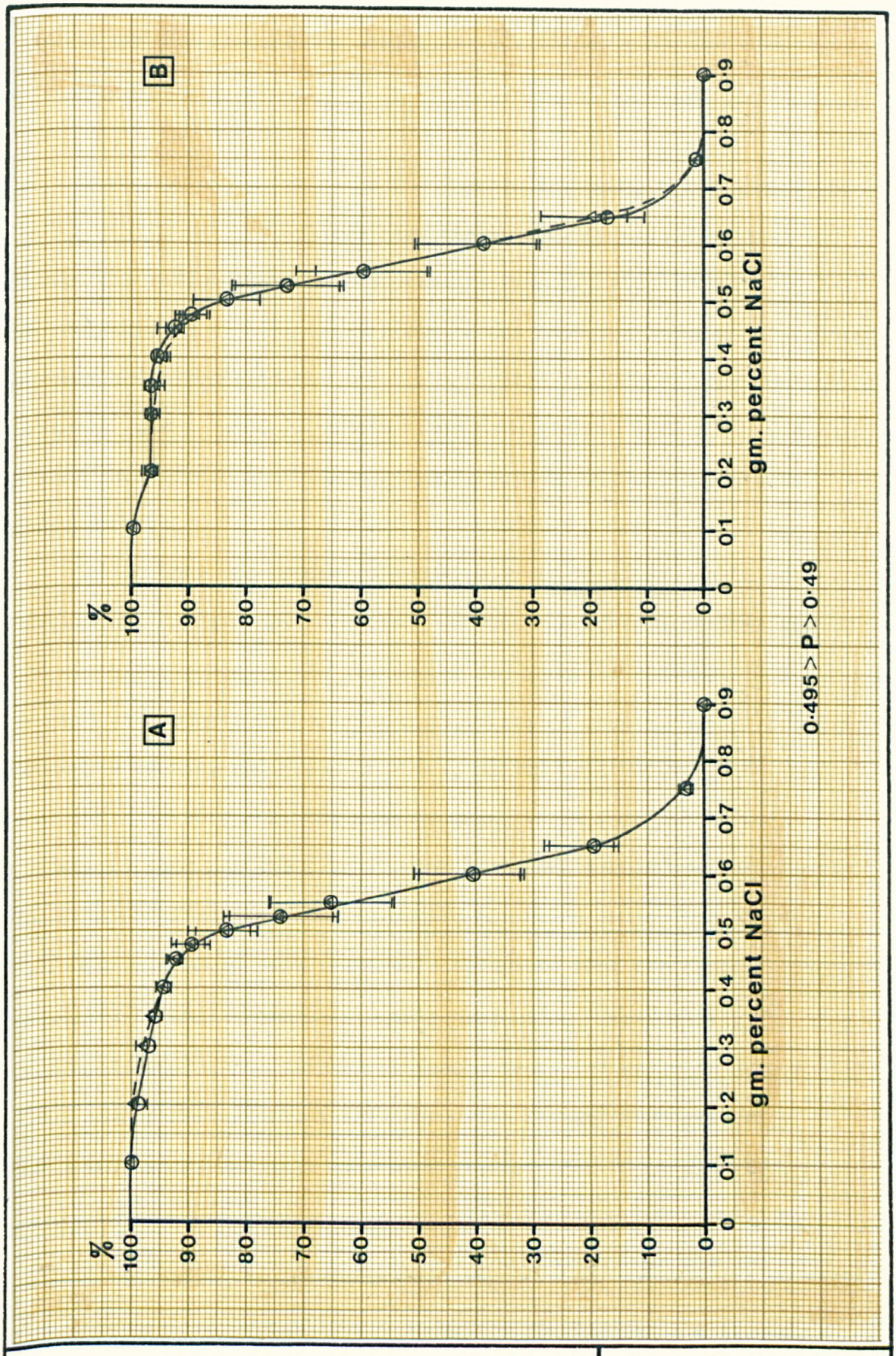

Osmotic fragility tests
without insonification A beginning
with insonification B end of experiment
± 2 SE.

Figure 5.10
Referred to on
pp. 204, 210

circuit and the circuit containing the activated transducer and mounting assembly, either before or following circulation ($0.495 > P > 0.49$).

Graphical presentation of the results for whole blood haemoglobin (g/100 ml/100 passes), plasma haemoglobin (mg/100 ml/100 passes) and screen filtration pressure measurements (mm. Hg) are shown in Fig.5.11 In each case no significant difference was observed between the control circuit and circuit containing the activated transducer and mounting assembly ($0.4 > P > 0.35$, whole blood haemoglobin, $0.45 > P > 0.4$, plasma haemoglobin and $0.45 > P > 0.4$, screen filtration pressure measurements).

Cell counts are presented graphically in Fig.5.12. Again no significant differences were noted between the control circuit and the circuit containing the transducer and mounting assembly ($0.3 > P > 0.25$ erythrocyte counts, $0.475 > P > 0.45$, platelet counts, $0.45 > P > 0.4$, leucocyte counts, and $0.45 > P > 0.4$, packed cell volume).

Fig.5.13represents the average count rates for bubbles with respect to time for the circuit containing the transducer and clearly indicates a steady increase in bubble formation and/or bubble persistence. It would seem reasonable to assume that the control circuit exhibited a similar trend in bubble production, particularly in view of the insignificant differences in the tests for cellular damage. Blood smears revealed that the aggregates present were generally small in numbers and that none were greater than 40 μm diameter.

Discussion

In attempting to relate the results of these experiments to those of a conventional bypass it was necessary to consider the frequency with which any one volume of blood was subjected to the influence of ultrasound. It was therefore necessary to establish the number of passes the blood makes through the circuit in a given period of time.

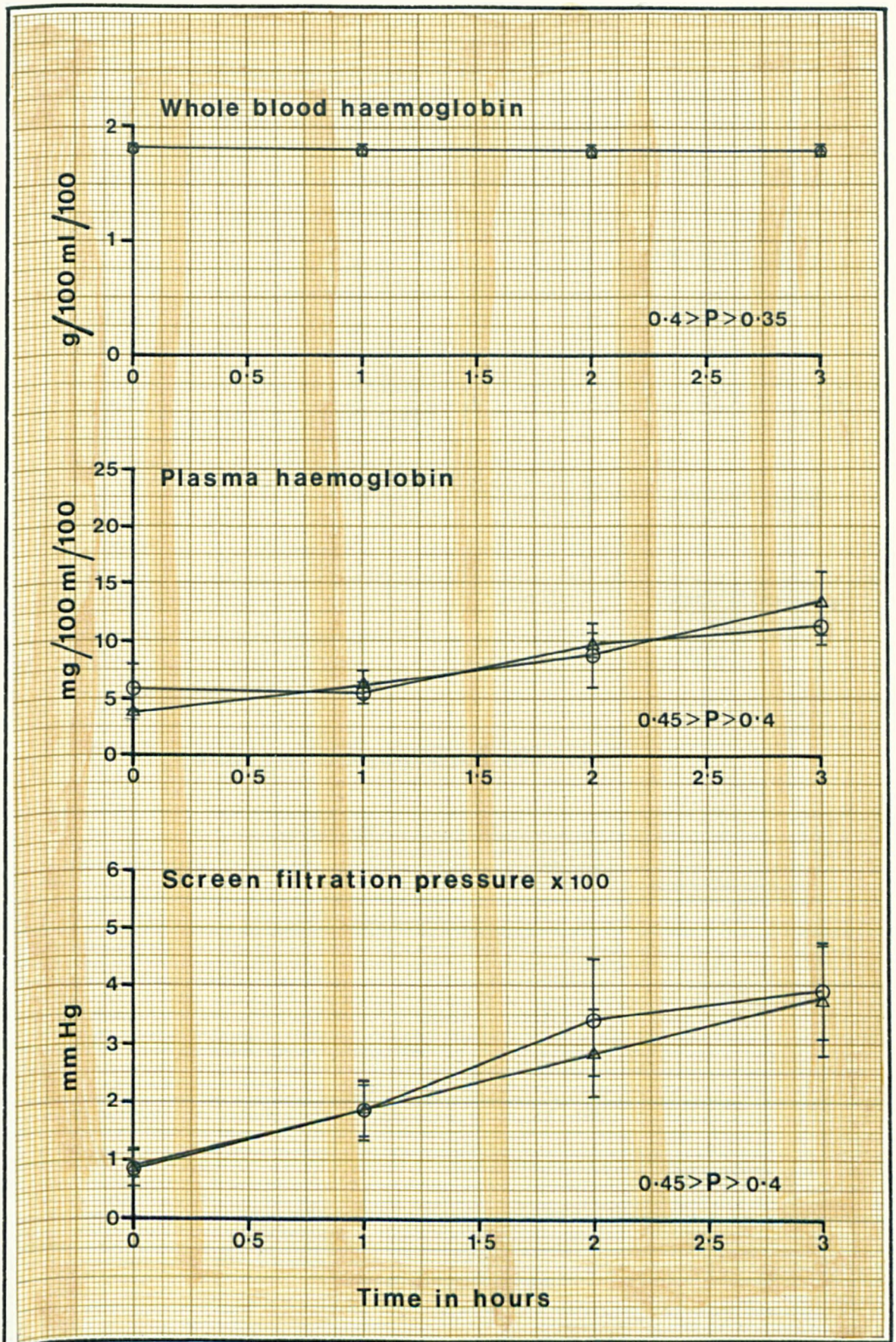

Cellular response characteristics
△ with insonification
○ without insonification
I± 2 SE.

Figure 5.11
Referred to on
pp. 204, 210

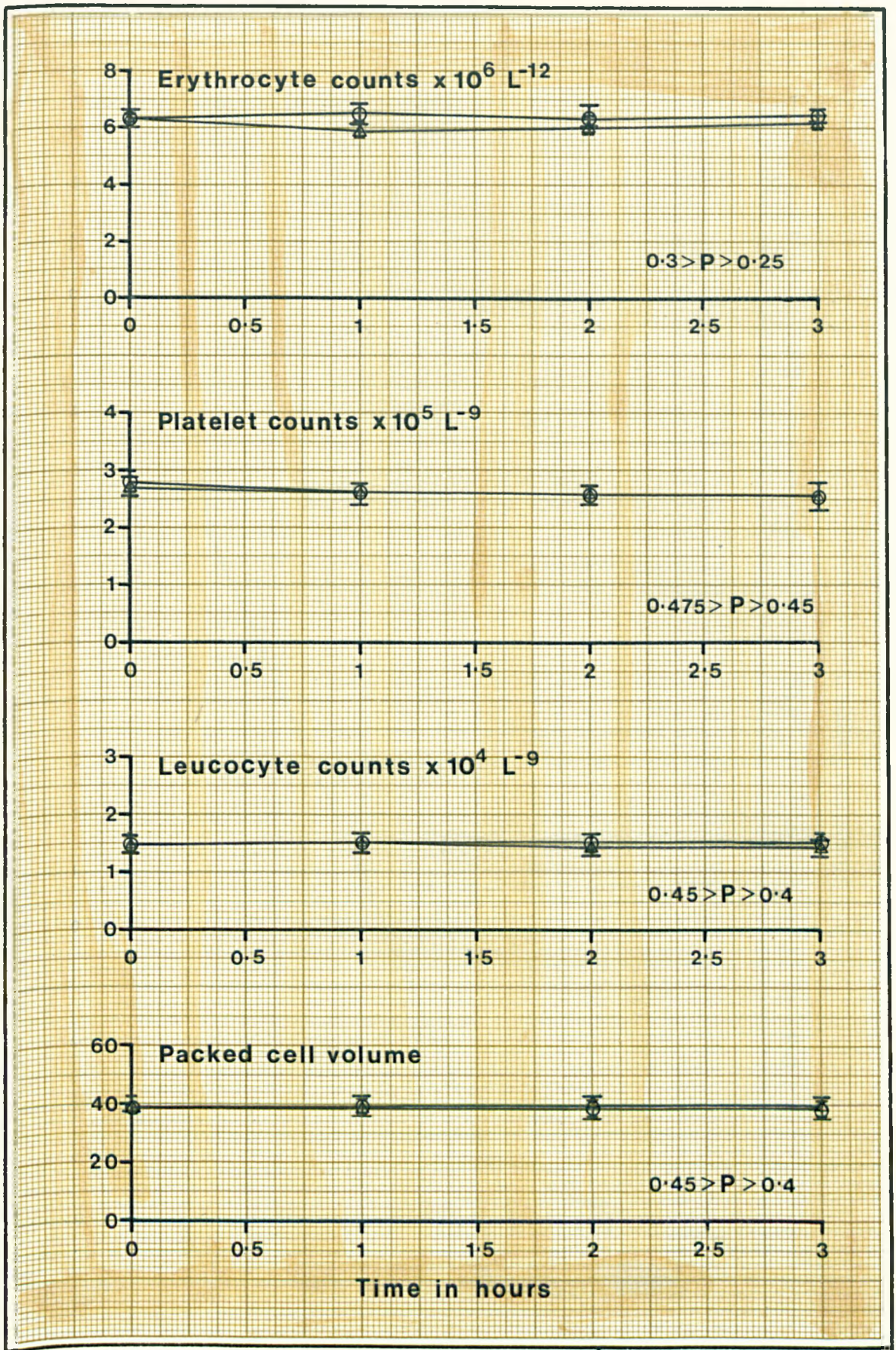

Cell count characteristics
△ with insonification

○ without insonification ⊥ + 2 SE.

Figure 5.12
Referred to on
pp. 204, 210

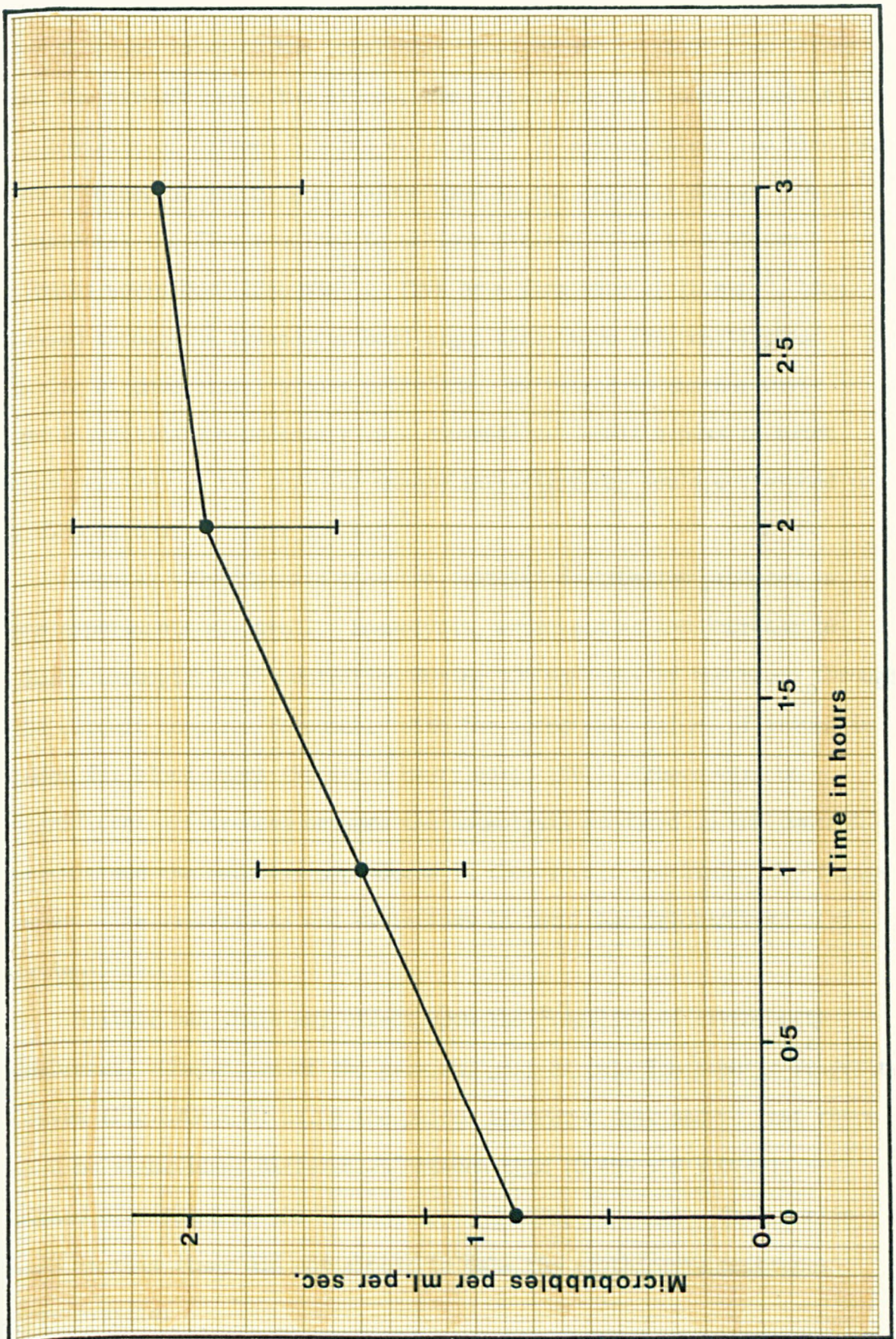

Microbubble Liberation Characteristic for Trauma experiment.

I $\pm$ 2 SE

Figure 5.13

Referred to on P.206

For a bypass in which the total body blood volume is about five litres and the circuit prime two litres, the circulation time corresponding to a flow rate of between 3.5 and 4.0 $L.min^{-1}$ is approximately two minutes. For a volume of 250 ml (the volume used in the cellular damage investigations) the flow required to achieve a circulation time of two minutes would be $0.125L.min^{-1}$. Thus at a flow rate of $1L.min^{-1}$, blood passed throughthe transducer head eight times more frequently than during a conventional bypass procedure. Expressed in another way, the insonification necessary in a conventional adult bypass to match that received in the cellular damage investigations would correspond to a flow rate of at least $30L.min^{-1}$.

Figures 5.10-12indicate that the cellular destruction produced in the experiments was small. Haemolysis, expressed as the increase in plasma haemoglobin concentration during 100 passages of the blood through the circuit compares favourably with the acceptable values of traumatic index for blood pumps (Koller & Hawrylenko, 1967). There were no significant differences between the haemolysis produced in the control circuit and the haemolysis produced in the circuit containing the transducer. The differences and variations in total haemoglobin were also insignificant.

Neither was there any effect upon the fragility of erythrocyte membranes. Comparison of the pre- and post-circulation osmotic fragility curves (Fig.5.10A & B) using the paired Student-t test showed that there were no significant differences between them ($0.495 > P > 0.49$). Pulsed ultrasound at the intensities and pulse repetition frequencies used in this study did not appear to make the erythrocyte membranes more fragile.

Screen filtration pressure was measured to assess changes in intra-cellular adhesion and aggregation (Swank, Roth & Jansen, 1964). As shown in Fig.5.11, there was a steady increase in cellular aggregation

during blood circulation. Regression analysis revealed a close correlation between cellular aggregation and the bubble population size ($r = 0.98$; $t = 4.9$; $y = 0.45x + 0.51 \pm 0.025$). In view of this correlation it may be suspected that the cellular aggregates have contributed to the acoustic perturbations taken to represent bubble sources. However significant correlation does not necessarily indicate a relationship. Blood smears indicated that the aggregates were both small in number and small in size; none greater than 40 μm in diameter. The differential scattering cross section for cellular aggregates of 40 μm diameter at 10 MHz is substantially less than that of a bubble of 10 μm diameter. Therefore, the detector would not be expected to indicate the presence of the cellular aggregates observed in this study unless they were present in very large numbers and thickly distributed. No evidence was obtained to suggest the presence of large numbers of aggregates.

Since there was no significant difference between the screen filtration pressure measurements for the control circuit and those for the transducer circuit it would seem reasonable to assume that the cellular aggregation was a consequence of the blood gas interface rather than the influence of acoustic energy.

On the basis of the tests performed, including cell counts, there is no evidence to suggest that the acoustic energy was responsible for any cellular damage.

Conclusions

In addition to revealing the capabilities of the microbubble detector the tests reported in this section have also revealed the improvements that need to be made to enhance the capabilities of the instrument. More uniform field distributions may be realised in the design of a new transducer by using a theoretical model of the type discussed by Marini & Rivenez (1974). Estimation of the Fresnel integrals necessary in the formulation of these models may be computed reasonably accurately using sine and cosine terms modulated by auxiliary functions as proposed by Smith (1975). However it would be necessary to formulate a model specifically for the very near field, since the model proposed by Marini & Rivenez (1974) includes a geometrical assumption that precludes accurate prediction of the field distribution very close to the transducer.

The transducer mounting assembly could be considerably improved to reduce the inlet disturbance and improve the flow characteristics within the region of insonification. Better flow visualisation facilities would be necessary to examine such an arrangement. With improvements in the uniformity of the field and methods of sterilizing transducers, advantages may be gained by reconsidering the use of a mounting assembly that allows direct contact of the transducer with the blood, so eliminating coupling effects.

Calibration techniques present particular problems, because of difficulties in controlling the number and distribution of scatter sources and the physical conditions under which the tests are performed. Lubbers & van den Berg (1977) have reported a method of calibration using bubbles in a flow situation, but the method is not applicable when there is more than one bubble per field. This criticism also applies to static calibration methods.

Since an in-field population of bubbles and their positions in

relation to one another will influence the magnitude of the echo strength nominally received from a single bubble it may be important to consider the effect of population size upon echo strength. Some attempt has been made in this study to achieve this requirement by estimating the resolution of the detector. However, further progress is impeded by the difficulty in controlling both the number of scatter sources within the field at any instance in time and the positional relationship of those scatter sources.

Blood would be the ideal medium for calibration tests but the loss of a direct visual check, together with the possibility of bubble fission (Hills, 1974) and the variable influences of the physical and chemical conditions prevailing within the blood make blood unsuitable. More attention is clearly needed to resolve these calibration problems, including rationalisation of the conditions under which the tests are performed.

Improvements could also be made in the signal processing and display instrumentation. Such improvements are those to be expected following a subsequent phase of development. For the purpose of demonstrating the potential of a flow dependent technique the prototype instrumentation has been adequate.

The advantages of having a system incorporating two or more transducers are obvious, not least of which would be the facility for bubble lifetime studies and the estimation of input/output relationships for extracorporeal circuit components. Such a system could be readily developed to allow the addition of more transducers by incorporating a multiplexer controlled by the flow dependent trigger circuit. Compound transducers incorporating two or more active elements could similarly be included in an attempt to average out sizing errors.

In spite of these criticisms the system fulfils the criteria for sizing, counting and rate determination with flow dependent error

elimination, hitherto unavailable for microbubble analysis during extracorporeal circulation.

Chapter 6

MICROBUBBLE INVESTIGATIONS

The objects of these investigations were to determine the significance of quantification in the study of microbubble sources and their elimination during extracorporeal circulation and to establish the validity of reported conclusions that have hitherto been based upon qualitative techniques. An additional objective was to establish the effectiveness of arterial line filtration in removing microbubbles.

Studies were performed in two groups, in vitro experiments using closed circuits and saline prime, and in vivo cardiopulmonary bypass experiments using adult beagle dogs.

In vitro studies - materials and methods

The circuits consisted of a small Rygg-Kyvsgaard disposable bubble oxygenator (HL-054, Polystan), a Bio-Med. Engineering stainless steel torpedo - type heat exchanger, a Pall extracorporeal blood filter (EC 3840, Johnson & Johnson), a Sarns roller pump, a 9.6 mm internal diameter PVC tubing (6LF pumpset, Travenol). The circuits were primed with 2-3 litres of 0.9% sodium chloride solution.

Circuit conditions were varied in the following ways in order to facilitate particular investigations;

Saline flow rate. The circuit saline volume was maintained at 2 litres, and the flow of oxygen maintained at 3 $L.min^{-1}$. Whilst maintaining these conditions measurements of microbubble rate, size, and number were obtained for increases in saline flow rate of 1 $L.min^{-1}$ up to 6 $L.min^{-1}$. At each flow rate the conditions were maintained for a period of five minutes. Measurements were then repeated at each of the specified flow rates, commencing at 6 $L.min^{-1}$ and reducing in 1 $L.min^{-1}$ steps, at two minute intervals down to 1 $L.min^{-1}$.

Gas flow rate. Commencing with zero gas flow and a saline flow rate of 1 $L.min^{-1}$, measurements of microbubble rate, size and number were

obtained for increases in oxygen flow rate of 1 $L.min^{-1}$ steps up to 5 $L.min^{-1}$ and maintained for two minutes at each level. The flow of oxygen was then returned to 1 $L.min^{-1}$, the arterial line filter was introduced and conditions were allowed to stabilize for 10 minutes. Following this period the filter was bypassed and the saline flow rate was increased to 2 $L.min^{-1}$. Measurements of microbubble rate, size and number were repeated at oxygen flow rates of 1 to 5 $L.min^{-1}$ in 1 $L.min^{-1}$ steps. The whole procedure was then repeated for a saline flow rate of 3 $L.min^{-1}$. In all cases the circuit volume of saline was maintained at 3 litres.

Reservoir level. With the circuit volume of saline maintained at 2 litres and the oxygen flow rate maintained at 3 $L.min^{-1}$, measurements of microbubble rate, size and number were obtained for saline flow rates of 1 $L.min^{-1}$ to 6 $L.min^{-1}$ in 1 $L.min^{-1}$ steps. For these measurements the reservoir level remained within 30 mm of the initial 200 mm level above the outlet port of the oxygenator. Contact between the saline and the defoaming sponge was minimal (30 mm contact on the bubble chamber side and 30 mm below the defoaming sponge on the reservoir side).

Following these measurements the volume of saline was increased to 3 litres. This raised the reservoir level to 270 mm above the outlet port and provided a defoamer contact depth of 60 mm (maximum on the bubble chamber side) and 30 mm (minimum on the reservoir side). The measurements described above were repeated at this reservoir level.

Further measurements were obtained for an oxygen flow rate of 5 $L.min^{-1}$ at both reservoir levels and saline flow rates of 1 to 6 $L.min^{-1}$ in 1 $L.min^{-1}$ steps.

Temperature. The circuit volume of saline was maintained at 3 litres and the conditions were allowed to stabilize for a period of 15 minutes whilst maintaining the oxygen flow rate at 3 $L.min^{-1}$. Following this period the temperature of the prime was raised at a rate of approximately

$1^{o}C.min^{-1}$ by means of the heat exchanger and a Grant Instruments Ltd., SB2 thermostatically controlled water bath. Measurements of microbubble rate, size and number were obtained at five minute intervals.

Filter response. The measurements described for the investigation of the saline flow rate - microbubble relationship were repeated and filter response investigated by introducing a micropore filter following a period of stabilization at each flow rate. The variation in microbubble rate, size and number were noted for each flow rate and for each introduction of the micropore filter into the flow line. The filter response was also observed over a 3 hour period of microbubble insult (3 $L.min^{-1}$ saline flow, 3 $L.min^{-1}$ gas flow and 2 L saline prime).

In vitro studies - results

Saline flow rate. Figs. 6.1 and 6.2 show the relationship between saline flow rate and microbubble population. Fig. 6.2 shows the actual rate recording for the microbubble population at flow rates from 1-6 $L.min^{-1}$. The analysis of size distribution based upon echo counts over the specified time intervals is shown in Fig. 6.1. The temperature of the saline prime remained within $\pm$ $1^{o}C$ of $19^{o}C$ during the period of the measurements. The most unequivocal feature of these results is the non-linear increase in bubble count rate with respect to flow rate (Fig. 6.2). However the concentration per second indicates a direct proportionality (Fig. 6.1). At all of the flow rates considered, the majority of bubbles were in the size range 20-80 μm diameter. A trend toward the release of larger bubbles (80-140 μm diameter) was indicated for flow rates above 2 $L.min^{-1}$. However the number of larger bubbles was small in comparison with the 20-80 μm diameter population.

Gas flow rate. Fig. 6.3 and 6.4 show the relationship between oxygen flow rate and microbubble population. They also illustrate the influence of the saline flow rate. The increase in the oxygen flow rate was accompanied by an increase in the rate of liberation of microbubbles.

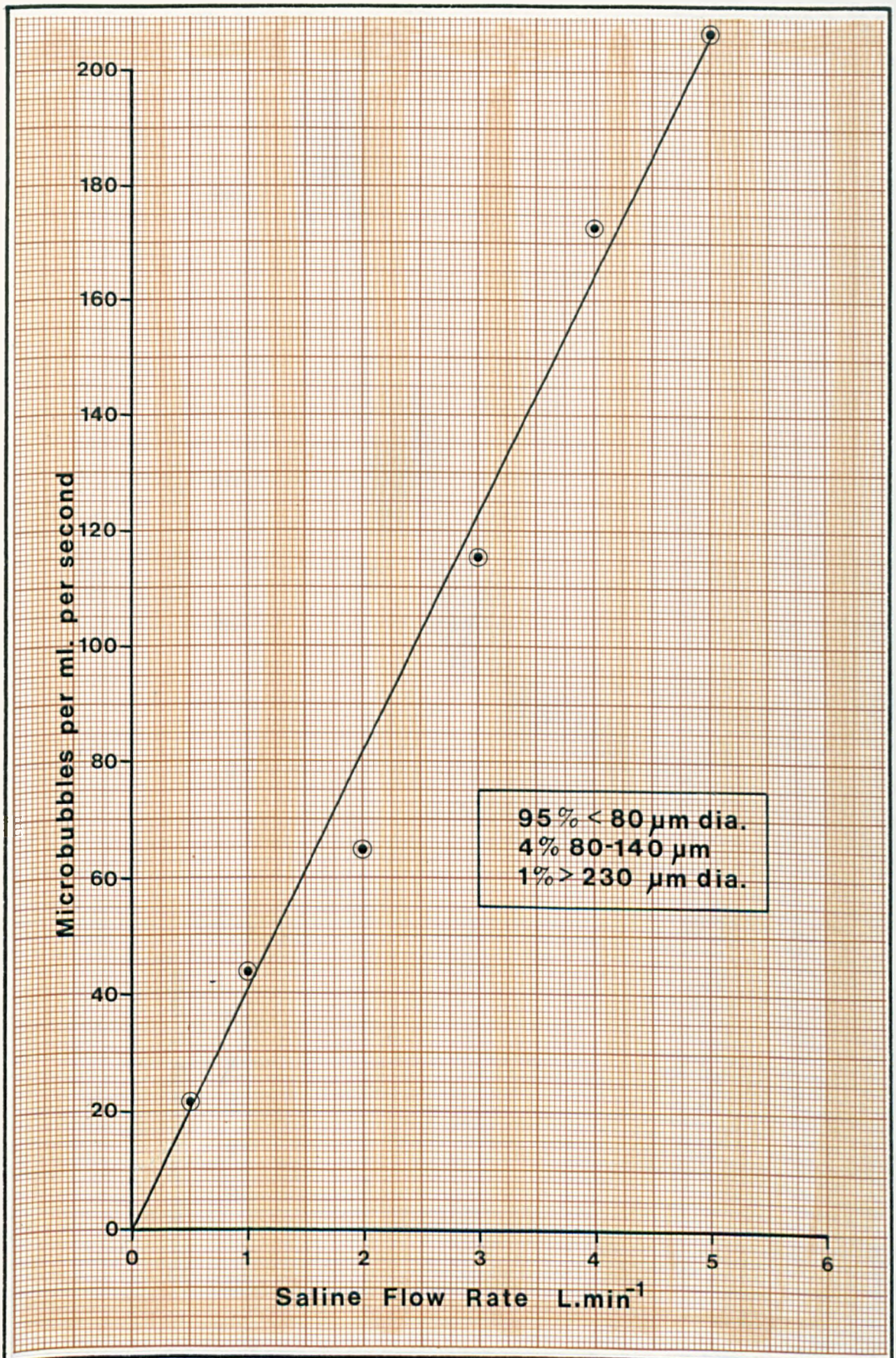

Microbubble Liberation - Saline Flow Rate Relationship
Oxygen Flow Rate 3L. min^{-1}
Temp $19^{o} \pm 1^{o}C$

Fig. 6.1

Referred to on P.217

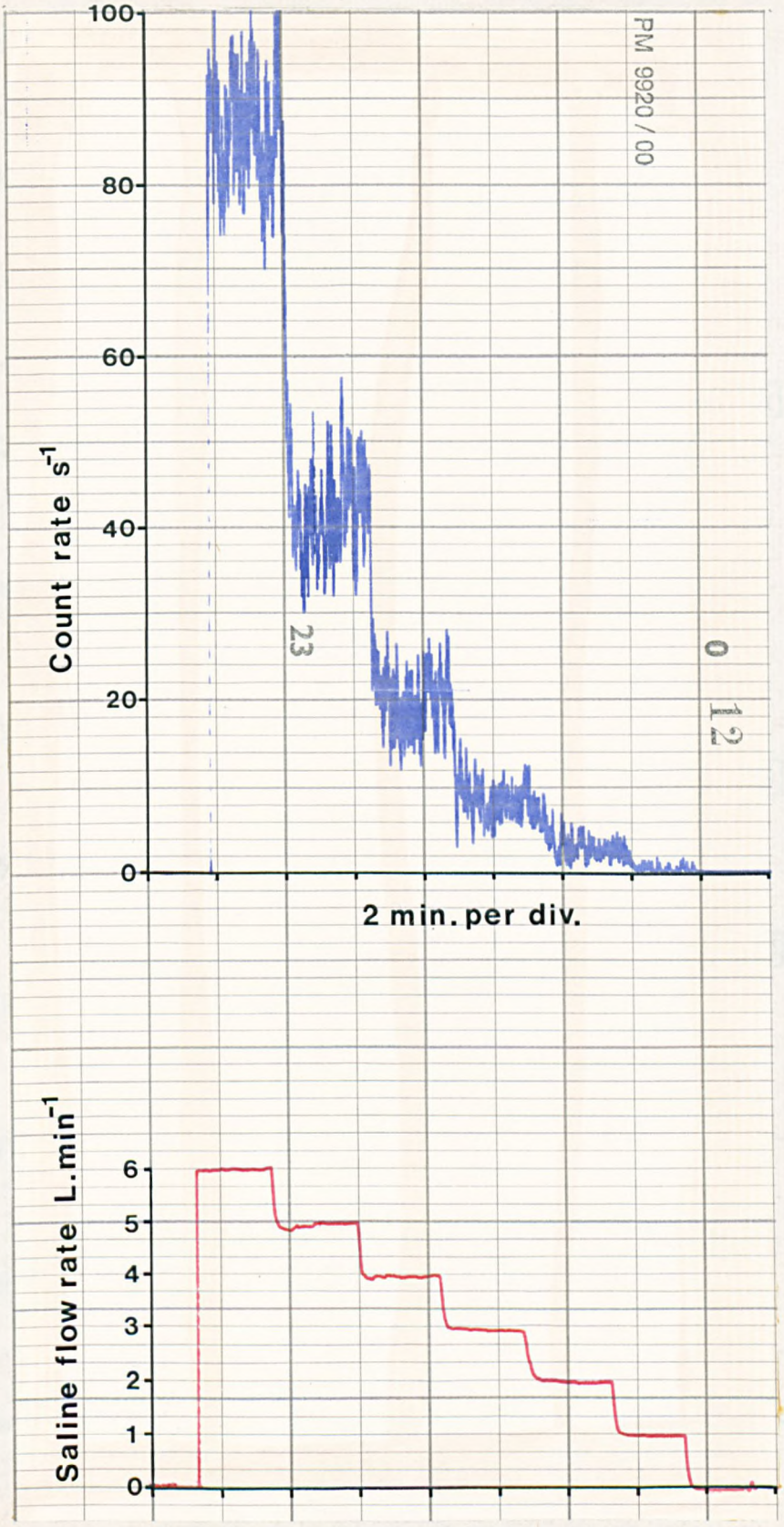

Flow rate - microbubble count rate recording
Oxygen flow rate 3L min^{-1}
Circuit volume 2L
No filter

Fig. 6.2

Referred to on P.217

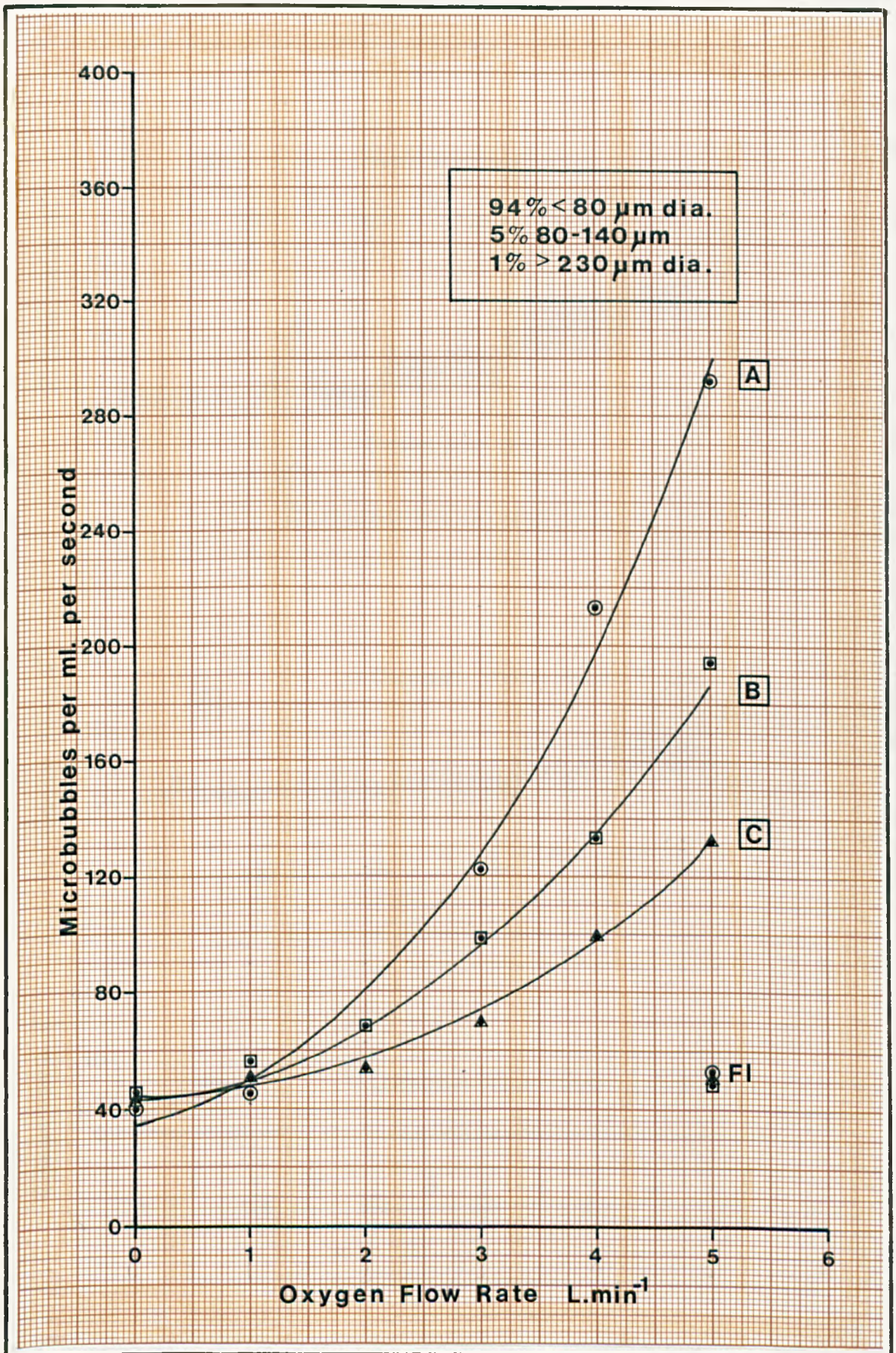

Microbubble Liberation - Oxygen flow rate Relationship
Saline Flow Rates, A:3L min^{-1}, B:2L min^{-1}, C:1L min^{-1}
Fl Filter in Circuit. Temp. 15.5 $\pm$ 1°C

Fig. 6.3

Referred to on P.217

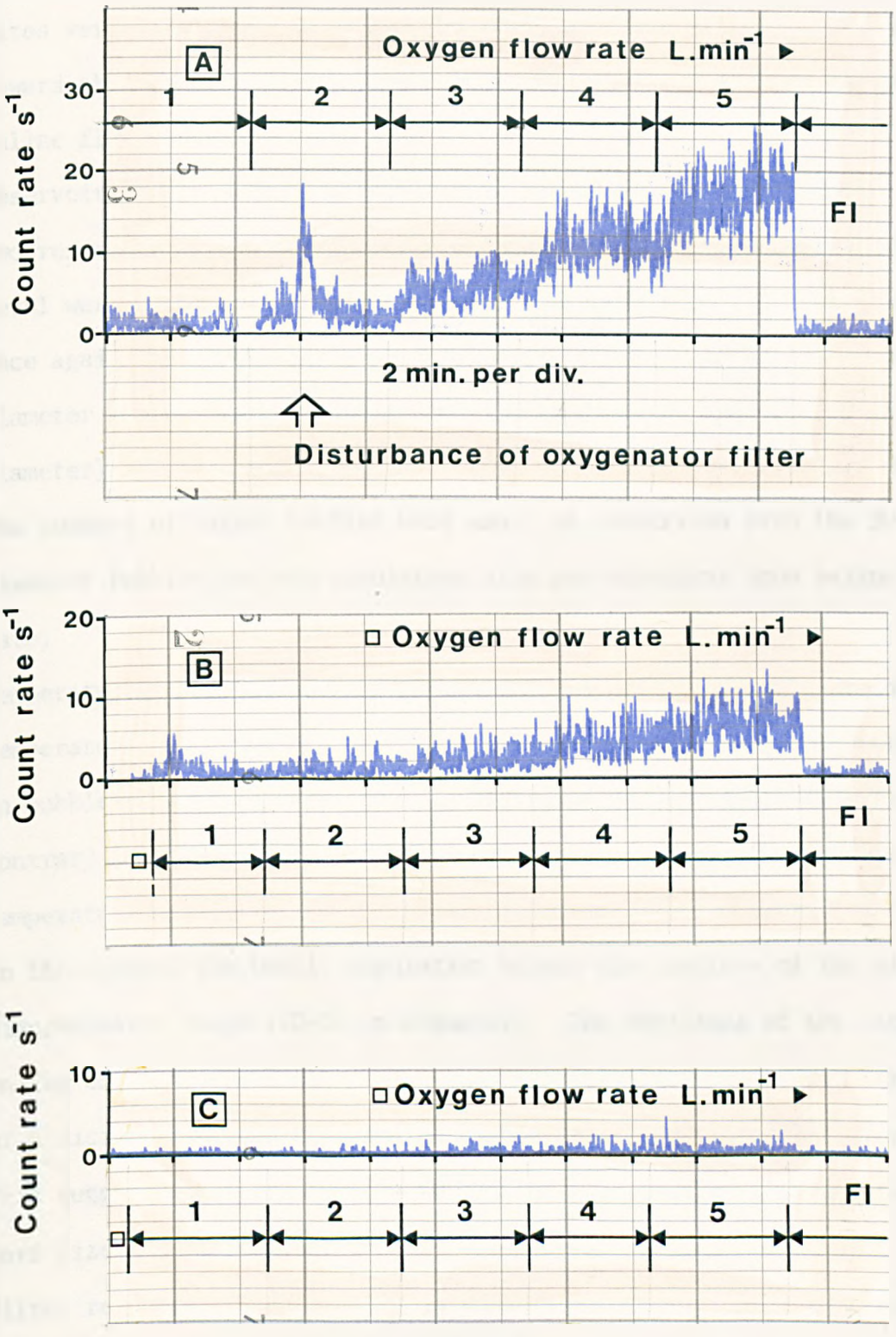

Oxygen flow rate - microbubble count rate recordings.

A 3L min^{-1} Saline Flow Rate
B 2L min^{-1} Saline Flow Rate
C 1L min^{-1} Saline Flow Rate

Fig. 6.4

Referred to on P. 217

This effect was greater than that predicted on the basis of flow dependent proportionality. As in the saline flow rate investigation, the bubble sizes were predominantly within the 20-80 μm diameter range. A tendency toward the liberation of larger bubbles was observed at high gas and saline flow rates.

Reservoir level. The microbubble rate recordings corresponding to the two reservoir levels considered are shown in Fig.6.5. Reductions in level were accompanied by increases in the numbers of liberated bubbles. Once again the bubble sizes were primarily confined to the 20-80 μm diameter range. Larger bubbles (80-120 μm diameter and 120-150 μm diameter) appeared more frequently with lower reservoir levels. However the numbers of larger bubbles were small in comparison with the 20-80 μm diameter bubbles and the population size was dependent upon saline flow rate.

Temperature. For both of the experiments in which the influence of temperature rise upon microbubble population was studied, the variations in bubble liberation rate and size distribution were small (Fig.6.6). Contrary to expectation a slight reduction in rate was observed as the temperature was increased. This was accompanied by an overall increase in the sizes of the bubble population within the confines of the minimum discriminator range (20-80 μm diameter). The amplitude of the signals on the oscilloscope display were only slightly increased. The introduction of a micropore filter reduced the bubble liberation rate still further. This suggests that the bubbles so removed were greater than the filter pore size (40 μm diameter).

Filter response. In all cases in which a micropore filter was introduced into the flow line, the reduction in the measured population of microbubbles was considerable. Fig.6.7 shows the rate recording for the bubble populations arising at flow rates of 1 to 6 $L.min^{-1}$ in 1 $L.min^{-1}$ steps and the effect of introducing the micropore filter after each step

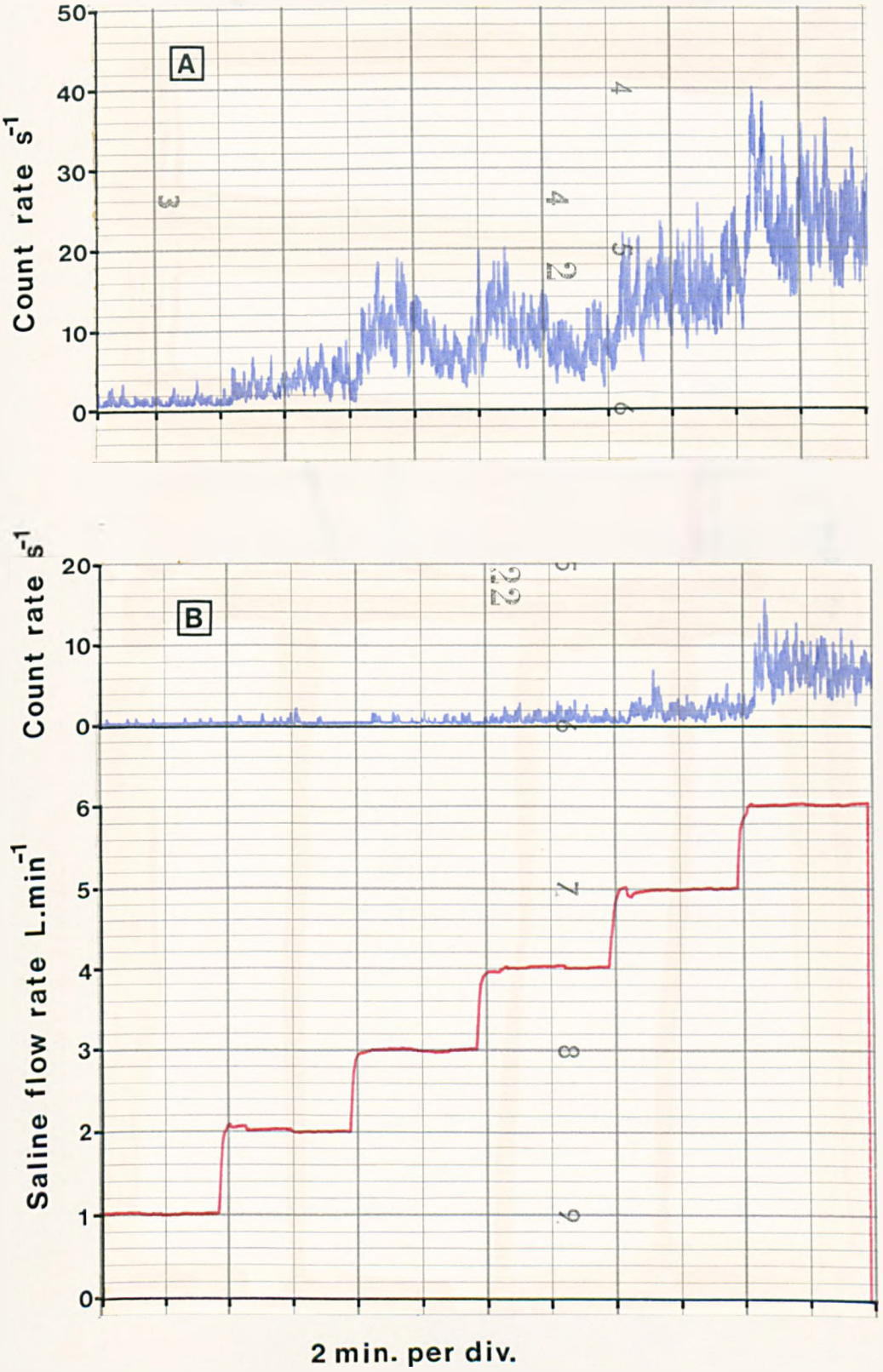

Reservoir Level Response
Gas Flow 3L min^{-1}
A. Circuit volume 2L
B. Circuit volume 3L
Filter in Circuit

Fig. 6.5

Referred to on P.222

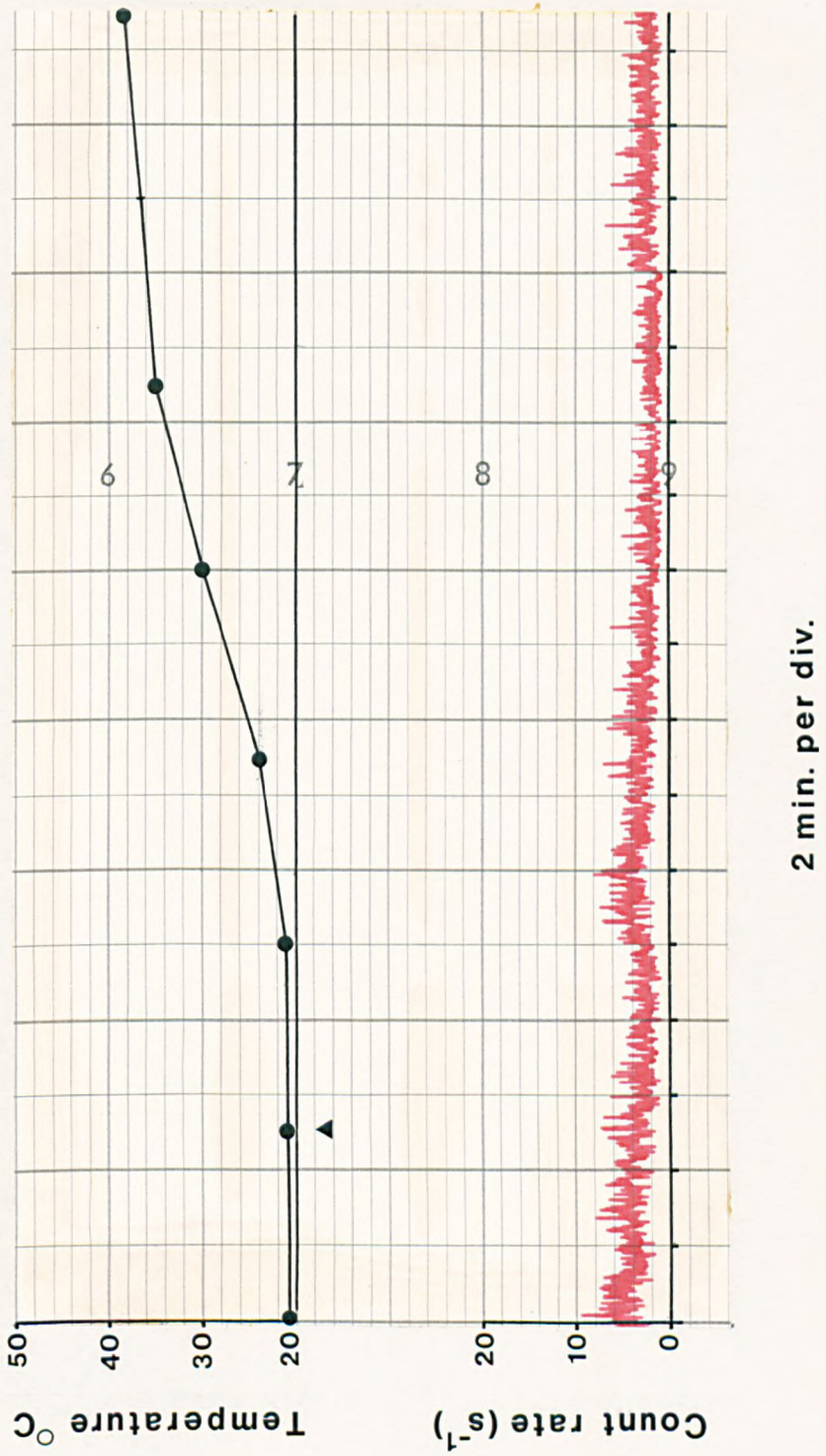

Temperature microbubble count rate response
Saline Flow Rate 1L min^{-1}
Oxygen Flow Rate 3L min^{-1}

Fig. 6.6

Referred to on P.222

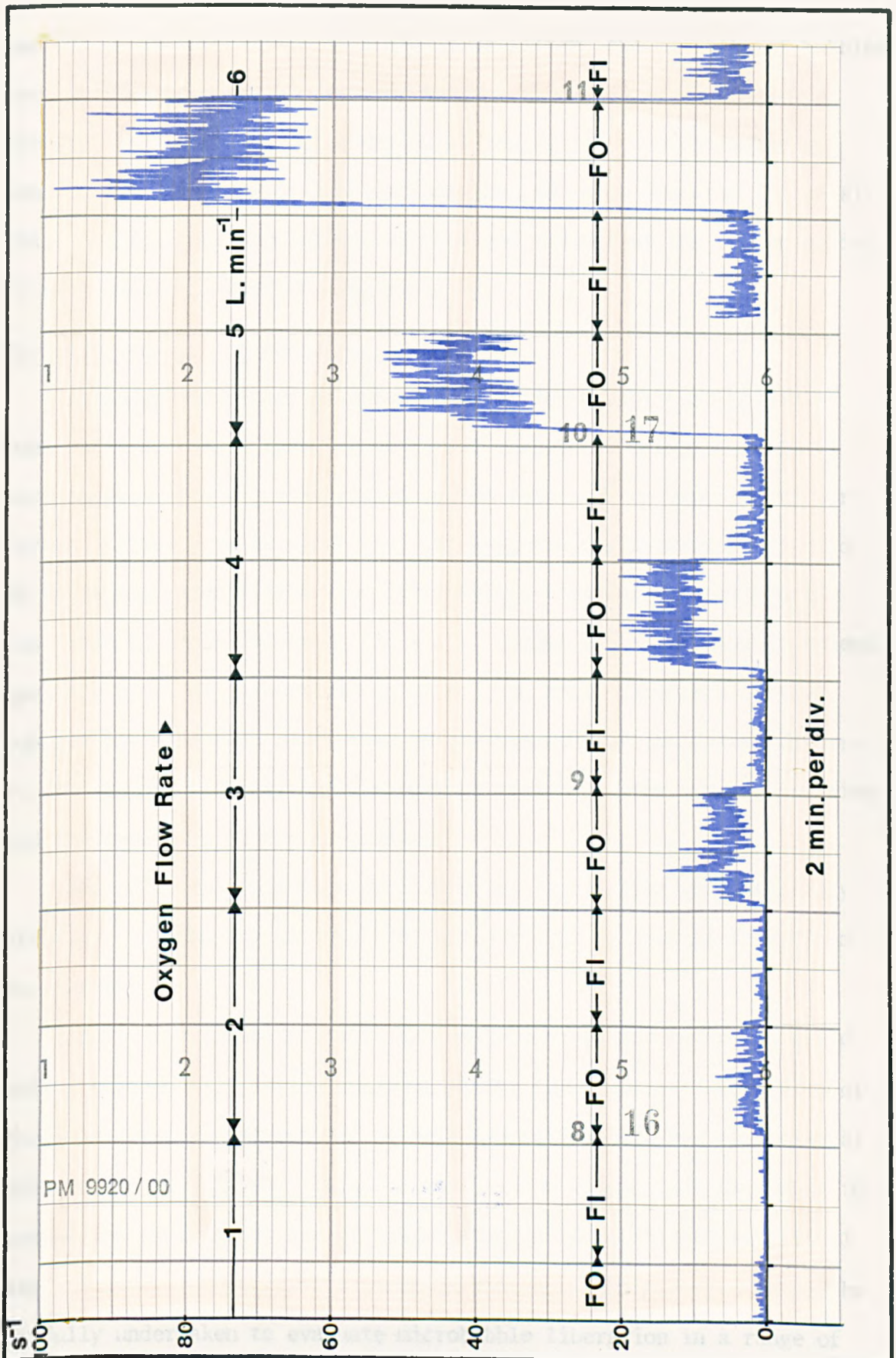

Filter Response (count rate S^{-1})
Blood Flow Rate 1L min^{-1}

FI Filter in
FO Filter out

Fig. 6.7

Referred to on P.222

increase. In the absence of a micropore filter, the majority of bubbles were within the 20-80 μm diameter range. The residual population of bubbles, following the introduction of the filter, was estimated to consist predominantly of bubbles less than 40 μm in diameter (Fig.6.8). This same residual population was observed throughout the 3 hour period of microbubble filtration (Fig.6.9).

In vitro studies - discussion

Although the number of experiments performed for each physical constraint was small (one repeat in all cases) two unequivocal facts have emerged from a consideration of the total of ten experiments performed. Firstly it is clear that the Rygg-Kyvsgaard oxygenators used in these experiments liberated microbubbles that were predominantly less than 80 μm in diameter, the actual number and rate being dependent upon the physical constraints imposed. The small diameters of the bubbles may have been partly due to the presence of two coarse filters ($\sim$ 140 μm pore size) within the outflow regions of the defoamer section and the reservoir of the oxygenator.

Secondly, the Pall micropore arterial line filter was remarkably effective in removing microbubbles estimated to be greater than 40 μm in diameter.

Apart from these two facts the results presented by the in vitro saline experiments provide implicit rather than explicit statements of the relationships between microbubble liberation rate and the physical constraints considered. Insufficient time or finance was available to repeat the experiments in sufficient numbers to establish statistical significance. However it is proposed that a separate project could be usefully undertaken to evaluate microbubble liberation in a range of extracorporeal components, preferably with a whole blood prime.

A number of interesting observations have been made concerning the individual results of the in vitro experiments.

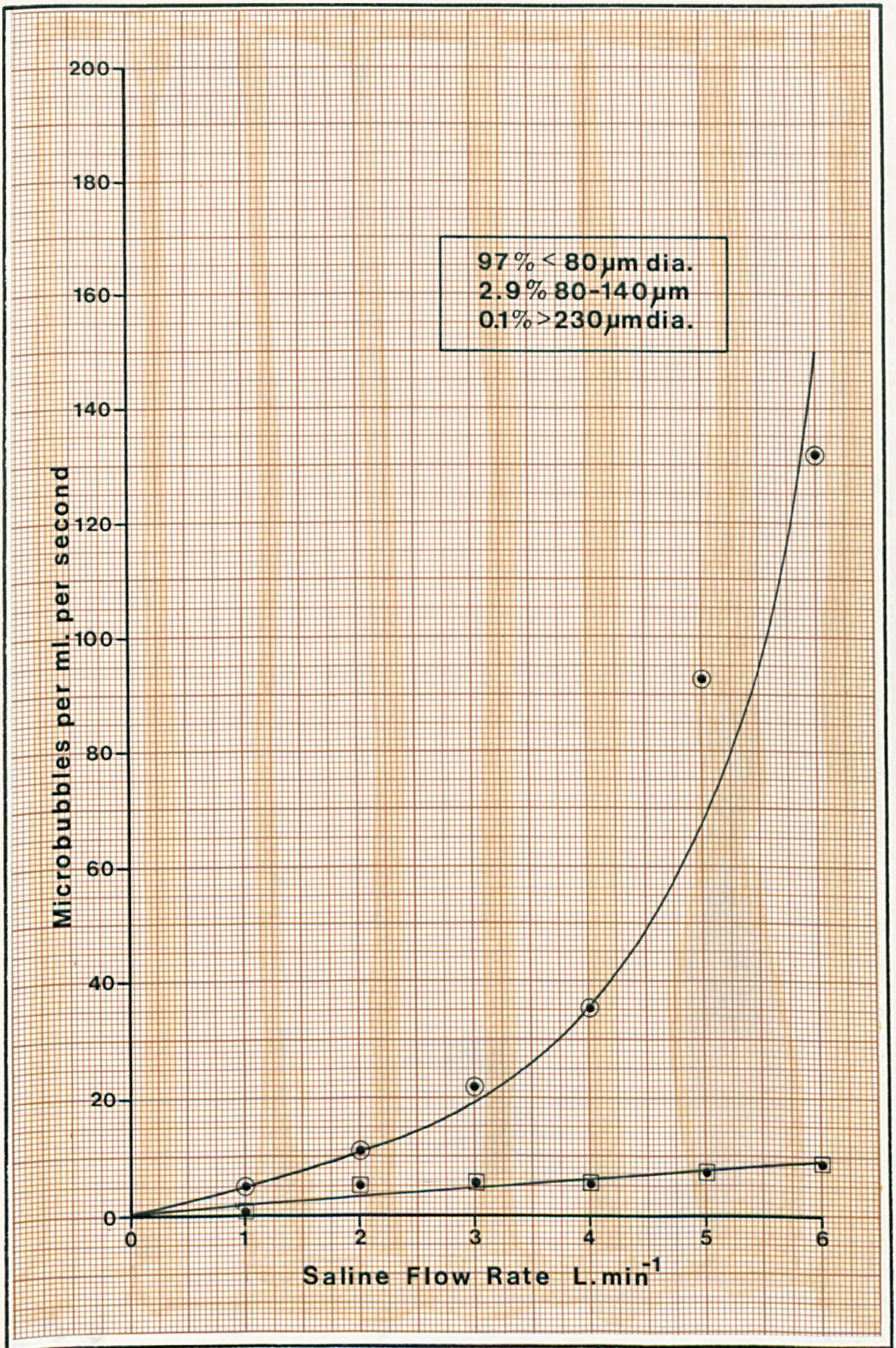

Microbubble Liberation & Filter Response
Oxygen flow rate 3L min^{-1} Temp. $16^{o} \pm 1^{o}C$
High reservoir level
◉ Without filter in circuit
▣ With filter in circuit

Fig. 6.8

Referred to on P.226

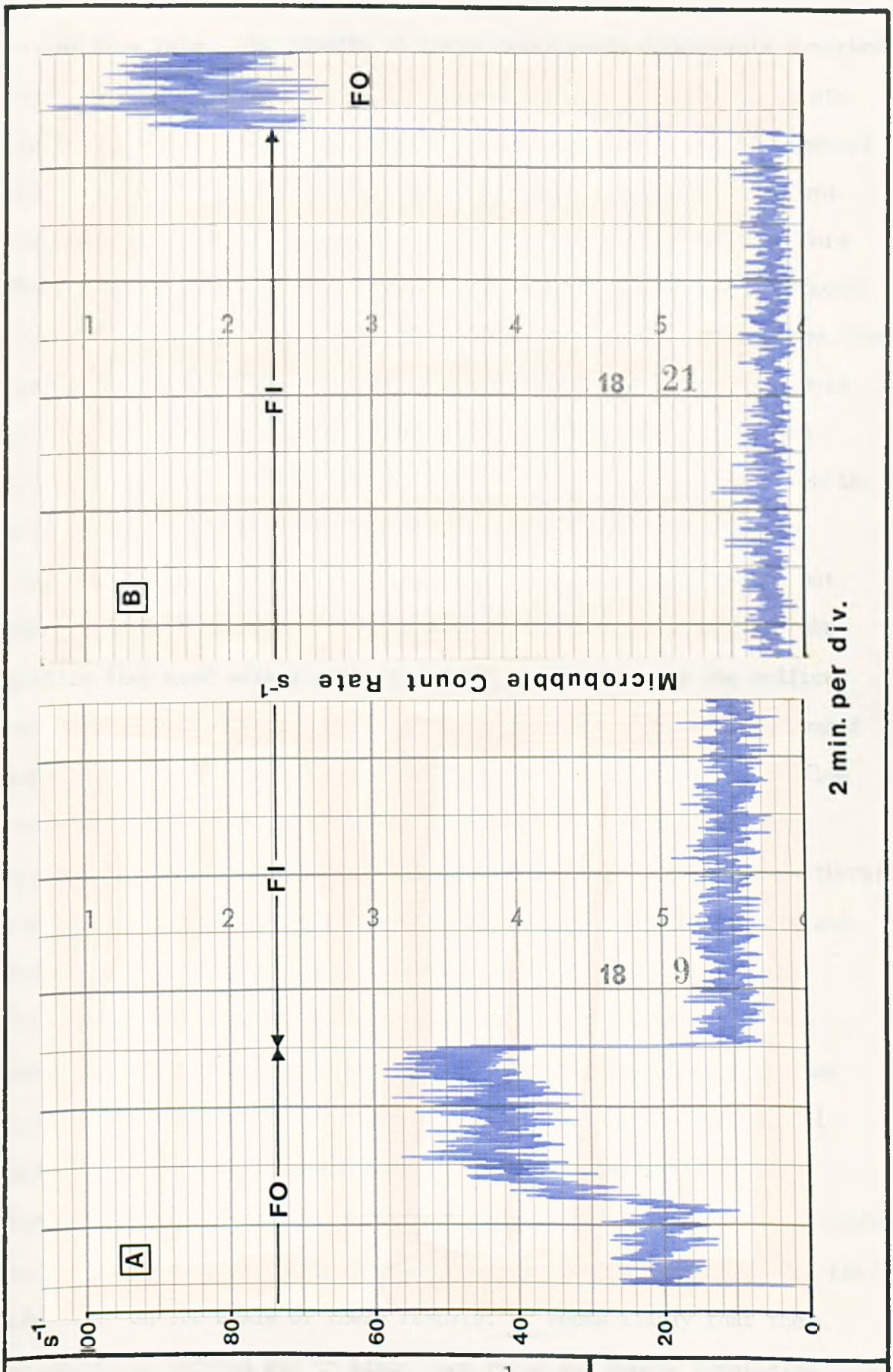

3 hour Filter Response (count rate S^{-1})

A Begining
B End

FI Filter in
FO Filter out

Fig. 6.9

Referred to on P.226

Saline flow rate. The results of these experiments demonstrate a marked relationship between microbubble liberation rate and saline flow rate. The use of flow dependent triggering of the ultrasonic detector enabled the increase to be resolved into a component directly related to proportional increases in flow rate and a component due to other factors. The component directly related to flow rate was insufficient to account for the increase in bubble liberation rate over the range of saline flow rates considered. This may have been due to a reduction in reservoir settling time and/or reduced contact with the defoaming agent. An additional, but less likely mechanism may have been that larger bubbles were undergoing fission as they were forced through the oxygenator filters at higher flow rates. Tanasawa et al (1970) have shown that bubbles may undergo fission at an imposed flow constriction, but the bubbles they used were greater than 1000 μm diameter and the orifices through which they were forced were of comparable size. The increased rigidity of smaller bubbles may preclude such a mechanism at the flow velocities encountered within an oxygenator. The more plausible explanation for the increase in the measured bubble population is therefore that more microbubbles were carried through the defoaming section and settling reservoirs at higher saline flow rates.

Gas flow rate. Even at the lowest oxygen flow rates used in these experiments (1 $L.min^{-1}$) it would seem reasonable to expect rapid and complete saturation of the prime with oxygen. The relatively small quantity of detectable bubbles observed at low saline flow rates indicates that the defoaming section, filters and the chambers are highly efficient in moderating the release of microbubbles to the rest of the circuit. On the basis of these results, it seems likely that the relationship between gas to blood flow ratio and bubble population size described by Gallagher & Pearson (1973) is an oversimplification. It is necessary to describe the bubble populations at various saline or

blood flow rates with constant gas flow rate and also at various gas flow rates with constant saline or blood flow rate.

Reservoir level. Although the influence of reservoir level was considered for only two volumes of circuit prime, the levels obtained were representative of the operating limits encountered during conventional clinical cardiopulmonary bypass, with the Rygg-Kyvsgaard oxygenator. The increase in the detectable bubble population when the circuit was operated at the lower reservoir level suggests that the reduced settling time, defoamer contact time, and volume of fluid in contact with the defoaming agent were the important factors. However the cascade of prime from the defoamer section to the reservoir was observed to result in the formation of bubbles. Many of these bubbles were readily discernable with the naked eye, and were prevented from entering the reservoir by the intervening coarse mesh filter. It is reasonable to expect that smaller bubbles may also be formed in this manner and pass, undetected by the naked eye, into the reservoir. Even for the conditions imposed by a low reservoir level, the sizes of bubbles that were detected were small (20-80 μm diameter). This observation supports the view that the coarse mesh filters are effective in trapping the larger bubbles.

The cascade effect further suggests that the geometry of the oxygenator, the local flow velocities and flow patterns may also exhibit a significant influence upon the propensity of oxygenators to liberate microbubbles.

Temperature. It is generally accepted that the rate of rewarming during extracorporeal circulation should not exceed $0.5^{o}C.min^{-1}$. The rate of temperature increase in both of the experiments performed using a saline prime was approximately $1^{o}C.min^{-1}$. Very little changes in the bubble population was noted during the warming period. Donald & Fellows (1961) reported that the rapid rewarming of blood ($17^{o}C$ in 4 to 10 minutes) within an experimental circuit was unaccompanied by a detectable release

of bubbles. Bubbles were formed only when a 17°C temperature gradient (20-37°C) was maintained in different parts of the circuit for at least 10 minutes. The visual technique of bubble detection used by Donald & Fellows (1961) prevented them from observing bubbles of very small size. However the flow dependent ultrasonic detector indicated the presence of very small bubbles throughout the warming procedure. Whilst the rate remained reasonably constant, the size of the bubbles detected was observed to be larger as the temperature increased. Unfortunately the increases in size were insufficient to register as changes in the channel activity of the signal discriminator, the reliance for the observation being based upon the oscilloscope display.

The observed changes in size may be attributed to the expansion of gas within the bubbles and to the diffusion of oxygen into the bubbles as the solubility of oxygen in saline decreased. The lack of accurate sizing data precluded an estimate of size increase to be expected on the basis of thermal expansion alone. This raised an important question. If bubble growth is initiated in this manner what is the subsequent fate of these bubbles in a conventional bypass? In these experiments the oxygenator was possibly forming a sink for growing bubbles. During cardiopulmonary bypass for open heart surgery the subject being perfused would constitute the sink for these bubbles. Experiments performed in the manner described, with the detector close to the heat exchanger, may therefore be misleading. More distal measurement of the bubble population together with an estimate of the rate of bubble growth would be more informative.

Caution must also be exercised in applying the results of saline primed experiments to situations involving a whole blood prime. Judicious control of blood saturation may considerably moderate the release of gases during a period of warming.

Filter response. The importance of arterial line filtration for the

removal of potentially embolic particulate matter has been well documented and the need for arterial line filtration during extracorporeal circulation strongly asserted (Swank & Hissen, 1965; Hill et al., 1970; Tufo et al., 1970; Osborn et al., 1970; Patterson, Kessler & Bergland, 1971; Patterson & Twichell, 1971; Ashmore et al., 1972; Egeblad et al., 1972; Dutton et al., 1973; Patterson, Wasser & Porro, 1974; Connell, 1975). Microfiltration has also been considered to be effective in the removal of microbubbles (Spencer et al., 1965; Patterson & Kessler, 1969; Gallagher & Pearson, 1973). Although attempts have been made to provide quantitative evidence of filter effectiveness (Lubbers et al., 1974), the limitations inherent in the detection technique, as discussed earlier, raise an element of doubt in the significance of the results. It has been generally reported the Pall filter is 40-90% effective in removing potentially embolic material without reference to the particle size being removed. The evidence of these experiments indicate that the Pall filter is extremely effective in removing microbubbles that are greater than 50 μm in diameter. This is in agreement with the conclusions provided by Lubbers et al., 1974, in spite of the limitations suggested.

The capacity of the filter to remove microbubbles has not been adequately assessed in these experiments, although a 3 hour insult with microbubbles (3 $L.min^{-1}$ oxygen flow rate, and 2 litre saline prime) revealed consistent microbubble removal. No evidence of the breakthrough of bubble showers, occasionally suggested as a disadvantage of screen type filters, was obtained during this period. More long term experiments are required to fully evaluate the capacity of filters for microbubble removal. Moreover, more experiments are required to evaluate the different types of filter for use in cardiopulmonary bypass.

In vivo studies - general and surgical methods

Adult beagle dogs weighing 10-15 Kg were used for these experiments.

General anaesthesia was induced by intra-venous injection of 0.4-0.5 g of sodium pentothal (Intraval). Following endotracheal intubation, the dogs were artificially ventilated in a semi-closed loop system containing a carbon dioxide absorber and an East-Radcliffe ventilator producing intermittent positive pressures of 20 cm water at 13 strokes min^{-1}, and light anaesthesia was maintained with a variable mixture of 0.5-2.0% halothane (Fluothane) in nitrous oxide and oxygen in the ratio of approximately 1:1. Following right femoral venesection, the halothane anaesthesia was replaced by a 0.4% drip of Intraval in 0.9% sodium chloride at a flow rate of 1 $ml.min^{-1}$.

The extracorporeal circuit consisted of a small Rygg Kyvsgaard disposable bubble oxygenator (HL-054, Polystan), a Bio-Med. Engineering stainless steel torpedo-type heat exchanger, a Pall extracorporeal blood filter (EC 3840, Johnson & Johnson), a Sarns roller pump, a 9.6 mm internal diameter cannulating electromagnetic flow probe (Nycotron), an in-line thermocouple temperature probe (Ellab) and the microbubble detector assembly, as shown in Fig 6.10. The components were connected by 9.6 mm internal diameter PVC tubing (6LF pumpset, Travenol). The circuits were primed with 500-1000 ml, 5% Dextrose solution, 200 ml., 10% low molecular weight dextran in 0.9% sodium chloride (Rheomacrodex), 500-700 ml Ringer-Lactate solution (Hartmanns), 10-30 ml, 20% sodium bicarbonate solution and 10 mg of heparin.

Using conventional clean surgical techniques the right and left femoral blood vessels were exposed. The right femoral vein was catheterised using a French number 6 catheter and coupled to a saline filled column, graduated in millimetres to allow direct measurement of venous pressure. A 2.1 mm internal diameter nylon catheter with a single end hole was introduced into the right femoral artery and coupled via a three-way tap to a Bell & Howell (4-422-0001-1-B4MS) pressure transducer, 0-750 mm Hg (0-101 kPa) range, for the measurement

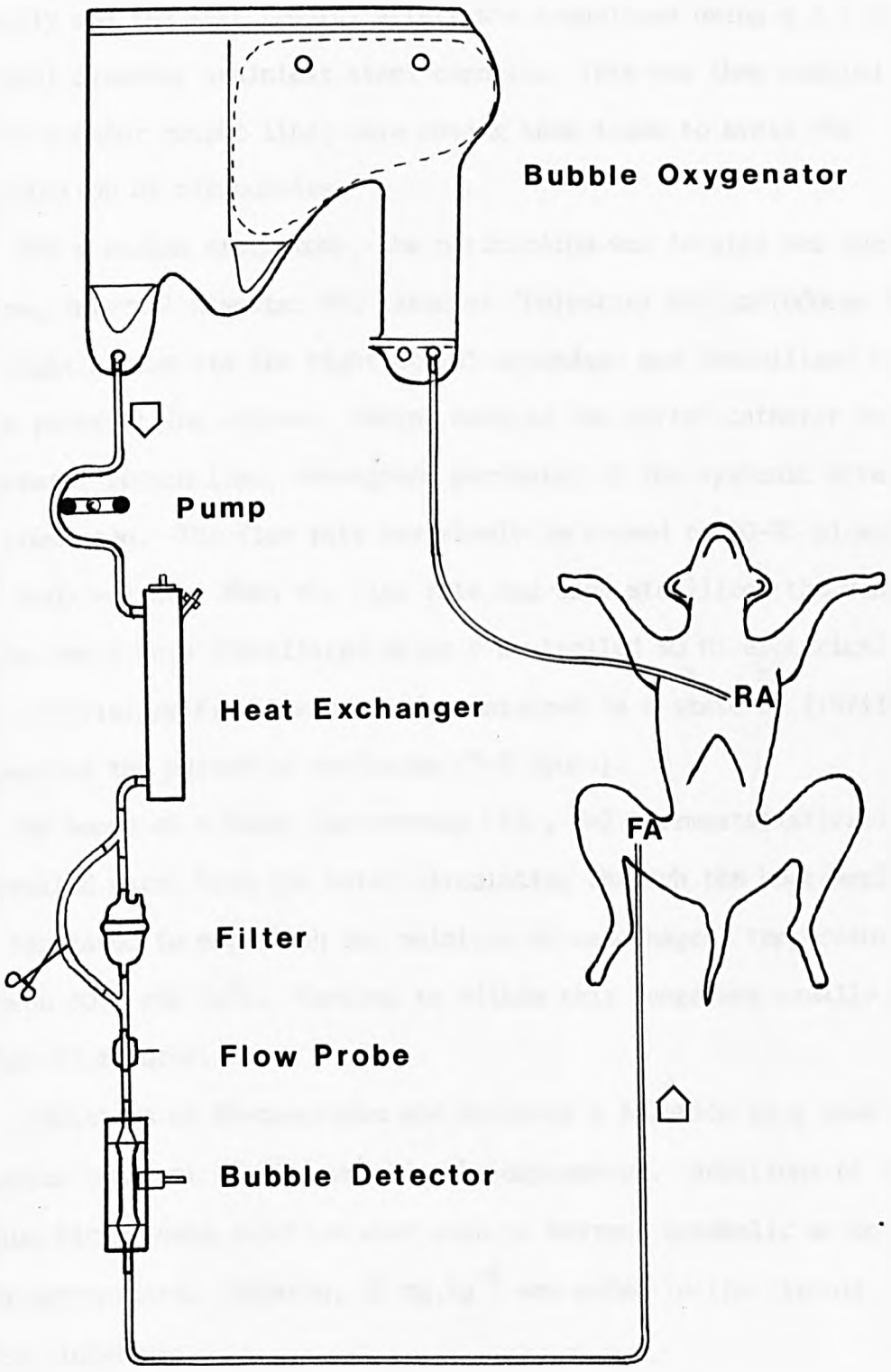

In vivo circulation circuit
RA Right Atrium
FA Femoral Artery

Fig. 6.10

Referred to on P. 233

of arterial pressure. Sodium heparin, 3 mg. Kg^{-1} was given intravenously and the left femoral artery was cannulated using a 3.5 mm internal diameter stainless steel cannula. This was then coupled to the oxygenator output line, care having been taken to avoid the introduction of air bubbles.

Via a median sternotomy, the pericardium was located and opened. A 6 mm, internal diameter PVC catheter (Polystan) was introduced into the right atrium via the right atrial appendage and immobilised by a nylon purse-string suture. Having coupled the atrial catheter to the oxygenator return line, retrograde perfusion of the systemic arteries was commenced. The flow rate was slowly increased to 80-85 $ml.min^{-1}$, Kg^{-1} body weight. When the flow rate had been stabilized the ventricles of the heart were fibrillated using a controlled 50 Hz electrical shock (non-proprietary fibrillator) and maintained in a state of fibrillation throughout the period of perfusion (3-5 hours).

By means of a Grant Instruments Ltd., SB2 thermostatistically controlled water bath the water circulating through the heat exchanger was regulated to establish and maintain an oesophageal temperature between $30^{o}C$ and $36^{o}C$. Cooling to within this range was usually achieved within 15 minutes.

Additions of Rheomacrodex and Hartmann's solution were made to maintain constant fluid levels in the oxygenator. Additions of 8.4% sodium bicarbonate solution were made to correct metabolic acidosis when appropriate. Heparin, 10 $mg.Kg^{-1}$ was added to the circuit at hourly intervals.

Arterial blood pressure, venous pressure, blood flow rate, oxygen flow rate, oesophageal temperature, circuit temperature, electrocardiogram, microbubble liberation, and arterial blood oxygen tension, carbon dioxide tension, pH, standard bicarbonate, and base excess were measured at intervals throughout the experiments. Screen filtration

pressure and packed cell volumes were also measured at intervals throughout the bypass. With the exception of the biochemical analyses of blood samples and the measurements of screen filtration pressure and packed cell volume, measurements were recorded at 10 minute intervals following the induction of ventricular fibrillation. Blood sample measurements were undertaken at 20 minute intervals.

Arterial blood pressure. The Bell & Howell arterial pressure transducer was coupled to a Devices DC.2D/SUB.1C signal conditioner and calibrated against a mercury column. Continuous monitoring of the arterial pressure waveform was provided by an Airmec display oscilloscope, whilst mean arterial pressure measurements were obtained from a calibrated meter output.

Venous pressure. A vertical saline filled column and a millimetre scale were used to monitor venous pressure. The venous catheter was coupled to the column via a three-way tap.

Blood flow rate. A Nycotron '376' flowmeter connected to a 9.6 mm, internal diameter cannulating electromagnetic flow probe was used to monitor blood flow rate. Continuous monitoring of the flow rate was achieved using a Philips PM8221 pen recorder, recording at a speed of 5 $mm.min^{-1}$.

Oxygen flow rate. A British Oxygen medical grade rotameter was used to monitor oxygen flow rate, up to a maximum of 6 $L.min^{-1}$.

Oesophageal temperature. An Ellab probe thermocouple passed into the oesophagus and connected to an Ellab multichannel temperature recorder was used to continuously monitor oesophageal temperature.

Circuit temperature. The extracorporeal circuit temperature was also monitored using an Ellab thermocouple probe and multichannel recorder.

Electrocardiogram. An Elema-Schonander Mingograph 81 pen recorder and associated ECG conditioner were used to monitor the electrocardiogram. The output was coupled to the Airmec display oscilloscope for continuous

monitoring.

Microbubble liberation. The microbubble liberation rate was continuously monitored using the Philips PM8221 pen recorder, recording at a speed of 5 mm.min^{-1}. Counts corresponding to different size ranges were also obtained at specified intervals from the amplitude discriminator-counter equipment.

Biochemical estimations. Measurements of arterial oxygen tension and blood pH were obtained using micro-Astrup equipment (Radiometer Ltd.). Measurements of pH obtained from the initial blood sample and from samples of blood equilibrated with two different oxygen/carbon dioxide mixtures (4% and 8% carbon dioxide) were used to estimate the base excess, standard bicarbonate and carbon dioxide tension (Astrup et al., 1960; Siggaard-Anderson & Engel, 1960; Siggaard-Anderson et al., 1960). The latter measurements were obtained to determine the respiratory and metabolic states of the animals.

Screen filtration pressure measurements. Screen filtration pressure measurements were obtained as an indication of platelet and leucocyte aggregation. Measurements were obtained according to the method described by Swank et al (1964).

Packed cell volume. A Gelman-Hawksley micro-haematocrit centrifuge was used to determine packed cell volume.

The constraint upon the range of variation of blood flow rate imposed by the perfusion of an experimental animal precluded the repeat of the in vitro studies. Consequently, the objectives of the in vivo experiments were confined to determining the sizes of bubbles delivered into the extracorporeal circuit from a proprietary bubble oxygenator (Rygg-Kyvsgaard, HL-054), establishing the effectiveness of arterial line filtration in removing microbubbles and establishing the significance of increased oxygen flow rate, variations in reservoir level and rapid rewarming upon the liberation of microbubbles. Because the majority

of microbubbles detected during the in vitro experiments were less than 80 μm diameter, the discriminator 'window' settings for these experiments were reduced in order to obtain further discrimination within the 20 μm to 80 μm diameter range. The lower threshold of the discriminator could not be set to a value as low as the rate recorder threshold because of a low offset voltage. However the rate recorder was set to provide a measure of the full range of bubble sizes.

Oxygen flow rate and filter response. The investigations into the effect of increased oxygen flow rate upon microbubble liberation and the effectiveness of arterial line filtration for eliminating microbubbles were combined. Oxygen flow rate was increased in 1 $L.min^{-1}$ steps up to a maximum of 6 $L.min^{-1}$. For each step increase the flow rate was maintained for a period of 10 minutes, at the end of which measurements were obtained for microbubble count, size ranges and, liberation rate. The arterial line filter was then introduced and the above measurements were repeated following a further period of 10 minutes. Thus at each oxygen flow rate the microbubble liberation characteristics were determined for both the situation in which a filter was included in the arterial line and for the situation without an arterial line filter. The reservoir level was maintained to within 20 mm $\pm$ 5 mm of the initial level (150-190 mm above the outlet port of the oxygenator) and the temperature within the range 33-36^{o}C.

Reservoir level. The arterial reservoir of the oxygenator was graduated in 10 mm $\pm$ 2 mm steps above the outlet port. The influence of reservoir level upon microbubble liberation was then investigated by removing aliquots of fluid to achieve step reductions in level of 10 mm $\pm$ 2 mm down to zero. Each level was maintained for 3 minutes but, below the 100 mm level, the reservoir volume was progressively depleted and the level rapidly reduced to zero. The arterial line filter was introduced before the reservoir emptied completely. At each reservoir level in

the range 200 mm to 100 mm, the microbubble liberation numbers, size range and rate were derived over a 3 minute period.

Temperature. Whilst maintaining a constant reservoir level the temperature of the blood was increased as rapidly as the thermostatically controlled waterbath and heat exchanger would allow. This amounted to an increase of approximately 0.6-0.7^{o}C.min^{-1}. Measurements of microbubble liberation rate, number and size ranges were obtained at 2 minute intervals. The oxygen flow rate was maintained at 6 L.min^{-1} and the temperature was not allowed to exceed 39^{o}C.

In vivo studies - results

While performing these experiments it became clear that the factors influencing the liberation and detection of microbubbles were difficult to control. In particular there was considerable variation between the groups of measurements for arterial and venous blood pressure, pO_2 and pCO_2 (Figures 6.11 to 6.22). On the other hand there was considerably less variation in the values of packed cell volume, screen filtration pressure, pH and temperature between experiments (Figures 6.11 to 6.22). The variations in measured microbubble liberation from one experiment to another were noticeably large (Figures 6.11 to 6.22). Moreover discrepancies in recorded rate and computed rate were noted and attributed to a marginal difference in the lower threshold settings for the discriminator and the frequency to voltage converter or rate recorder.

Whilst precautions were taken to avoid artefacts, the possibility must be recognised that the observed variations in counts between experiments may not be entirely influenced by in-circuit, physical parameter variations. A disturbing limitation on discriminator sensitivity was revealed following the final experiment in this series. The large discrepancies (300% max., 50% typical) observed during the course of these experiments, between recorded rates and rates computed from

KEY TO ABBREVIATIONS USED IN THE GRAPHICAL REPRESENTATION OF IN-VIVO RESULTS

LR	:	Microbubble liberation rate expressed in number per millilitre per minute.
AP	:	Arterial pressure expressed in millimetres of mercury.
VP	:	Venous pressure in millimetres of water.
pCO_2	:	Partial pressure of carbon dioxide expressed in millimetres of mercury.
pO_2	:	Partial pressure of oxygen expressed in millimetres of mercury.
O_2sat	:	Oxygen saturation expressed as a percentage.
GF	:	Oxygen flow rate in litres per minute.
SFP	:	Screen filtration pressure expressed in millimetres of mercury.
PCV	:	Packed cell volume.
BE	:	Base excess expressed in milli equivalents per litre.
pH	:	Hydrogen ion concentration expressed on the conventional logarithmic (pH) scale.
T	:	Temperature expressed in degree Centrigrade.
*	:	Figures in brackets indicate the multiplication necessary to obtain actual value from value indicated on scale.
**	:	All relevant quantities have been corrected for temperature, pressure and pH.

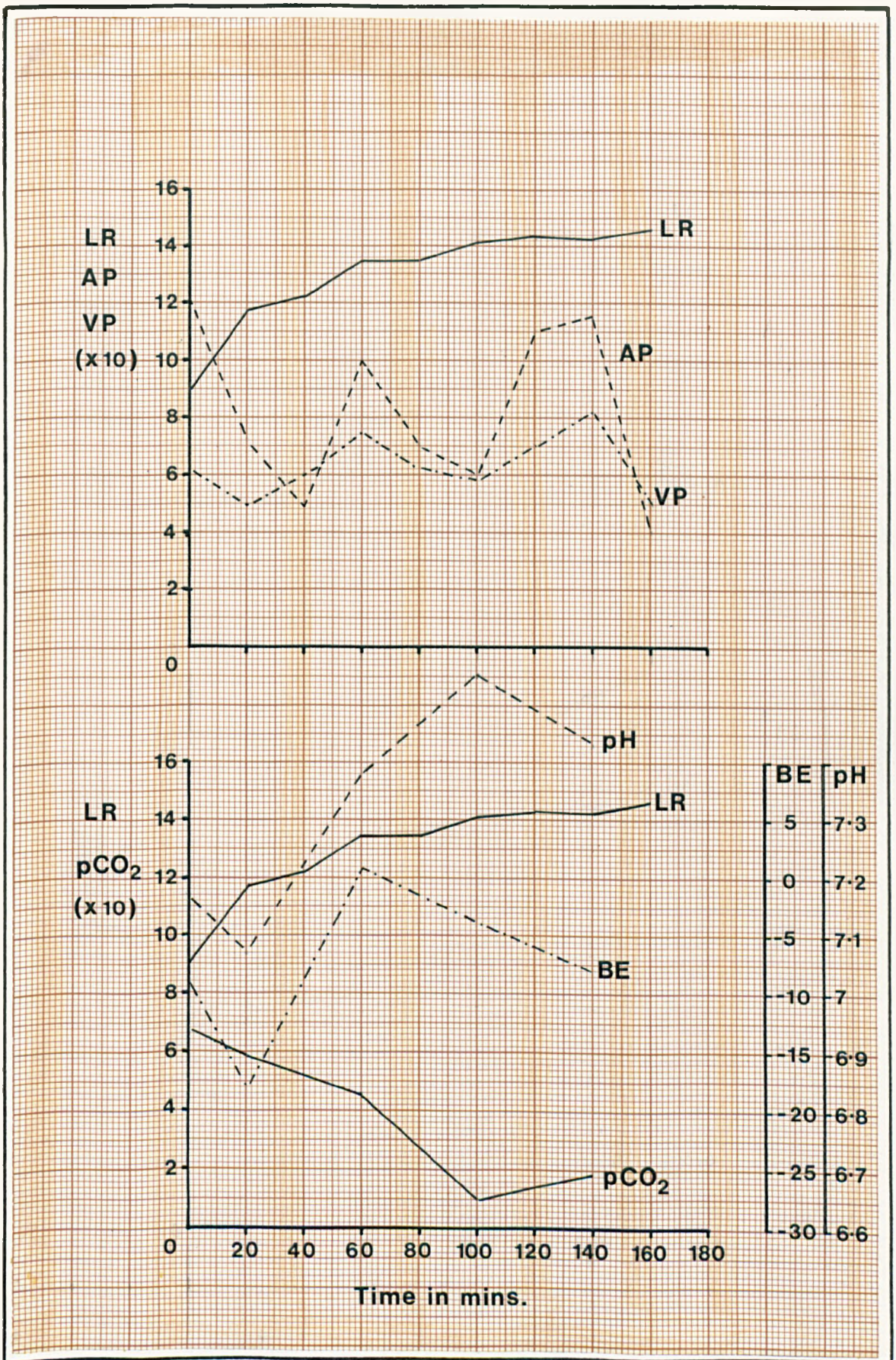

Experiment E1
Beagle ♀ Weight : 15.4Kg.

Fig. 6.11
Referred to on p. 239

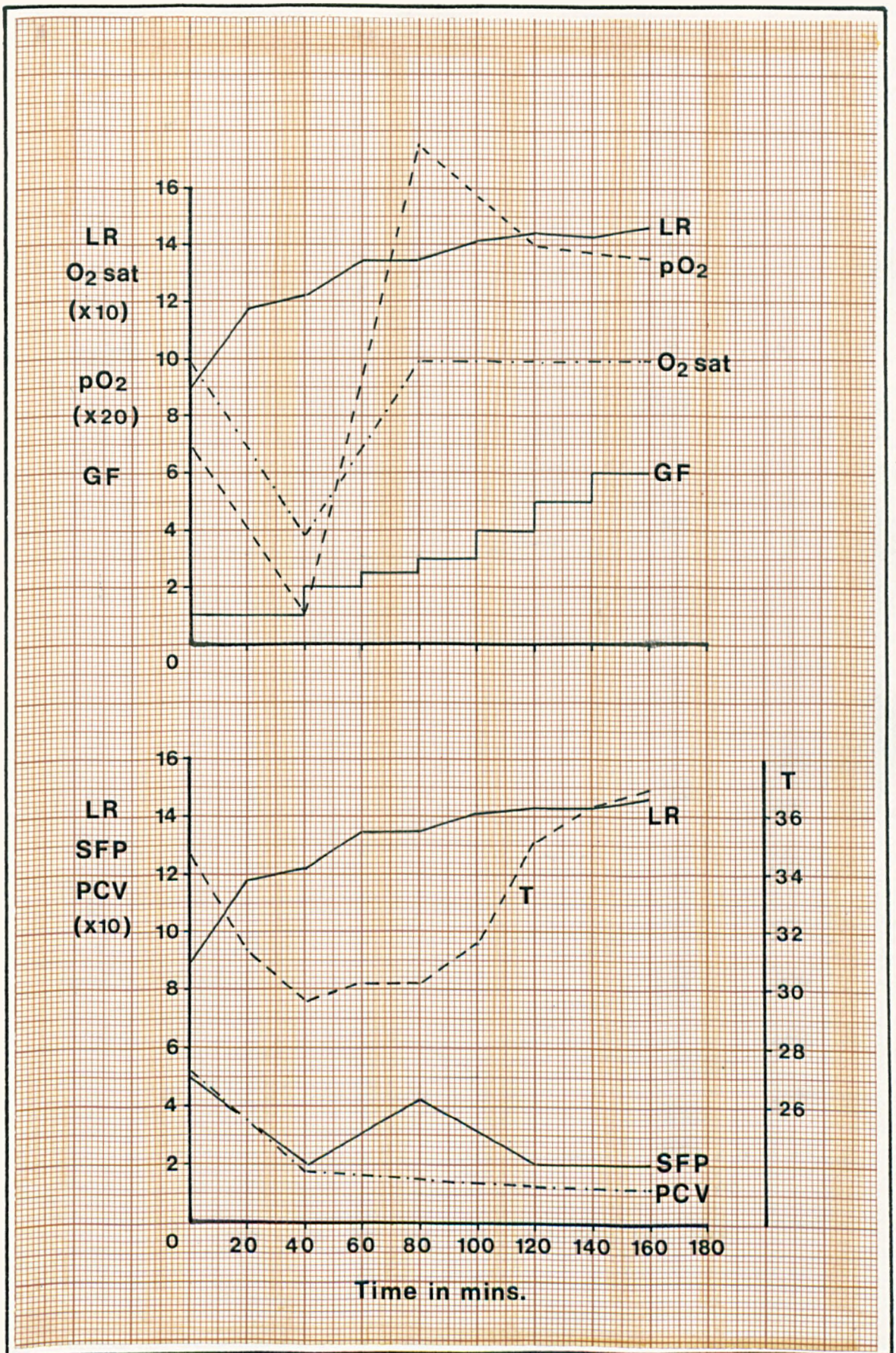

Experiment E1

Beagle ♀ Weight : 15.4Kg.

Fig. 6.12

Referred to on p. 239

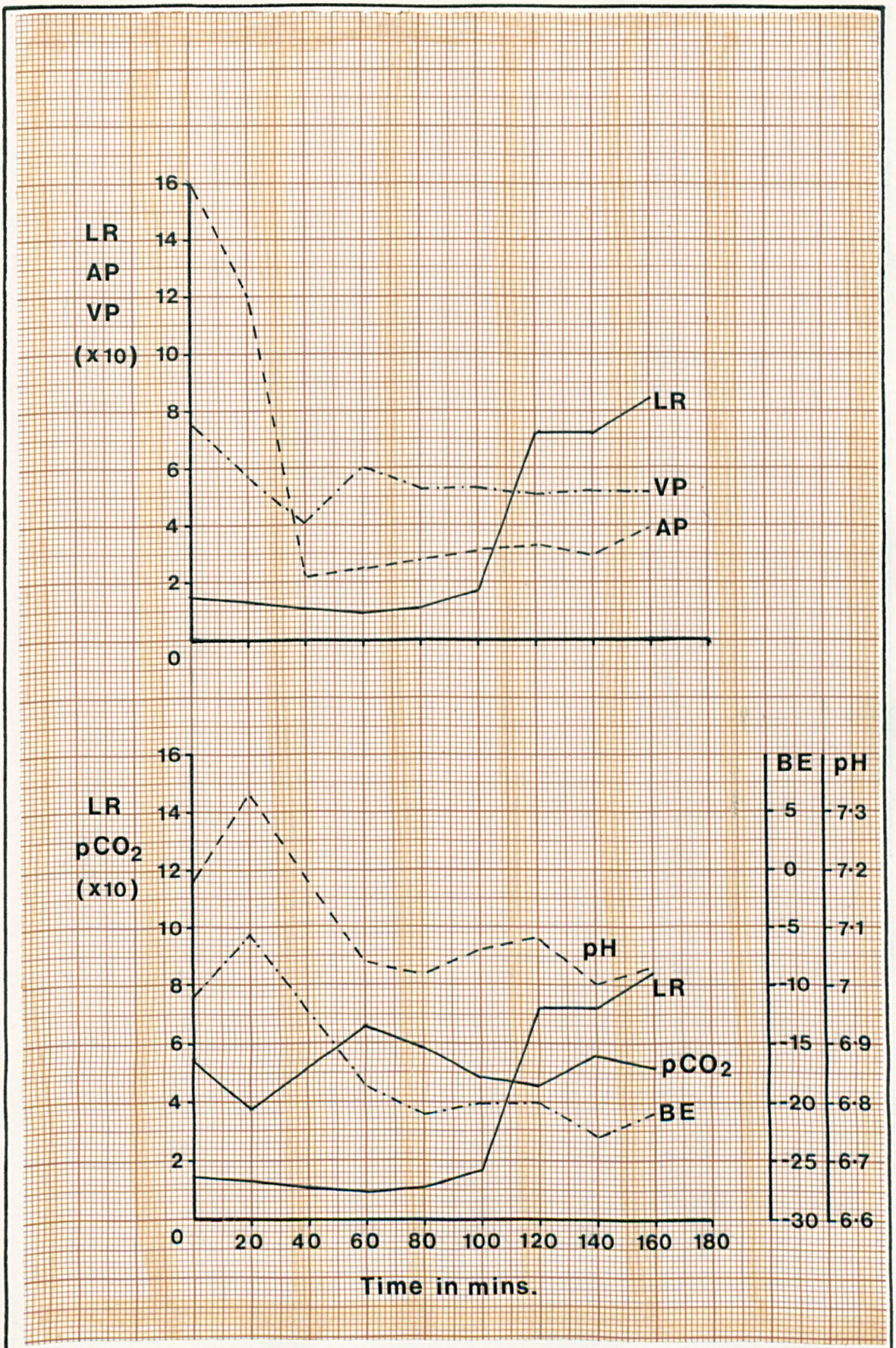

Experiment E2

Beagle ♂ Weight : 13.1Kg.

Fig. 6.13

Referred to on p. 239

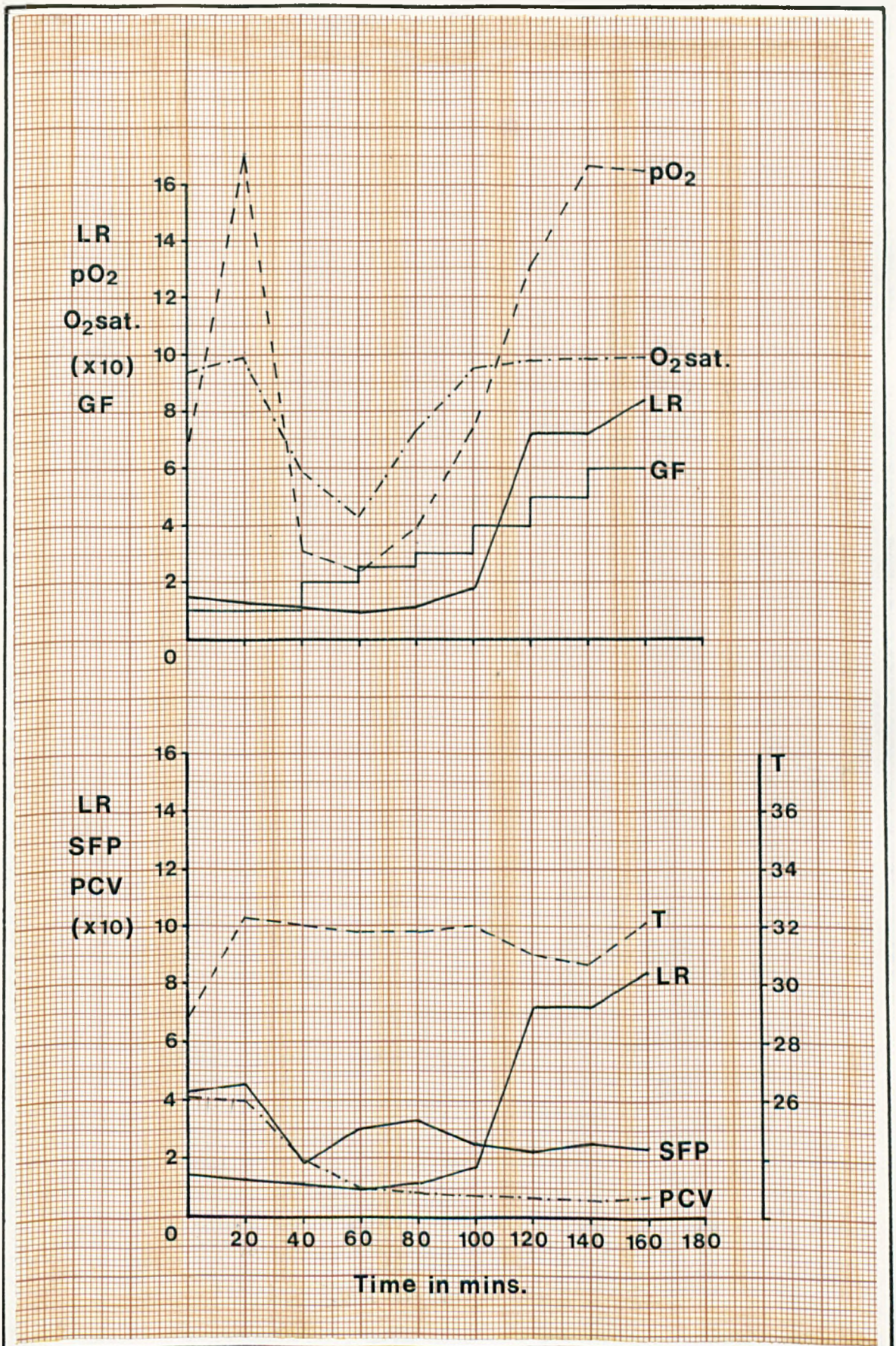

Experiment E2

Beagle ♂ Weight : 13.1Kg.

Fig. 6.14

Referred to on p. 239

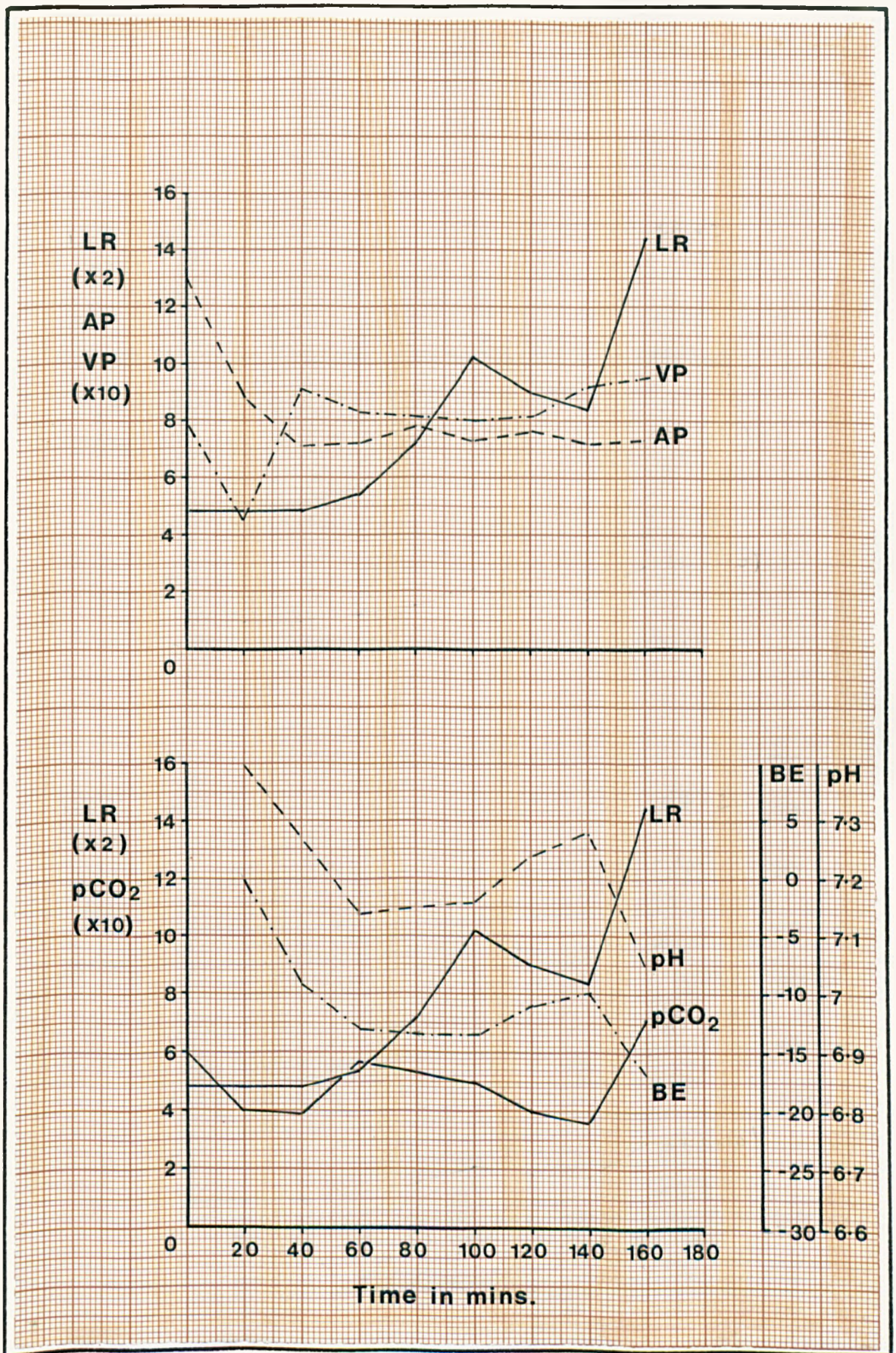

Experiment E3

Beagle ♂ Weight : 14.1Kg.

Fig. 6.15

Referred to on p. 239

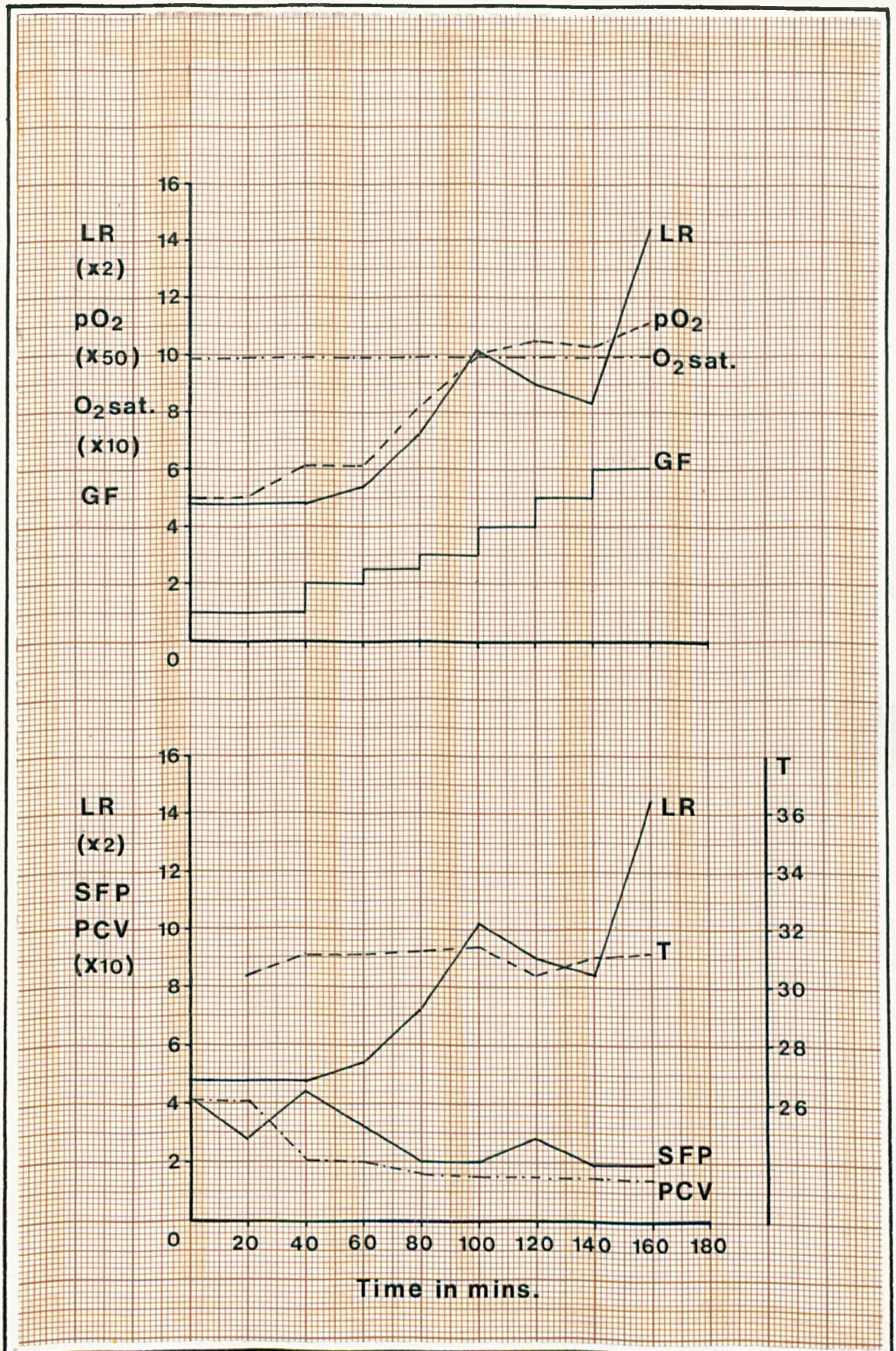

Experiment E3

Beagle ♂ Weight : 14.1Kg.

Fig. 6.16

Referred to on p. 239

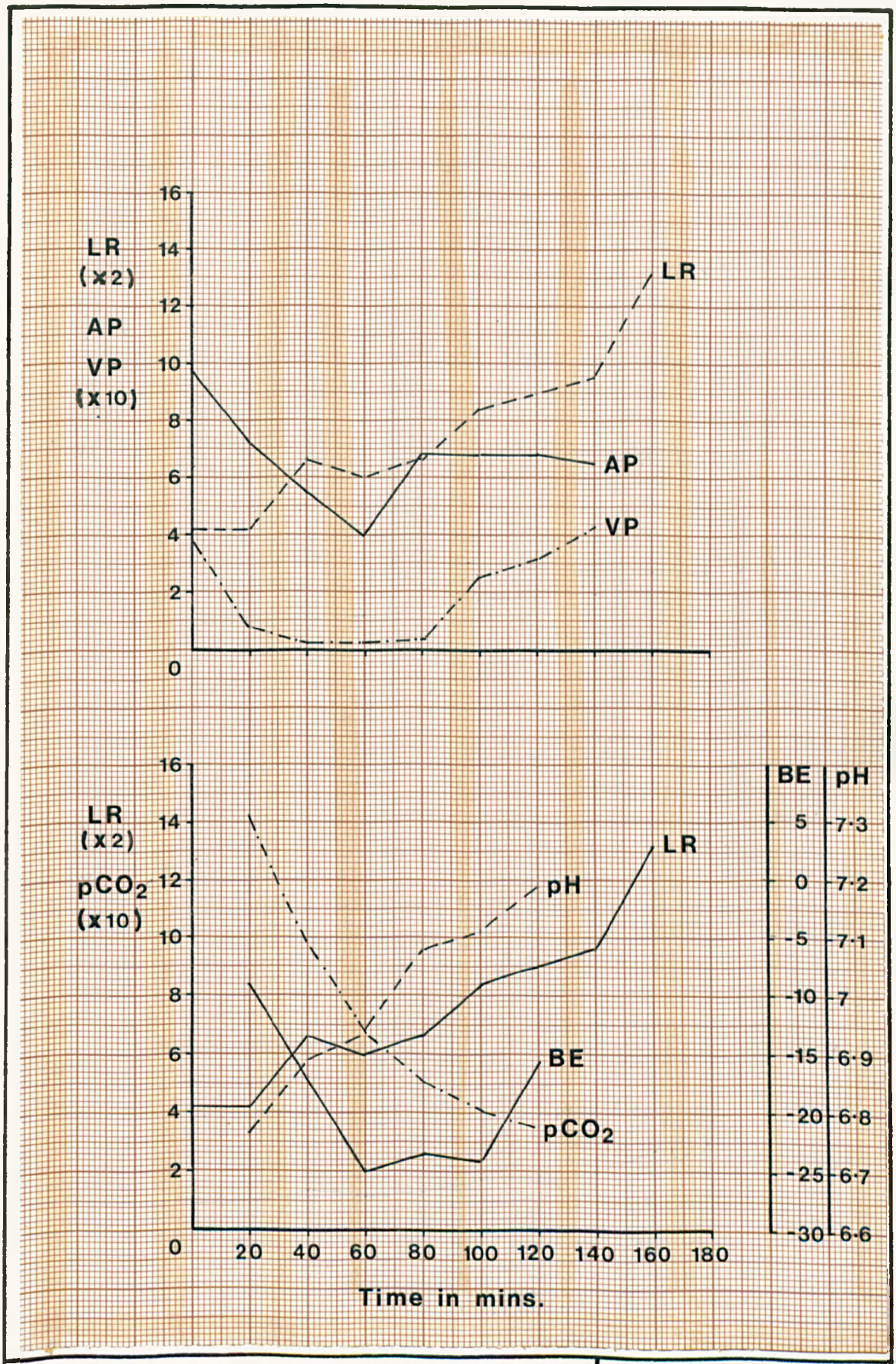

Experiment E4

Beagle ♀ Weight : 10Kg.

Fig. 6.17

Referred to on p. 239

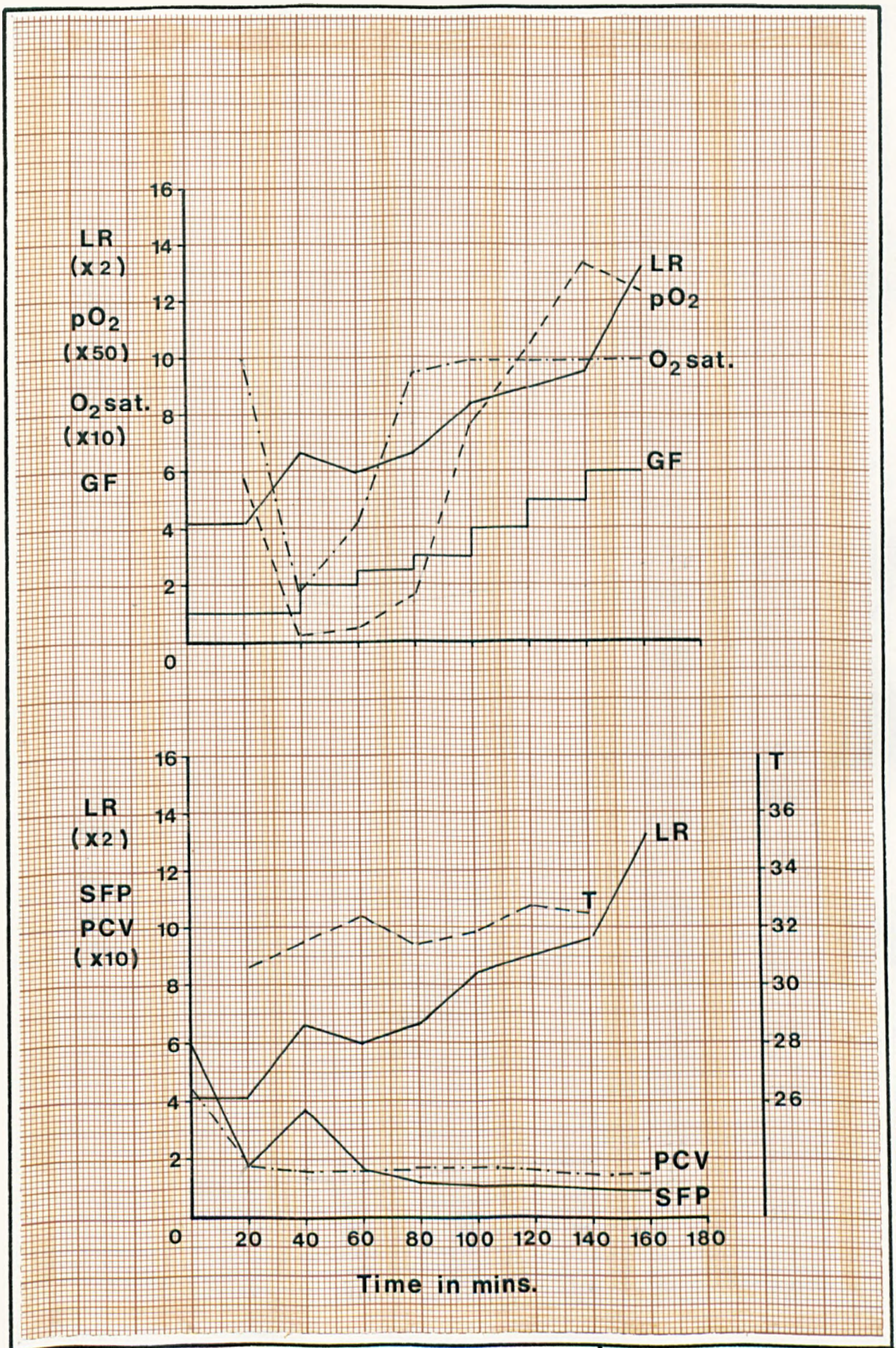

Experiment E4

Beagle ♀ Weight : 10Kg.

Fig. 6.18

Referred to on p. 239

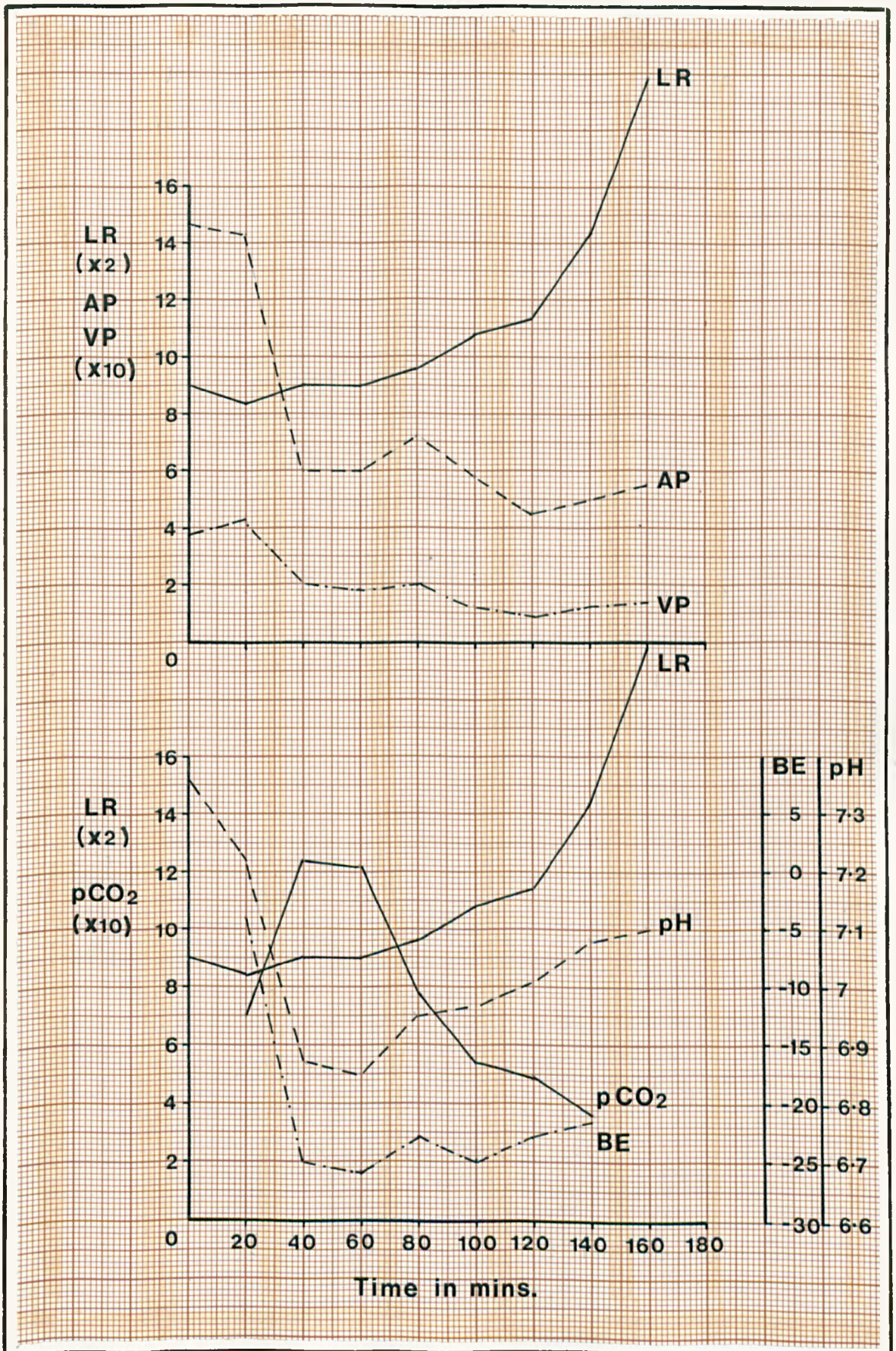

Experiment E5

Beagle ♀ Weight : 15.4Kg.

Fig. 6.19

Referred to on p. 239

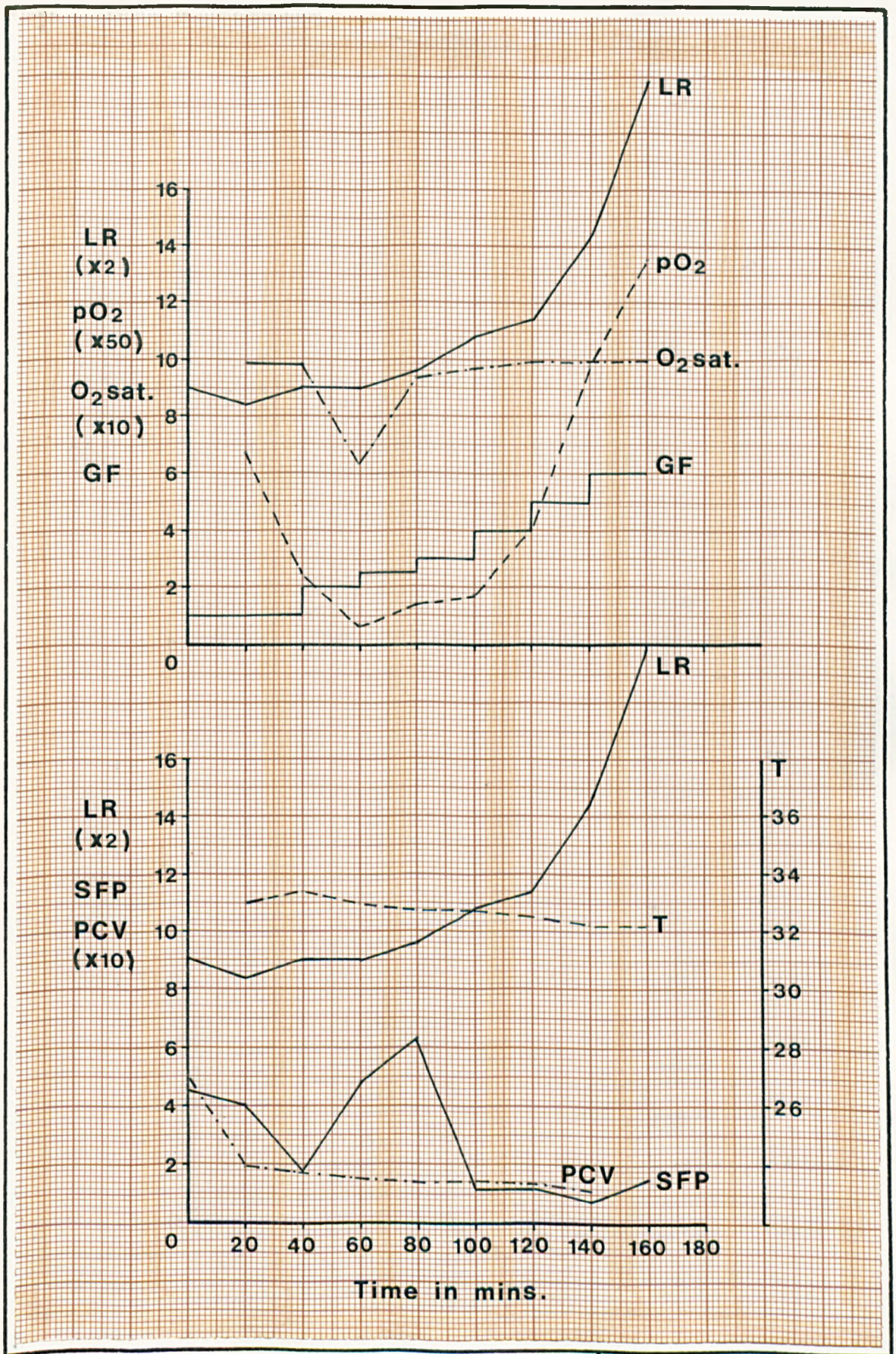

Experiment E5

Beagle ♀ Weight : 15.4Kg.

Fig. 6.20

Referred to on p. 239

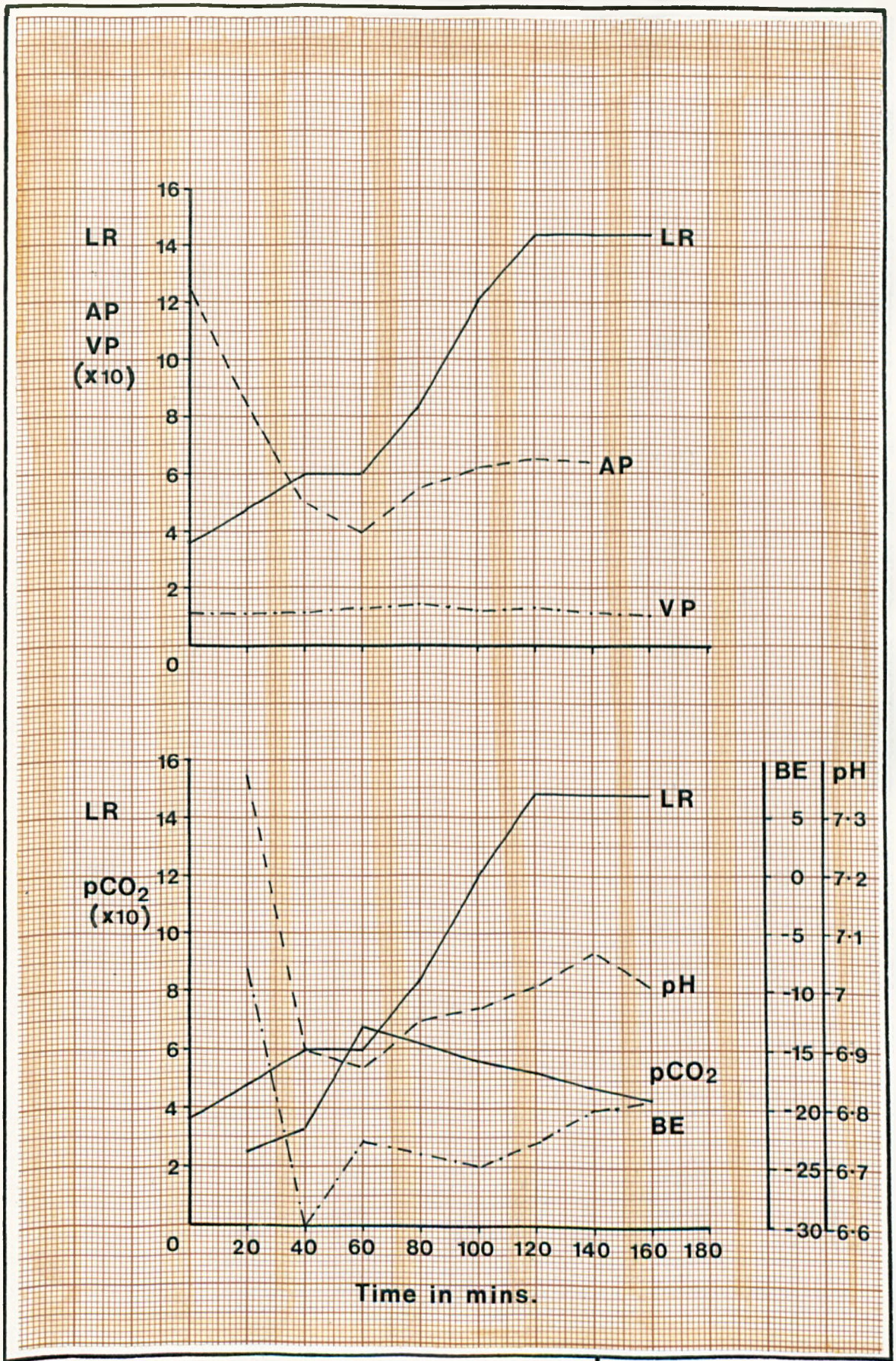

Experiment E6

Beagle ♂ Weight : 14.5Kg.

Fig. 6.21

Referred to on p. 239

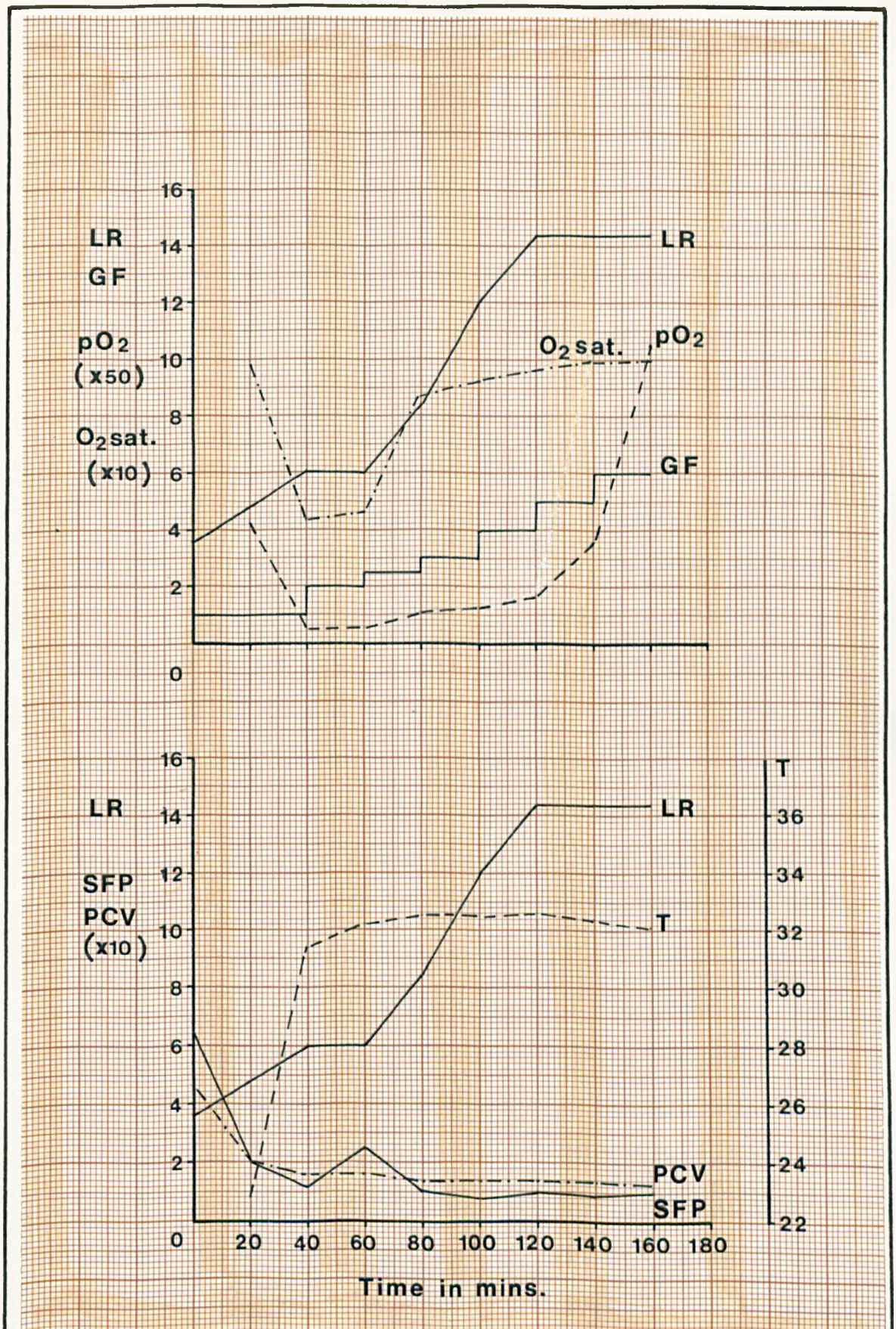

Experiment E6

Beagle ♂ Weight 14.5Kg.

Fig. 6.22

Referred to on p. 239

totalised counts over a measured period of time were thought, in retrospect, to be too large to be accounted for on the basis of marginally lower threshold settings for the discriminator and the rate recorder (approximately 10 mV difference). In a closed circuit saline experiment, using a circuit as described for the in vitro studies, the lower threshold levels for the discriminator and rate recorder were matched. Subsequent detection of liberated microbubbles revealed a smaller, but still large discrepancy between the recorded rate and the computed rate (100% max., 30% typical). Because such large discrepancies had not been observed during the in-vitro studies in which wider discriminator windows were used, the influence of size range threshold settings was investigated. Increasing the difference between the upper and lower threshold levels, produced an apparent increase in discriminator sensitivity for the detection of the irregular shaped echo responses. This effect was not observed for well defined rectangular pulses.

The reason for this effect has been attributed to the finite response time of the discriminator circuits and the relative time for which the signal peaks remain within the appropriate 'window' of the discriminator (Fig. 6.23). If the peak is just within the 'window' (Fig. 6.23A) it may not be detected because of insufficient time for the circuit to respond. This is so irrespective of the difference between the upper and lower threshold levels for the channel concerned. Consequently a marginally lower threshold may allow sufficient pulse peak to enter the 'window' and effect a response (Fig. 6.23B). The marginally lower threshold of the rate recorder compared with the discriminator can therefore account for a large part of the variations in counts observed from one experiment to another, but not all of the discrepancies. By reducing the difference between the upper and lower threshold levels the probability of a peak just exceeding a channel threshold setting and being undetected is increased (Fig. 6.23C). The

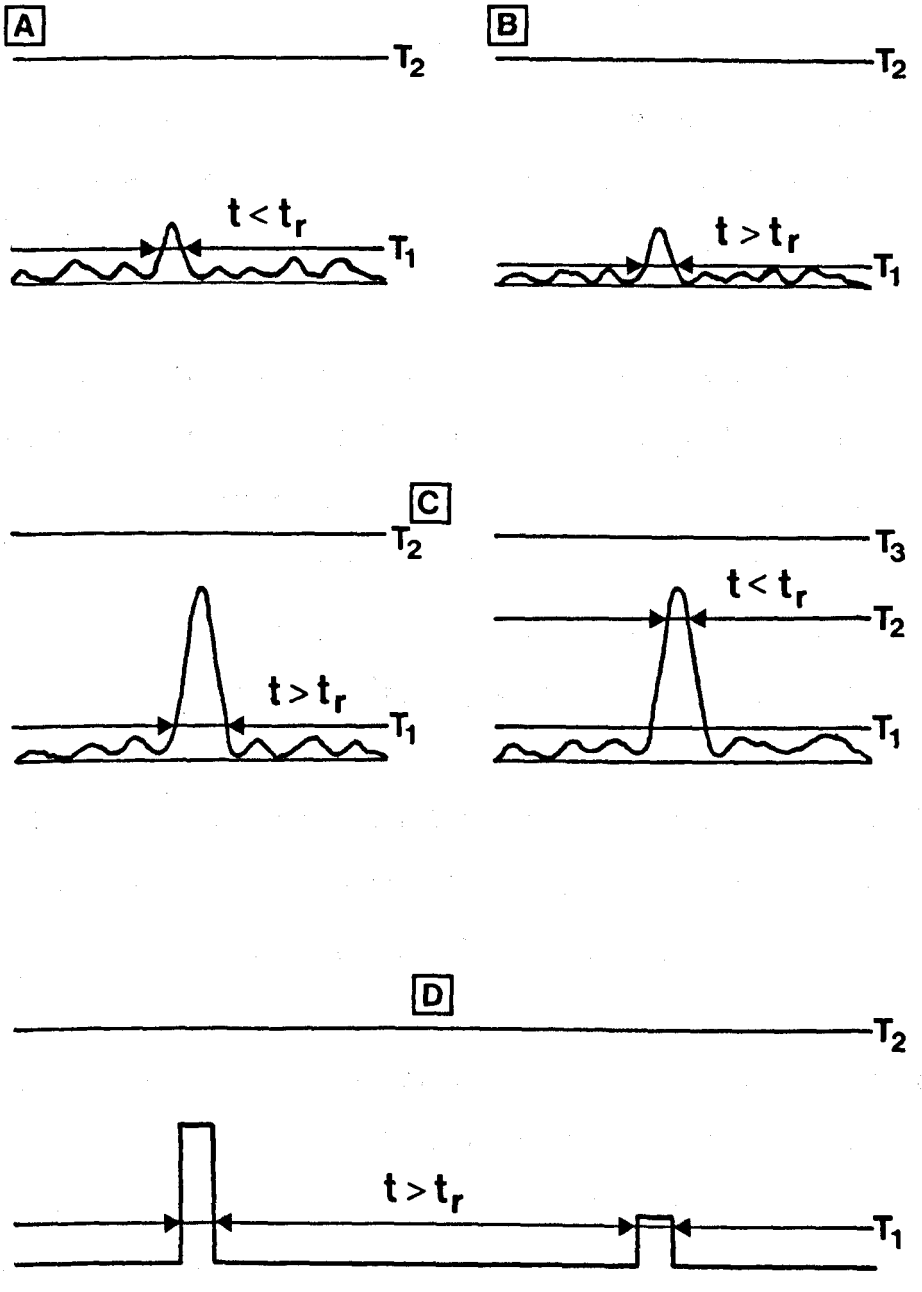

DISCRIMINATOR DETECTION LIMITATIONS
$t > t_r$ signal is detected,
t_r circuit response time
$t < t_r$ signal undetected (see text)

Fig. 6.23

Referred to on p. 253, 255

time for which a rectangular pulse exceeds a threshold level is determined by the pulse duration (Fig.6.23D). Consequently the consistent response to rectangular pulses can be readily appreciated provided the duration is sufficiently long (> 0.2 μs). On the basis of these observations it was concluded that the rate recorder was capable of detecting all the received signals corresponding to bubbles greater than 20 μm diameter, whereas the close setting discriminator channels were not.

Noise was considered as a possible source of artefact. However the noise level was observed to be no greater than 6 dB up on the level observed with a clear prime throughout the experiments. Measurements of packed cell volume and screen filtration pressure which may be considered to provide some guide to the expected level of noise, complement this observation. Little variation was noted for these parameters from one experiment to another.

In spite of the discriminator limitation and the variations in blood gas and pressure measurements from one experiment to another, some interesting results and observations have been derived from the in vivo experiments.

Bubble sizes. Although there is clear evidence to indicate that the discriminator channels have not been responding to all the received signals, the oscilloscope observations made throughout the experiments support the sizing indications provided by the discriminator. There is little doubt that the predominant size range for the microbubbles liberated in all of these experiments is 20 μm-80 μm diameter. The rate recordings for all the experiments at low oxygen flow rates (1-2.5 $L.min^{-1}$) and high reservoir level (170-190 mm above the outlet port) appear to substantiate this, since the introduction of the arterial line filter produced little change in the observed rate. However, a noticeable change was observed whenever the oscilloscope and the

discriminator provided indications of increased bubble sizes (Fig. 6.24). Taking the discriminator records to be representative of the trends in size range variation, no less than 89% of the unfiltered bubble population, liberated under the high level reservoir conditions were below 50 μm diameter, irrespective of oxygen flow rate. The remaining microbubbles were estimated to be within the 50-80 μm, 80-110 μm and > 230 μm diameter ranges, whilst the percentages were dependent upon oxygen flow rate and reservoir level. Few microbubbles were counted within the ranges between 110 μm and 230 μm diameter. Since this could have been due to non-functional channels, bubbles were generated electrolytically following these experiments and the channels found to be in working order.

Oxygen flow rate and filter response. Table 6.1 indicates the changes in the liberated microbubble population for the conditions imposed by having a high reservoir level (170-190 mm above the outlet port) and increasing oxygen flow rate. In general the effect of increasing the oxygen flow rate, while maintaining a fixed blood flow rate, was an increase in the number of microbubbles released and a shift toward the formation of larger bubbles. (Figures 6.12 to 6.22 alternate).

Table 6.1 also indicates the effect upon the release of microbubbles of introducing an arterial line filter. In general the result was an increase in the population of bubbles less than 50 μm in diameter and a reduction in the larger size range. It would therefore appear that the Pall arterial line filters used in these experiments are particularly effective in removing microbubbles above 50 μm diameter, but relatively ineffective below 50 μm diameter. The increase in the release of bubbles less than 50 μm in diameter suggests that the filters may be causing the larger bubbles to break-up and pass through the filter. Unfortunately, without monitoring both the input and output of the

Table 6.1

Microbubble Liberation Rate-Oxygen Flow Rate Relationship and Filter Response during extracorporeal circulation in dogs (microbubbles ml^{-1}. min^{-1}.)

	Bubble Diameter	< 50μm		50-80μm		80-110μm		> 230μm	
	Filter*	FO	FI	FO	FI	FO	FI	FO	FI
	1	10.49	10.56	0.02	0.002	0.05	0	0	0
Gas	2	11.42	11.5	0.01	0.01	0.007	0.01	0.014	0
Flow	2.5	10.99	11.14	0.14	0.12	0.05	0.02	0.12	0
Rate	3	12.62	12.96	0.38	0.22	0.07	0.02	0.096	0.005
L. min^{-1}	4	15.05	17.11	2.11	0.38	0.22	0.02	0.17	0.002
	5	19.39	25.2	9.62	4.94	0.96	0.07	0.26	0.005
	6	27.12	31.68	9.6	6.82	1.61	0.02	0.31	0.007

* FO : Filter out

FI : Filter in

filter simultaneously it is not possible to establish a relationship between the undissolved gas entering the filter and that leaving the filter via the arterial line.

In considering the relevance of these observations it must be borne in mind that the variations in microbubble liberation rates between experiments were large (Table 6.1). Although the mean values suggest an overall slight increase or decrease in the measured rate following the introduction of an arterial line filter conditions were noted in which the reduction in rate was very marked (Fig.6.24).

Reservoir level. Each reduction in reservoir level was accompanied by an increase in the rate of microbubble liberation (Table 6.2) and an increase in the liberation of larger bubbles (Fig.6.25). When the reservoir level reached approximately 20 mm the arterial line filter was introduced into the circuit. A marked reduction in the liberation of microbubbles greater than 80 μm diameter was noted immediately. The reservoir level continued to fall towards zero but the rate of liberation of microbubbles less than 50 μm diameter was reduced to a level below that initially observed for a reservoir depth of 170 mm without a filter in the arterial line (Fig.6.25).

At zero reservoir level, the flexible reservoir walls became appressed and further suction by the roller pump produced cavitation in the pump insert and the release of large numbers of microbubbles (Fig.6.26) With the filter in the arterial line the microbubbles entering the systemic circulation under these conditions were predominantly confined to the < 50 μm diameter range.

Temperature. The results of the experiments performed to assess the effect of increasing temperature merely indicated that the rate of liberation of microbubbles either increased or remained steady following a rapid increase in circuit temperature (Fig.6.27). They also suggested a tendency towards the release of microbubbles larger in size than those

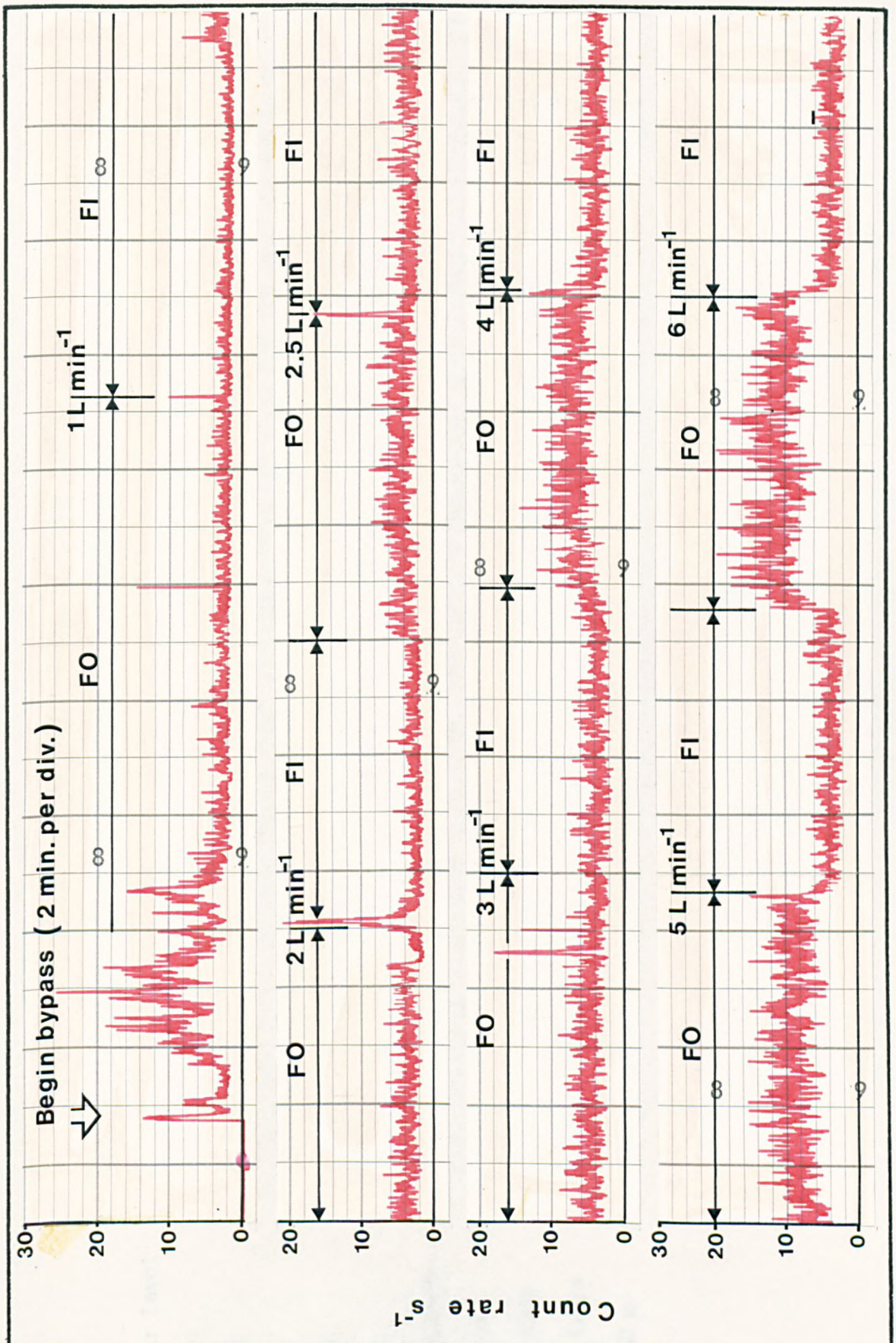

Filter Response
Blood Flow Rate 1L min^{-1}
Oxygen Flow Rate 1 - 6L min^{-1}

Fig. 6.24
Referred to on P.256

Table 6.2

Microbubble Liberation Rate at various Reservoir Levels

during extracorporeal circulation in dogs (microbubbles ml^{-1}. min^{-1}.)

Reservoir Level	Filter out									Filter in
(mm)	170	160	150	140	130	120	110	100	<100	< 100
$\bar{x}$	17.64	18.84	24.84	26.4	36	39.96	45.6	47.16	48.84	12.84
σ	3.84	4.2	9.36	9.6	15	6.96	8.64	8.04	7.68	12.36
SE	2.16	2.4	5.4	5.52	8.64	3.96	5.07	4.68	4.44	7.08
Bubble diameter										
< 50µm	17.04	18.41	23.88	25.44	33.24	30.96	32.28	24.97	15.91	12.79
50 - 80µm	0.11	0.14	0.3	0.28	0.58	1.61	3.04	2.72	2.42	0.03
80 - 110µm	0.24	0.26	0.55	0.58	2.08	5.52	6.78	10.37	14.54	0.01
> 230 m	0.07	0.04	0.1	0.06	0.12	1.9	3.48	9.10	15.91	0.008

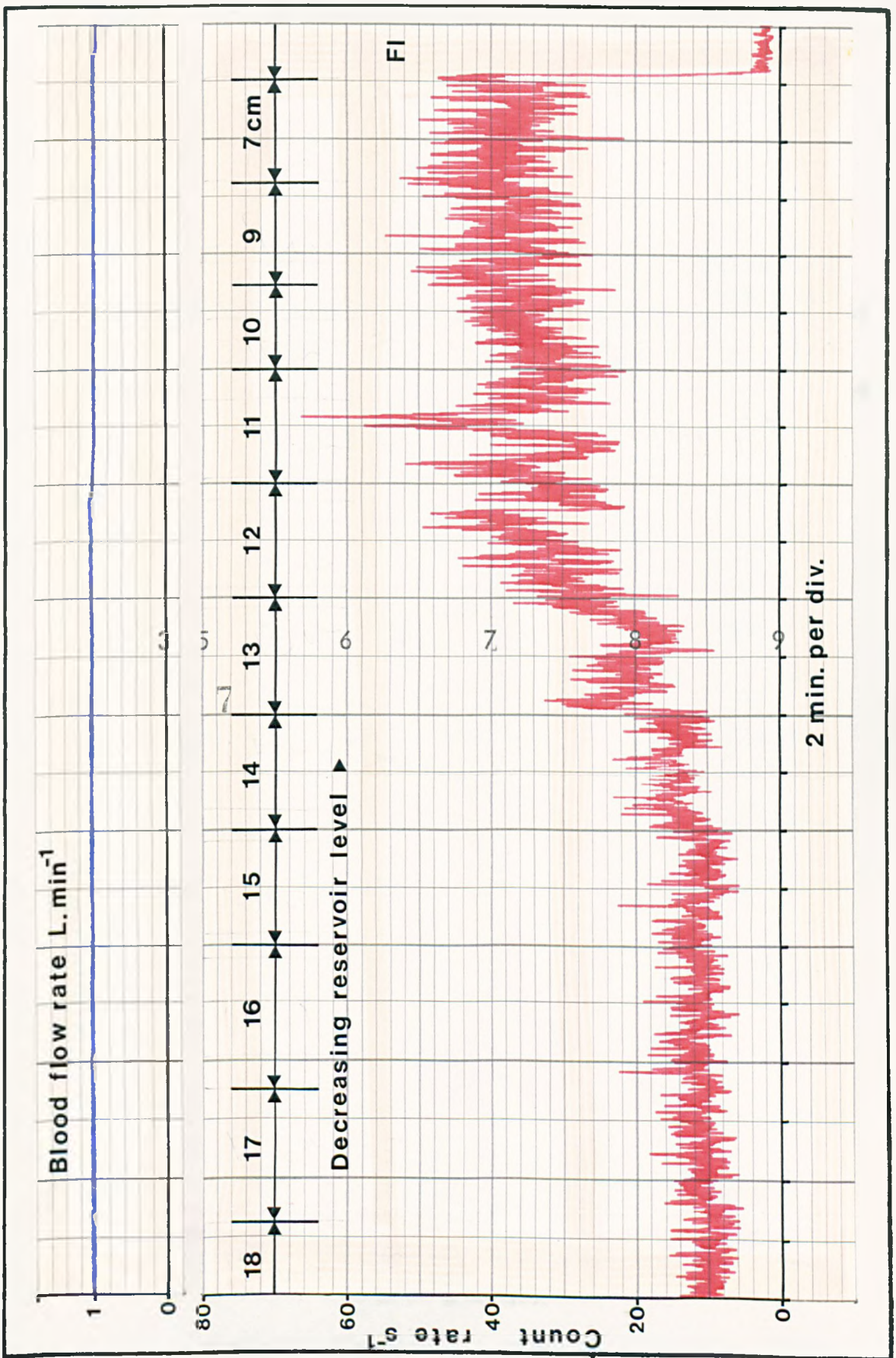

Reservoir Level - Microbubble Count Rate Recording

FI : Filter In

Fig. 6.25

Referred to on P.258

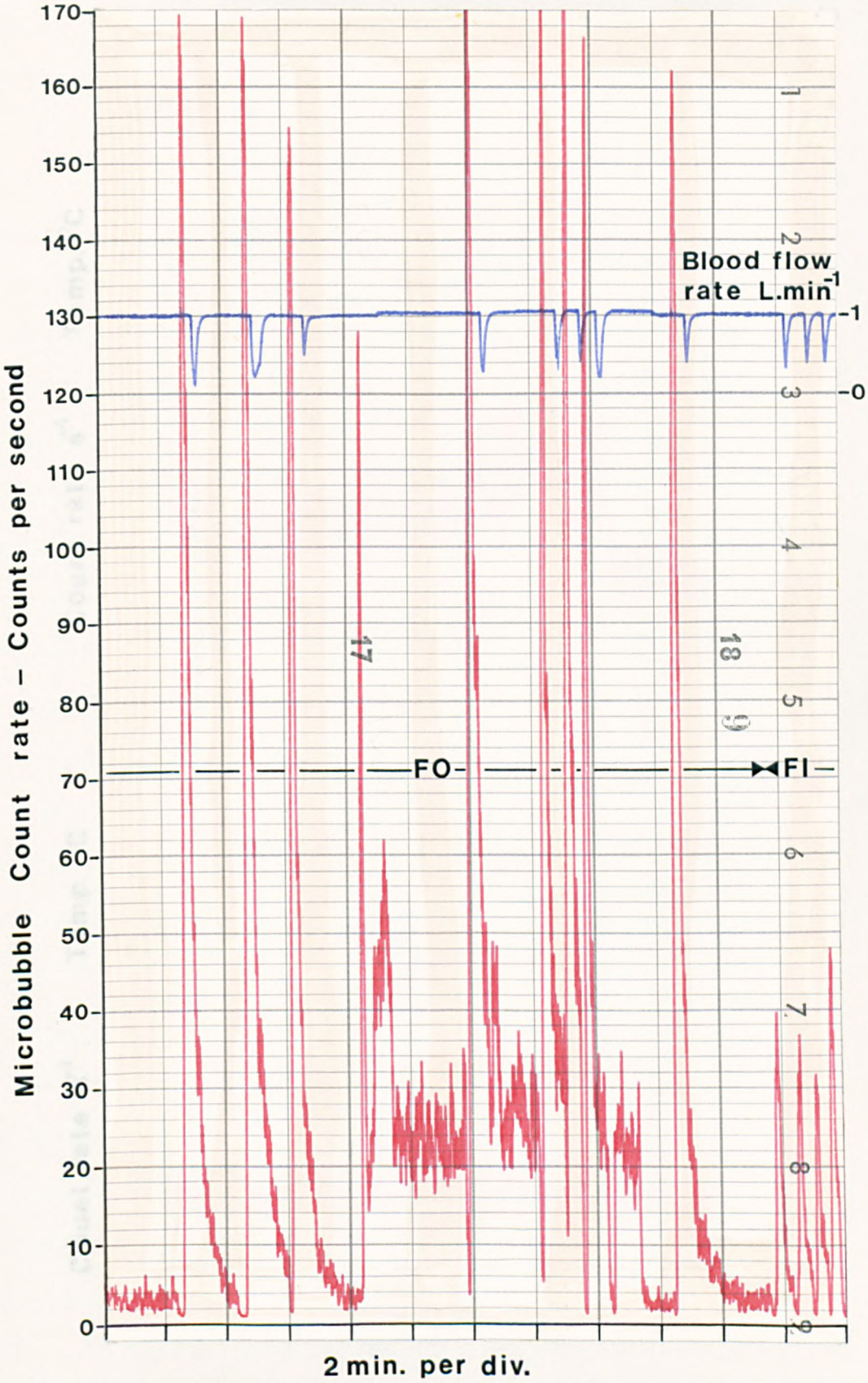

Microbubble Liberation as a Result of Cavitation

FO : Filter out
FI : Filter in

Fig. 6.26

Referred to on P.258

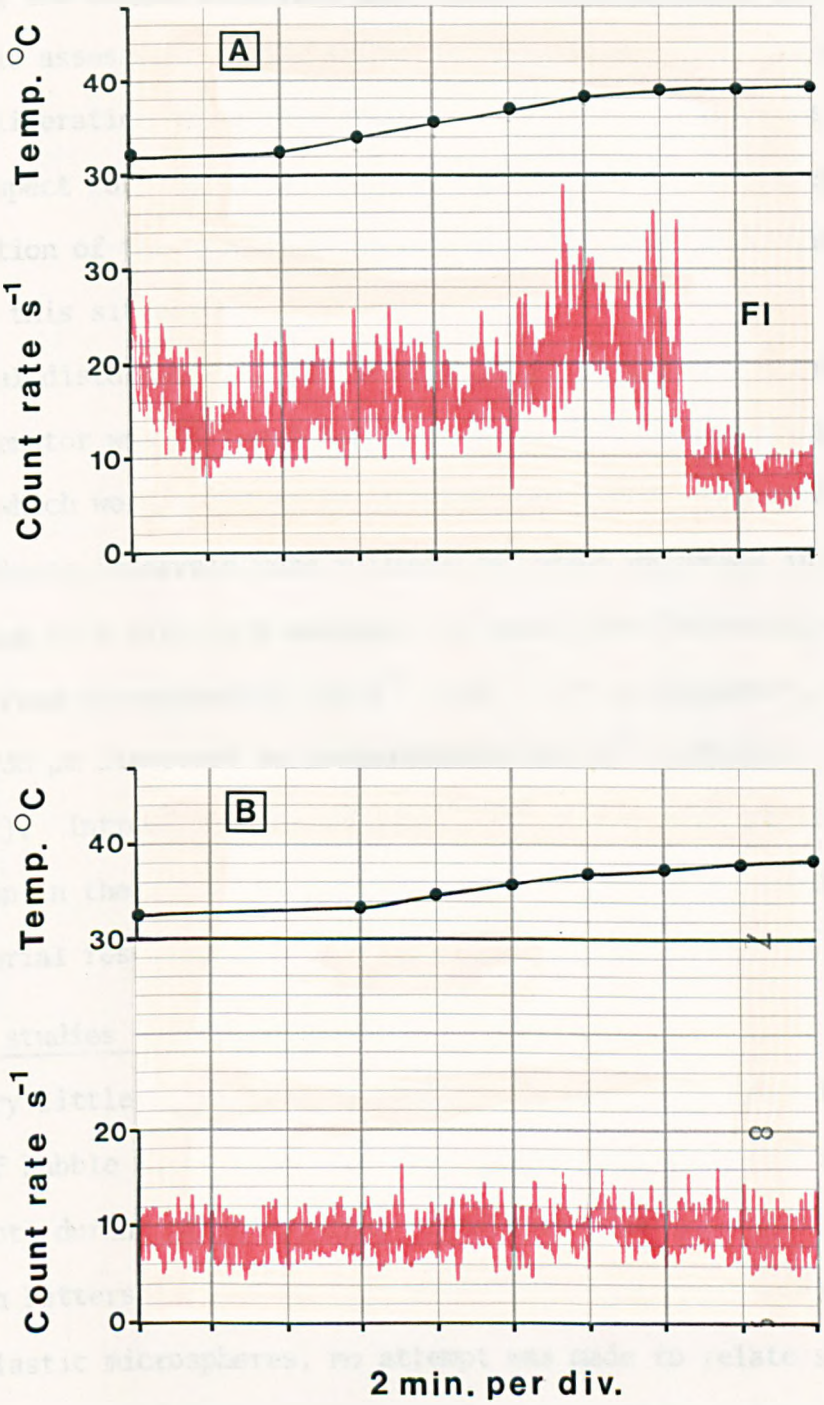

Temperature Effects
Blood Flow Rate 1L min^{-1}
FI : Filter In

Fig. 6.27
Referred to on P.258

present within the pre-warming population.

Difficulties were encountered in maintaining a constant rate of temperature increase, which together with differences in conditions following the oxygen flow rate and filter investigations precluded any reasonable assessment of the effect of temperature increase upon the rate of liberation of microbubbles. Moreover the criticisms presented in retrospect for the in vitro temperature studies, with respect to the position of the transducer relative to the heat exchanger, also apply to this situation.

Mechanical disturbance. Briefly massaging the arterial reservoir of the oxygenator was followed by the release of a shower of microbubbles, most of which were $\geq$ 230 μm in diameter (Fig 6.28). Repeated massage at 2-3 minute intervals were followed by rapid increases in microbubble liberation rate with each massage, the peak rate decreasing with successive massage from approximately 200 s^{-1} (590 230 μm diameter), to 150 s^{-1} (275 230 μm diameter) to approximately 105 s^{-1} (138-205 230 μm diameter). Introducing the arterial line filter produced a marked reduction in the number of microbubbles detected as a result of massaging the arterial reservoir.

In vivo studies - discussion

Very little definitive information is available concerning the range of bubble sizes liberated from oxygenators and other circuit components during extracorporeal circulation for open-heart surgery. Although Patterson et al (1972) calibrated their microbubble detector using plastic microspheres, no attempt was made to relate signal amplitude to bubble size or to provide a quantitative analysis of bubble populations arising during extracorporeal circulation. On the basis of compressibility and density the detection of 50 μm diameter soft plastic spheres would indicate that their instrument was capable of detecting microbubbles of approximately 5 μm diameter (Lubbers et al., 1974).

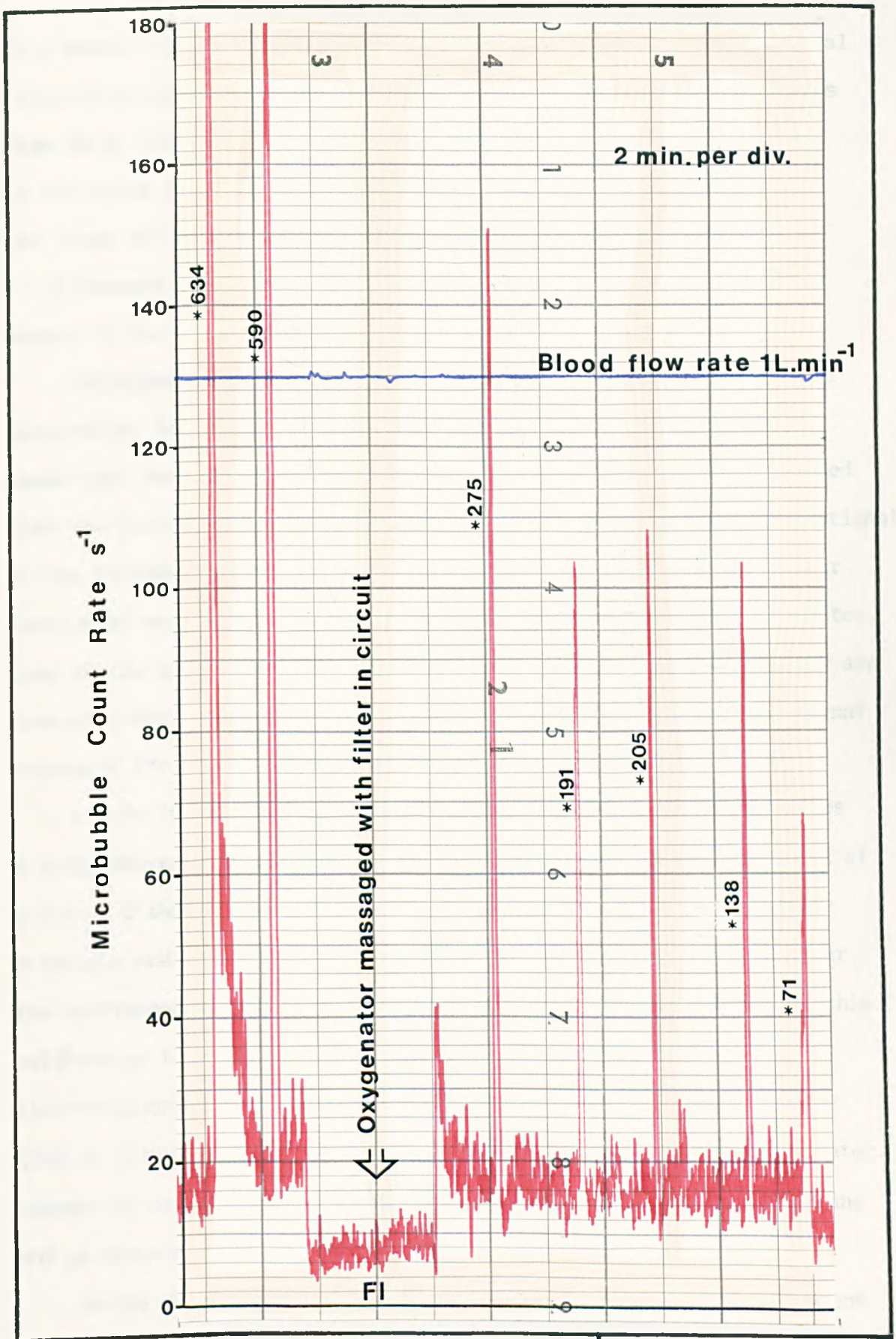

Microbubble Liberation Due to Oxygenator Massage

FI : Filter In
* Microbubbles > 230 µm diameter

Fig. 6.28

Referred to on P.264

This would suggest that the bubbles detected during the extracorporeal circulation experiments performed by Patterson et al (1972) were less than 20 μm diameter. However, the limitations of the technique used by Patterson et al (1972), as discussed in chapter 2 , indicate that the sizes of bubbles could be under-estimated because of the scatter of ultrasound within the region between the transducer and the gated region of the blood volume.

Gallagher & Pearson (1973), in attempting to present a figure of sensitivity for their own instrument, made an incorrect assumption based upon data presented by Patterson & Kessler (1969). They assumed that the sensitivity of the ultrasonic technique was directly proportional to the frequency of the source of ultrasound and concluded that their instrument was capable of detecting emboli greater than 125 μm diameter. Even if the techniques and instrumentation were the same, which they are certainly not, there would be no appreciable differences between signal responses for microbubbles greater than 10 μm diameter.

A more justifiable approach to the determination of bubble sizes arising during extracorporeal circulation was reported by Lubbers et al (1974). Although the technique they used was based upon the Doppler principle and as such subject to the limitations discussed in Chapter 2 the instrument was calibrated using microbubbles. On the basis of this calibration they have concluded that the predominant bubble sizes liberated during extracorporeal circulation (incorporating a Bentley Q100 or Q110 bubble oxygenator) were within the range 60-90 μm diameter. Lubbers et al (1974) also noted the occasional detection of 300 μm and 800 μm diameter bubbles, particularly at the beginning of bypass.

As far as it is possible to compare bubble sources from different oxygenators the predominant size range established for these experiments (20 μm-80 μm diameter) are similar to those detected by Lubbers et al (1974). The measured rates of liberation, on the other hand were

markedly different, those of Lubbers et al (1974) being as much as a factor of 10 lower. However it is asserted on the basis of the discussion presented in chapter 2 on the limitations of continuous wave techniques that such techniques are inherently less capable of counting and for determining the rate of microbubble liberation than pulsed ultrasound techniques.

Oxygen flow rate. Increased liberation of microbubbles, associated with high oxygen flow rate has been observed on a number of occasions (Maloney et al., 1958; Tepper et al., 1958; Landew et al., 1960; Patterson & Kessler, 1969; Fisk et al., 1972; Gallagher & Pearson, 1973; Patterson, Rosenfeld & Porro, 1976). In addition to supporting these observations, the results of the in vivo experiments have indicated the quantitative significance of such increases. A predominance of bubbles < 50 μm in diameter was characteristic under the conditions considered, together with an increase in the rate of microbubble liberation and a trend towards the release of larger bubbles (50-80 μm diameter) with increasing oxygen flow rate. Not surprisingly, oxygen flow rate has been considered as a principal determinant of the quantity of microbubbles released during extracorporeal circulation.

Lubbers et al (1974) claimed that the number of small bubbles (60-90 μm diameter) liberated during extracorporeal circulation was mainly determined by oxygen tension (PO_2) and blood flow rate. Ostensibly, it appears to be at variance with the statement made above. In actual fact it is not since it specifically refers to the size as the point of issue and in consequence only specifies the agents that moderate or exacerbate a source of bubbles and not the agents, such as oxygen flow rate and cardiotomy suction that determine the initial bubble population. However, it is misleading in that it suggests that oxygen tension is the most important parameter in the moderator mechanism to which it relates, the rate at which microbubbles dissolve.

In the discussion presented in chapter 1 , it was suggested that the degree of saturation is the important parameter in determining bubble dissolution time and not gas tension. Gas tension is a direct consequence of solubility and the concentration of gas in solution. Oxygen tension is also related to the saturation of haemoglobin by its influence upon the haemoglobin dissociation curve, but it is not the only influential factor. Carbon dioxide tension, temperature and pH also influence the degree of saturation.

The basis that Lubbers et al (1974) used for claiming that oxygen tension was a principal determinant factor in the release of microbubbles was the correlation (which appears to have been a loose use of the term rather than a statement based upon statistical analysis) that they observed between oxygen tension and microbubble liberation rate. A similar relationship was suggested by the results of the in vivo experiments reported in this chapter. It was noted that a general increase in microbubble liberation rate was accompanied by a general increase in oxygen tension (Figs.6.11 to 6.22)Because of the small number of experiments in the series, an estimate of statistical correlation was not attempted. A positive correlation, statistical or not, would not prove a cause and effect relationship and a failure to establish a statistical correlation would not have proved the absence of one. The misuse of correlation in this way obscures the fact that oxygen tension is a moderator and not a direct determinant of the microbubble source.

Gas tension within the blood during extracorporeal circulation is dependent upon the dynamic relationships that exist between the gas phases introduced into the blood, the degree of saturation, the blood flow rate, and the gas phases being removed from solution. Consequently oxygen tension may be considered to be primarily dependent upon the oxygen flow rate and the dissolution of microbubbles. In view of this assertion

it is possible to appreciate the distinction between oxygen flow rate as a deterministic factor, and oxygen tension, or more correctly oxygen saturation, as a moderating factor in the liberation of microbubbles.

Blood flow rate. The same distinction between moderator and determinant functions must also be applied to blood flow rate. By determining the settling time for the blood within the arterial reservoir, the blood-flow rate is moderating the microbubble population by influencing the time available for the microbubbles to dissolve. Unfortunately, because of the restrictions imposed by the perfusion, it was not possible to investigate the significance of blood flow per se during the in vivo experiments. However the results of the in vitro experiments suggested that blood flow rate could be a significant moderator of microbubble numbers.

Filter response. The in vivo experiments have revealed some interesting results on filter response. On the basis of these results it would appear that the filter response is dependent upon the relative proportions of microbubbles within the various size ranges. Thus the filter was more effective under conditions, such as low reservoir level and high oxygen flow rate, for which the bubbles released were > 50 μm diameter.

The increase in liberation rate that was observed on occasions suggests a bubble fission mechanism of the type proposed by Hills (1974) based upon the presence of surfactant agents within the plasma. The release of larger bubbles was suggested by Lubbers et al (1974) to be due to inadequate purging of the filter before use.

Although filters have been strongly recommended for the removal of particulate matter (Swank & Hissen, 1965; Hill et al., 1970; Tufo et al., 1970; Osborn et al., 1970; Brennan et al., 1971; Patterson, Kessler & Bergland, 1971; Patterson & Twichell, 1971; Ashmore et al., 1972; Egeblad et al., 1972; Dutton et al., 1973; Patterson, Wasser & Porro, 1974; Connel, 1975) and microbubbles (Spencer et al., 1965; Patterson &

Kessler, 1969; Kessler & Patterson, 1970; Lichti, Simmons & Almond, 1972) the case for recommending micropore filtration for the removal of microbubbles is less emphatic. This is undoubtedly due in part to the lack of adequate discrimination between particulate and gaseous matter detected in these studies. Bartlett & Gazzaniga (1976), in a short review of neurological damage during extracorporeal circulation for open heart surgery suggested that brain damage was due to microbubble embolism and that arterial line filters should be used with bubble oxygenators for the purpose of trapping microbubbles. On the other hand Lubbers et al (1974) suggested that the use of arterial line filters for the removal of microbubbles is unwarranted. The basis for this suggestion was the observation that the predominant bubble sizes encountered in their experiments were comparable with the pore size of the filters they used (30 μm pore size). For similar conditions, the results presented in this chapter for the in vivo experiments support the conclusion of Lubbers et al (1974), particularly for instances in which the liberation rate was observed to increase. However for the conditions in which larger bubbles were released and effectively removed, the use of an arterial line filter would appear to be justified. Indeed for the conditions of high oxygen flow rate and very low reservoir level the use of an arterial line filter appeared to be particularly beneficial, the microbubble liberation rate being less than that observed using a high reservoir level with or without a filter. Furthermore the use of an arterial line filter would appear to offer some degree of protection should the arterial reservoir of the oxygenator empty completely. Although the microbubble population is dependent upon the prevailing conditions, these conditions cannot be measured with sufficient accuracy and speed to enable the size and number of bubbles to be predicted.

Reservoir level. Reduction in the volume of blood within the arterial reservoir of a bubble oxygenator, with a consequent reduction in the

fluid level has been generally considered to result in the liberation of large numbers of microbubbles (Patterson & Kessler, 1969; Kessler & Patterson, 1970; Fisk et al., 1972; Gallagher & Pearson, 1973; Patterson, Rosenfeld & Porro, 1976). The results of the in vivo experiments support this assertion, but there was also a trend towards the release of larger bubbles (Table 6.2). The increase in rate was attributed to reduced settling time and the inclusion of additional undissolved gas by turbulence within the reservoir. The trend towards the release of larger bubbles was attributed to increased turbulence and in particular the cascade of fluid from the defoaming section into the arterial reservoir.

In view of the increased rate of microbubble liberation with decreasing reservoir level it has been generally recommended that the reservoir level should be maintained at a high level. However, on the basis of these experiments, low level operation with an arterial line filter could result in lower liberation rates and bubble sizes than those observed with high level reservoir operation. Further investigations are necessary to establish the effectiveness of such a regime over prolonged periods of time. Its value, should it be found to be consistent, might be more important in the design of new bubble oxygenators than in the attempt to improve techniques of using conventional bubble oxygenators. Low level operation increases the risk of complete reservoir depletion following a sudden reduction in the venous return to the oxygenator and it is not to be recommended for general use.

Temperature. The same observations and criticisms that were presented for the in vitro experiments also apply to the results of the in vivo temperature investigations.

Mechanical disturbance. The dislodgement of microbubbles by mechanical disturbance of the arterial reservoir of a bubble oxygenator has been previously observed (Patterson & Kessler, 1969; Gallagher & Pearson, 1973). The results of the in vivo experiments support these reports

and indicate, in addition, that the bubbles released are notably larger than those within the population prevailing before massage. By incorporating a micropore filter within the arterial line, the carry through of these large bubbles was prevented.

Whilst it is prudent to avoid unnecessary disturbance of the arterial reservoir during bypass, accidental disturbance or the excessive build up of bubbles and subsequent sudden release cannot be disregarded. An arterial line filter would therefore offer some degree of protection against such eventualities.

Instrumentational limitations. From the realisation of the practical limits on discriminator sensitivity, three particular points of importance have emerged. Firstly there is a need for more decisive tests for evaluating the discriminator under conditions to be expected in practise. The use of rectangular pulses for the functional evaluation of the discriminator was clearly unrepresentative of the practical situation. However the static tests using microbubbles to evaluate the detector provided little indication of the problem, partly because of the multiple counts per bubble as a result of fixed rate pulsing, partly because of the wide initial channel settings on the discriminator and partly because of the unexpectedly small predominant bubble sizes encountered in the practical situations considered, requiring lower discriminator settings.

Secondly, the value of an alternative device or procedure as a check upon the effectiveness of a new system has become apparent. Had the oscilloscope display and the rate recorder not been included in the system, the limitations described might have remained unrecognised. Thirdly, results obtained with other microbubble detection techniques in which a single discriminator is used to size irregular shaped pulses are subject to the same potential errors.

As a short term solution to the problem, the discriminator may be

operated with broader channel settings. However the need for a more responsive instrument may be satisfied by using two discriminators with their channel settings interleaved so that a signal that is missed in the appropriate channel of one discriminator will appear well within the corresponding channel of the second and so be detected. Unfortunately such a system would require scaling of the totalised counts and would be subject to error due to signals being detected in both discriminators. Alternatively, the received signals may be shaped into rectangular pulses using high speed Schmitt triggers in order to present well defined pulses to the discriminator. Even so, it would probably be more accurate to use two discriminators with slightly different channel settings.

Because of the predominance of small bubbles (< 50 μm diameter) in both the in vitro and in vivo experiments, discrimination may be improved by further amplification of the received signals. However, to effectively accommodate the range of bubble sizes found in these experiments it would be necessary to have two amplification systems, high gain for small bubbles (< 50 μm diameter) and low gain for large bubbles (> 50 μm diameter).

Cardiotomy suction experiments

Whilst it was not possible to include an investigation of cardiotomy suction in the in vivo experiments an opportunity was presented for an in vitro investigation of microbubble liberation during suction as part of a series of tests to compare cardiotomy reservoirs.

Materials and methods

Two independent circuits were constructed as illustrated in Fig.6.29A. Each circuit consisted of a cardiotomy reservoir with its outlet port positioned 300 mm ± 5 mm above the head of a Sarns roller pump and connected to it by 9.6 mm internal diameter P.V.C. tubing. A blood

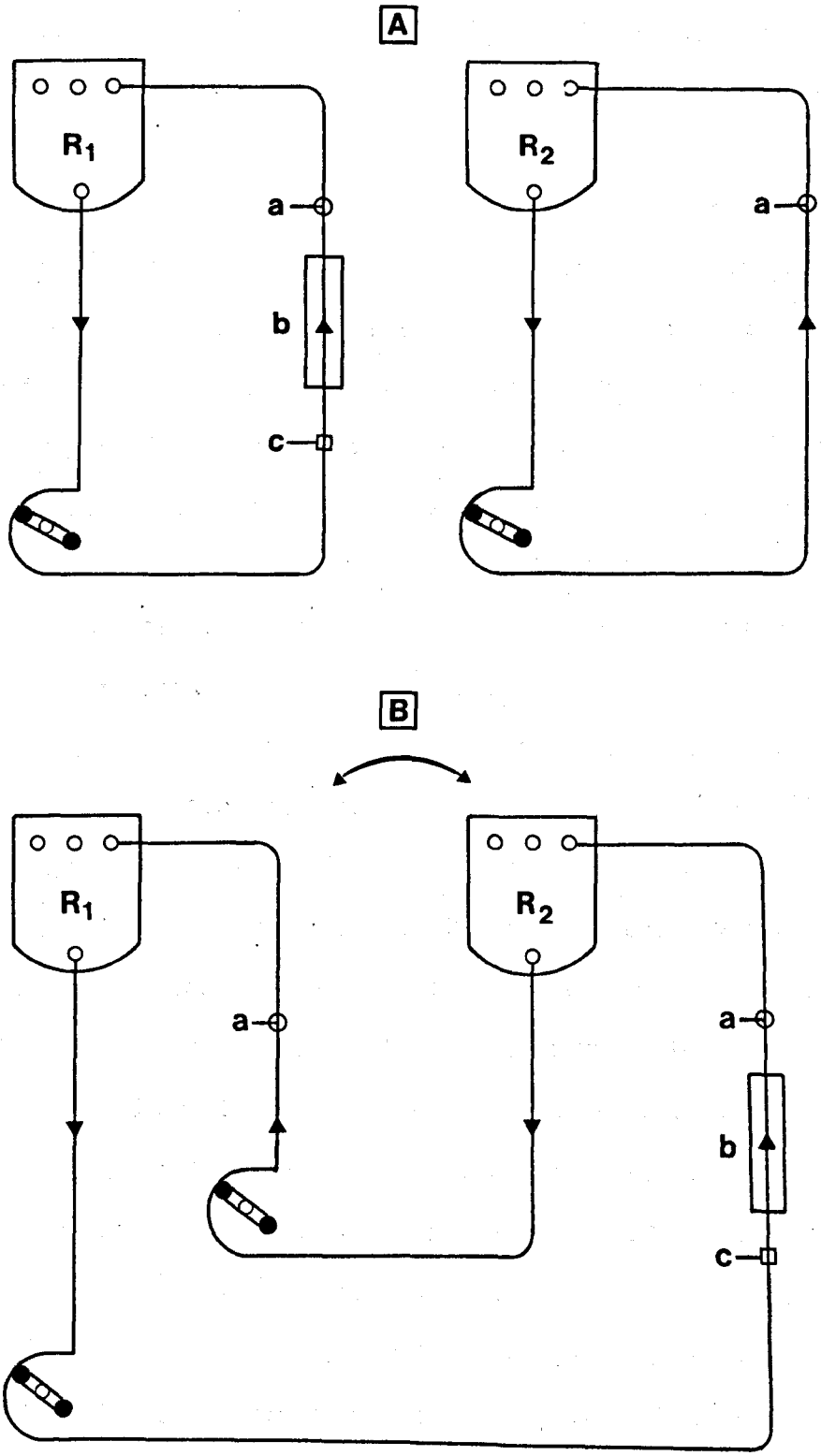

Cardiotomy Suction Circuits
A Cellular Damage Investigation
B Reservoir Bubble Performance Test
a: Sample Port b: Bubble Dector c: Flow Probe
P Pump R_1 & R_2 cardiotomy reservoirs

Fig. 6.29

Referred to on P. 273, 275

sampling port (9.6 mm internal diameter, stainless steel) and cannulating electromagnetic flow probe (Nycotron) was included within the line between the reservoir outlet and the pump. Microfiltered (Biotest mikrofiltrationsgerat, ME10B) heparinised two-day old dog blood (250 ml) was used to prime each circuit.

For the comparison of blood trauma, the circuits were operated independently at a flow rate of 1L.min^{-1} for 2 hours at room temperature (18^{o}C). The volume of blood in each reservoir was approximately 60 ml. During the series of tests a Polystan reservoir (new product incorporating a 40 μm pore diameter Dacron filter) was compared with both a Travenol 5M-03-91 flexible cardiotomy reservoir (120 μm pore diameter filter) and a Bromlus polycarbonate shell cardiotomy reservoir (45 μm pore diameter microfilter). Samples (5 ml) were taken at 30 minute intervals and measurements of screen filtration pressure (Swank et al., 1964) total haemoglobin concentration (cyanmethaemoglobin method), plasma haemoglobin concentration (benzidene technique), packed cell volume, erythrocyte, platelet and leucocyte counts were obtained.

For the investigation of microbubble liberation, the two circuits were interconnected (Fig.6.29B) and the ultrasonic transducer assembly was placed within the outlet line of the reservoir under test. The two pumps were started and the speeds increased together to a level corresponding to 1 L.min^{-1} (based upon Nycotron pre-test calibration curve). The speed of one pump was then increased in 0.2 L.min^{-1} steps at 10 minute intervals in order to pump 1 L.min^{-1} of blood together with 0-1 L.min^{-1} of air into the reservoir under test. During each set of tests the Polystan reservoir was tested twice to bracket a test run on the alternative reservoir. The microbubble liberation rate was recorded throughout the tests with hard copy records obtained using a Philips PM8221 pen recorder operating at 5 mm.min^{-1}. Microbubble size ranges and counts over 10 minute periods every 30 minutes

were also obtained.

Results

Screen filtration pressure and plasma haemoglobin concentrations for the series of tests are shown graphically in Fig.6.30. Packed cell volume and cell counts remained reasonably constant throughout the tests. The blood trauma was much less for the Polystan and Bromlus reservoirs than for the Travenol reservoir.

The relationships between air flow rate and microbubble liberation rate for each reservoir are shown in Fig.6.31. Rate recordings for the response of each reservoir to increases in air flow rate are shown in Figs.6.32 to 6.34. At each air flow rate, the rate of microbubble liberation remained reasonably constant. The sizes of the microbubbles released were predominantly within the range 20-80 μm diameter (98%), the remaining 2% being > 230 μm diameter. No intermediate sizes were detected and the same distribution was observed for all of the reservoirs tested. Abrupt increases in the microbubble liberation rate upon commencing the combined flow of blood and air through the reservoir under test was particularly apparent for the Travenol and Bromlus reservoirs (Figs.6.32& 6.33)whilst a slight decrease was evident for the Polystan reservoirs (Fig 6.34).

Discussion

Cardiotomy suction has been considered to be a serious source of microbubbles during extracorporeal circulation (Miller & Allbritten, 1960; Baird & Mujagishima, 1964; Spencer et al., 1965; Spencer et al., 1969; Gallagher & Pearson, 1973). However Lawrence, McKay & Sherensky (1971) suggested that cardiotomy suction systems incorporating an in-line filter reduce the liberation of microbubbles to insignificant levels. Such a statement pre-supposes a knowledge of the quantity of microbubbles released and the quantitative significance of microbubbles in relation to embolic damage. Since the latter has never been directly

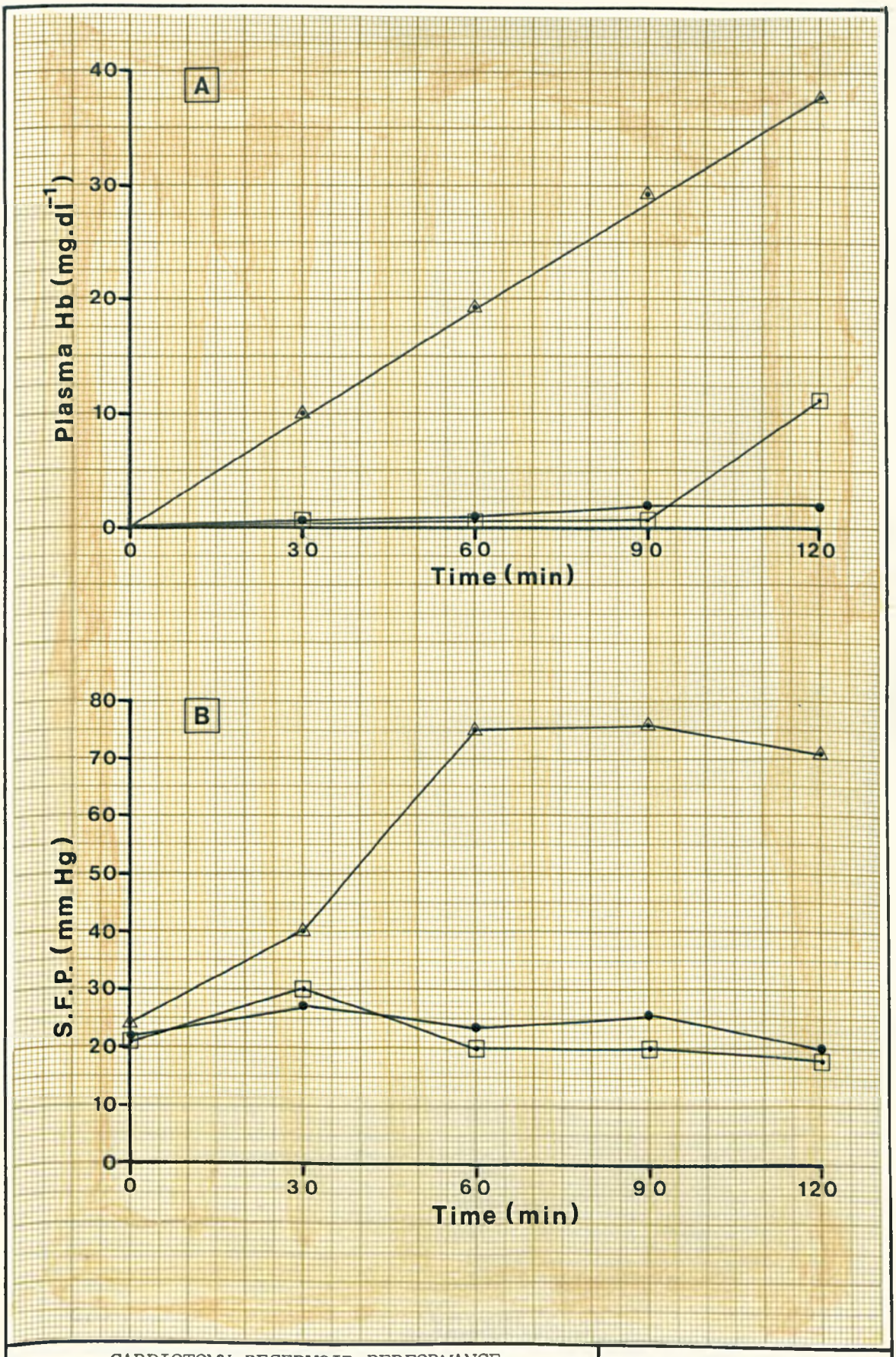

CARDIOTOMY RESERVOIR PERFORMANCE

△ TRAVENOL
• POLYSTAN
⊡ BROMLUS

A HEMOLYSIS

B CELLULAR AGGREGATION

Fig. 6.30

Referred to on P.276

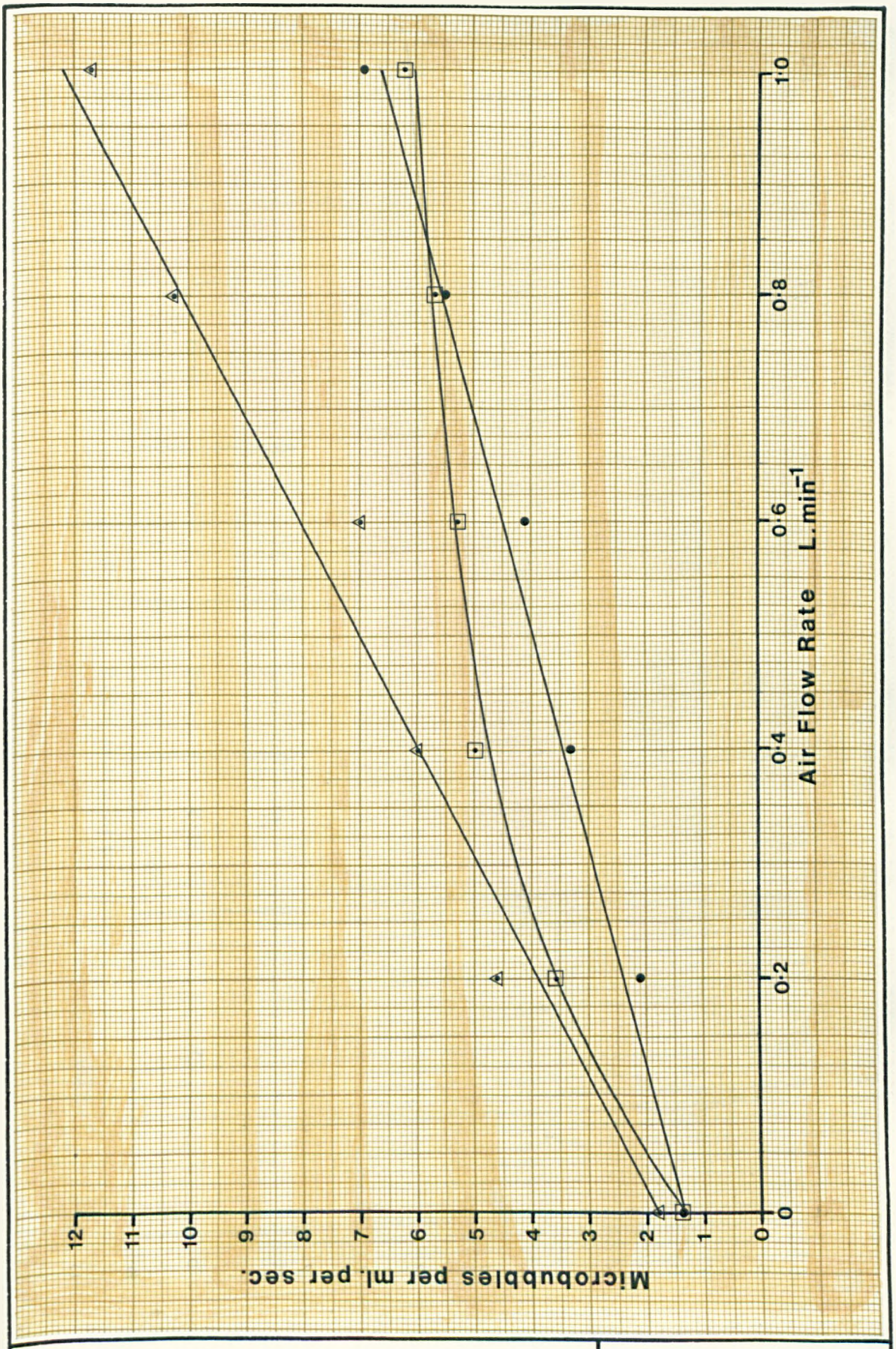

MICROBUBBLE LIBERATION RATE

△ TRAVENOL

● POLYSTAN

⊡ BROMLUS

Fig. 6.31

Referred to on P.276

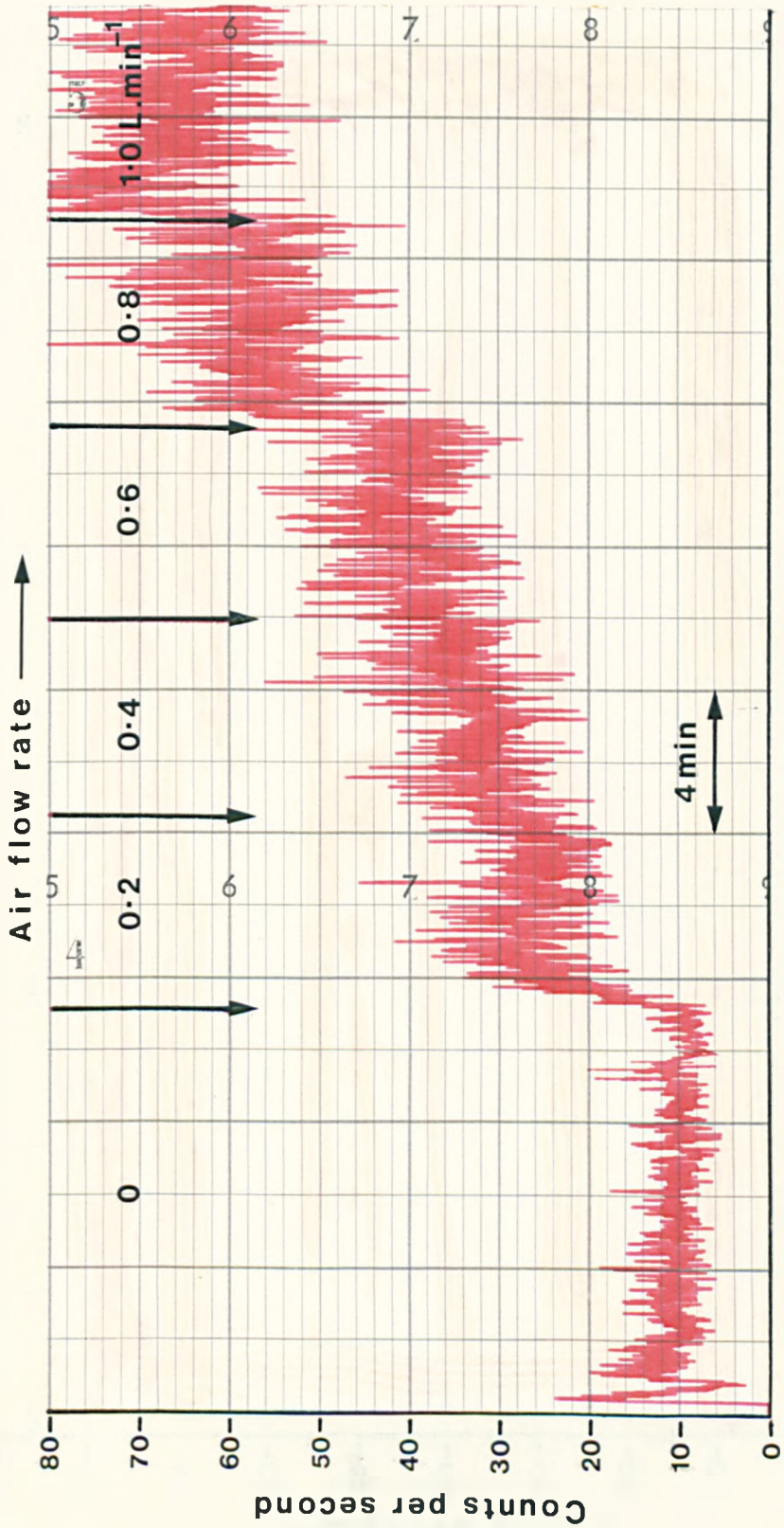

TRAVENOL CARDIOTOMY RESERVOIR

Fig. 6.32

Referred to on P.276

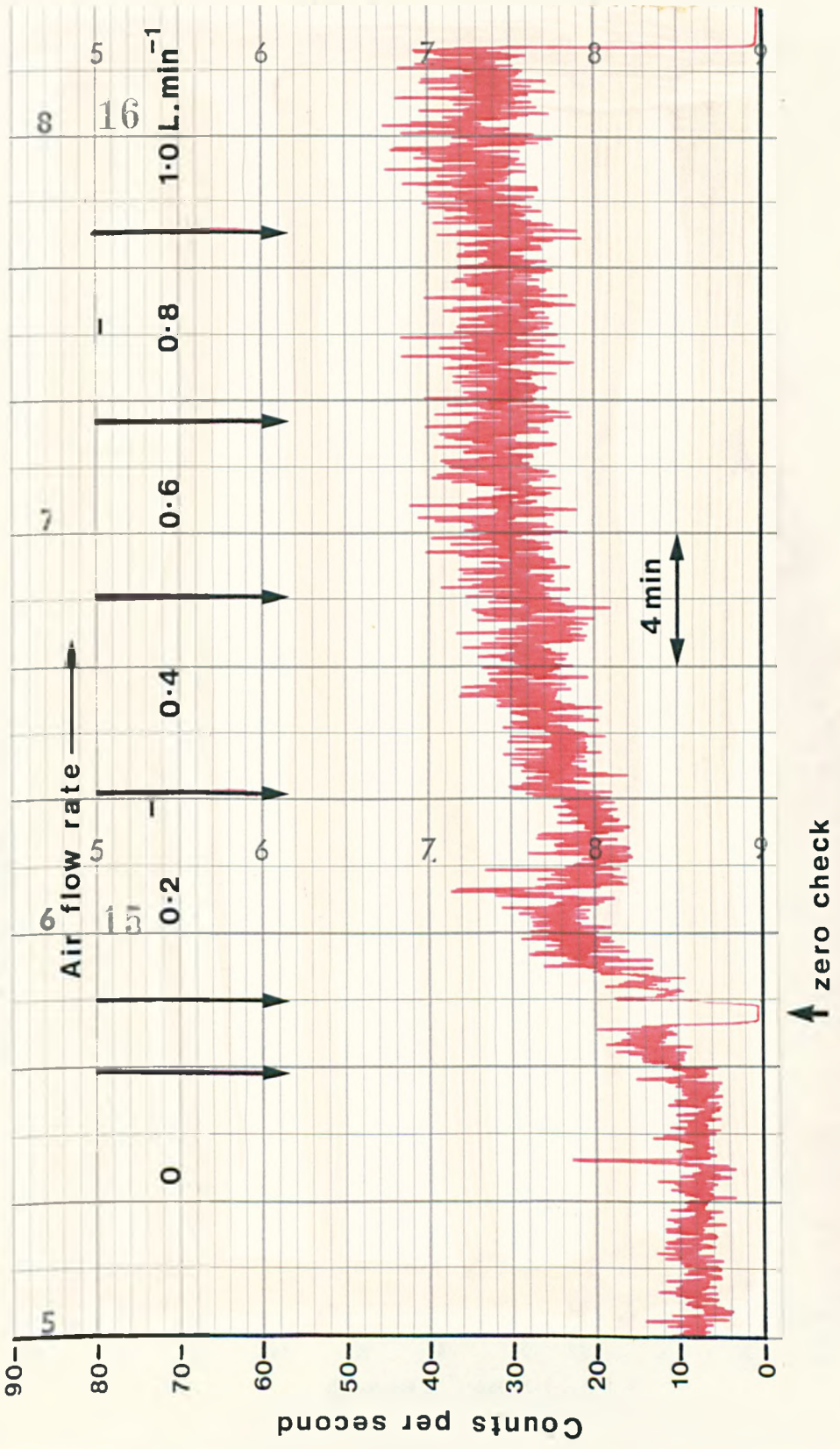

BROMLUS CARDIOTOMY RESERVOIR

Fig. 6.33

Referred to on P.276

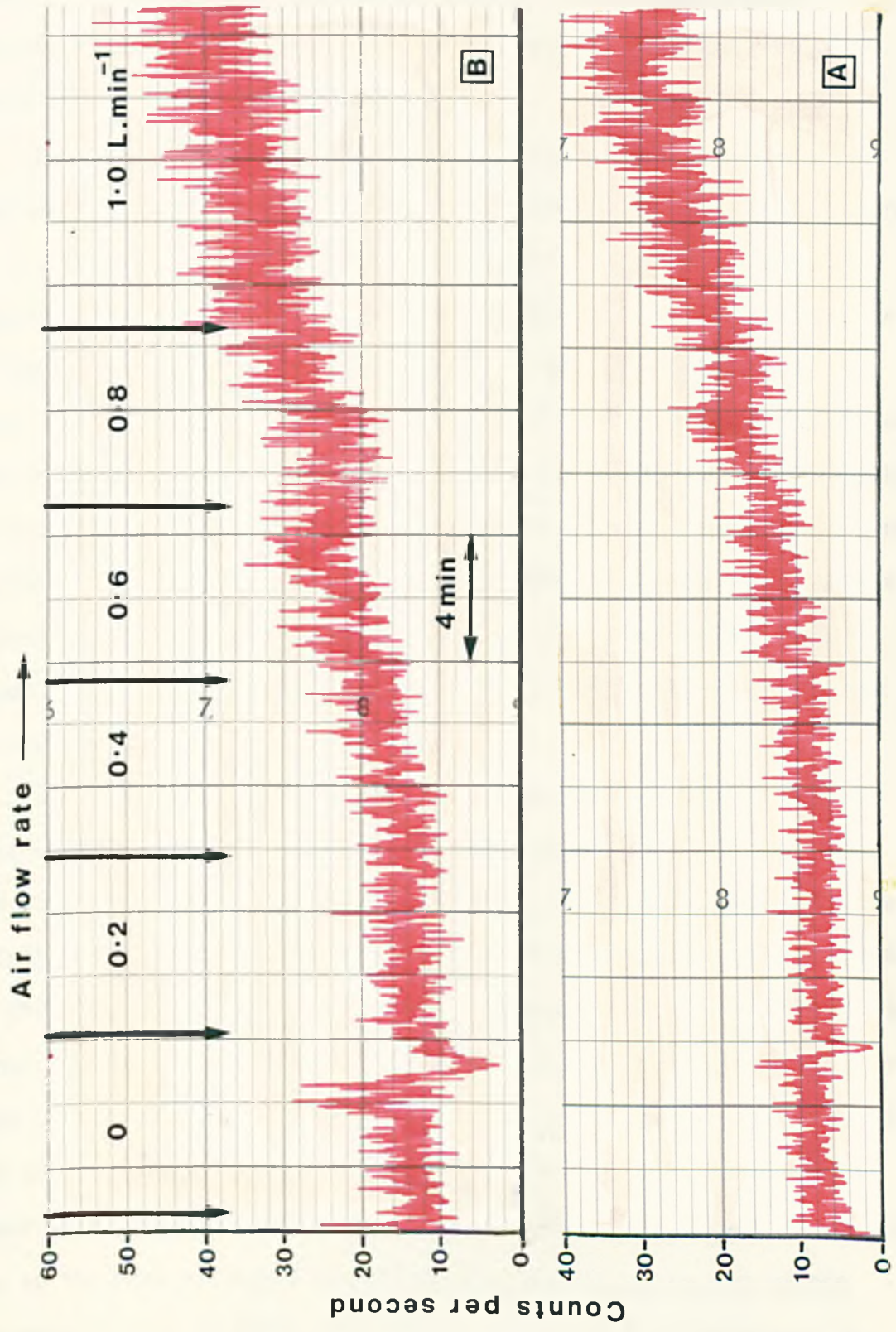

POLYSTAN CARDIOTOMY RESERVOIR

A BEFORE TRAVENOL TEST

B FOLLOWING TRAVENOL TEST

Fig. 6.34

Referred to on P.276

demonstrated either clinically or experimentally, and since the technique used by Lawrence, McKay & Sherensky (1971) for the detection of microbubbles was qualitative rather than quantitative, there is no basis for accepting their conclusion.

The results of these experiments tend to support the view that cardiotomy suction, even using cardiotomy reservoirs with in-line filters, is a potentially large source of microbubbles. However, it must be appreciated that the results obtained in these in vitro studies relate to the initial source of microbubbles. During a clinical bypass procedure the cardiotomy suction is returned to the venous reservoir of the oxygenator. Consequently the suction line population of microbubbles is then subjected to the influence of bubble sinks and moderating agents within the oxygenator, such as defoaming material, coarse mesh filters within the separate compartments, and the circuit conditions that determine the time available for bubbles to rise to the blood surface or dissolve.

The comparisons between the three reservoirs considered indicate that blood trauma, characterised by plasma haemoglobin concentration and screen filtration pressure measurements was about the same for the Polystan and Bromlus reservoirs, but much less than the trauma produced by the Travenol reservoir. The late increase in the plasma haemoglobin concentration for the Bromlus reservoir appeared to be due to slightly more blood flow turbulence towards the end of the test. The relatively low screen filtration pressure values for the Polystan and Bromlus reservoirs compared with those for the Travenol reservoir were probably due to the more efficient filtration of cellular aggregates within the microfilters of these reservoirs. Similarly the differences in pore size may also account for the lower liberation rates of microbubbles for the Polystan and Bromlus reservoirs.

The small pore size of the Polystan filter mesh did not appear to

offer any serious disadvantage, although a small amount of blood pooling was observed within the filter sock after about 4 hours of pumping. This was attributed to loss of patency of some of the pores due to the retention of cellular aggregates.

In view of the small number of reservoirs tested (4) the results obtained can only be considered to be preliminary. However the procedure adopted and the tests performed would appear to provide a useful method for comparing cardiotomy reservoirs.

Whilst the results obtained in these experiments cannot be quantitatively related to those expected during cardiopulmonary bypass on human patients, they do demonstrate the existence of primary sources of microbubbles, the value of in-line filtration as a sink and the quantitative effect of various modifying agents. The results also suggest ways of using the microbubble detector in the future, for example in the comparison of the performance of circuit components such as cardiotomy reservoirs.

Chapter 7

GENERAL DISCUSSION

The advent of cardiopulmonary bypass secured for open heart surgery an increase in available operating time that had hitherto been denied even by the use of profound hypothermia. As a result, the range of corrective procedures has been extended and improved. However the expedient of temporarily replacing the function of the heart and lungs by an artificial pump oxygenator has not been without complications. Not the least of these has been the incidence of post operative neurological complications ranging from slight psychological disturbances to gross cerebral damage characterised by excessive mental derangement and/or paralysis (Ehrenhaft & Claman, 1961; Blachy & Starr, 1964; Gilman, 1965; Sachdev, 1967; Hill et al., 1969; Javid et al., 1969; Tufo, Ostfeld,& Skekelle, 1970; Lee et al., 1971; Branthwaite, 1972; Frank et al., 1972; Branthwaite, 1973; Aberg, 1974; Branthwaite, 1975; Aberg, 1976; Matts, 1976).

Wright (1971), having reviewed the available reports of neurological damage following cardiopulmonary bypass concluded that two principal groups of neurological and psychiatric complications could be distinguished. One group was characterised by slow recovery from anaesthesia with somnolence and affective disorders persisting for only a few days. The prognosis for this group was generally considered to be good, with no persistent symptoms being discernible after three months. The second group was characterised by localised motor defects, often with attendant affective states such as severe depression. Loss of memory for specific items, reduced facility for mental arithmetic, and loss of muscular co-ordination could also be symptomatic of this group. The characteristics of the first group are reminiscent of generalised cerebral depression whilst the second group is more representative of localised cerebrovascular accidents such as arteriolar

embolism.

Incidence of neurological disorders

The incidence of these disturbances has fallen appreciably in recent years. In a prospective study of 100 cases following cardio-pulmonary bypass, Tufo et al (1970) reported a 44% incidence in neurological abnormalities early after recovery from anaesthesia. Lee et al (1971) reported a 23% incidence of neurological deficit, 14% incidence of psychiatric complications, and an overall incidence of central nervous system disturbance of 31%. Branthwaite (1972) reporting upon a retrospective study of 417 cases following open heart surgery quoted a 19.2% incidence of neurological injury characterised by impairment of consciousness, voluntary movement, or vision, in the first few days following surgery. Aberg (1974) reporting upon a study of 252 cases quoted a 15% incidence of cerebral complications. In a later study by Branthwaite (1975) based upon a patient population of 538 the incidence of cerebral damage was reported to be 7.4% and the incidence of neurological injury not attributable to any specific feature of the operative period was quoted to be 3.4% compared with 11.5% in the 1972 study. Although the incidence of neurological disturbance can now be considered to be quite low, the fact that there is still evidence to indicate the continued presence of neurological sequalae precludes any complacency in efforts to eliminate the causes.

Pathological indications of cerebral damage

Pathological evidence of cerebral damage attributed to extracorporeal circulation is generally characterised by diffuse nerve cell changes, focal lesions and cerebral haemorrhages (Wright, 1975). Diffue nerve cell changes which are typical of those associated with ischaemia, hypoxia or hypotension, have been attributed to the loss of blood flow pulsatility during extracorporeal circulation (Sanderson Wright & Sims, 1972) and to persistently low arterial blood pressure

during bypass (Javid et al., 1969; Tufo, Ostfeld & Shekelle, 1970).

Aetiology of cerebral damage

Focal lesions have been attributed to particulate matter in the form of fat (Miller at al., 1962; Caguin & Carter, 1963; Evans & Wellington, 1964; Hill et al., 1969; Danielson, Dubilier & Bryant, 1970; Aguilar, Gerbode & Hill, 1971) calcium salt deposits (Baglie & Hunter, 1959) antifoam (Cassie, Riddell & Yates, 1960; Smith, 1960; Bleifield, 1961; Lindberg et al., 1961; Thomassen et al., 1961), denatured protein (Lee et al., 1961) aggregated blood cells (Swank & Porter, 1963; Sachdev, Carter & Swank, 1967; Osbourn et al., 1970), undissolved gas in the form of microbubbles (Starr, 1960; Groves & Effler, 1964; Fishman, Carlsson & Roe, 1969; Patterson & Kessler, 1969; Patterson et al., 1972; Fisk et al., 1972; Gallagher & Pearson, 1973; Patterson, Rosenfeld & Poro, 1976) and unvented air following surgery (Nichols et al., 1958; Gott & Lillehei, 1959; Groves et al., 1964; Jones et al., 1964; Fishman et al., 1969; Taber, Moraan & Tomatis, 1970; Lawrence, McKay & Sherensky, 1971; Padula et al., 1971; Gallagher & Pearson, 1973; Borike et al., 1973; Cleland & Ghadiali, 1976; Lemole & Pinder, 1976). Embolic episodes may also be partly responsible for cerebral haemorrhage (Wright, 1975).

Microbubbles as a potential source of embolic damage

Of the various aetiologies suggested for cerebral damage as a result of extracorporeal circulation for open heart surgery, cerebral embolism by microbubbles remains a largely indeterminant issue. There is little doubt that microbubbles perfused in sufficient numbers can cause neurological dysfunction or death (Friedman et al., 1962). However the mechanism for these effects and direct evidence of tissue damage is yet to be shown. The point at issue is not that arterial embolism by gas microbubbles is potentially hazardous but that the numbers and sizes of bubbles produced during extracorporeal circulation

are sufficient to produce the reported neurological and pathological symptoms. Complementary to this has been the need to establish the sources of microbubbles during extracorporeal circulation, the factors that moderate these sources and the methods that can be used to eliminate them.

Of the studies undertaken to determine the effects of arterial embolism by microbubbles in quantitative terms, that of Friedman et al (1962) is the most definitive. Using a double syringe device, microbubbles (25 μm to 100 μm diameter, mean 70 μm diameter) were produced in a gelatin medium and the microbubble mixture was injected, in various doses, into the left carotid artery of dogs via a thin-walled polyethylene catheter placed in a retrograde fashion to the level of the aortic arch. Perfusion was achieved over an average period of 32.4 minutes. A bypass circuit from the right femoral artery to the right femoral vein, containing a lucite chamber was used to observe the intra-arterial bubble population directly. Temperature and oxygen tension measurements were also taken from within this circuit. Friedman et al (1962) concluded that up to 1.2 $ml.Kg^{-1}$ body weight of air administered in the form of microbubbles intra-arterially had negligible effects, whereas 1.5 $ml.Kg^{-1}$ was 100% fatal. Moreover, they concluded that 5 $ml.Kg^{-1}$ of oxygen could be administered in the same manner without serious effect.

While these values are similar to the values derived by Geoghegan & Lam (1953) for death induced by bolus injection of air into the left ventricles of dogs (1.5 $ml.Kg^{-1}$) they are at variance with values obtained by Benjamin, Turbak & Lewis (1957) for bolus injection (0.5 $ml.Kg^{-1}$) into the left ventricle, but compare well with bolus injection into the descending aorta (1.5 $ml.Kg^{-1}$, without adverse effects). Less favourable comparisons exist between the values derived by Friedman et al (1962) and those derived by Landew et al (1960) based upon microbubble estimations during partial bypass using a bubble

oxygenator. Landew et al (1960) reported that all dogs given more than 0.19 ml.Kg^{-1} of air in microbubble form died. Oxygen was less toxic than air, but they found that 20% of the dogs given 0.43 ml.Kg^{-1} of oxygen developed neurological sequalae. Although Landew et al (1960) admitted an error of 30%-50% in the estimation of gas volumes, this was insufficient to account for the large differences in the effects reported for air and oxygen. Friedman et al (1962) suggested that the difference was due to other factors such as the use of partial perfusion per se, oxygen toxicity, cerebral embolisation by Antifoam A or incompatibility of blood. In view of the bubble detection technique used by Landew et al (1960) (visual observation of sample volumes) it is difficult to understand how they derived their error of 30%-50%. Even if their estimate was correct, they should also have considered that microbubble infusion rate as well as the total number of microbubbles infused might have considerable importance in accounting for the differences. Microbubble stability and dissolution time may also have been important, yet no consideration was given to the significance of microbubbles as dynamic entities in either of these studies. Microbubble dynamics has been similarly ignored in subsequent studies of embolic tissue damage as a result of extracorporeal circulation.

Other factors, such as carbon dioxide tension and its influence upon cerebral vasodilation may also influence the effects of microbubbles introduced into the blood circulation. Temperature certainly appears to influence the effect. Friedman et al (1962) reported that hypothermia (30 $\pm$ 1^{o}C) mitigates the deleterious effects of microbubbles observed during normothermia (50% survival at 1.5 ml.Kg^{-1} of air). Amongst the hypotheses proposed for this mitigation has been the reduction of arterial spasm due to the irritant effect of undissolved gas (Durrant et al., 1949) and the reduced metabolic demands of the tissues under hypothermic conditions. An explanation based upon the

increased solubility of gas at reduced temperatures was rejected by Friedman et al (1962) on the grounds that the arterial blood was already equilibrated with respect to the gases dissolved in the plasma at the hypothermic level established before the perfusion of microbubbles. This is not entirely valid since the ability of a bubble to dissolve is primarily determined by the localised conditions of saturation and the concentration gradient.

A further complication to determining definitive levels of microbubbles responsible for cerebral complications has been the nature of the gas. Friedman et al (1962) have shown that oxygen is better tolerated than air, whilst Kunkler & King (1959) have shown, on the basis of bolus injections that carbon dioxide is better tolerated than oxygen and that oxygen is better tolerated than air.

It is clear that the variety and variations in conditions that could influence the pathological effects of microbubbles make comparisons and definitive statements of hazardous limits very difficult. Whilst the results of Friedman et al (1962) provide some indication of the danger of microbubbles as possible embolic agents they are not necessarily representative of the results that may arise during conventional cardiopulmonary bypass. The results and conclusions presented by Landew et al (1960) may not be entirely representative of the effects produced by microbubbles, since other agents, such as particulate emboli may have contributed to the outcome. Histological examination of cerebral tissue revealed venous distention and petechial haemorrhages. Both of these are well known in pathological material and they are thought to develop during the process of dying as the cardiac output declines and the venous pressure increases (Wright, 1975).

It is surprising that no attempt has been made to quantitatively relate cerebral tissue damage to microbubble sources detected during cardiopulmonary bypass, since that of Landew et al (1960). Subsequent

studies of extracorporeal microbubbles have been largely confined to the identification of microbubble sources, the factors that influence microbubble liberation and measures to eliminate them (Miller & Allbritten, 1960; Donald & Fellows, 1961; Baird & Mujagishima, 1964; Spencer et al., 1965; Austen & Howry, 1965; Selman, McAlpine & Ratan, 1967; Aronstam et al., 1968; Patterson & Kessler, 1969; Patterson, Kessler & Bergland, 1971; Patterson & Twichell, 1971; Lawrence, McKay & Sherensky, 1971; Fisk et al., 1972; Lichti, Simmons & Almond, 1972; Patterson et al., 1972; Gallagher & Pearson, 1973; Patterson, Wasser & Porro, 1974; Lubbers et al., 1974; Clarke, Dietz & Miller, 1975; Patterson, Rosenfeld & Porro, 1976).

Source-sink representation

Collectively, the results of these studies provide the ingredients for a source-sink representation of the extracorporeal circuit with respect to microbubble formation, variation, and elimination. By developing this source-sink representation a framework emerges for presenting the variables that govern the introduction of microbubbles and secondary related products, such as denatured protein, into the systemic circulation during cardiopulmonary bypass (Appendix B). Additionally it provides a framework for considering the nature of the agents involved. Thus it is possible to distinguish discrete and distributed sources, sinks and mediators (agents that moderate or enhance the characteristics of the microbubble population) and coupled sources (sources that directly influence the source of a secondary agent such as lipid globules). The fact that any agent that influences the microbubble population may be classified according to its function as a source, sink or mediator reduces confusion over the significance of each of these agents at any point within the circuit. A summary of the sources, sinks and mediators for which there is documented evidence is presented in the Tables 7.1 to 7.3. The functional

Table 7.1

Sources of microbubbles during cardiopulmonary bypass

SOURCE	TYPE	FUNCTIONAL DEPENDENCE OF SOURCE	REFERENCES
Oxygenator Column or Membrane	Discrete	Gas flow rate, Counter diffusion, exchange rate supersaturation, Sparger design, membrane design	Jordan et al, 1958; Maloney et al, 1958; Spencer et al, 1965; Selman, McAlpine & Ratan, 1967; Aronstam et al, 1968; Patterson & Kessler, 1969; Fisk et al, 1972; Ward & Zingg, 1972; Gallagher & Pearson, 1973; Graves et al, 1973; Quinn, Graves & Smock, 1974.
Cardiotomy Suction	Discrete	Suction flow rate and gas content	Miller & Allbritten, 1960; Baird & Mujagishima, 1964; Spencer et al, 1969 Gallagher & Pearson, 1973.
Dissolved gas	Distributed	Rise in gas tension above system pressure (including the influence of temperature)	Donald & Fellows, 1959; 1961; Drew et al, 1959; Gordon et al, 1960; Kaplan et al, 1962.
Cavitation	Discrete	Negative pressure gradient	Willman et al, 1958; Bass & Longmore, 1969.
Mechanical Disturbance	Discrete	Dislodgement of adherent microbubbles, splashing	Patterson & Kessler, 1969; Gallagher & Pearson, 1973.
Surgical	Discrete	Inadequate venting	Nichols et al, 1958; Gott & Lillehei, 1959; Groves et al, 1964; Jones et al, 1964; Anderson et al, 1965; Spencer et al, 1965; Carlson et al, 1967; Fishman et al, 1969; Tuber, Moraan & Tomatis, 1970; Lawrence, MacKay, Sherensky, 1971; Gallagher & Pearson, 1973; Lemole & Pinder, 1976.

Table 7.2

Mediators for microbubbles during cardiopulmonary bypass

MEDIATOR	TYPE	FUNCTIONAL DEPENDENCE OR MEDIATOR	REFERENCES
Settling time	Discrete	Blood flow rate and reservoir level (volume)	Patterson & Kessler, 1969; Kessler & Patterson, 1970; Fisk et al, 1972; Gallagher & Pearson, 1973; Lubbers et al, 1974.
Dissolution rate	Distributed	Saturation level	Christoforides & Hedley-Whyte, 1969; Yang et al, 1971; Lubbers et al, 1974.
Counter diffusion	Distributed	Differential gas concentrations between contents of bubble and gases in solution	Nunn, 1959; Tisovec & Hamilton, 1967.
Surfactants	Distributed	Surfactant concentration, surface energy and bubble collisions	Hills, 1974.

Table 7.3

Sinks for microbubbles during cardiopulmonary bypass

SINKS	TYPE	FUNCTIONAL DEPENDENCE OF SINK	REFERENCES
Defoamer	Discrete	Active area and duration of contact, surface energy	Rygg, 1973
Arterial reservoir	Discrete	Bubble rise time (including influence of outflow velocity)	Reed & Clark, 1975
Chemical union	Distributed	Concentration of reactants and reaction rates	Yang et al, 1971
Physical solution	Distributed	Solubility and saturation level	Yang et al, 1971
Filters	Discrete	Pore size and bubble sizes	Spencer et al, 1965; Patterson & Kessler, 1969; Lichti, Simmons & Almond, 1972; Kessler & Patterson, 1970
Microvasculature	Discrete	Vessel sizes, bubble sizes and vasotone	

dependencies stated in these tables have been derived from a consideration of the references quoted rather than an acceptance of individually reported statements. Moreover, the recognition and classification of the various sources, sinks, and mediators have been based upon the source-sink representation discussed in Appendix B, as distinct from the more loose classifications generally encountered in the references quoted. In many of these reports microbubble liberation has been merely related to one or more of the functionally dependent parameters associated with a particular source, sink or mediator.

Quantification in microbubble detection

A fundamental criticism of previous studies of factors that influence microbubble liberation during cardiopulmonary bypass has been the lack of quantification. In most cases this shortcoming can be attributed to the limitations of the microbubble detection techniques. Inadequate recognition of the criteria that must be fulfilled in order to achieve useful quantification has caused problems when quantification has been attempted.

As indicated in chapter 2 Doppler and continuous wave ultrasonic techniques in general are inherently less suitable for quantitative microbubble detection than pulsed ultrasonic techniques, particularly with respect to coincidence errors and the avoidance of multiple counts per bubble. Flow dependent pulse triggering of the ultrasound source has largely avoided these problems.

The technical and physical considerations presented in chapters 3 and 4 have revealed that the physical principle of the technique, the choice of source frequency, the intensity level, the field uniformity, the transducer configuration and the shape of the transducer are fundamental to the design of an ultrasonic microbubble detector. It is therefore surprising that so few researchers have appreciated these fundamental requirements when selecting an ultrasonic microbubble

detection technique for use in cardiopulmonary bypass studies. The low cost and availability of Doppler flow devices may in some measure account for the widespread, uninformed use of these instruments and the disregard for the physical basis of the method when considered for the purpose of microbubble detection. Only in more recent reports has there been evidence of physical considerations in the design of a detection system (Lubbers et al., 1974; Lubbers et al., 1977). Unfortunately these considerations did not include the limitations of the physical principle upon which the instrument was based (Doppler) or the limitations imposed by a continuous wave source of ultrasound with microbubble detection unrelated to field uniformity and flow. Moreover the reports of Lubbers et al (1974; 1977) suggest the use of a proprietory Doppler instrument, yet no reference was made to any possible limitations imposed by instrumentation characteristics of the type discussed in Chapter 2.

It is clear from earlier discussion that the previously used techniques of microbubble detection have been inadequate for obtaining quantitative results. In general the results obtained were confined to estimations of microbubble liberation rate or number, but without reference to concentration or size (Patterson & Kessler, 1969; Spencer et al., 1969b; Kessler & Patterson, 1970; Simmons et al., 1972). Unfortunately these results may be further criticised for errors inherent in the methods used to obtain bubble counts. These criticisms have been discussed for each technique in chapter 2 , the principal conclusion being that they do not necessarily provide counts that are proportionally related to microbubble numbers. In view of these limitations it is disturbing that so many studies have been reported in which a need for quantification has been clearly indicated, both for comparative and non-comparative studies, and yet inadequate instruments have been used. For example, instruments in which the bubble detector

output was not flow-related have been used to compare oxygenators (Spencer et al., 1965; Selman et al., 1967; Patterson & Kessler, 1969; Spencer et al., 1969b; Kessler & Patterson, 1970; Simmons et al., 1972). Although the conclusions derived in these studies may be valid, they cannot be accepted with certainty.

Complementary to the need for quantification in microbubble investigations is the need to consider the factors that influence bubble lifetime (Furness, 1975; Bethune, 1976). Bethune (1976) in a letter to the editor of Lancet discussed two such factors and speculated upon their relevance to neurological dysfunction as a result of cardiopulmonary bypass. The two factors discussed were the pressure gradient causing a bubble to dissolve and the diffusion of anaesthetic gases into a bubble nucleus causing it to increase in size.

By considering only the pressure gradient as a mechanistic factor in the dissolution of microbubbles Bethune (1976) confined his discussion to general comments on bubble lifetime as determined by the physical solution of the bubble contents. He claimed that increased system pressure would favour more rapid solution of gas and suggested that this was the mechanism by which vasopressors prevent neurological changes at the beginning of cardiopulmonary bypass (Branthwaite, 1975). By taking precautions, such as the use of a carbon dioxide flush to remove air from the circuit, and the avoidance of pre-bypass oxygenation of the prime, Bethune (1976) concluded that microbubbles could be completely or almost completely eliminated from the prime, thereby obviating the need for vasopressors at the start of bypass.

This hypothesis would be difficult to test since it would be necessary to evaluate microbubble population characteristics quantitatively and to obtain estimates of microbubble lifetimes. The latter would be particularly difficult at the beginning of bypass because of the variable composition of the perfusate and because information other than system

pressure would be required for estimating bubble lifetimes (see chapter 1)

Irrespective of the influence of microbubbles at the beginning of bypass, the absence of microbubbles would not eliminate hypotension due to dilution of the blood by the prime. Consequently the use of vasopressors could continue to be necessary to maintain adequate cerebral perfusion.

Bubble growth as a result of soluble anaesthetic gases such as nitrous oxide diffusing into a bubble has been observed on a number of occasions (Nunn, 1959; Munson & Merrick, 1966; Tisovec & Hamilton, 1967). Bethune (1976) has suggested that the growth of bubbles as a result of the high concentration of nitrous oxide within the patient's arterial blood before bypass may be the factor responsible for neurological damage in some patients (Branthwaite, 1973). The basis for this observation was the lack of evidence from either cerebral function monitor tracings (Prior et al., 1971) or other clinical manifestations of inadequate cerebral blood circulation at the start of bypass when the nitrous oxide ventilation was discontinued ten minutes previously. This procedure can reduce the level of nitrous oxide to less than 10% of its previous concentration and minimise bubble growth (Bethune, 1976). However the relationship between bubble growth and clinical manifestations of cerebral disturbance has not been demonstrated. Again it would be difficult, if not impossible to test the hypothesis, particularly since it would be functional within the systemic circulation and complicated by other influential factors, including the system pressure effect on bubble dissolution.

Two important points emerge from these considerations. Firstly the factors influencing bubble lifetime may be complicated and difficult to measure. Nevertheless it is important that hypotheses derived to explain events or phenomena should be falsifiable (Magee, 1975). However the practical expedient of eliminating microbubbles from the

extracorporeal circuit is a justifiable and commendable procedure.

Quantification of microbubbles and neurological damage

Friedman et al (1962) reported that 5 ml.Kg^{-1} of oxygen delivered into the left carotid artery of dogs, in microbubble form (25 μm to 100 μm diameter, mean, 70 μm diameter) had no apparent effect. In the in vitro and in vovo studies the predominant microbubbles were 50 μm in diameter and the liberation rate was less than 100 s^{-1}. At these sizes and rates, the volumes of oxygen delivered within the cardiopulmonary bypass period would be well below the value of 5 ml.Kg^{-1}. For the values of size and rate quoted, a bypass period of 212 hours.Kg^{-1} would be necessary to deliver such a quantity of gas as microbubbles.

Considering the estimate of Landew et al (1960) of 0.43 ml.Kg^{-1} of oxygen to produce neurological sequalae, a bypass period of 18 hours.Kg^{-1} would be required to deliver 0.43 ml.Kg^{-1} of oxygen as 50 μm diameter bubbles at a rate of 100 s^{-1}.

On the basis of these considerations the modern bubble oxygenator, incorporating coarse mesh filters would appear to offer a considerable margin of safety with respect to microbubble liberation. However this statement assumes that the results of Landew et al (1960) and Friedman et al (1962) are directly applicable to the human bypass situation. Furthermore it only relates to gross neurological disturbances and to the contribution made by the smaller bubbles identified during the bypass experiments. Smaller concentrations of microbubbles may be responsible for more minor disturbances, and the contribution made by larger bubbles, although smaller in number, may be significant because of the relationship of volume to the cube of the radius.

More information is necessary in order to define the quantities of microbubbles, including their size range, rate and contents, that present a serious hazard during bypass. The seriousness of the insult is of course difficult to determine when external criteria become inadequate.

However, more definitive studies of cerebral tissue damage may help to resolve this difficulty. Patterson, Rosenfeld & Porro (1976) have reported some qualitative results that indicate that microbubbles may be responsible for transient neurological sequalae that may arise as a result of cardiopulmonary bypass (Tufo et al., 1970; Aberg, 1974; Branthwaite, 1975).

Flow dependent detector development

The construction of the flow dependent ultrasonic technique for microbubble detection has been based upon an analysis of the limitations of previously used techniques, a consideration of the behaviour of microbubbles in an acoustic field, and a formulation of the criteria that must be fulfilled in order to obtain quantitative results.

The criteria proposed for deriving quantitative information has been the measurement of number, size range and rate for a known volume of insonification. These measurements were then combined to provide an expression of results in terms of the number of microbubbles per unit volume per unit time for each size range considered. The accuracy of the results presented in this manner is dependent upon the accuracy of the component parts, some of which are difficult to specify exactly. However, the rates recorded in the experiments appeared to be well within the resolving capability of the instrument (5 microbubbles per ml).

In keeping with other ultrasonic techniques, the flow dependent detector design is also subject to errors due to coincidence, but the probability of these occurring has been limited by the chosen size of the volume of insonification. By reducing the width of the volume of insonification still further, coincidence errors may also be further reduced. Unfortunately it is not at present possible to estimate the incidence of such errors under bypass conditions.

Errors in estimating the size of the microbubbles may have been as high as 15-50%, depending upon the position of the microbubble within

the field (chapter 5). The regions in which a 50% error would have been obtained are relatively small and the consistency of the signal responses for microbubbles < 50 μm diameter, suggests that the error in sizing was mainly well below 50%. Greater accuracy in sizing may be achieved by improvement in the transducer design, but again the possibility of coincidence errors must be considered as an agent that can influence the accuracy in sizing.

An important pre-requisite in the design of a microbubble detector is the range of bubble sizes to be accommodated. At the design stage of the flow dependent detector this information was not available and an estimate had to be made on the basis of earlier studies (Landew et al., 1960; Friedman et al., 1962). Subsequent use of the instrument revealed that the predominant size of microbubbles detected during both the in vitro and in vivo experiments was less than 50 μm diameter, with a much smaller population being detected within the 50-80 μm diameter and > 230 μm diameter ranges under various conditions. In view of these observations, further signal conditioning facilities could be usefully incorporated in order to separately accommodate bubble sizes below say, 80 μm diameter and those greater than 80 μm diameter. In this way the signals corresponding to the smaller bubble sizes could be considerably enhanced by further amplification and so enable greater delineation of bubble sizes and more accuracy in discriminating between them.

Field uniformity has featured as an important consideration in the design of the detector and plots of the acoustic field have indicated that such consideration is justified. No previously reported detection technique for microbubbles has included any reference to field uniformity. The facility for predicting field patterns for different transducer configurations (Marine & Rivenez, 1974) provides a useful basis for designing transducers that exhibit more uniform field characteristics within the region of interest. However the model would need

to be developed for predictions within the very near field.

The choice of source frequency for the flow dependent detection technique was made difficult by a lack of knowledge of the bubble sizes to be expected. A compromise was therefore adopted that allowed a reasonable differentiation margin between gaseous and particulate matter, together with a reasonably linear and large dynamic range. On the basis of the results obtained the choice appears to be acceptable. No evidence has been acquired to suggest that blood cell aggregates or other particulate matter have been detected together with microbubbles. However, a greater margin of confidence may be achieved by reducing the source frequency to about 5 MHz, thus putting the resonant bubble size at approximately 1 μm diameter. Such a reduction may also allow some improvement in the uniformity of the field characteristics. The signal conditioning instrumentation for the flow dependent detector has been adequate for the purpose of demonstrating the potential of the technique for quantitative analysis of microbubble populations arising during cardiopulmonary bypass. A programme of system development is now indicated in order to extend the capabilities of the technique. A number of additions and improvements may be suggested. These include:-

1. Multiplexed, triple element transducers providing narrow, low volume regions of insonification and uniform field characteristics in order to reduce coincidence errors and errors in sizing.
2. Improvements in the transducer mounting assembly to reduce counting errors that may arise due to the nature of the flow velocity profile.
3. Two tier system of microbubble size analysis based upon higher amplification of small bubble signals, and separate discrimination.
4. Signal conditioning electronics to replace the modified Ekoline ultrasonoscope. The retention of an oscilloscope display would provide a very valuable adjunct to the signal

discriminators, counters and rate recorders.

5. Pre-discriminator pulse shaping circuitry to improve discriminator performance.
6. Inclusion of rate recorder facilities for all selectable size ranges.
7. Computer control and analysis of counter contents with provision for teletype output.
8. Multiplexed transducer facilities for 'simultaneous' input-output investigations.

Such improvements would obviously be costly and could only be justified on the basis of the degree of quantification that such a system could offer and the demands for quantification in future studies of extracorporeal bubble phenomena. Institutional discussions to establish standards for extracorporeal components, together with the interests of manufacturers to completely specify their products may favour the development of such a system. But in considering such a development, it must be borne in mind that an error free ultrasonic system is most assuredly unattainable. The distribution of microbubbles within the volume of insonification will always present the possibility of coincidence errors and multiple scattering would introduce further limits on what is physically possible in discriminating both size and number. In spite of these physical limitations, the flow related pulsed ultrasound microbubble detector is a substantial improvement over techniques previously available for the quantitative analyses of microbubble populations in whole blood.

Prospective work

The work completed to date has helped to re-establish the foundations for further study of microbubbles during cardiopulmonary bypass in particular and extracorporeal circulation in general. In addition to the natural development of the microbubble detector, prospective

work also includes the evaluation of extracorporeal circuit components with respect to microbubble liberation. For example the trend towards the use of membrane oxygenators instead of bubble oxygenators introduces the need to investigate the exchange rate and counter diffusion mechanisms for bubble formation in membrane devices and the significance of these mechanisms during long term cardiac and respiratory support.

At present the evaluation of cardiotomy reservoirs for the removal of suction liberated microbubbles is being investigated as part of a wider study to determine their effectiveness.

Once the detector has been further developed a study to establish the embolic potentiality of microbubbles is envisaged. Studies are also envisaged for investigating further the general properties of sources, sinks and mediators.

Conclusions and recommendations

The main conclusions of this work are as follows;

1. Ultrasonic Doppler and continuous wave techniques in general are less suitable than pulsed ultrasound techniques for quantitative microbubble detection.
2. By developing a new flow dependent ultrasonic detection technique, a more quantitative approach to microbubble analysis has been achieved.
3. Flow dependent pulse triggering has been found to be effective in avoiding multiple counts per bubble and in discriminating changes in microbubble populations due to flow from those due to other factors.
4. Measurement of field uniformity is extremely important if attempts are to be made to quantitatively analyse microbubble populations.
5. The predominant bubble sizes liberated in both in vitro and in vivo studies were < 50 μm diameter. These sizes are possibly representative of the sizes generally encountered during cardiopulmonary bypass in which the same oxygenators, or oxygenators having the

same filter characteristics are used.

6. Blood flow rate and reservoir level are mediators that directly influence reservoir settling time. Increases in blood flow rate and reductions in reservoir level increase the rate of microbubble liberation and also favour the release of larger bubbles.
7. Gas flow rate is a principal determinant in the rate of formation of microbubbles, the rate at which they are liberated into the system being dependent upon the effectiveness of intermediary mediator characteristics.
8. Micropore filters of the type used in these studies can be extremely effective in removing microbubbles providing the microbubble diameters are greater than the filter pore sizes (> 50 μm diameter in these studies).
9. Micropore filters appear to offer a reasonable degree of protection should the arterial reservoir become depleted of blood.
10. Consideration of bubble dynamics is an important requirement in any study of the effects of microbubbles during cardiopulmonary bypass. Theoretical analysis indicates that oxygen saturation is an effective mediator in the lifetime of oxygen microbubbles. A small reduction in saturation level results in a reasonably large reduction in dissolution time.
11. The flow dependent detection technique may be of value in decompression studies in which an arterio-venous shunt can be established in order to detect circulating microbubbles. Similarly the detector may be used in studies of extracorporeal circulation for renal dialysis.
12. It has still not been demonstrated that microbubbles cause cerebral tissue damage as a result of cardiopulmonary bypass.

To reduce the liberation of microbubble into the arterial line during cardiopulmonary bypass it is recommended that the following

precautions be taken:-

1. The oxygen flow rate should be kept as low as possible, consistent with adequate oxygenation whilst maintaining a saturation level below 90%.
2. The oxygenator arterial reservoir level (Rygg-Kyvsgaard HL-054) should be maintained to within 20 mm of the defoamer chamber level in order to increase reservoir settling time and eliminate large bubble formation due to turbulence and splashing.
3. A micropore arterial line filter should be included in the extra-corporeal circuit to eliminate large bubbles.
4. A cardiotomy reservoir incorporating a micropore filter should be included in the cardiotomy suction line.
5. Attention should be given to any agents that influence microbubble sources and mediate microbubble liberation. Further work is required to establish the quantitative significance of blood warming upon microbubble liberation.

APPENDIX A

DETECTION OF MICROBUBBLES BY USE OF ULTRASONIC DOPPLER DEVICES

In chapter 2 an analysis of ultrasonic Doppler devices having a transcutaneous arrangement of the transmit and receive transducers was presented. Below the analysis is repeated for a cuff type arrangement of the transducers.

Doppler principle. The frequency of an ultrasound signal reflected from a moving surface will differ from that of the transmitted signal by an amount determined by the velocity of the reflecting surface and the velocity of sound propagation of the medium in which the sound waves are travelling. The frequency shift will result in either an increase or a decrease in frequency depending upon the direction of movement of the reflecting surface. Movement towards the transmitter/receiver assembly will yield an increase in frequency, whereas movement away from the assembly will yield a decrease.

Analysis for cuff type arrangement of transducers

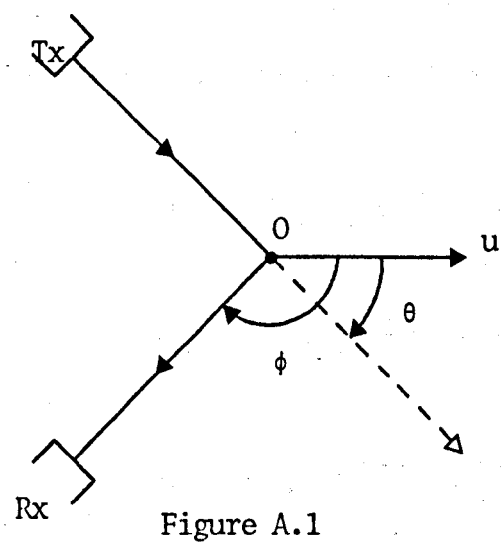

Figure A.1

At O (Fig. A.1)a decrease in frequency is observed due to the movement of the object away from the source of the transmitted ultrasound such that the secondary source of reflected ultrasound has a frequency ω_{R1} related to the transmitted frequency ω_T by the expression:

$$\frac{\omega_{R1}}{\omega_T} = \frac{c - u\cos\theta}{c}$$

Where v is the velocity of sound propagation within the medium and u is the velocity of the object.

At the receiver, a second change in frequency is observed due to the movement of the secondary source of ultrasound such that the received frequency ω_{R2} is related to the secondary source of ultrasound by the expression:

$$\frac{\omega_{R2}}{\omega_{R1}} = \frac{c}{c - u\cos\phi}$$

$$\therefore \quad \omega_{R2} = \left(\frac{u}{c - u\cos\phi}\right)\omega_{R1}$$

But $\omega_{R1} = \left(\frac{c - u\cos\theta}{c}\right)\omega_T$

$$\therefore \quad \omega_{R2} = \left(\frac{c}{c - u\cos\phi}\right)\left(\frac{c - u\cos\theta}{u}\right)\omega_T$$

$$= \left(\frac{c - u\cos\theta}{c - u\cos\phi}\right)\omega_T$$

The change in frequency with respect to the transmitted frequency, ω_T,

$$\Delta\omega = \left(\frac{c - u\cos\theta}{c - u\cos\phi}\right)\omega_T - \omega_T$$

$$\Delta\omega = \omega_T\left(\frac{c - u\cos\theta}{c - u\cos\phi} - 1\right)$$

$$\Delta\omega = \omega_T\left(\frac{c - u\cos\theta - c + u\cos\phi}{c - u\cos\phi}\right)$$

$$= \omega_T\left(\frac{u(\cos\phi - \cos\theta)}{c - u\cos\phi}\right)$$

For $v >> u$

$$\Delta\omega = \omega_T \left(\frac{u(\cos\phi - \cos\theta)}{c} \right)$$

$$\Delta\omega = \frac{u\omega_T}{c} (\cos\phi - \cos\theta)$$

Now $\cos\phi - \cos\theta = -2 \sin\left(\frac{\phi+\theta}{2}\right) \sin\left(\frac{\phi-\theta}{2}\right)$

$$\therefore \Delta\omega = \frac{-2u\omega_T}{c} \sin\left(\frac{\phi+\theta}{2}\right) \sin\left(\frac{\phi-\theta}{2}\right)$$

For a fixed mounting of the transmitter and receiver transducers $-\sin\left(\frac{\phi-\theta}{2}\right)$ is a constant K'

$$\therefore \Delta\omega = \frac{2u\omega_T}{c} K' \sin\left(\frac{\phi+\theta}{2}\right)$$

$u \sin\left(\frac{\phi+\theta}{2}\right)$ defines a unit vector along the bisector of the angle between the transmitter and receiver axes such that:

$$u \sin\left(\frac{\phi+\theta}{2}\right) = \bar{u} \cdot \bar{k}'$$

$$\therefore \Delta\omega_i = \frac{2\omega_T}{c} (\bar{u} \cdot \bar{k}') K'$$

Developed in the same manner as the analysis for the transcutaneous arrangement of transducers, the expression for change in frequency due to both blood particles and a small population of microbubbles is of the form:

$$\Delta\omega_{av} = \frac{2\omega_T}{c} (k' \cdot u_{av}) K' \frac{1}{N} \sum_{i=1}^{N_b} \frac{2\omega_T}{c} K' (\bar{u}_{ib} \cdot \bar{k}'_{ib})$$

with $(\bar{u}_{ib} \cdot \bar{k}'_{ib})$ having a possible range of values from 0 to u_{ib}.

APPENDIX B

SOURCE-SINK REPRESENTATION OF THE EXTRACORPOREAL CIRCUIT

The extracorporeal circuit is, by virtue of the many and varied factors inherent within it, extremely complex. Analysis of relationships between individual factors and their physiological and pathological effects is difficult. Because of this difficulty the use of a conceptual framework as an aid to experimental design and the interpretation of complex observations is an appropriate expedient. For the analysis of the factors concerned with the formation and elimination of microbubbles during extracorporeal circulation a source-sink representation provides a useful framework.

A source is defined as any device or process that introduces microbubbles into the circulation, whilst a sink is defined as any device or process that directly eliminates microbubbles from the circulation. In addition to sources and sinks it is necessary to collectively define the agents that mediate the function of sources and sinks. Thus a mediator may be defined as any agent that influences action of a source or sink. For example blood flow is a mediator in the elimination of microbubbles by its influence upon settling time.

Having defined the sources, sinks and mediators in this manner the extracorporeal-intracorporeal circuit may be represented by a flow diagram showing the location for each component within the circuit relative to the subject being perfused (Fig.B1). Such an arrangement may simplify the selection of sites for obtaining particular measurements. Unfortunately it is only of value for sources and sinks that are confined to a particular part of the circuit, i.e. discrete sources and sinks.

Distributed sources and sinks

Non-discrete sources and sinks may be recognised, the effects of which are manifest throughout the circuit. These may be called

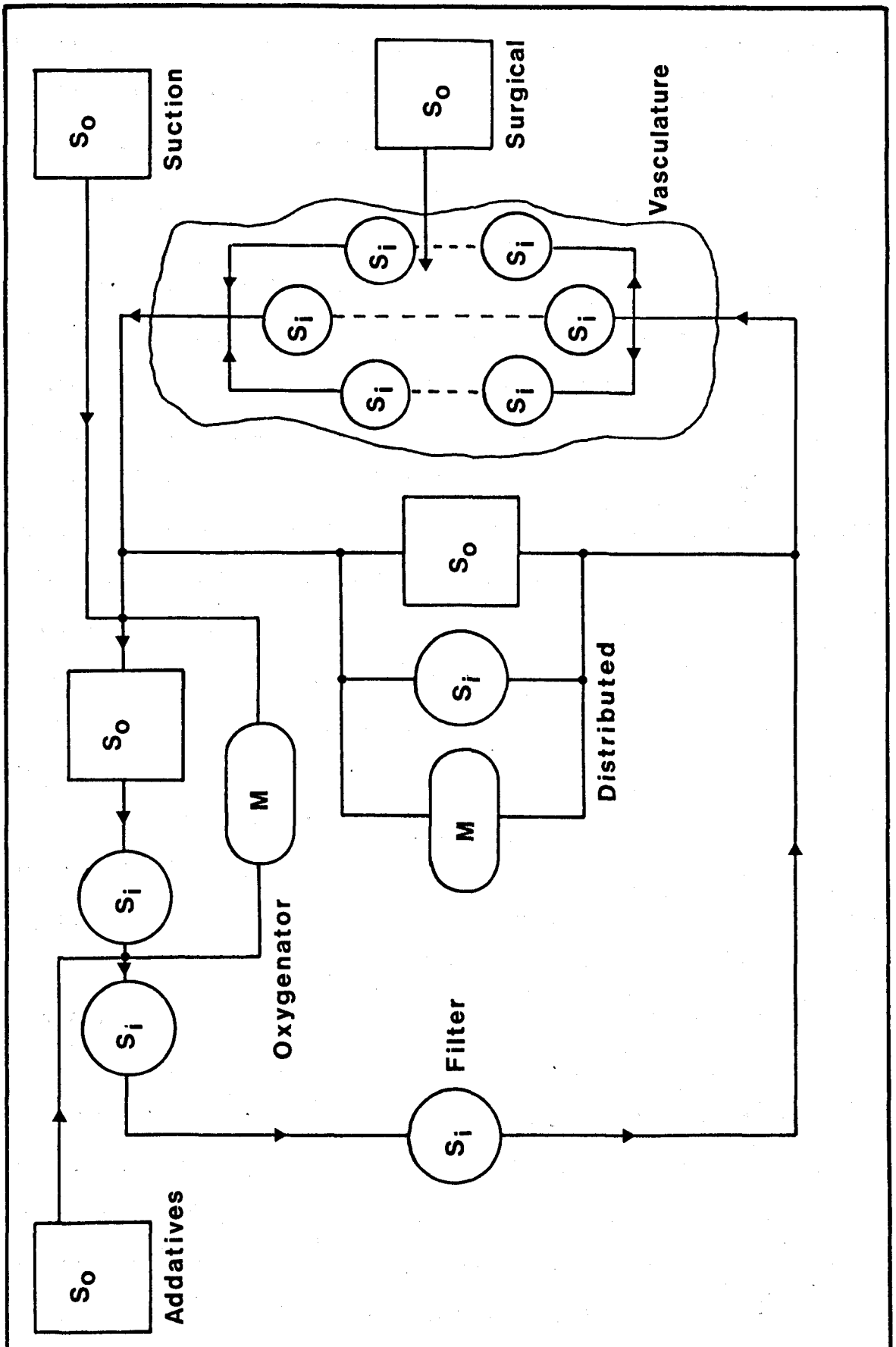

Generalised Source - Sink representation for the extracorporeal-intracorporeal circuit

S_o : source; S_i : sinks; M : mediators

Figure 8.1

Referred to on P.309

distributed sources or sinks. The prime example of a distributed sink is the dissolution of microbubbles in the circulating blood, whilst an example of a distributed source is the release of dissolved gas from solution, in the form of microbubbles, due to blood warming or system pressure decrease.

The presence of distributed sources and sinks indicatesthe need for recognising the functions that describe the variability of the microbubble population as it courses through the circuit. A knowledge of these functions, which would include the influence of mediators, may be used to estimate the value of a particular parameter at or within a region of interest. However, an estimate of this nature could only be expected to be of value within the region between discrete sources or sinks. From a more practical standpoint the functional behaviour of a distributed source or sink may be used to recognise the means of reducing the microbubble population.

Coupled sources

Because of the nature of the blood-gas interface a source of microbubbles is capable of yielding a source of other material that may also influence the physiological or pathological state for which a relationship with microbubbles is being sought. A situation of this type may be defined as a coupled source. Denatured protein, lipid globules and blood cell aggregates may all represent products of microbubble blood-gas interface activity. By identifying that such sources exist, the possibility of each source distinguished within the circuit having such a couple must be considered. Having recognised the existence of particular coupled sources it is important to establish the nature of the coupled source products and their function with respect to the physiological and pathological effects being investigated.

Lumped representation

Where a relationship is sought between the microbubble population

entering the intracorporeal circuit and a selected physiological or pathological effect the individual sources and sinks within the extracorporeal circuit may be considered lumped together as a single source of bubbles. Whilst it is difficult, if not impossible, to characterise the various vascular beds within the intracorporeal circuit as sinks for microbubbles the distribution of the input population may, to some extent, be resolved by knowing or measuring the relative flows to these regions during total bypass. In partial bypass the contribution provided by the heart would negate a prediction of bubble distribution. Thus it is possible to distinguish various sinks in the intracorporeal circuit providing a distribution in flow is known otherwise the intracorporeal circuit may be represented as a single sink. The lumped representation of the extracorporeal circuit is shown below, the function for diffuse source and/or sink activity being defined for the region between the source measurement point and the intracorporeal circuit.

REFERENCES

Abdulla, U., Talbert, D., Lucas, M., & Mullarkey, M. (1972) Effect of ultrasound on chromosomes of lymphocyte cultures. British Medical Journal, 3, 797.

Abelson, D. & Müller, H.R. (1973) Reciprocal movement of the right and left heart demonstrated by directional Doppler ultrasound. American Heart Journal, 86, 651.

Aberg, T. (1974) Effect of open heart surgery on intellectual functions. Scandinavian Journal of Thoracic and Cardiovascular Surgery - Supplement 15.

Aberg, T. & Kilhgren, M. (1976) Effect of open heart surgery on intellectual function. Scandinavian Journal of Thoracic & Cardiovascular Surgery, 10, 221.

Adams, J.E., Owens, G., Mann, G., Headrick, J.R., Munoz, A. & Scott, H.W. Jr. (1959) Experimental evaluation of Pluronic F68 (a non-ionic detergent) as a method of diminishing systemic fat emboli resulting from prolonged cardiopulmonary bypass. Surgical Forum, 10, 585.

Aquilar, M.J., Gerbode, F. & Hill, J.D. (1971) Neuropathological complications of cardiac surgery. Journal of Thoracic & Cardiovascular Surgery, 61, 676.

Allardyce, D.B., Yoshida, S.H. & Ashmore, P.C. (1966) The importance of microembolism in the pathogenesis of organ dysfunction caused by prolonged use of the pump oxygenator. Journal of Thoracic and Cardiovascular Surgery, 52, 706.

Anderson, R.M., Fritz, J.M. & O'Hare, J.G. (1965) Pulmonary air emboli during cardiac surgery. Journal of Thoracic & Cardiovascular Surgery, 49, 440.

Aronstam, E.M., Geiger, J.P., Morris, J.A. & Rigby, B.T. (1968) Preliminary observations on the performance of the Bramson membrane lung oxygenator. Annals of Thoracic Surgery, 5, 367.

Arts, M.G.J. & Roevros, J.M.J.G. (1972) On the instantaneous measurement of bloodflow by ultrasonic means. Medical & Biological Engineering, 10, 23.

Ashmore, P.G., Sirtek, V. & Ambrose, P. (1968) The incidence and effects of particulate aggregation and microembolism in pump-oxygenator systems. Journal of Thoracic and Cardiovascular Surgery, 55, 691.

Ashmore, P.G., Swank, R.L., Gallery, R., Ambrose, P. & Prichard, K.H. (1972) Effect of Dacron wool filtration on the microembolic phenomenon in extracorporeal circulation. Journal of Thoracic & Cardiovascular Surgery, 63, 240.

Austen, W.G. & Howry, D.H. (1965) Ultrasound as a method to detect bubbles or particulate matter in the arterial line during cardio-pulmonary bypass. Journal of Surgical Research, 5, 283.

Baglio, C.M. & Hunter, W.C. (1959) Calcific arterial embolization accompanying commissurotomy. Journal of Thoracic Surgery, 37, 490.

Baird, R.J. & Miyagishima, R.T. (1963) The danger of air embolism through pressure perfusion cannula. Journal of Thoracic & Cardiovascular Surgery, 46, 212.

Balldin, U.I. & Borgstrom, P. (1976) Intra arterial bubbles during decompression to altitude in relation to decompression sickness in man. Aviation Space & Environmental Medicine, 47, 113.

Bartlett, R.H. & Gazzaniga, A.B. (1976) Physiology and pathophysiology of extracorporeal circulation. In Current techniques in extracorporeal circulation (Ed. M.I. Ionescu & G.H. Wooler) Butterworths, London.

Bass, R.M. & Longmore, D.B. (1969) Cerebral damage during open heart surgery. Nature, 222, 30.

Benjamin, R.B., Turbak, C.E. & Lewis, F.J. (1957) The effects of air embolism in the systemic circulation and its prevention during open heart surgery. Journal of Thoracic Surgery, 34, 548.

Bernstein, E.F. (1971) Certain aspects of blood interfacial phenomena - red blood cells. Federation Proceedings, 30, 1510.

Bethune, D.W. (1976) Organ damage after open heart surgery. Lancet, 1410.

Blacky, P.H. & Starr, A. (1964) Post-cardiotomy delirium. American Journal of Psychiatry, 121, 371.

Bleifeld, W. (1961) Cerebrale "fett" embolie nach operationen mit der Herz-Lungen-Maschine. Thoraxchirurgie, 9, 12.

Borik, S., Davey, T.B., Kaufman, B., Smeloff, E.A. & Miller, G.E. (1973) A new method for intraoperative detection of intracardiac air prior to discontinuance of bypass. Annals of Thoracic Surgery, 16, 344.

Bove, A.A., Ziskin, M.C. & Mulchin, W.L. (1969) Ultrasonic detection of in-vivo cavitation and pressure effects of high speed injections through catheters. Investigative Radiology, 4, 236.

Bradley, E.L. & Sacerio, J. (1972) The velocity of ultrasound in human blood under varying physiologic parameters. Journal of Surgical Research, 12, 290.

Branthwaite, M.A. (1973)Detection of neurological damage during open heart surgery. Thorax, 28, 464.

Branthwaite, M.A. (1975) Prevention of neurological damage during open heart surgery. Thorax, 30, 258.

Brennan, R.W., Patterson, R.H. & Kessler, J. (1971) Cerebral blood flow and metabolism during cardiopulmonary bypass: Evidence of microembolic encephalopathy. Neurology, 21, 665.

Bradley, E.L. & Sacerio, J. (1972) The velocity of ultrasound in human blood under varying physiological parameters. Journal of Surgical Research, 12, 290.

Caguin, F. & Carter, M.G. (1963) Fat embolism with cardiotomy with the use of cardiopulmonary bypass. Journal of Thoracic & Cardiovascular Surgery, 46, 665.

Carlson, R.G. & Lillehei, C.W. (1967) A useful modification to the aortic needle-vent for prevention of air embolism during open heart surgery. Journal of Thoracic & Cardiovascular Surgery, 53, 848.

Carlson, R.G. Landé, A.J., Twichell, J., Baxter, J. & Lillehei, C.W. (1972) Prolonged cardiopulmonary support with disposable membrane oxygenator. N.Y. State Journal of Medicine, 72, 2513.

Carlson, R.G., Landé, A.J., Landis, B., Rogoz, B., Baxter, J., Patterson, R.H., Stenzel, K. & Lillehei, C.W. (1973) The Lande-Edwards membrane oxygenator during heart surgery. Journal of Thoracic and Cardiovascular Surgery, 66, 894.

Carrel, A. (1914) Experimental operations on the orifices of the heart. Annals of Surgery, 60, 1.

Cartensen, E.L. & Schwan, H.P. (1959) Acoustic properties of haemoglobin solutions. Journal of the Acoustical Society of America, 31, 305.

Cassie, A.B., Riddell, A.G. & Yates, P.O. (1960) Hazard of antifoam emboli from a bubble oxygenator. Thorax, 15, 22.

Chan, K.S. & Yang, W-J. (1969) Survey of literature related to the problems of gas embolism in human body. Journal of Biomechanics, 2, 299.

Chan, K.S. & Yang, W-J. (1969) Behaviour of gas emboli subjected to pressure variation in biological systems. Journal of Biomechanics, 2, 151.

Chan, K.S. & Yang, W-J. (1969) Survey of literature related to the problems of gas embolism in human body. Journal of Biomechanics, 2, 299.

Christoforides, C. & Hedley-Whyte, J. (1969) Supersaturation of blood with O_2. Journal of Applied Physiology, 26, 239.

Clark, L.C. (1958) Optimal flow rate in perfusion. In Extracorporeal Circulation (Ed. Allen, J.G.) Charles C. Thomas, Springfield III.

Clark, L.C. (1959) Blood gas exchange devices. I.R.E. Transactions on Medical Electronics, 6, 18.

Clark, R.E. & Weldon, C.S. (1972) Metabolic responses to extracorporeal circulation in cardiac surgery. (Ed. Norman, J.C.) Appleton Century Crofts pp. 183-194.

Clarke, R.E., Dietz, D.R. & Miller, J.G. (1975) Continuous detection of microemboli during cardiopulmonary bypass in animals and man. Circulation, Supplement II (51 & 52) II - 75, 287.

Cleland, W.P. & Ghadiali, P.E. (1976) Protection of the myocardium during extracorporeal circulation for intracardiac surgery. In. Current techniques in extracorporeal circulation. (Ed. Ionesen, M.I. & Woller, G.H.) Butterworths, London.

Connell, R. (1975) Filtration characteristics of three new in-line blood transfusion filters. Annals of Surgery, 181, 273.

Connolly, C.C. (1963) Ultrasonic stable cavitation and its effects on human erthrocytes. M.Sc. thesis, University of Vermont, cited in Howkins & Weinstock.

Crosley, W.H. & Furth, F.W. (1956) A modification of the benzidene method for measurement of haemoglobin in plasma and urine. Blood 11, 380.

Dacie, J.V. & Lewis, S.M. (1968) Practical Haematology. J. & A. Churchill Limited, London.

Daigle, R.E., Morgan, R.J. & Budak, A. (1973) Window discrimination using integrated circuits. I.E.E.E. Transactions on Biomedical Engineering BME-20, 303.

Danielson, G.K., Dubilier, L.D. & Bryant, L.R. (1970) Use of Pluronic F-68 to diminish fat emboli and hemolysis during cardio-pulmonary bypass. Journal of Thoracic & Cardiovascular Surgery, 59, 178.

DeJong, D.A., Megens, P.H.A., DeVlieger, M., Thon, H.& Holland, W.P.J. (1975) A directional quantifying Doppler system for measurement of transport velocity of blood. Ultrasonics, May, 138.

Devin, C. (1959) Survey of thermal, radiation, and viscous damping of pulsating air bubbles in water. Journal of the Acoustical Society of America, 31, 1654.

De Wall, R.A., Long, D.M., Gemmill, S.H. & Lillehei, C.W. (1959) Certain blood changes in patients undergoing extracorporeal circulation. Journal of Thoracic Surgery, 37, 325.

Dewhurst, C.J. (1971) The safety of ultrasound. Proceedings of the Royal Society of Medicine, 64, 996.

Donald, D.E. & Fellows, J.L. (1959) Relation of temperature, gas tension, and hydrostatic pressure to the formation of gas bubbles in extracorporeally oxygenated blood. Surgical Forum, 10, 589.

Donald, D.E. & Fellows, J.L. (1961) Physical factors relating to gas embolism in blood. Journal of Thoracic and Cardiovascular Surgery, 42, 110.

Drew, C.E., Keen, G. & Benazon, D.B. (1959) Profound hypothermia, Lancet, 1, 745.

Durrant, T.M., Oppehheime, M.J., Webster, M.R. & Lang, J. (1949) Arterial air embolism. American Heart Journal, 38, 481.

Dutton, R.C., Edmunds, L.H., Hutchinson, J.C. & Benson, B.R. (1973) Platelet aggregate emboli produced in patients during cardiopulmonary bypass with membrane and bubble oxygenators and blood filters. Journal of Thoracic & Cardiovascular Surgery, 67, 258.

Edmonds-Seal, J. & Maroon, J.C. (1969) Air embolism diagnosed with ultrasound. Anaesthesia, 24, (3), 438.

Edmonds-Seal, J., Prys-Roberts, C. & Adams, A.P. (1971) Air Embolism: A comparison of the various methods of detection. Anaesthesia, 26, 202.

Egar, E.I. & Saidman, L.J. (1965) Hazards of nitrous oxide anesthesia in bowel obstruction and pneumothorax. Anesthesiology, 26, 61.

Egeblad, K., Osborn, J., Burns, W., Hill, J.D. & Gerbode, F. (1972) Blood filtration during cardiopulmonary bypass. Journal of Thoracic & Cardiovascular Surgery, 63, 384.

Ehrenhaft, J.L. & Cloman, M.A. (1961) Cerebral complications of open heart surgery. Journal of Thoracic & Cardiovascular Surgery, 41, 503.

Emerson, L.V., Hempleman, H.V. & Lentle, R.G. (1967) The passage of gaseous emboli through the pulmonary circulation. Respiratory Physiology, 3, 213.

Epstein, P.S. & Plesset, M.S. (1950) On the stability of gas bubbles in liquid-gas solutions. Journal of Chemistry & Physics, 18, 1505.

Evans, E.A. & Wellington, J.S. (1964) Emboli associated with cardiopulmonary bypass. Journal of Thoracic & Cardiovascular Surgery, 48, 323.

Evans, A., Barnard, E.E.P. & Walder, D.N. (1972) Detection of gas bubbles in man at decompression. Aerospace Medicine, 43, 1095.

Ferguson, T.B., Burbank, A. & Burford, T.H. (1967) The disposable bubble oxygenator. Evaluation of an improved model. Surgery, 61, 260.

Fishman, N.H., Carlsson, E. & Roe, B.B. (1969) The importance of the pulmonary veins in systemic air embolism following open heart surgery. Surgery, 66, 655.

Fisk, G.C., Lawrence, J., Stacey, R.B., Wright, J.S. & Horton, D.A. (1972) Bubbles in an infant oxygenator at very low flow rates. Journal Thoracic & Cardiovascular Surgery, 64, 98.

Flax, S.W., Webster, J.G. & Updike, S.J. (1973) Pitfalls using Doppler ultrasound to transduce blood flow. I.E.E.E. Transactions on Biomedical Engineering, BME-20, 306.

Forster, R.E. (1964) Rate of gas uptake by red cells. Handbook of Physiology - section 3 Respiration. (Ed. Fenn, W.O. & Rahn, H.)

Forster, R.E. & Van der Lindt, W.J. (1959) Calculations of the rates of uptake of O_2 and CO by red cells using a digital computer. Federation Proceedings, 18, 47.

Frank, K.A., Heller, S.S., Kornfeld, D.S. & Malm, J.R. (1972) Long-term effects of open heart surgery on intellectual functioning. Journal of Thoracic & Cardiovascular Surgery, 64, 811.

Freedman, A. (1960) Sound field of a rectangular piston. Journal of the Acoustical Society of America 32, 197.

Freedman, A. (1970) Transient field of acoustic radiators. Journal of the Acoustical Society of America, 48, 135.

Friedman, I.H., Gelman, S., Lowenfels, A.B., Landew, M. & Lord, J.W. (Jr.) (1962) The effects of intra-arterial microbubbles on normothermic and hypothermic dogs. Journal of Surgical Research, 2, (1), 19.

Furness, A. (1975) The detection of microbubbles in extracorporeal circulation. Journal of Cardiovascular Technology, 18, 28.

Geoghegan, T. & Lam, C.R. (1953) The mechanism of death from intra cardiac air and its reversability. Annals of Surgery, 138, 351.

Gianelli, S., Moltham, M.F., Best, R.J.,Diell, J.A. & Kirby, C.K. (1957) The effects produced by various types of pump oxygenators during two-hour partial infusions in dogs. Journal of Thoracic Surgery, 34, 563.

Gillis, M.F., Karagianes, M.T. & Peterson, P.O. (1968) Bends detection of circulating gas emboli with external sensor. Science, 161, 579.

Gillis, M.F., Karagianes, M.T. & Peterson, P.O. (1969) Detection of gas emboli associated with decompression using the Doppler flowmeter. Journal of Occupational Medicine, 11, 245.

Gillis, M.F., Peterson, P.L. & Karagianes, M.T. (1968) In vivo detection of circulating gas emboli associated with decompression sickness using the Doppler flowmeter. Nature, 217, 965.

Gilman, S. (1965) Cerebral disorders after open heart operations. New England Journal of Medicine, 272, 489.

Goldford, D. & Bannson, H.T. (1963) Early and late effects on the heart of small amounts of air in the coronary circulation. Journal of Thoracic & Cardiovascular Surgery, 46, 368.

Goldstein, S. (1938) Modern developments in fluid dynamics. Oxford - Clarendon Press.

Gordan, A.S., Jones, J.C. & Luddington, L.G. (1960) Deep hypothermia for intracardiac surgery. American Journal of Surgery, 100, 332.

Gosling, R.G., King, D.H., Newman, D.L. & Woodcock, J.P. (1969) Transcutaneous measurement of aterial blood-velocity by ultrasound. Journal of Ultrasonics, U.S.I. Conf. papers, 16.

Gott, V.L. & Lillehei, C.W. (1959) An instrument for the prevention of air embolism during direct vision closure of atrial septal defects and mitral valvulop. . Surgery,Gynaecology & Obstetrics, 108, 747.

Gottlieb, J.D., Ericsson, J.A. & Sweet, R.B. (1965) Venous air embolism. Anesthesia & Analgesia, 44, 773.

Graff, T.D., Arbegast, N.R., Phillips, O.C., Harris, L.C. & Frazier, T.M. (1959) Gas embolism, A comparative study of air and carbon dioxide as embolic agents in the venous system. American Journal of Obstetrics & Gynaecology, 78, 259.

Graves, D.J., Idicula, J., Lambertsen, C.J. & Quinn, J.A. (1963) Bubble formation resulting from counterdiffusion supersaturation a possible explanation for isobaric inert gas 'urticaria' and vertigo. Physics in Medicine & Biology, 18, 256.

Graves, D.J., Idicula, J., Lambertsen, C.J. & Quinn, J.A. (1973) Bubble formation in physical and biological systems: a manifestation of counterdiffusion in composite media. Science, 179, 582.

Greenfield, J.G. & Meyer, A. (1963) General pathology of the nerve cell and neuroglia. Greenfield's Neuropathology (2nd. Edition) Ed. Blackwood, W., McMenemey, W.H., Meyer, A., Norman, R.M. & Russell, D.S. Edward Arnold Ltd.

Groves, L.K. & Effler, D.B. (1964) A needle-vent safeguard against systemic air embolus in open heart surgery. Journal of Thoracic & Cardiovascular Surgery, 47, 349.

Grulke, D.C., Marsh, N.A., & Hills, B.A. (1973) Experimental air embolism; measurement of microbubbles using the Coulter counter. British Journal of Experimental Pathology, 54, 684.

Halley, M.M., Reemstma, M.D. & Creech, O. Jr. (1958) Cerebral blood flow, metabolism, and brain volume in extracorporeal circulation. Journal of Thoracic & Cardiovascular Surgery, 36, 506.

Harkens, H. & Harmon, P. (1934) Embolism by air and oxygen: experimental studies. Proceedings of the Society for Experimental Biology & Medicine, 32, 178.

Hasbrouk, J.D. & Rigor, B.M. (1969) The oxygen tension of cerebrospinal fluid during cardiopulmonary bypass. Journal of Thoracic & Cardiovascular Surgery, 58, 754.

Helps, E.P.W. & McDonald, D.A. (1954) Observations on laminar flow in veins. Journal of Physiology, 124, 631.

Hickling, R. (1962) Analysis of echoes from a solid elestic sphere in water. Journal of the Acoustical Society of America, 34, 1582.

Hickling, R. (1964) Analysis of echoes from a hollow metallic sphere in water. Journal of the Acoustical Society of America, 36, 1124.

Hill, R.C. (1968) The possibility of hazard in medical and industrial applications of ultrasound. British Journal of Radiology, 41, 561.

Hill, C.R. (1970) Calibration of ultrasonic beams for biomedical applications. Physics in Medicine & Biology, 15, 241.

Hill, C.R. (1972) Proceedings of the first World Congress on Ultrasonic Diagnostics in Medicine. Academy of Science, Vienna.

Hill, C.R., Clark, P.R., Crowe, M.R. & Hammick, J.W. (1969) Ultrasonics for Industry Conference Papers (Ed. Crawford, A.) Illife Scientific and Technical Publications, Guildford, 26.

Hills, B.A. (1974) Air embolism: fission of microbubbles upon collision in plasma. Clinical Science and Moelcular Medicine, 46, 629.

Hills, B.A. & Grulke, D.C. (1975) Evaluation of ultrasonic bubble detectors in vitro using calibrated microbubbles at selected velocities. Ultrasonics, July, 181.

Hollenberg, M., Pruett, R. & Thal, A. (1963) Vasoactive substances liberated by prolonged bubble oxygenation. Journal of Thoracic & Cardiovascular Surgery, 45, 402.

Howkins, S.D. & Weinstock, A. (1970) The effect of focused ultrasound on human blood. Ultrasonics, 8, 174.

Hughes, D.E. & Nyborg, W.L. (1962) Cell disruption by ultrasound. Science, 138, 108.

Javid, H., Tufo, H.M., Najafi, H., Dye, W.J., Hunter, J.A. & Julian, O.C. (1969) Neurological abnormalities following open heart surgery. Journal of Thoracic & Cardiovascular Surgery, 58, 502.

James, T.N., Geoghegan, T. & Lam, C.R. (1953) Electro-cardiographic manifestations of air in the coronary arteries of dying and resusitated hearts. American Heart Journal, 46, 215.

Jones, H.B. (1950) Respiratory system: nitrogen eleimination. In Medical Physics (Ed. O. Glosser) Chicargo, Ill. 2, 857.

Jones, R.D. & Cross, F.S. (1964) A vent valve to minimise air embolism during open heart surgery. Journal of Thoracic & Cardiovascular Surgery, 48, 310.

Jordan, P. (Jr.), Tolstedt, G.E. & Beretta, F.F. (1958) Microbubble formation in artificial oxygenation. Surgery, 43, 266.

Justice, C., Leach, J. & Edwards, W.S. (1972) The harmful effects and treatment of coronary air embolism during open heart surgery. Annals of Thoracic Surgery, 14, 47.

Kaplan, S., Clark, L.C., Fox, R.P., Daoud, G. & Shemtob, A. (1962) Oxygen embolization during deep hypothermia. Archives of Surgery, 84, 140.

Kapustina, O.A. (1970) Gas bubbles in a small amplitude sound field. Soviet Physics - Acoustics, 15, 427.

Kayser, K.L. (1974) Blood-gas interface oxygenators versus membrane oxygenators. Annals of Thoracic Surgery, 17, 459.

Kessler, J. & Patterson, R.H. (1970) The production of microemboli by various blood oxygenators. Annals of Thoracic Surgery, 9, 221.

Koller, Th., & Hawrylenko, A. (1967) Contribution to the in vitro testing of pumps for extracorporeal circulation. Journal of Thoracic & Cardiovascular Surgery, 54, 22.

Kunkler, A. & King, H. (1959) Comparison of air, oxygen and carbon dioxide embolization. Annals of Surgery, 149, 95.

Kremkau, F.W., Gramiak, R., Carstensen, E.L., Shah, P.M. & Kramer, D.H. (1970) Ultrasonic detection of cavitation at catheter tips. American Journal of Roentgenology, 110, 177.

Landew, M., Bowles, T., Gelman, S., Lowenfels, A.B., Tepper, R. & Lord, J.W. (Jr.) (1960) Effects of intra-arterial microbubbles. American Journal of PHysiology, 199, 485.

Lawrence, G.H., McKay, H.A. & Sherensky, R.T. (1971) Effective measures in the prevention of intraoperative aerombolus. Journal of Thoracic & Cardiovascular Surgery, 62, 731.

Lee, W.H. Jr. & Hairston, P. (1971) Structural effects on blood proteins at the glood-gas interface. Federation Proceedings, 30, 1615.

Lee, W.H., Krumhaar, D., Foukalsrud, E.W., Schjeide, O.A. & Maloney, J.V. (1961) Denaturation of plasma proteins as a cause of morbidity and death after intra-cardiac operations. Surgery, 50, 29.

Lee, W.H., Brady, M., Rowe, J. & Miller, W. (1971) Effects of extracorporeal circulation upon behaviour, personality and brain function. Part II Haemodynamic metabolic and psychometric correlations. Annals of Surgery, 173, 1013.

Lemole, G.M. & Pinder, G.C. (1976) A method of preventing air embolus in open heart surgery. Journal of Thoracic & Cardiovascular Surgery, 71, 557.

Lichti, E.L., Simmons, E.M. & Almond, C.A. (1972) Detection of microemboli during cardiopulmonary bypass. Surgery, Gynaecology & Obstetrics, 134, 977.

Lindberg, D.A.B., Lucas, F.V., Sheagren, J. & Malm, J.R. (1961) Silicone embolization during clinical and experimental heart surgery employing a bubble oxygenator. American Journal of Pathology, 39, 129.

Lubbers, J., Ten Hof, J.P., Van der Veen, P.H., Van den Berg, J.W., Dorlas, J.C. & Horman Van der Heide, J.N. (1974) Microgasemboli in a pump oxygenator during open heart surgery. Archivum Chirurgicum. Neerlandium 26, 41.

Lubbers, J. & Van der Berg, Jw. (1977) An ultrasonic detector for microgasemboli in a bloodflow line. Ultrasonics in Medicine & Biology. In press.

Lucas, M., Mullarkey, M. & Abdulla, U. (1972) Study of chromosomes in the newborn after ultrasonic fetal heart monitoring in labour. British Medical Journal, 3, 795.

Lypacewicz, G. & Hill, C.R. (1974) Choice of standard target for medical pulse echo equipment evaluation. Ultrasound in Medicine & Biology, 1, 287.

Magee, B. (1975) Popper, Fontana Modern Masters, William Collins Sons & Co.

Maloney, J.V. (1958) Discussion on air embolism In : Allen, J.G. Extracorporeal circulation. Charles C. Thomas, Springfield Ill. 305.

Maloney, J.V. (Jnr.), Longmire, W.P. (Jnr.), Schmutzen, K.S., Marable, S.A., Raschee, E., Walanobe, Y., Lobpresis, E.L., & Aryouman, J.E. (1958) An experimental and clinical comparison of the bubble dispersion and stationary screen pump oxygenators. Surgery, Gynaecology & Obstetrics, 107, 577.

Manley, D.M.J.P. (1969) Ultrasonic detection of gas bubbles in blood. Ultrasonics, 7, 102.

Manley, D.M.J.P., & Cole, E.M. (1974) The detection of micro-inclusions in flowing liquids. Eighth International Congress on Acoustics, London. 1974.

Marini, J. & Rivenez, J. (1974) Acoustical fields from rectangular ultrasonic transducers for non-destructive testing and medical diagnosis. Ultrasonics, 12, 251.

Maroon, J.C., Edmonds-Seal, J. & Campbell, R.L. (1969) An ultrasonic method for detecting air embolism. Journal of Neurosurgery, 31, 196.

Maroon, J.C., Goodman, J.M., Horner, T.G. & Campbell, R.L. (1968) Detection of minute venous air emboli with ultrasound. Surgery Gynaecology & Obstetrics, 127, 1236.

Mats, G. & Hane, M. (1976) Changes in mental functions after open heart operations. Scandinavian Journal of Thoracic & Cardiovascular Surgery, 10, 215.

Matten, C.F.T., Brackett, F.S., Olson, B.J. (1957) Determination of number and size of particles by electrical gating : blood cells. Journal of Applied Physiology, 10, 56.

Mifo, H.M., Ostfeld, A.M. & Shakelle, R. (1970) Central nervous system dysfunction following open heart surgery. Journal of the American Medical Association, 212, 1333.

Miller, D.R. & Allbritten, F.F. (1960) Coronary suction as a source of air embolism: an experimental study using the Kay-Cross oxygenator. Annals of Surgery, 151, 75.

Miller, B.J., Gibbon, J.H., Greco, V.F., Cohn, C.H. & Allbritten, F.F. (1953) The use of a vent for the ventricle as a means of avoiding air embolism to the systemic circulation during open cardiotomy with the maintenance of the cardiorespiratory function of animals by pump oxygenator. Surgical Forum, 4, 29.

Morse, P.M. & Ingard, K.U. (1969) Theoretical Acoustics. McGraw-Hill.

Munson, E.S. & Merrick, H.C. (1966) Effect of nitrous oxide on venous air embolism. Anesthesiology, 27, 783.

McDonald, D.A. (1975) Blood flow in arteries. Edward Arnold.

Nichols, H.T., Morse, D.R. & Hirose, T. (1958) Coronary and other air embolization occuring during open heart surgery. Surgery, 43, 236.

Nicks, R. (1969) Air embolism in cardiac surgery: incidence and prophylaxis. Australian & New Zealand Journal of Surgery, 38, 328.

Nishi, R.Y. (1972) Ultrasonic detection of bubbles with Doppler flow transducers. Ultrasonics, 10, 173.

Nishi, R.Y. (1975) The scattering and absorption of sound waves by a gas bubble in a viscous liquid. Acustica, 33, 65.

Nishi, R.Y. & Livingstone, S.D. (1973) Intravascular changes associated with decompression: theoretical considerations using ultrasound. Aerospace Medicine, 44, 179.

Nunn, J.F. (1959) Letter to editor. Anaesthesia, 14, 413.

Osborne, J.J., Swank, R.L., Hill, J.D., Agiular, M.J. & Gerbode, F. (1970) Clinical use of a Dacron wool filter during perfusion for open heart surgery. Journal of Thoracic & Cardiovascular Surgery, 60, 575.

Padula, R.T., Eisenstat, T.E., Bronstein, M.H. & Camishion, R.C. (1971) Intracardiac air following cardiotomy. Journal of Thoracic & Cardiovascular Surgery, 62, 736.

Patterson, R.H. & Kessler, J. (1969) Microemboli during cardiopulmonary bypass detected by ultrasound. Surgery, Gynaecology and Obstetrics, 129, 505.

Patterson, R.H., Kessler, J. & Bergland, R.M. (1971) A filter to prevent cerebral damage during experimental cardiopulmonary bypass. Surgery Gynaecology & Obstetrics, 132, 71.

Patterson, R.H., Kessler, J., Brennan, R.W. & Twichell, J.B. (1972) Ultrasonic detection of microemboli from artificial surfaces: evidence of microembolic tissue damage. Bulletin of the New York Academy of Medicine 48, (2) 452.

Patterson, R.H., Rosenfeld, L. & Porro, R.S. (1976) Transitory cerebral microvascular blockade after cardiopulmonary bypass. Thorax, 31, 736.

Patterson, R.H. & Twichell, J.B. (1971) Disposable filter for Microemboli. Journal of the American Medical Association, 215, 76.

Patterson, R.H., Wasser, J.S. & Porro, R.S. (1974) The effects of various filters on microembolic cerebrovascular blockade following cardiopulmonary bypass. Annals of Thoracic Surgery, 17, 464.

Peacocke, A.R. & Pritchard, N.J. (1968) Some biophysical aspects of ultrasound. Progress in Biophysics, 18, 185.

Philp, R.B., Inwood, M.J. & Warren, B.A. (1972) Interaction between gas bubbles and components of the blood: implications in decompression sickness. Aerospace Medicine, 43, 946.

Pierce, E.C. (1966) A new concept in membrane support for artificial lungs. Transactions of the American Society for Artificial Internal Organs, 12, 334.

Pierce, E.C. (1974) Is the Blood-gas interface of clinical importance? Annals of Thoracic Surgery, 17, 526.

Powell, M.R. (1972) Leg pain and gas bubbles in the rat following decompression from pressure: monitoring by ultrasound. Aerospace Medicine, 43, 168.

Powell, M.R. (1972) Gas phase separation following decompression in asymptomatic rats : visual and ultrasound monitoring. Aerospace Medicine 43, 1240.

Powell, M.R. (1974) Doppler ultrasound monitoring of venous gas bubbles in pigs decompression with air, helium and neon. Aerospace Medicine, 45, 505.

Prior, P.F., Maynard, D.E., Sheaff, P.C., Simpson, B.R., Strunin, L., Weaver, E.J.M. & Scott, D.F. (1971) Monitoring Cerebral Function : Clinical experience with new device for continuous recording of electrical activity of brain. British Medical Journal, 2, 736.

Quinn, J.A., Graves, D.J. & Smock, R.A. (1974) Bubbles generated in membrane oxygenators : N_2 washout and counter diffusion supersaturation. Journal of Applied Physiology, 37, 479.

Reed, C.C. & Clark, D.K. (1975) Cardiopulmonary Perfusion. Texas Medical Press Inc., Texas.

Rittenhouse, E.A., Hessel, E.A., Ito, C.S. & Merendino, K.A. (1972) Effect of dipyridamole on microaggregate formation in the pump oxygenator. Annals of Surgery, 175, 1.

Robinson, D.E. & Kossoff, G. (1972) Performance tests of ultrasonic echoscopes for medical diagnosis. Radiology 104, 123.

Ross, J. (Jr.) (1959) Factors influencing the formation of bubbles in blood. Transactions American Society for Artifical Internal Organs, 5, 140.

Rott, H-D., Huber, H.J., Soldner, R. & Schwanitz, G. (1972) Examinations of chromosomes after in-vitro exposure of human lymphocytes to ultrasound. Electromedica, 1, 14.

Rschevsky, S.N. (1963) A course of lectures on the theory of sound. Pergamon Press.

Rubissow, G.J. & Mackay, R.S. (1971) Ultrasonic imaging of in vivo bubbles in decompression sickness. Ultrasonics, 9, 225.

Rubissow, G.J. & Mackay, R.S. (1974) Decompression study and control using ultrasonics. Aerospace Medicine, 45, 473.

Rygg, I.H. (1973) Studies in Extracorporeal Circulation. F.A.D.L.'s Forlag A/S København, Denmark.

Sachdev, N.S., Carter, C.C., Swank, R.L. & Blacky, P.H. (1967) Relationships between postcardiotomy delirium, clinical neurological changes and EEG abnormalities. Journal of Thoracic & Cardiovascular Surgery, 54, 557.

Sanderson, J.M., Wright, G. & Sims, F.W. (1972) Brain Damage in Dogs immediately following pulsatile and non-pulsatile blood flows in extracorporeal circulation. Thorax, 27, 275.

Schwarz, S.I., De Weese, J.A. & Nigualdula, F.N. (1958) Tissue oxygen 'tension' at various flow rates of extracorporeal circulation. Surgical Forum, 9, 151.

Selman, M.W., McAlpine, W.A. & Ratan, R.S. (1967) The effectiveness of various heart lung machines in the elimination of microbubbles from the circulation. Journal of Thoracic & Cardiovascular Surgery, 53, 613.

Senning, A. (1952) Ventricular fibrillation during extracorporeal circulation to prevent air embolism and to facilitate intracardiac operations. Acta Scandanavica Chilurgicum. Supplement, 171, 7.

Sigel, B., Gibson, R.J., Amatneek, K.V., Felix, W.R., Edelstein, A.L. & Popky, G.L. (1970) A Doppler ultrasound method for distinguishing lamina from turbulent flow. Journal of Surgical Research, 10, 221.

Simmons, E., MaGuire, C., Lichti, E., Helvey, W. & Almond, C. (1972) A comparison of the microparticles produced when two disposable-bag oxygenators and a disc oxygenator are used for cardiopulmonary bypass. Journal of Thoracic & Cardiovascular Surgery, 63, 613.

Smith, J.M. (1975) Scientific Analysis on the pocket Calculator. Wiley-Interscience Publication. John Wiley & Sons.

Smith, K.H. & Spencer, M.P. (1970) Doppler indices of decompression sickness: Their evaluation and use. Aerospace Medicine 41, 1396.

Solis, R.T., Wright, C.B., Gibbs, M.B. & Stevens, P.M. (1974) Quantitative studies of microaggregate formation in vitro and in vivo. Chest, 65, 445.

Spencer, M.P. (1976) Decompression limits for compressed air determined by ultrasonically detected blood bubbles. Journal of Applied Physiology, 40, 229.

Spencer, M.P. & Clarke, H.T. (1972) Precordial monitoring of pulmonary gas embolism and decompressed bubbles. Aerospace Medicine, 43, 762.

Spencer, M.P., Campbell, S.D., Sealey, J.L., Henry, F.C. & Lindbergh, J. (1969a) Experiments on decompression bubbles in the circulation using ultrasonic and electromagnetic flowmeters. Journal of Occupational Medicine, 11, 238.

Spencer, M.P., Lawrence, G.H., Thomas, G.I. & Sauvage, L.R. (1969b) The use of ultrasonics in the determination of arterial aeroembolism during open heart surgery. Annals of Thoracic Surgery, 8, 489.

Spencer, F.C., Rossi, N.P., Yu, S.C. & Koepke, J.A. (1965) The significance of air embolism during cardiopulmonary bypass. Journal of Thoracic & Cardiovascular Surgery, 49, 615.

Starr, A. (1960) The mechanism and prevention of air embolism during correction of congenital cleft mitral valve. Journal of Thoracic & Cardiovascular Surgery, 39, 808.

Starr, E.G. & Fisher, F. (1976) Ultrasonic monitoring for early diagnosis of air embolism during neurosurgical procedures. Der Anaesthetist, 25, 290.

Stepanischen, P.R. (1970) Transient radiation from pistons in an infinite planar baffle. Journal of the Acoustical Society of America, 49, 1629.

Stormorken, H. (1971) Platelets, thrombosis and hemolysis. Federation Proceedings, 30, 1551.

Swank, R.L. (1961) Alteration of blood on storage. Measurement of adhesiveness of "ageing" platelets and leucocytes and their removal by filtration. New England Journal of Medicine, 265, 728.

Swank, R.L. & Hissen, W. (1965) Isolated cat head perfusion by donor dog. Archives of Neurology, 13, 93.

Swank, R.L. & Porter, G.A. (1963) Disappearance of microemboli transfused into patients during cardiopulmonary bypass. Transfusion, 3, 192.

Swank, R.L., Roth, J.G. & Jansen, J. (1964) Screen filtration pressure method and adhesiveness and aggregation of blood cells. Journal of Applied Physiology, 19, 340.

Taber, R.E., Maraan, B.M. & Tomatis, L. (1970) Prevention of air embolism during open heart surgery. A study of the role of trapped air in the left ventricle. Surgery, 68, 685.

Tanasawa, I., Wotton, D.R., Yang, W-J. & Clark, D.W. (1970) Experimental study of air bubbles in a simulated cardiopulmonary bypass system with flow constriction. Journal of Biomechanics 3, 417.

Tanasawa, I., Echigo, R., Wotton, D.R., Nomura, M. & Yang, W-J. (1971) Measurement of mass diffusivity of gases in plasma and reaction velocity constant in bloods. Journal of Biomechanics, 4, 265.

Tarssanen, L. (1976) Hemolysis by ultrasound - A comparative study of the osmotic and ultrasonic fragility tests. Scandinavian Journal of Haematology, Supplement No. 29.

Taylor, K.J.W. & Dyson, M. (1972) Possible hazards of diagnostic ultrasound. British Journal of Hospital Medicine, 571.

Tepper, R., Gelman, S., Lowenfels, A.B. & Lord, J.W. (1958) A method for the detection of microbubbles resulting from the passage of blood through heart-lung machines. Surgical Forum, 9, 171.

Thomassen, R.W., Howbert, J.P., Win, D.F. & Thompson, S.W. (1961) The occurence and characterization of emboli associated with the use of a silicone antifoaming agent. Journal of Thoracic & Cardiovascular Surgery, 41, 611.

Thompson, P.D., Mennel, R.G. & Joyner, C.R. (1970) The effect of hematocrit on signal strength of Doppler velocity meters. Proceedings of 15th Annual Meeting of the American Institute of Ultrasound in Medicine, Cleveland, Ohio, U.S.A. 12-15 October, 1970.

Tinker, J.H., Gronert, G.A., Messick, J.M. & Michenfelder, J.D. (1975) Detection of air embolism, a test for positioning of right atrial catheter and Doppler probe. Anesthesiology, 43, 104.

Tisovec, L. & Hamilton, W.K. (1967) Newer considerations in air embolism during operation. Journal of the American Medical Association, 201, 376.

Tucker, D.G. & Welsby, V.G. (1968) Ultrasonic monitoring of decompression. Lancet, June 8, 1253.

Tufo, H.M., Ostfield, A.M. & Skekelle, R. (1970) Central nervous system dysfunction following open heart surgery. Journal of the American Medical Association, 212, 1333.

Ward, C.A. & Zingg, W. (1972) Bubble formation at a liquid-membrane interface during oxygen transfer. Proceedings of the Conference on Engineering in Medicine & Biology, 25th Bal. Harbour, Florida, 14, 14.

Warren, B.A., Philp, R.B. & Inwood, M.J. (1973) The ultrastructural morphology of air embolism: platelet adhesion to the interface and endothelial damage. British Journal of experimental Pathology, 54, 163.

Walder, D.N., Evans, A. & Hempleman, H.V. (1968) Ultrasonic monitoring of decompression. Lancet, April 27th. 897.

Weissler, A. (1960) Effects of ultrasonic irradiation on haemoglobin. Journal of the Acoustical Society of America, 32, 1208.

Wells, P.N.T. (1975) Absorption and dispersion of ultrasound in biological tissue. Ultrasound in Medicine & Biology, 1, 369.

Welsby, V.G. (1969) Acoustic Detection of Gas-Bubbles in Liquids. Joint Conference on Industrial Ultrasonics, Loughborough. I.E.R.E. Conference Proceedings, No. 16, 97.

Welsby, V.G. & Safar, M.H. (1969-70) Acoustic non-linearity due to microbubbles in water. Acustica 22, 177.

Willman, V.L., Zafiracopoulos, P. & Hanlon, C.R. (1958) Air Embolism, In Extracorporeal Circulation (Ed. Allen, J.G.). Springfield, Illinois.

Wladimiroff, J.W. & Talbert, D.G. (1973) The changing fine structure of erythrocyte formations when trapped in ultrasonic standing waves. Physics in Medicine & Biology, 18, 888.

Womersley, J.R. (1957) An elastic tube theory of pulse transmission and oscillatory flow in mammalian arteries. Wright Air Development Centre Technical Report, TR56-614.

Wright, G. (1971) Brain damage in dogs resulting from pulsatile and non-pulsatile blood flows in extracorporeal circulation. Ph.D. thesis, Keele University.

Wright, G. (1975) Brain damage druing extracorporeal circulation for open heart surgery. Journal of Cardiovascular Technology, 17, 36.

Wright, G. & Sanderson, J.M. (1976) Cellular aggregation and destruction during blood circulation and oxygenation. Thorax, 31, 405.

Yang, W-J. (1971) Dynamics of gas bubbles in whole blood and plasma. Journal of Biomechanics, 4, 119.

Yang, W-J., Echigo, R., Wotton, D.R. & Hwang, J.B. (1971a) Experimental studies of the dissolution of gas bubbles in whole blood and plasma: I Stationary bubbles. Journal of Biomechanics, 4, 275.

Yang, W-J., Echigo, R., Wotton, D.R. & Hwang, J.B. (1971b) Experimental studies of the dissolution of gas bubbles in whole blood and plasma: II Moving bubbles or liquids. Journal of Biomechanics, 4, 283.

Yang, W-J. & Yeh, H-C. (1966) Theoretical study of bubble dynamics in purely viscous fluids. American Institute of Chemical Engineers Journal, 12, 927.

Yeh, H.C. & Yang, W-J. (1968) Dynamics of bubbles in moving liquids with pressure gradients. Journal of Applied Physics, 39, 3156.

Yellin, E.L. (1966) Laminar-turbulent transition process in pulsatile flow. Circulation Research, 19, 791.